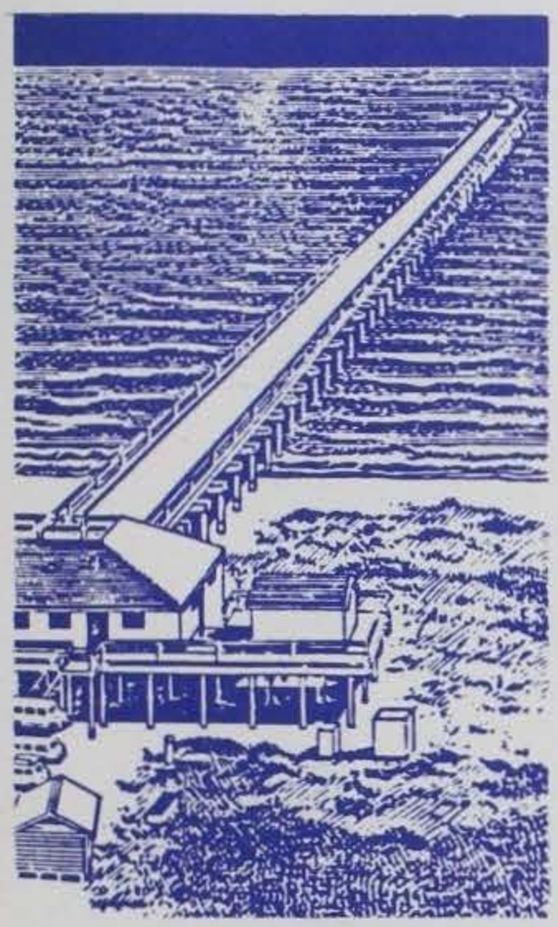

MISCELLANEOUS PAPER CERC-86-3

FLOATING BREAKWATER PROTOTYPE TEST PROGRAM: SEATTLE, WASHINGTON

by

Eric E. Nelson

US Army Engineer District, Seattle
PO Box C-3755, Seattle, Washington 98124-2255

and

Laurie L. Broderick

US Army Engineer District, Portland
PO Box 2946, Portland, Oregon 97208-2946

March 1986
Final Report

Prepared for

DEPARTMENT OF THE ARMY
US Army Corps of Engineers
Washington, DC 20314-1000

Unclassified
SECURITY CLASSIFICATION OF THIS PAGE *(When Data Entered)*

REPORT DOCUMENTATION PAGE

READ INSTRUCTIONS BEFORE COMPLETING FORM

1. REPORT NUMBER: Miscellaneous Paper CERC-86-3
2. GOVT ACCESSION NO.:
3. RECIPIENT'S CATALOG NUMBER:

4. TITLE *(and Subtitle)*: FLOATING BREAKWATER PROTOTYPE TEST PROGRAM: SEATTLE, WASHINGTON

5. TYPE OF REPORT & PERIOD COVERED: Final report

6. PERFORMING ORG. REPORT NUMBER:

7. AUTHOR(s):
Eric E. Nelson
Laurie L. Broderick

8. CONTRACT OR GRANT NUMBER(s):

9. PERFORMING ORGANIZATION NAME AND ADDRESS:
US Army Engineer District, Seattle
PO Box 4-3755, Seattle, Washington 98124-2255

US Army Engineer Waterways Experiment Station
Coastal Engineering Research Center
PO Box 631, Vicksburg, Mississippi 39180-0631

10. PROGRAM ELEMENT, PROJECT, TASK AREA & WORK UNIT NUMBERS:

11. CONTROLLING OFFICE NAME AND ADDRESS:
DEPARTMENT OF THE ARMY
US Army Corps of Engineers
Washington, DC 20314-1000

12. REPORT DATE: March 1986

13. NUMBER OF PAGES: 202

14. MONITORING AGENCY NAME & ADDRESS*(if different from Controlling Office)*:

15. SECURITY CLASS. *(of this report)*: Unclassified

15a. DECLASSIFICATION/DOWNGRADING SCHEDULE:

16. DISTRIBUTION STATEMENT *(of this Report)*:
Approved for public release; distribution unlimited.

17. DISTRIBUTION STATEMENT *(of the abstract entered in Block 20, if different from Report)*:

18. SUPPLEMENTARY NOTES:

19. KEY WORDS *(Continue on reverse side if necessary and identify by block number)*:

Anchor line forces
Field monitoring
Floating breakwaters
Puget Sound, Washington
Wave attenuation

20. ABSTRACT *(Continue on reverse side if necessary and identify by block number)*:

Because of increased interest in the use of floating breakwaters to provide wave protection, the US Army Corps of Engineers initiated the Floating Breakwater Prototype Test Program in February 1981. The objectives of the program, which utilized two types of breakwaters--a concrete box and a pipe-tire mat--was designed to answer several important engineering questions which included the following: determining the most efficient breakwater for a particular wave climate, predicting the forces that act upon structures and
(Continued)

DD FORM 1 JAN 73 1473 EDITION OF 1 NOV 65 IS OBSOLETE

Unclassified
SECURITY CLASSIFICATION OF THIS PAGE *(When Data Entered)*

20. ABSTRACT (Concluded):

anchoring systems, determining the optimum construction materials, and providing a low-cost means of connecting or fendering the individual breakwater modules. After construction and mooring at an exposed site in Puget Sound, the breakwaters were monitored to evaluate their performance and structural response. The results are being compiled to aid designers of future floating breakwaters.

FOREWORD

In February 1981 the US Army Corps of Engineers initiated a prototype test program to provide guidance for floating breakwater applications in semiprotected coastal waters, lakes, and reservoirs. The test was designed not only to obtain field information on construction methods and materials, connector systems, and maintenance problems but also to measure wave transmission characteristics, anchor loads, and structural response. Program planning, engineering, and design work were completed in September 1981. Monitoring and data collection ended in January 1984.

The Office, Chief of Engineers (OCE), US Army Corps of Engineers, had overall responsibility for program management. Technical guidance was provided throughout the program by the Prototype Test Working Group. The membership of the group changed over the 4-year span of the program; however, all members contributed to its successful completion. The following individuals comprised the Prototype Test Working Group: Messrs. Bruce L. McCartney, Jesse A. Pfeiffer, Jr., Fred A. Anderson, and Ivar R. Paavola, OCE; Messrs. Robert M. Sorenson, Richard L. Weggel, Rudolph P. Savage, and D. Donald Davidson, Coastal Engineering Research Center (CERC) of the US Army Engineer Waterways Experiment Station (WES); Mr. Paul F. Mlakar, Structures Laboratory, WES; Ms. Laurie L. Broderick, formerly at CERC/WES; Mr. John G. Oliver, US Army Engineer Division, North Pacific; and Messrs. A. David Schuldt and Eric E. Nelson, US Army Engineer District, Seattle.

Additional guidance was provided by the faculty and staff of the University of Washington, including Professors Eugene P. Richey, Billy J. Hartz, and Ronald E. Nece and Mr. Derald R. Christensen. Guidance was also provided by Dr. Volker W. Harms, University of California, Berkeley. Observations and photographs of the marine flora and fauna that inhabited the breakwaters were provided by two Seattle Aquarium biologists, Mr. Richard Hocking and Ms. Kristine Nelson.

PREFACE

The study herein was conducted between 5 February 1981 and 31 January 1985, during which time personnel of the US Army Engineer District, Seattle (NPS), had primary responsibility for carrying out the design, construction, and testing phases. Analysis of the collected data was done by the Coastal Engineering Research Center (CERC) of the US Army Engineer Waterways Experiment Station (WES). The study was authorized by the Office, Chief of Engineers (OCE), US Army Corps of Engineers, with overall program management responsibilities being shared by Messrs. Bruce L. McCartney, Directorate of Civil Works, OCE, and Jesse A. Pfeiffer, Jr., Directorate of Research and Development, OCE.

The initial report, prepared for NPS, was written by Mr. Eric E. Nelson, NPS, and Ms. Laurie L. Broderick, US Army Engineer District, Portland (formerly with CERC). Commanders of NPS during the 4-year study were Colonels Leon K. Moraski, Norman C. Hintz, and Roger F. Yankoupe.

The final report was prepared for publication utilizing funds from Work Unit 31679, "Design of Floating Breakwaters," by Mr. Peter J. Grace, Wave Research Branch, CERC. The report was written under general supervision of Dr. James R. Houston, Chief, CERC; Messrs. Charles C. Calhoun, Jr., Assistant Chief, CERC; C. Eugene Chatham, Chief, Wave Dynamics Division; and D. Donald Davidson, Chief, Wave Research Branch. This report was edited by Ms. Shirley A. J. Hanshaw, Publications and Graphic Arts Division, WES.

Director of WES during publication of this report was COL Allen F. Grum, USA. Technical Director was Dr. Robert W. Whalin.

TABLE OF CONTENTS

CONVERSION FACTORS, SI TO NON-SI (METRIC)
UNITS OF MEASUREMENT

Non-SI units of measurement used in this report can be converted to SI (metric) units as follows:

Multiply	By	To Obtain
cubic feet	0.02831685	cubic metres
Fahrenheit degrees	5/9	Celsius degrees or Kelvins*
feet	0.3048	metres
foot-pounds (force)	1.355818	metre-newtons or joules
inches	2.54	centimetres
kips (force)	4.448222	kilonewtons
knots (international)	0.5144444	metres per second
miles (US statute)	1.609347	kilometres
ounces (US fluid)	0.02957353	cubic decimetres
pounds (force)	4.448222	newtons
pounds (mass)	0.4535924	kilograms
pounds (force) per foot	14.5939	newtons per metre
pounds (force) per square foot	47.88026	pascals
pounds (force) per square inch	6.894757	kilopascals
slugs (mass) per cubic foot	515.3788	kilograms per cubic metre
square feet	0.09290304	square metres
tons (2,000 pounds, mass)	907.1847	kilograms

* To obtain Celsius (C) temperature readings from Fahrenheit (F) readings, use the following formula: $C = (5/9)(F - 32)$. To obtain Kelvin (K) readings, use: $K = (5/9)(F - 32) + 273.15$.

SUMMARY

The US Army Corps of Engineers (Corps) initiated the Floating Breakwater Prototype Test Program with the following objectives: determining the most efficient breakwater for a particular wave climate, predicting the forces that act upon structures and anchoring systems, determining the optimum construc-tions materials, and providing a low cost means of connecting or fendering the individual concrete breakwater modules. This breakwater study involved the testing of two types of breakwaters--a concrete box and a pipe-tire structure. After they had been constructed and moored at an exposed site in Puget Sound, the breakwaters were monitored for 18 months to collect data on performance and structural response.

Results of the program indicate that the breakwaters provided wave protection which was similar to that predicted by model tests. However, anchor forces and internal concrete strains were lower than predicted. None of the flexible connector designs for the concrete breakwater survived undamaged, but both fendering and rigidly connecting the individual breakwater modules proved successful. The pipe-tire breakwater proved to be durable; however, several of the longitudinal pipes broke as a result of faulty welds, and the break-water had to be removed from the test site 6 months ahead of schedule. The concrete breakwater was undamaged by the testing and was reused in a nearby Corps marina project.

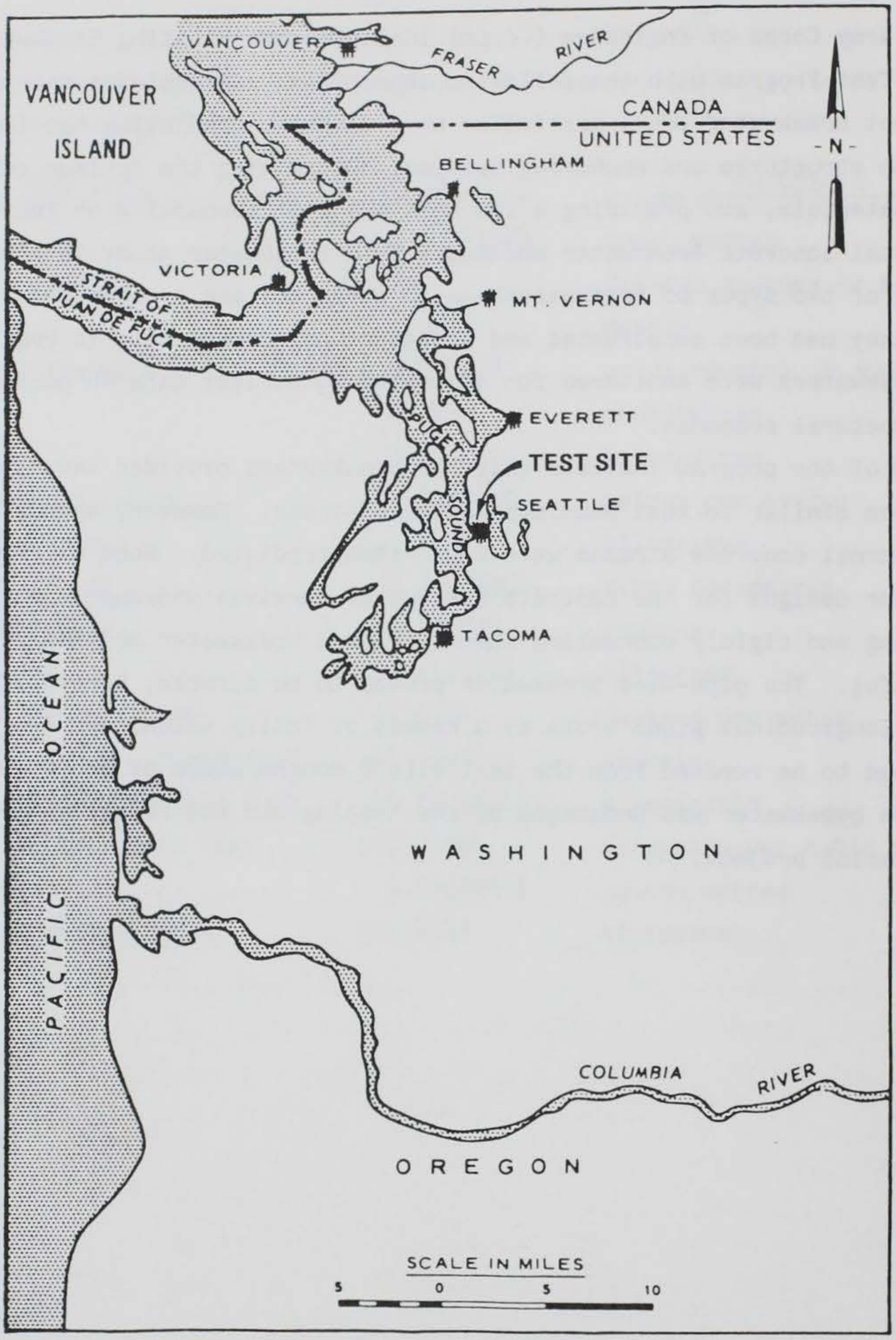

FIGURE 1. Location Map

FLOATING BREAKWATER PROTOTYPE TEST PROGRAM: SEATTLE, WASHINGTON

1.0 Introduction. This report documents a 4-year program in which two prototype floating breakwater designs were extensively field tested. The breakwater test site was in Puget Sound off West Point at Seattle, Washington (figure 1). This site was chosen to ensure that, within the period available for testing, wave conditions would approximate design waves normally associated with sites considered suitable for floating breakwaters. Water depth at the site varied between 30 and 50 ft* at mean lower low water (MLLW), and bottom materials consisted of gravel and sand. The diurnal tide range at the site was 11.3 ft, and the extreme range was 19.4 ft.

The prototype structures that were built and monitored were of two types: a concrete box (figure 2) and a pipe-tire design (figure 3). The 150-ft-long concrete breakwater was composed of two 75-ft-long units, each 16 ft wide and 5 ft deep (draft of 3.5 ft). The pipe-tire breakwater was composed of nine 16-in.-diam steel pipes and 1,650 truck tires fastened together with conveyor belting to form a structure that was 45 ft wide and 100 ft long.

2.0 Design and Construction. The concrete structure design was based on field and design experience from numerous floating structures now in use, available model test data, and detailed structural analysis of similar structures (references 1 through 4). The pipe-tire breakwater construction was based on a Sea Grant funded design by Harms (reference 5) and modified based on local site conditions and personal discussion with him. Other types of floating breakwaters, such as log bundles, twin pontoons, and A-frames, were considered; but either high construction costs, lack of broad applicability, or overall test program budget limited testing to the concrete box float and the scrap tire structures. Also, because Coastal Engineering Research Center (CERC) field studies (references 6 and 7) revealed that these two types of breakwaters were commonly used, the Prototype Test Working Group felt that

---

* A table of factors for converting non-SI to SI (metric) units of measurements is presented on page 4.

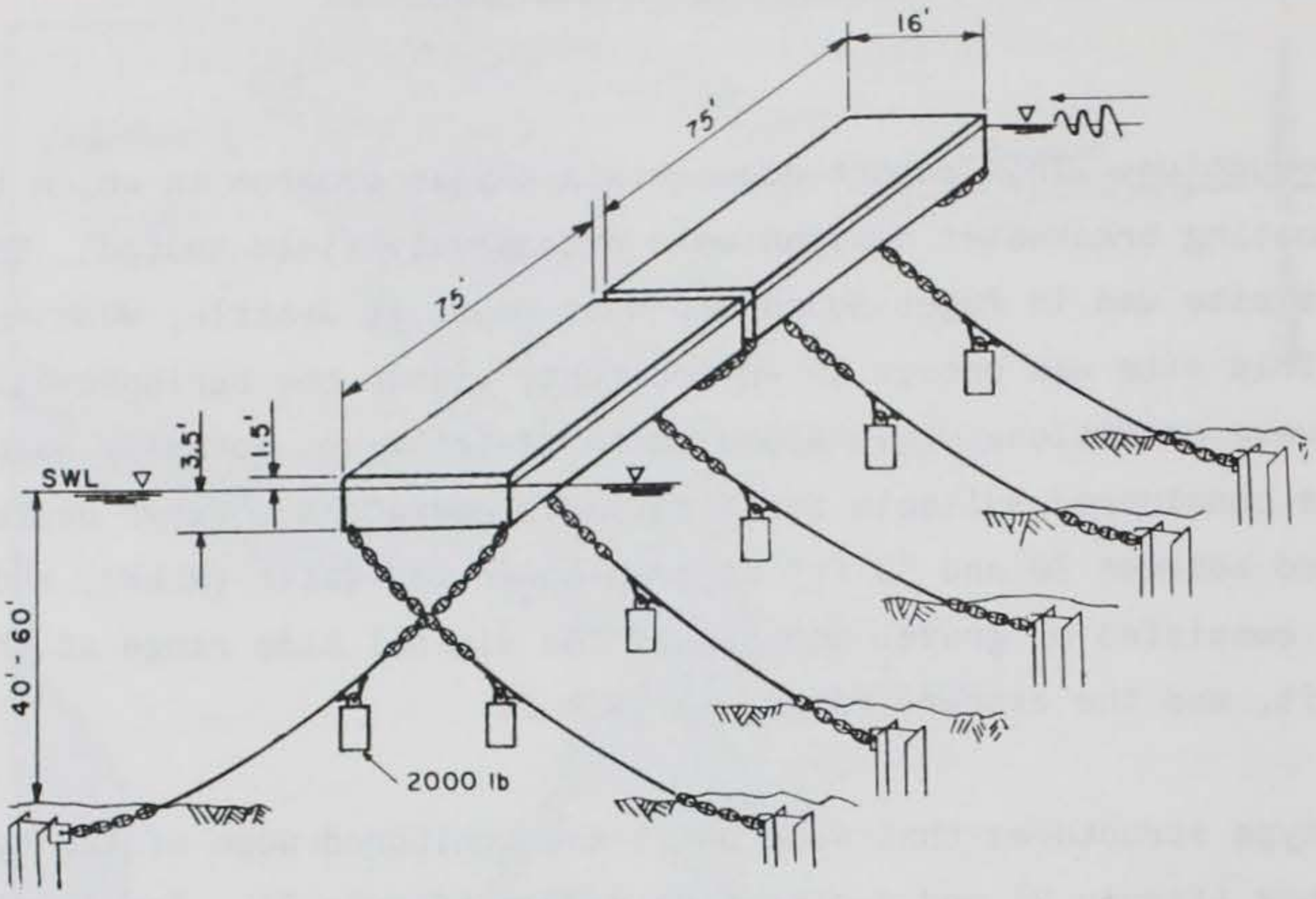

NOT TO SCALE

FIGURE 2. Concrete Breakwater

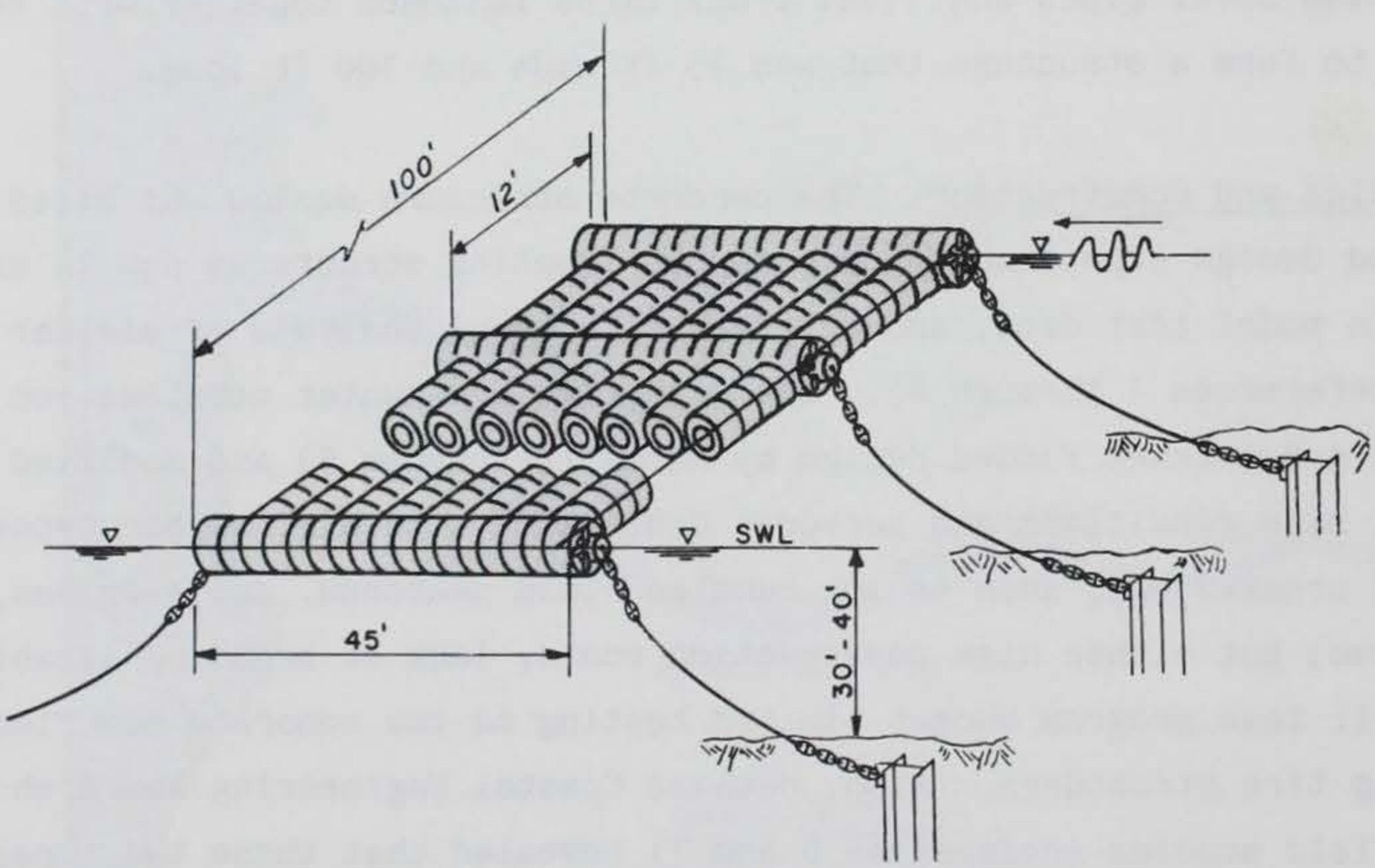

NOT TO SCALE

FIGURE 3. Pipe-Tire Breakwater

the concrete box and pipe-tire designs would be most promising for use in the future. Based on available design information, the breakwaters were sized to provide acceptable wave attenuation under conditions typical of sites where the future use of floating breakwaters is anticipated (i.e., significant wave height, H_s = 2 to 4 ft , wave period, T = 2 to 4 sec). However, the structures and anchor systems were designed to withstand the maximum wave predicted for the West Point site (H_s = 6 ft , T = 5 sec).

2.01 Concrete Breakwater Construction. The two 75-ft-long concrete breakwater units were cast in Bellingham, Washington, 90 miles from the test site. Work on these units began with the erection of exterior plate steel forms. Welded wire fabric (3/8 in. diam) were then placed on the sides, ends, and bottom of the forms, with the top left open to allow placement of styrofoam blocks during the concrete placement process. All small pieces of reinforcing steel were epoxy coated, and the welded wire parts were galvanized for corrosion protection. Prior to casting of the breakwater units, 16 rebar strain gages were fastened into the deck, sides, bottom, and corners of the west float as part of the monitoring system. The concrete placement began with pouring of the 4-3/4-in.-thick bottom. The styrofoam blocks that served as the interior forms were then dropped into place (photograph 1). Two-by-fours and PVC pipe were used as spacers to keep the reinforcing steel located properly between the styrofoam blocks and the outer steel plate forms. Steel beams were placed across the deck, and then wedges were hammered between these beams and the foam to keep the foam from floating up as the sides of the float were placed. After the sides of the floats had been placed to within 1 ft of the deck surface, the spacers and steel hold-down beams were removed. The deck reinforcing steel was laid, and the final stage of the concrete placement was begun (photograph 2). Placing and finishing of the deck completed the casting process (photograph 3). Test samples of concrete were taken throughout the placement. The concrete weight varied between 131 and 134 pcf, with an average 7-day strength of 4,000 to 5,000 psi and a 28-day strength of 5,000 to 6,000 psi. After the concrete had cured for 7 days, the ten 1/2-in.-diam strands in each of the six posttensioning tendons were tensioned to 25,000 lb (photograph 4).

On 28 May 1982, the 140-ton units were lifted from the casting area and

lowered into the waterway (photograph 5). The longitudinal strain gages in the lower center edges of the west float were monitored during the launching. A maximum strain of 1,700 microstrains was recorded, indicating that loads were about two-thirds of the yield strength of the reinforcing steel. After both units were launched, they were joined, end-to-end, with two flexible connectors (photograph 6) and towed approximately 90 miles south to the West Point test site. A detailed description of the concrete breakwater construction is given in Appendix A.

2.02 Pipe-Tire Breakwater Construction. The pipe-tire breakwater was assembled, one bay at a time, on a construction platform located adjacent to a waterway. As each 12- by 45-ft bay was completed, it was moved into the waterway (photograph 7). Construction of the breakwater followed closely the sequence described by Harms (reference 5). The prefoamed tires were brought to the assembly platform (photograph 8) where they were arranged as shown in figure 4 but without those tires labeled "free tires" (i.e., tires not connected to a conveyor belt). The matrix of 1,650 truck tires was bound by loops of 5-1/2-in.-wide, 3-ply conveyor belting. A special tool fabricated from a car jack was used to tighten the belting (photograph 9) before the loop ends were joined with five 1/2-in.-diam by 2-in.-long nylon bolts. The ends of the bolt threads were melted with a welding torch to prevent the nuts

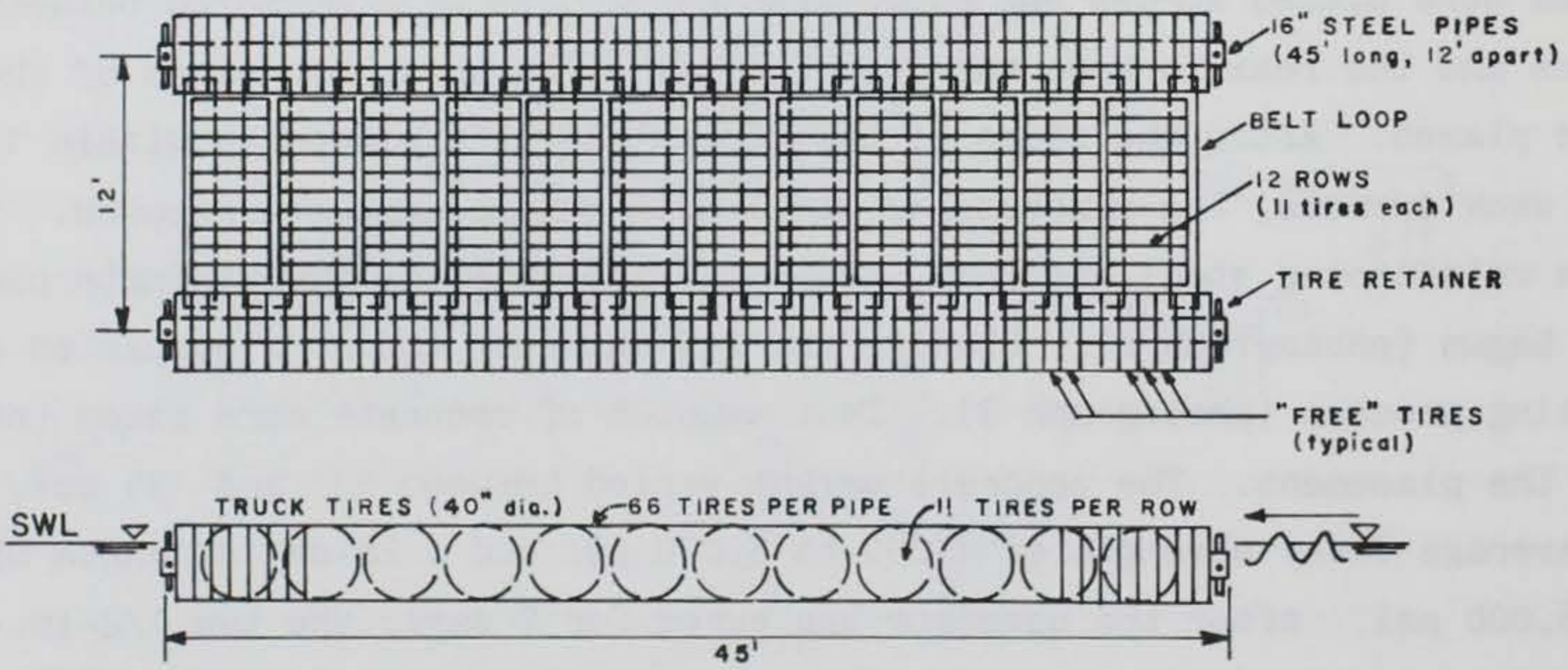

NOT TO SCALE

FIGURE 4. Pipe-Tire Breakwater Module

from working off the bolts. After 12 rows of 11 tires had been fastened together, additional tires were forced into the open spaces (free tire spaces) in the 45-ft-long beamwise row of tires.

The breakwater was then ready to have a 16-in.-diam styrofoam filled pipe inserted into the beamwise row. Because the tires were not perfectly aligned, a nose cone was placed on the end of the pipe. The pipe was moved into place with a large overhead crane and was shoved through the row of tires with a forklift (photograph 10). A tight structure was produced by compressing one additional tire onto each end of the pipe before the keeper pipes were installed (photograph 11). This procedure brought the total number of tires on each pipe to 66. The completed bay was dragged into the adjacent waterway by using the overhead crane and a small tugboat (photograph 12). This process was repeated for each of the eight bays (nine pipes). After construction procedures had been perfected, assembly time for each bay was approximately 8 hr for two men. Adding the free tires, inserting the pipe, and moving the completed bay off the assembly platform required an additional two men and took approximately 4 hr. Construction time was reduced by the use of heavy equipment and the special tools fabricated by the contractor. A detailed description of the pipe-tire breakwater construction is given in Appendix B.

2.03 Anchoring. The concrete breakwater was anchored in place by ten 30-ft-long steel H-piles (HP 14 by 102) embedded their full length (photograph 13). The pilings were driven using a Vulcan 010 hammer with a 10,000-lb ram weight and an 8,000-lb mandrel (photograph 14). A special fitting was attached to the mandrel to hold the piling in proper alinement while it was being driven. Anchor lines consisted of 1-3/8-in.-diam galvanized bridge rope with 15 to 25 ft of 1-1/4-in. stud link chain at each end. Anchor line lengths were sized to provide a scope no steeper than 1 vertical to 4.5 horizontal, and initial anchor line tensions were 5,000 ± 1,000 lb. A 2,000-lb concrete clump weight was attached 44 ft from the upper end of each anchor line. The purpose of this design was to produce a more even anchor line tension over the full range of tides and thereby to reduce the horizontal excursions of the breakwater, particularly at lower tide elevations. Four months prior to the termination of the field test, the clump weights were removed. During this 4-month period, the effects of

this clump weight removal on float motions, anchor forces, and wave attenuation were monitored.

The pipe-tire breakwater was anchored about 30 ft from the end of the concrete breakwater with ten 20-ft-long steel H-piles (HP 12 by 53) (photograph 15). Anchor lines consisting of 1-1/4-in.-diam three-strand nylon rope, with 10 ft of 3/4-in. stud link chain at each end, were attached to both ends of each pipe. The scope for these anchor lines was not steeper than 1 vertical to 4 horizontal. The center and end H-piles had one anchor line each, while the remaining four anchor piles were attached to three anchor lines apiece. The four end pilings were offset at an outward angle to counteract the opposing longitudinal component of force from the adjacent anchor lines. Anchoring details are given in Appendix C.

3.0 Observations of Performance and Durability. The prototype breakwater test site at West Point was selected because of its exposure to wind waves. This choice proved to be more than adequate for providing the desired wave conditions. During the 18-month test period, more than 20 storms moved through Puget Sound. One storm brought winds in excess of 60 knots and generated waves over 4 ft high. Most often, storm winds were in the 20- to 40-knot range with wave heights between 2 and 3.5 ft (photograph 16). Access to the breakwater was difficult when winds exceeded 10 knots; 15-knot winds made working conditions potentially hazardous.

Visual comparisons of incident and transmitted wave heights indicated that, under all observed wave conditions, the pipe-tire and the concrete breakwaters provided an adequate and very similar degree of wave protection for both wind waves and boat wakes (photograph 17). Moreover, the concrete breakwater reflected the wave energy, but the pipe-tire breakwater dissipated it through viscous damping. As a result of wave reflection, the windward side of the concrete breakwater was always noticeably rougher than the windward side of the pipe-tire breakwater (photograph 18).

Overtopping of the concrete breakwater by ship wakes and wind waves was quite pronounced (photograph 19). Sheet flow 6 in. deep was common. As a result, a lush crop of algae thrived on the deck of the structure, making the surface

treacherously slippery. The actual freeboard of the concrete breakwaters was about 13 in., 4 to 5 in. less than anticipated in the original design. The reduced freeboard undoubtedly contributed to the amount of overtopping.

The relatively high initial tension in the anchor lines of the concrete breakwater (5,000 lb with the 2,000-lb clump weights attached and 1,500 lb without the clump weights) appeared to minimize the lateral travel of the floats even during low tides and fast tidal current flows (2 knots). Lateral displacements were estimated to be less than 2 ft, even when the clump weights were removed.

Lateral displacement of the pipe-tire breakwater did not appear excessive (about 15 ft), but tidal currents running at a 45-deg angle to the anchor lines tended to carry the pipe-tire breakwater in a longitudinal direction to the near end of the concrete breakwater, a distance of about 30 ft.

Water leakage into the hollow end compartments of the concrete breakwater was a serious problem early in the test. Primary leak points were at the access hatches and the 2-in.-diam posttensioning bolt holes that were used when making the rigid connections between the two floats. Because calculations indicated that the breakwater could sink if the end compartments filled, emergency pumping operations were carried out on several occasions. Eventually, reworking the hatch covers and filling the bolt holes with sealant reduced the leakage rate to manageable levels.

One of the major goals of the test program was to investigate various methods of connecting (or fendering) the two 140-ton floats. Four different connection methods were tested: flexible connectors (two types), complete disconnection (with fendering), and rigid bolting of the units. Both the fendering (photograph 20) and the rigid connection were successful. None of the flexible connector designs survived their test period undamaged, although considerable progress was made toward a viable flexible connection design. Details of the connector testing are given in Appendix D.

Advantage was taken of calm periods to make repairs and to conduct additional tests. Four boat wake tests and an anchor line stiffness (pull) test were

conducted at various times in the program. For two of the boat wake tests, 41-ft Coast Guard cutters were used to generate waves (photograph 21). The other two tests used large (75- and 110-ft) tugboats. Boat generated waves were in the 2- to 3-ft range (see Appendix E for details). For the anchor stiffness test, a 4,000-horsepower tugboat was used to pull on the breakwater with varying loads, while surveying instruments measured displacements, and load cells in the anchor lines monitored anchor forces (photograph 22). This test was conducted to obtain simultaneous measurements of breakwater lateral displacement and the resisting anchor force, which are properties of the anchor system that affect overall float motions and internal loads.

Upon completion of the field test, diver inspections of the anchor lines and the concrete floats were made. No significant damage, wear, or cracking was found on the floats. The galvanized steel anchor lines were visibly corroded, and the shackles used to attach the clump weights to the anchor lines were worn; otherwise, the anchor line hardware, including the chain, was found to be in excellent condition.

For nearly a year, the pipe-tire breakwater proved to be remarkably durable. Except for minor repairs to the keeper pipes, it withstood the winter storms of 1982 without any maintenance (photograph 23). But in June 1983, almost a year to the day after the pipe-tire breakwater was installed, the first problem of any consequence developed. After a minor storm, routine inspection revealed that one of the longitudinal pipes had broken (photograph 24). A closer inspection revealed that the 45-ft pipe had been fabricated from a 40-ft section and a 5-ft section. A poor weld between the two sections had finally failed because of a combination of corrosion and fatigue, allowing the two pipe sections to pull out of the tires. One month later, when a second pipe failed in exactly the same manner, a decision was made to terminate testing of the pipe-tire breakwater. During the removal process, the anchor lines were inspected, and no major problems were found in the nylon anchor lines or connecting hardware. After the breakwater was removed, it was surplused and eventually reinstalled at a private marina in southern Puget Sound. Monitoring of the long-term durability of this unit is planned.

While the Prototype Test Program was under way, two projects using floating

breakwaters were designed and constructed by the US Army Engineer District, Seattle. In 1983, a 600-ft-long breakwater was constructed for the 800-boat East Bay Marina at Olympia, Washington (photograph 25). A year later, another floating breakwater, 1,600 ft long, was anchored at Friday Harbor, Washington (photograph 26). As originally planned, the prototype test breakwater was refurbished and incorporated into the Friday Harbor Project. Throughout the test program, information obtained from the construction and operation of the prototype breakwater was used to refine the East Bay and Friday Harbor designs. Preliminary prototype test data were used to confirm float sizing. Construction specifications were broadened to allow the use of either lightweight or standard weight concrete, with appropriate adjustments in float draft. Details of the East Bay connector system were changed to reduce maintenance, and the Friday Harbor fender system is a direct spinoff of the one developed during the prototype testing.

4.0 Data Collection. The monitoring program for the prototype test was conducted by the Civil Engineering Department of the University of Washington under contract with the US Army Corps of Engineers (Corps). The purpose of the monitoring program was to collect data that would serve as a basis for establishing and evaluating the fundamental behavior of the two breakwater types under study. The University designed a system to measure and record pertinent environmental and structural variables that are involved in the design and mathematical modeling of the test breakwaters and similar structures. The parameters that were measured included incident and transmitted waves, wind speed and direction, anchor line forces, stresses in the concrete units, relative float motion, rotational and linear accelerations, pressure distribution on the concrete breakwater, water and air temperatures, and tidal current data.

Off-the-shelf transducers for measuring many of the parameters were not available. A major effort was required to design and fabricate anchor force load cells (photograph 27), wave measuring spar buoys, a relative motion sensor (photograph 28), pressure sensor housings, and embedment strain gages. By the end of the monitoring program, approximately 60 transducers had been installed in and around the breakwater. Over 3 miles of underwater electrical cable was required to feed signals to the onboard data acquisition system that was

housed on the concrete breakwater (photograph 29). Using large lead-acid batteries for power, the system was completely self-contained. In addition to the input transducers, the system included a microprocessor controlled data logger and special purpose signal conditioning electronics which were designed and built by the University of Washington (photograph 30). The data acquisition system was programmed to sample selected transducers for 1 min on an hourly basis (because of power and storage requirements, the system was later programmed to take 1-min data every 2 hr). When either wind speed, current speed, anchor force, or significant wave height exceeded a preset threshold value, an 8-min record of all transducers was made at a sampling rate of 4 Hz. The microprocessor was capable of a limited amount of data processing, including calculations of maximum, minimum, mean, and standard deviation of selected parameters. After each data tape was retrieved from the breakwater, it was processed at the University. Selected statistics and data plots were analyzed to determine whether all critical components of the data acquisition system were operating properly. When problems were detected, repairs were made as soon as the breakwater was safely accessible. Keeping this complicated and extensive system operational in such a hostile environment proved to be a challenging enterprise. Salt water flooded instrumentation, waves and tidal currents broke transducers and tore out electrical leads, and logs, fish nets, and other debris caused damage continuously. Despite these difficulties in the 18 months of data collection, 121 data tapes were recorded, representing approximately one-quarter billion measurements. After initial processing at the University, the data were transferred to the Coastal Engineering Research Center for detailed analysis. Details of the monitoring program are given in Appendix F.

5.0 Data Analysis. Detailed analysis of the data was initiated in June 1984, with the major effort being directed toward the transmission and anchor force characteristics of the breakwaters. These two parameters had the highest priority because they were considered to be key factors in the effort to optimize the cost effectiveness of floating breakwater design. Other parameters such as the internal concrete strains and wave pressures were checked to ensure the reliability of the data, but detailed analysis was deferred.

Figures 5 and 6 present the wave transmission characteristics and anchor line

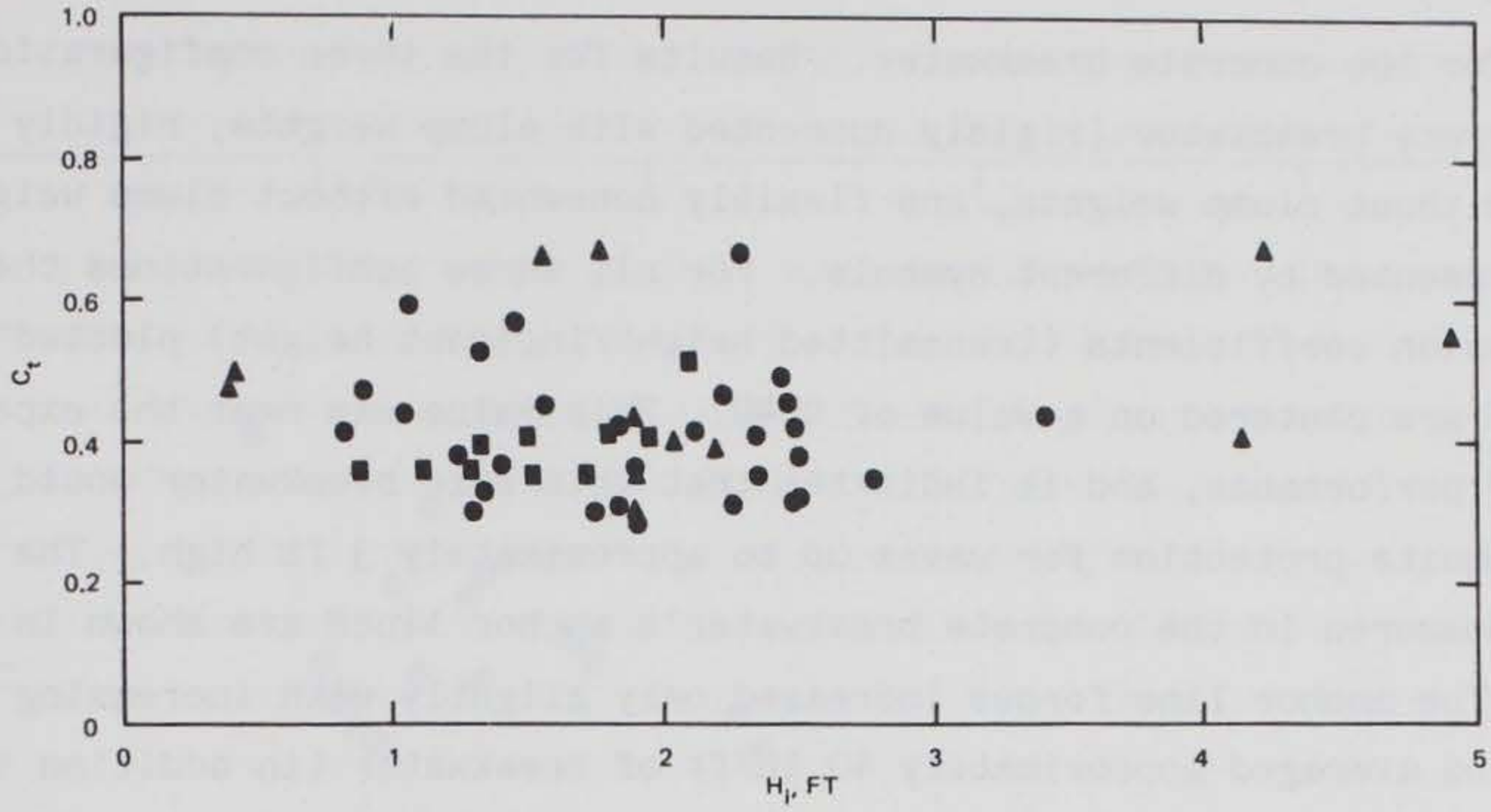

LEGEND

- ■ RIGID CONNECTION, WITH CLUMP WEIGHTS
- ▲ RIGID CONNECTION, NO CLUMP WEIGHTS
- ● FLEXIBLE CONNECTION, NO CLUMP WEIGHTS

FIGURE 5. Transmission Coefficient versus Incident Wave Height - Concrete Breakwater

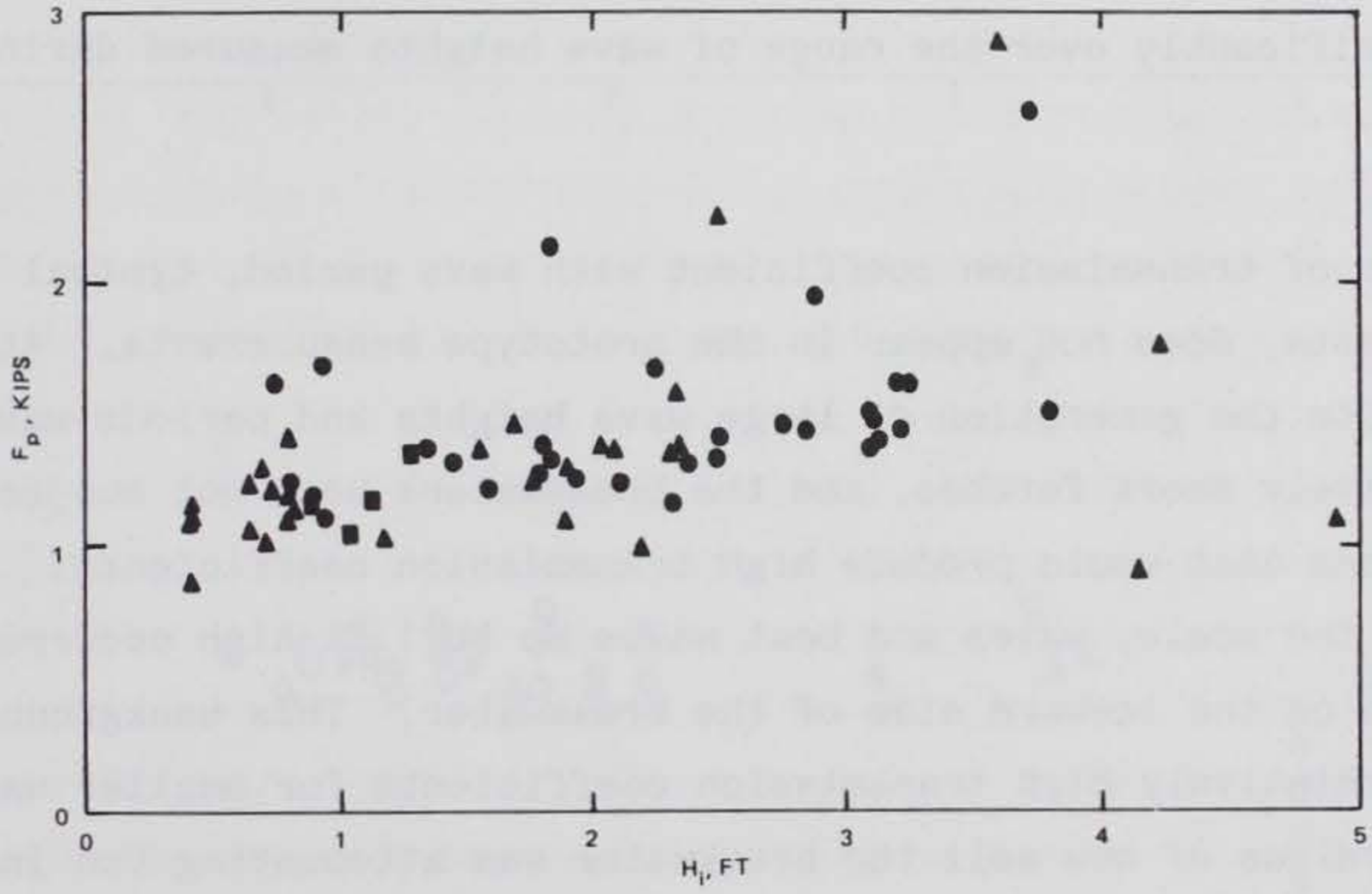

LEGEND

- ■ RIGID CONNECTION, WITH CLUMP WEIGHTS (PRETENSIONING ≃ 5000 LB)
- ▲ RIGID CONNECTION, NO CLUMP WEIGHTS
- ● FLEXIBLE CONNECTION, NO CLUMP WEIGHTS

(PRETENSIONING ≃ 1500 LB)

FIGURE 6. Peak Anchor Line Force versus Incident Wave Height - Concrete Breakwater

forces for the concrete breakwater. Results for the three configurations of the concrete breakwater (rigidly connected with clump weights, rigidly connected without clump weights, and flexibly connected without clump weights), are represented by different symbols. For all three configurations the wave transmission coefficients (transmitted height/incident height) plotted in figure 5 are centered on a value of 0.40. This value was near the expected level of performance, and it indicates that this size breakwater would provide adequate protection for waves up to approximately 3 ft high. The peak forces measured in the concrete breakwater's anchor lines are shown in figure 6. The anchor line forces increased only slightly with increasing wave height and averaged approximately 40 lb/ft of breakwater (in addition to the initial tension). The various configurations of the concrete breakwater seemed to have little effect on the peak anchor force. Figures 7 and 8 present the wave transmission characteristics and the anchor line forces for the pipe-tire breakwater. The average wave transmission coefficient of 0.42 is close to the expected value for the wave heights tested (figure 7). The peak anchor loads for the tire breakwater shown in figure 8 average approximately 75 lb/ft. Again, as for the concrete breakwater, the peak anchor load does not vary significantly over the range of wave heights measured during the test.

The variation of transmission coefficient with wave period, typical of most laboratory tests, does not appear in the prototype measurements. At the West Point test site the generation of large wave heights and periods was limited by the relatively short fetches, and the breakwaters were not subjected to wave conditions that would produce high transmission coefficients. At the lower end of the scale, waves and boat wakes up to 1 ft high occurred frequently, even on the leeward side of the breakwater. This background noise resulted in relatively high transmission coefficients for smaller wave heights regardless of how well the breakwater was attenuating the incident waves. These site-specific characteristics resulted in a concentration of wave attenuation measurements around 0.40. Selection of the concrete breakwater size was based on two-dimensional model tests which indicated a transmission coefficient of 0.40 could be expected for a range of wave periods for 2.0 to 3.5 sec. Prototype performance appears to closely follow the model test results, at least for this relatively narrow range of wave periods.

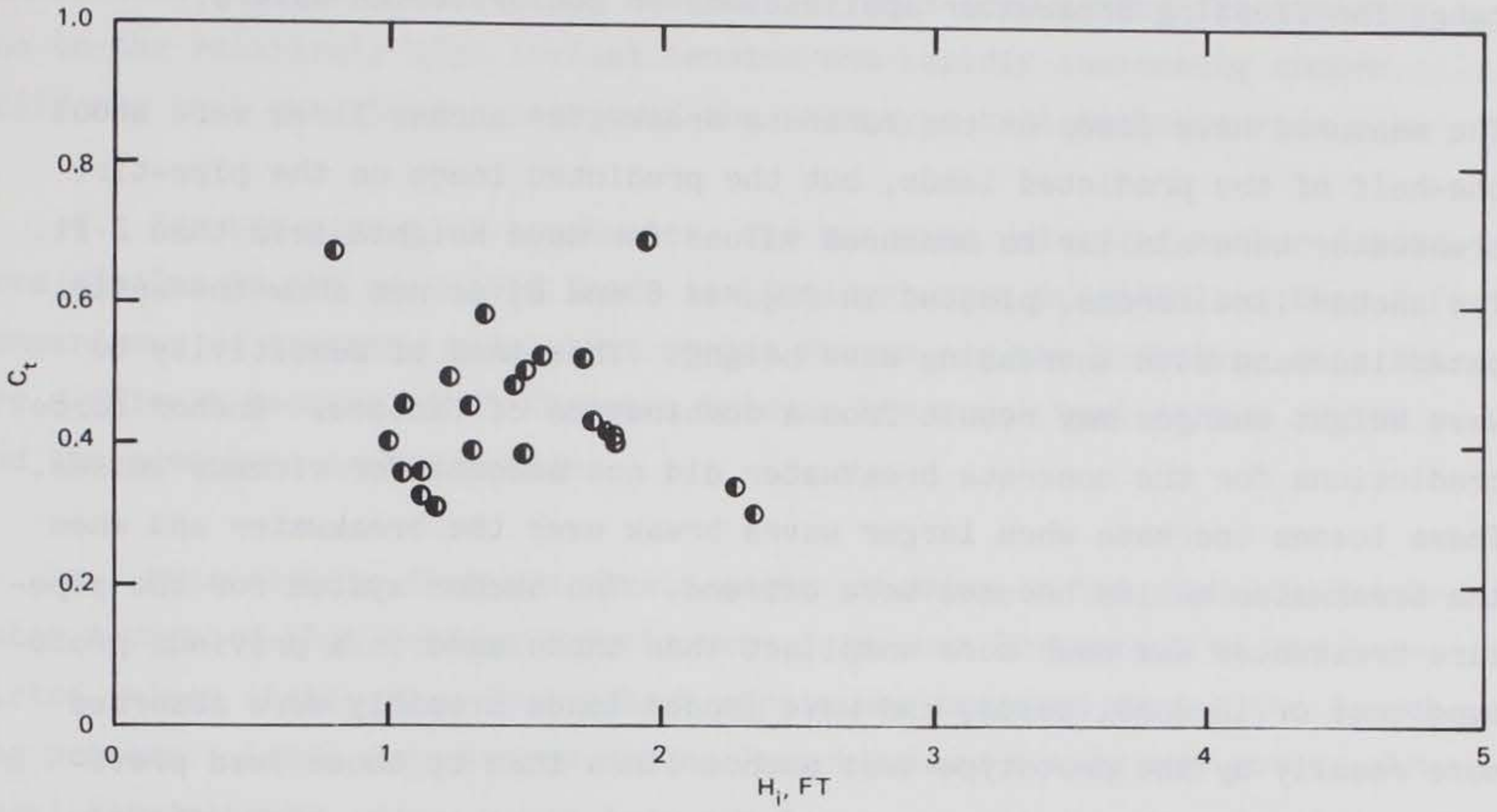

FIGURE 7. Transmission Coefficient versus Incident Wave Height - Pipe-Tire Breakwater

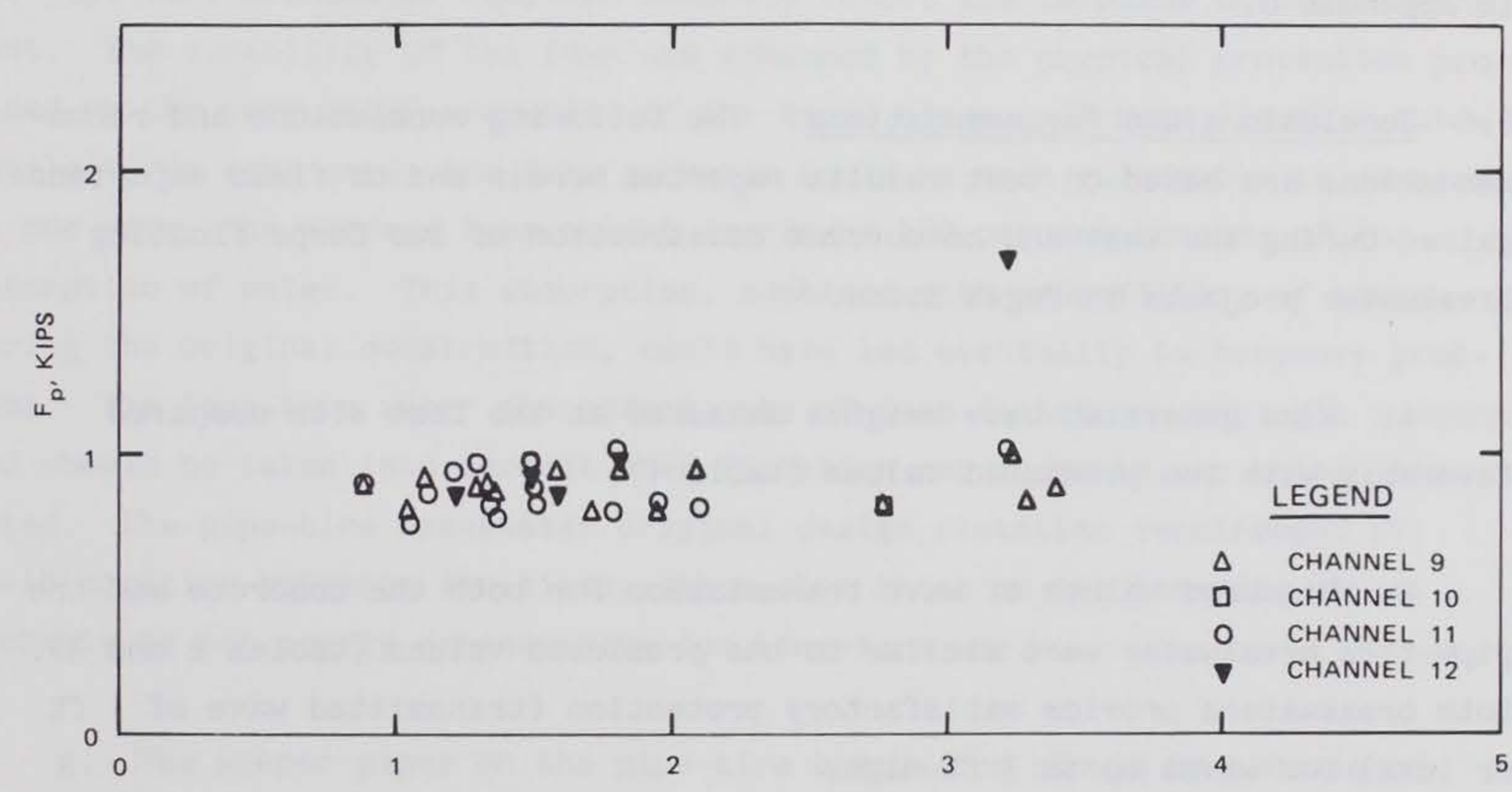

FIGURE 8. Peak Anchor Line Force versus Incident Wave Height - Pipe-Tire Breakwater

While the test site periods were limited, they do represent the most important range for floating breakwater applications in semiprotected waters.

The measured wave loads on the concrete breakwater anchor lines were about one-half of the predicted loads, but the predicted loads on the pipe-tire breakwater were similar to measured values for wave heights less than 2 ft. The anchor line forces, plotted in figures 6 and 8, do not show the anticipated increase with increasing wave height. This lack of sensitivity to wave height changes may result from a combination of factors. Anchor force predictions for the concrete breakwater did not account for viscous losses. These losses increase when larger waves break over the breakwater and when the breakwater motion becomes more extreme. The anchor system for the pipe-tire breakwater was much more compliant than those used in a previous prototype test or in model tests, and wave impact loads probably were absorbed more readily by the prototype-test anchor lines than by those used previously. Finally, the random nature of the wind waves at the test site complicates the correlation of the prototype test results with monochromatic model test data. The data analyses and results are discussed in more detail in Appendix G.

6.0 Conclusions and Recommendations. The following conclusions and recommendations are based on test results reported herein and on field experience gained during the test and concurrent construction of two Corps floating breakwater projects in Puget Sound.

a. Wind generated wave heights measured at the test site compared favorably with the predicted values (table 1).

b. Measured values of wave transmission for both the concrete and the pipe-tire breakwater were similar to the predicted values (tables 2 and 3). Both breakwaters provide satisfactory protection (transmitted wave of 1 ft or less) for waves up to 3 ft high.

c. For the concrete breakwater, measured values of anchor forces were about 50 percent of the predicted loads if the long-period sway component of the predicted value is ignored (table 2). The prototype test anchor force

records do not show the long-period component that was present in previous anchor line force measurements. The lack of this long-period force may be due to the relatively high initial tension and rapidly increasing anchor stiffness that was characteristic of the prototype test anchor system.

d. For the pipe-tire breakwater, the measured values of anchor forces were similar to the predicted loads for incident wave heights less than 2 ft. Comparisons of existing model test anchor forces and the prototype data set are difficult because of differences between the model test anchor system and the prototype anchor system.

e. Measurements from the strain gages embedded in the concrete breakwater indicated that bending moments were less than 50 percent of the predicted values (table 2). The highest strain was measured during the launching process. Loads encountered during launching and towing may govern structural requirements.

f. Most of the urethane foam flotation in the crowns of the tires of the pipe-tire breakwater remained securely intact and in place throughout the test. The durability of the foam was enhanced by the physical protection provided by the very stiff sidewalls of the truck tires. If more flexible automobile tires were used, the foam probably would be more vulnerable to damage. In one year, the average foam weight increased 250 percent because of the absorption of water. This absorption, combined with underfilling of tires during the original construction, could have led eventually to buoyancy problems. The long-term water absorption rate of foam flotation remains a concern and should be taken into account when flotation requirements are being calculated. The pipe-tire breakwater original design flotation requirement of 75-lb positive buoyancy for tires, other than those on the beamwise pipes, probably is not overly conservative for long-term use.

g. The keeper pipes on the pipe-tire breakwater should be redesigned. If a single 4-in.-diam by 40-in.-long keeper pipe were welded in place, the expensive 4-way cross coupler and 2-in. ID pipes which were vulnerable to corrosion and loosening could be eliminated. Also, designers should consider the potential for corrosion of all small metal parts such as cotter keys.

h. Although a number of the bolted connections had one or two broken bolts, none of the connections failed. Binding the tires of the pipe-tire breakwater with loops of conveyor belting and fastening the loops together with nylon bolts appeared to produce a strong durable structure, providing the bolt ends are melted and flattened to prevent the nuts from backing off.

i. The 16-in.-diam pipe for the pipe-tire breakwater should be used in standard lengths to avoid welding. If welding is required, all welds should be carefully inspected.

j. Construction cost of the prototype 150-ft-long concrete breakwater was approximately $2,600 per linear foot (1981). In 1983, construction of a 1,600-ft-long breakwater of similar design (anchored in a similar depth) cost $1,200 per linear foot indicating a considerable cost reduction.

k. Construction cost of the prototype test 100- by 45-ft pipe-tire breakwater was $1,600 per linear foot (1981) including anchors. Uncertainties in availability of used truck tires and in construction methods resulted in this relatively high cost.

REFERENCES

1. Adee, B. H., Richey, E. P., and Christensen, D. R., "Floating Breakwater Field Assessment Program for Friday Harbor, Washington," Final Report. Ocean Engineering Research Laboratory, University of Washington, Seattle, Washington, 1976.

2. Carver, R. D., "Floating Breakwater Wave Attenuation Tests for the East Bay Marina, Olympia Harbor, Washington," Hydraulic Model Investigation. U. S. Army Engineer Waterways Experiment Station, Technical Report HL-79-13, Vicksburg, Mississippi, 1979.

3. Davidson, D. D., "Wave Transmission and Mooring Force Tests of Floating Breakwaters at Oak Harbor, Washington," Hydraulic Model Investigation. U. S. Army Engineer Waterways Experiment Station, Technical Report H-71-3, Vicksburg, Mississippi, 1971.

4. Hales, L. Z., "Floating Breakwaters: State-of-the-Art Literature Review," CERC Technical Report No. 81-1, U. S. Army Engineer Waterways Experiment Station, Vicksburg, Mississippi, 1981.

5. Harms, V. W., Westerink, J. J., Sorensen, R. M., and McTamany, J. E., "Wave Transmission and Mooring-Force Characteristics of Pipe-Tire Floating Breakwaters," CERC Technical Paper No. 82-4, U. S. Army Engineer Waterways Experiment Station, Vicksburg, Mississippi, 1982.

6. Richey, E. P., "Floating Breakwater Field Experience, West Coast," CERC Miscellaneous Report No. 82-5, U. S. Army Engineer Waterways Experiment Station, Vicksburg, Mississippi, 1982.

7. Baird, A. V., and Ross, N. W., "Field Experiences with Floating Breakwaters in the Eastern United States," CERC Miscellaneous Report No. 82-4, U. S. Army Engineer Waterways Experiment Station, Vicksburg, Mississippi, 1982.

TABLE 1

COMPARISON OF PREDICTED AND MEASURED WAVES

Wind Speed 1/ (mph)	Significant Wave Height, H_s (ft)		Wave Period, T (sec)	
	Predicted	Measured	Predicted	Measured
15	1.3	1.5	2.5	2.8
15	1.3	1.8	2.5	3.0
16	1.4	2.1	2.6	3.3
* 2/	--	4.0	--	4.3

1/ Measurements of unlimited duration.
2/ No wind speed measurements obtained due to equipment malfunction.

TABLE 2

COMPARISON OF FIELD MEASUREMENT WITH PREDICTED VALUE FOR CONCRETE BREAKWATER

Significant Wave Height H_s (ft)	Wave Attenuation Coefficient, C_t		Peak Anchor Force (lb/ft)		Moment (ft-kips)	
	Predicted	Measured	Predicted 1/	Measured 2/	Predicted 3/	Measured
1.5	0.4	0.4	105	50	125	47
1.8	0.4	0.5	130	70	178	97
2.1	0.4	0.5	145	75	256	79
4.0	0.8	0.7	500	97	745	*4/

1/ Calculated using Miche-Rundgren method, neglecting sway load with wave load acting on a portion of the structure equal to the wave length, L , = $5.12T^2$; i.e., spatial correlation factor (SCF) = 1 ; also assumes 50 percent loss due to viscous effects. (Neither the predicted nor the measured anchor forces include either the anchor line pretension or long period loads such as current drag.)

2/ Peak load calculated statistically assuming wave loads follow Rayleigh distribution; F peak defined as equal to the average of the 1 percent highest loads; F peak = F1% = 1.67 F significant .

3/ Heave moments calculated using FLOATX.

4/ No strain data available for H_s = 4.0 ft .

TABLE 3

COMPARISON OF FIELD MEASUREMENT WITH PREDICTED VALUE FOR PIPE-TIRE BREAKWATER 1/

Significant Wave Height H_s (ft)	Wave Attenuation Coefficient C_t		Peak Anchor Force (lb/ft)	
	Predicted	Measured	Predicted 2/	Measured 3/
1.5	0.2	0.5	60	77
1.8	0.2	0.4	75	63
2.1	0.4	0.7	100	75
3.2	0.5	* 4/	250	134

1/ Neither the predicted nor the measured anchor forces include long period loads such as current drag. Anchor line pretension was negligible for the pipe-tire breakwater.

2/ From reference 5, figure 46.

3/ Peak load calculated statistically assuming wave loads follow Rayleigh distribution; F peak defined as equal to the average of the 1 percent highest loads; F peak = f1% = 1.67 F significant .

4/ No transmitted wave height data available for H_s = 3.2 ft .

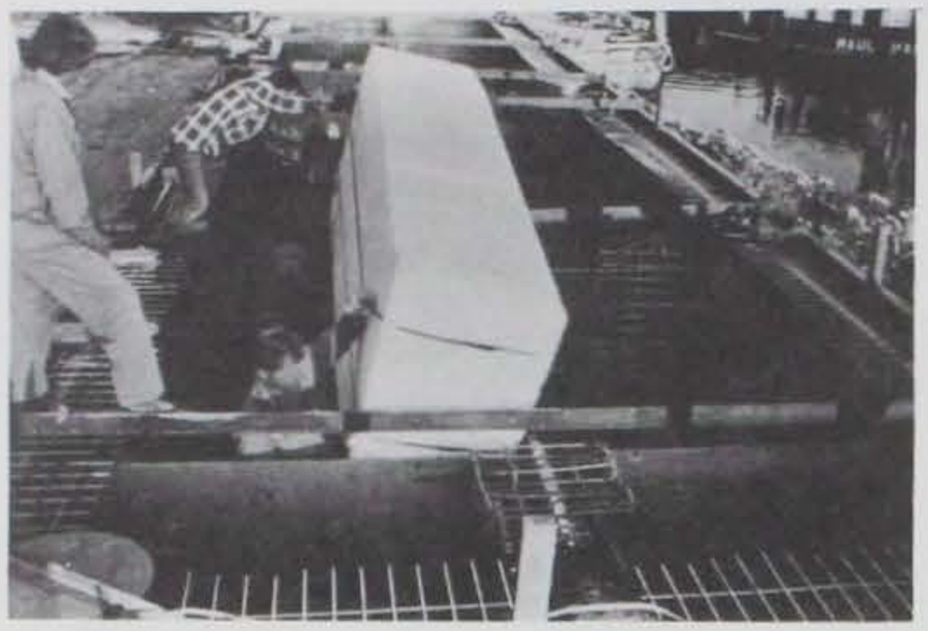

Photo 1. Starting concrete breakwater placement; internal foam blocks being positioned.

Photo 2. Placing concrete in sides and internal walls.

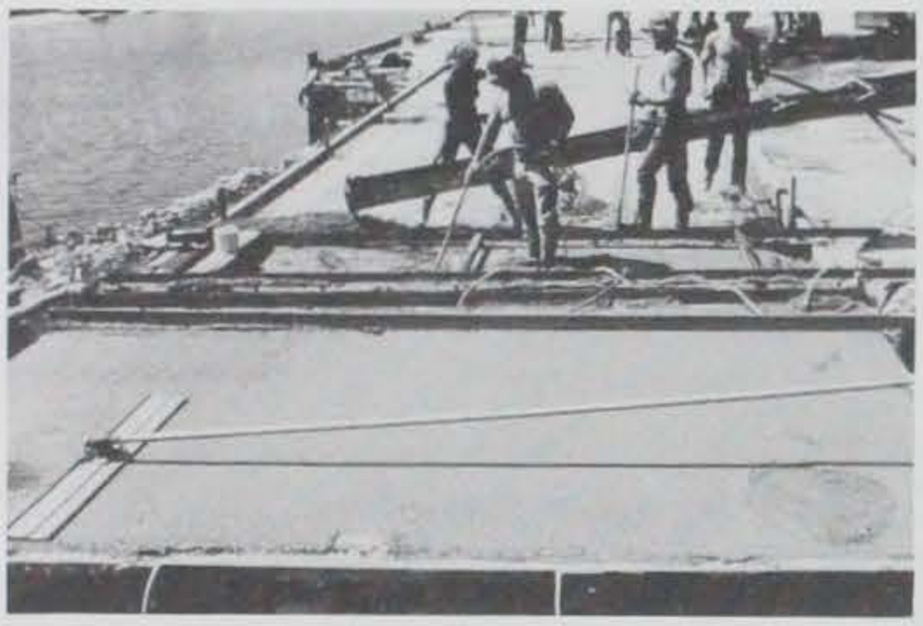

Photo 3. Placing and leveling deck.

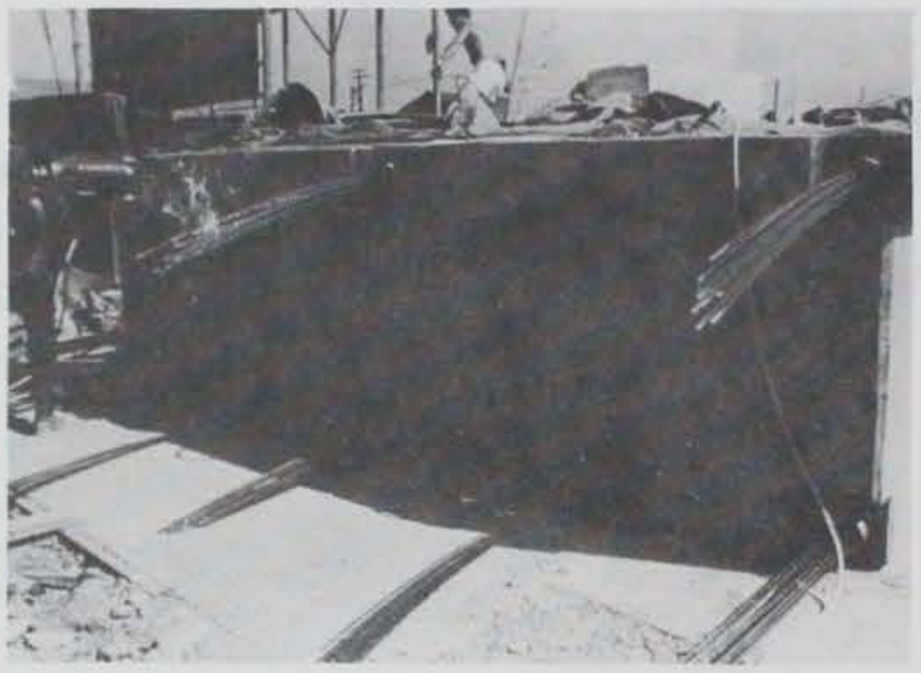

Photo 4. Posttensioning of concrete units.

Photo 5. Launching of concrete breakwater.

Photo 6. Joining units with flexible connectors.

Photo 7. Assembling pipe-tire breakwater (Four modules are complete).

Photo 8. Assembling a module.

Photo 9. Tensioning of belting using a modified car jack.

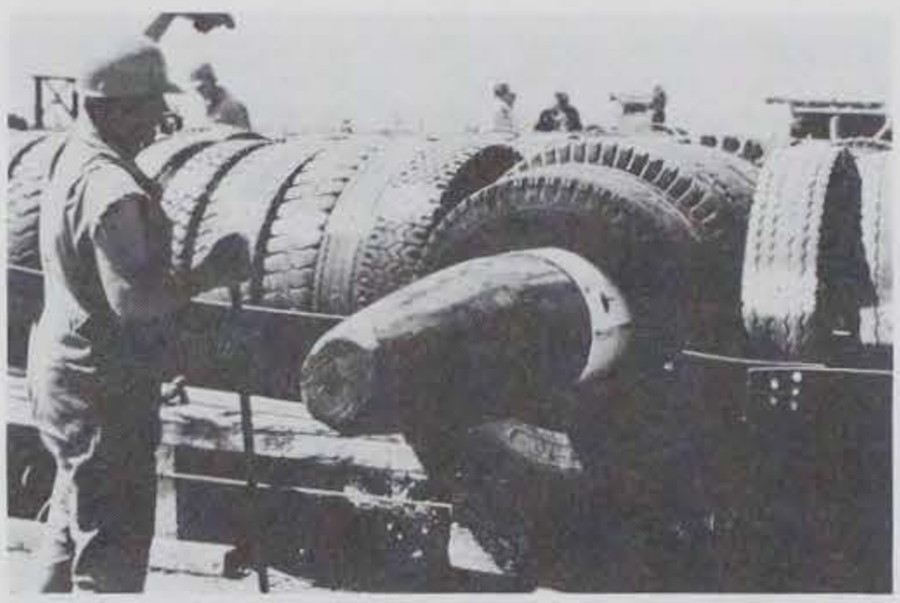

Photo 10. Shoving steel pipe through tires (tires around pipes not foamed).

Photo 11. Keeper pipes being secured (welding of keepers required to prevent loosening).

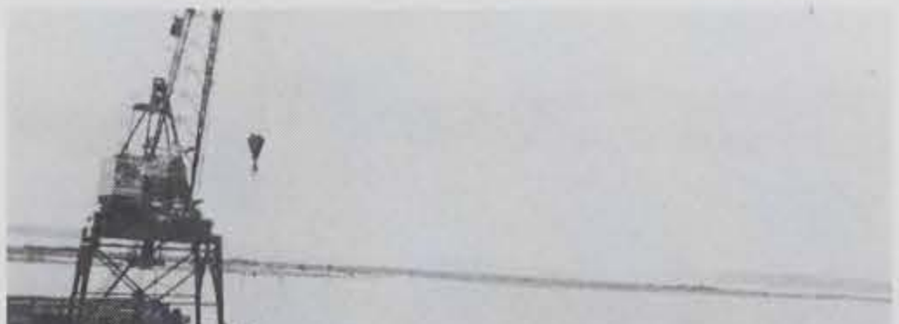

Photo 12. Launching of pipe-tire breakwater.

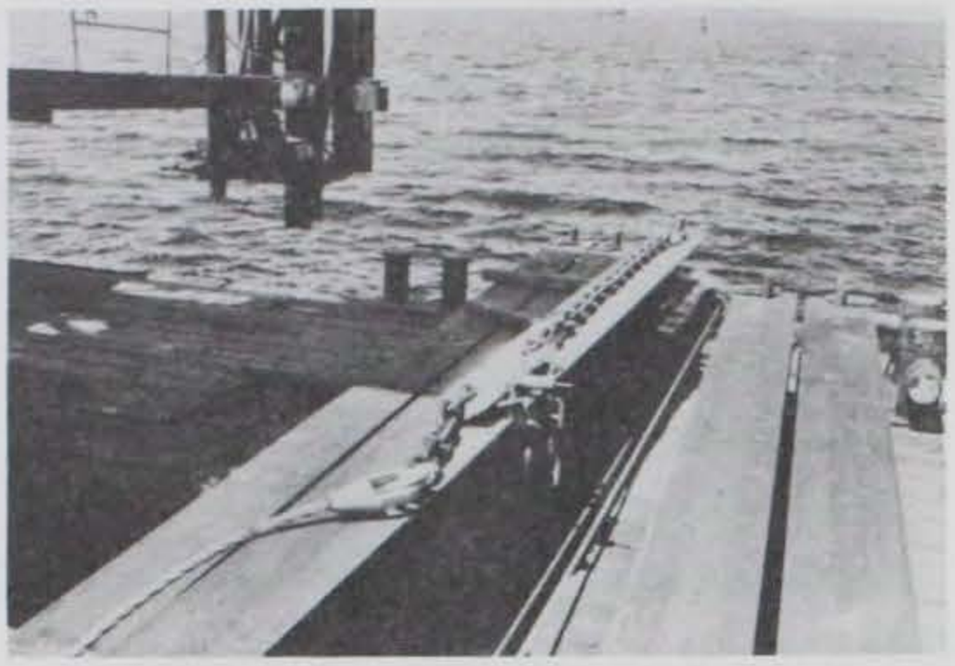

Photo 13. Photo showing H-pile with chain and steel rope attached (anchor force cell in chain).

Photo 14. Anchor piles being driven at test site.

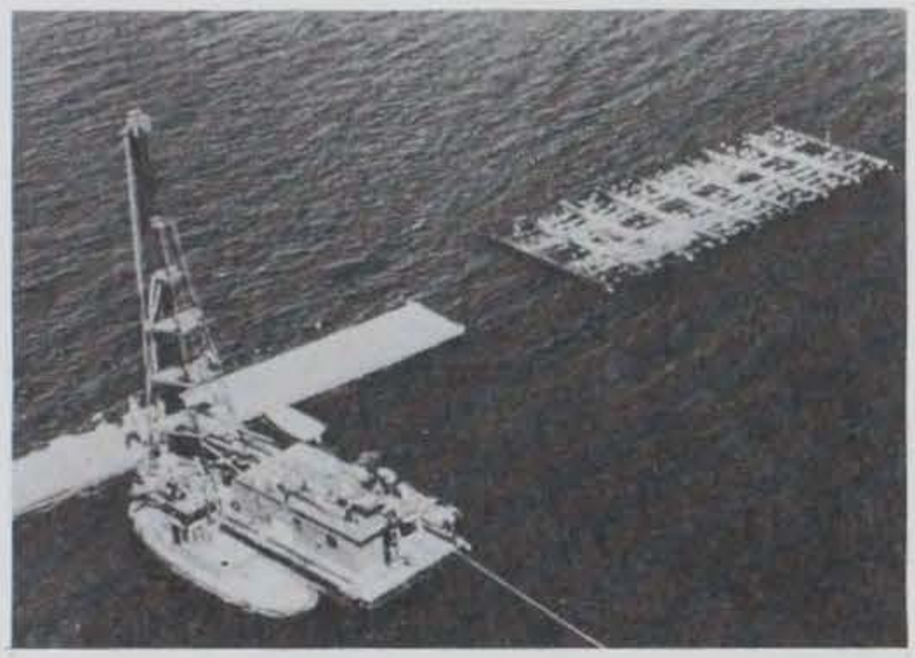

Photo 15. Final anchoring of breakwaters at test site.

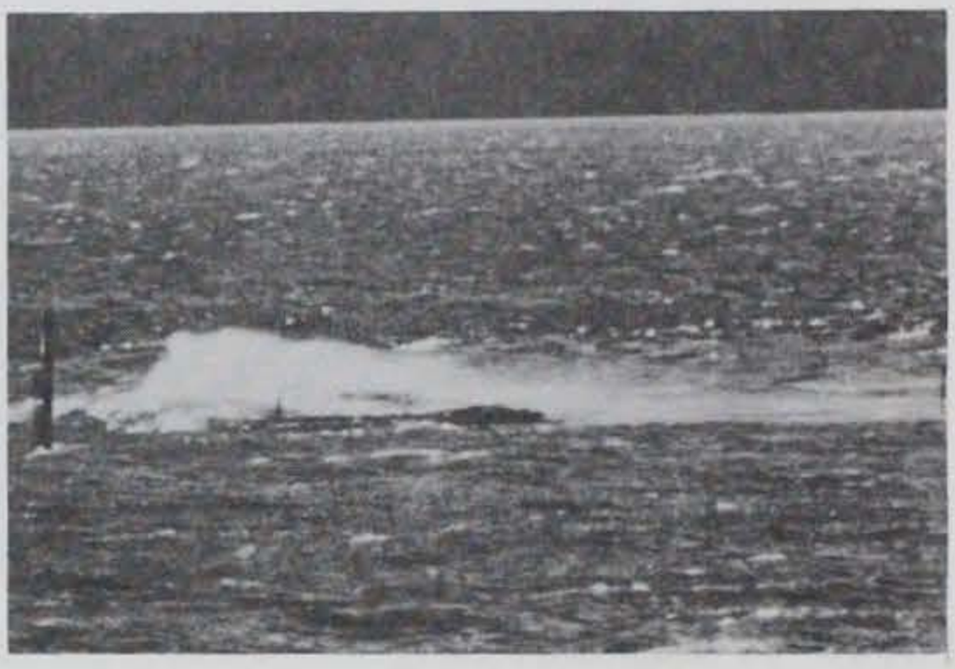

Photo 16. Waves reflecting from the concrete breakwater sending spray 20 ft into the air.

Photo 17. Example of both breakwaters providing good protection from storm waves.

Photo 18. Waves reflecting from windward side of concrete float.

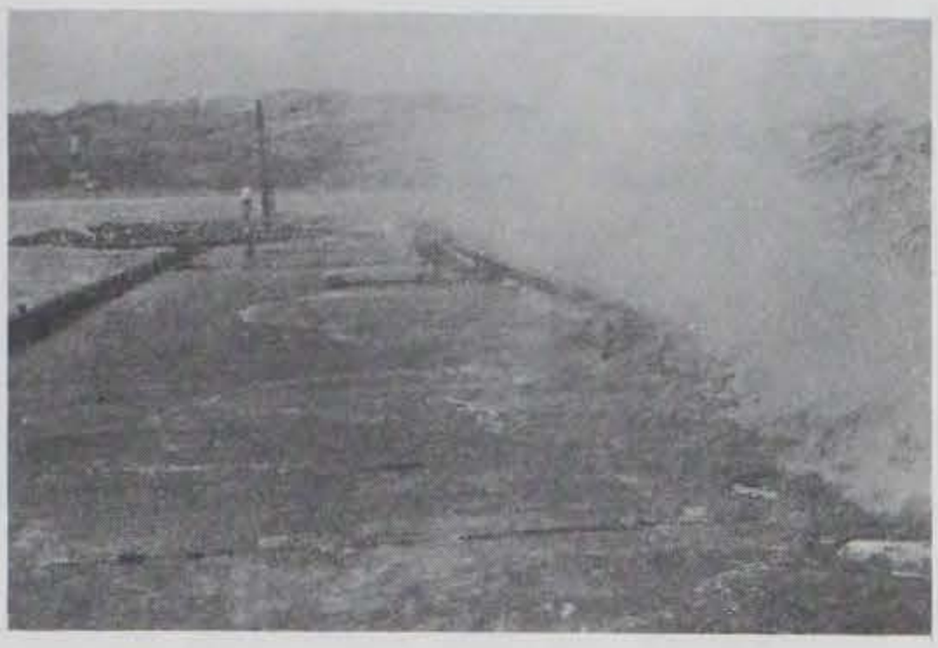

Photo 19. 1.5-ft waves overtopping the concrete breakwaters.

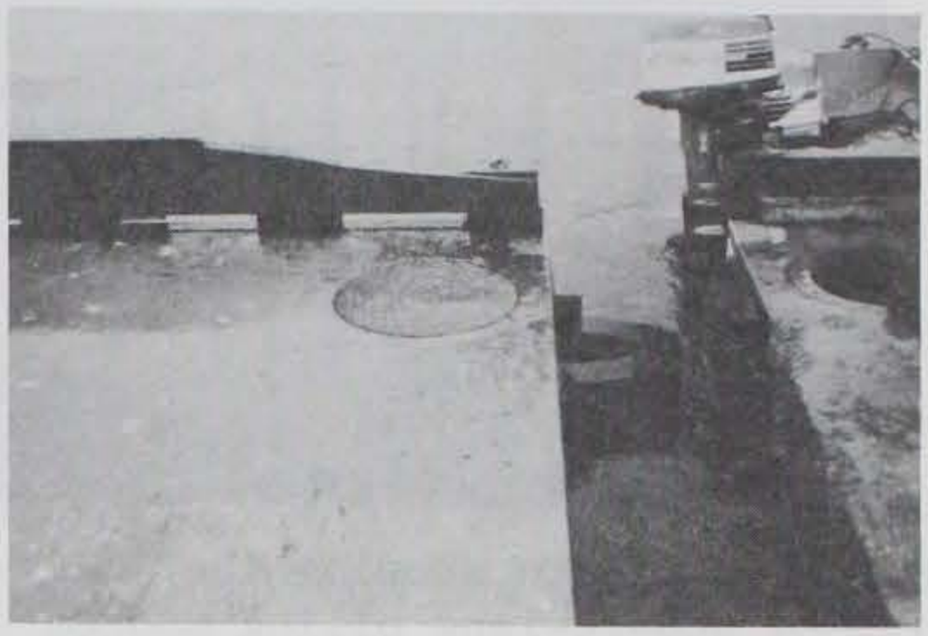

Photo 20. Concrete units in disconnected and fendered configuration.

Photo 21. 41-ft Coast Guard cutter passing the breakwaters during a boat wake test.

Photo 22. 4,000 hp tugboat pulling on concrete breakwater to determine anchor line stiffness.

Photo 23. Pipe-tire breakwater after having weathered numerous storms.

Photo 24. A broken longitudinal pipe pulling out of the tires.

Photo 25. Photo showing the 16-ft-wide by 600-ft-long piling moored breakwater at East Bay, Washington.

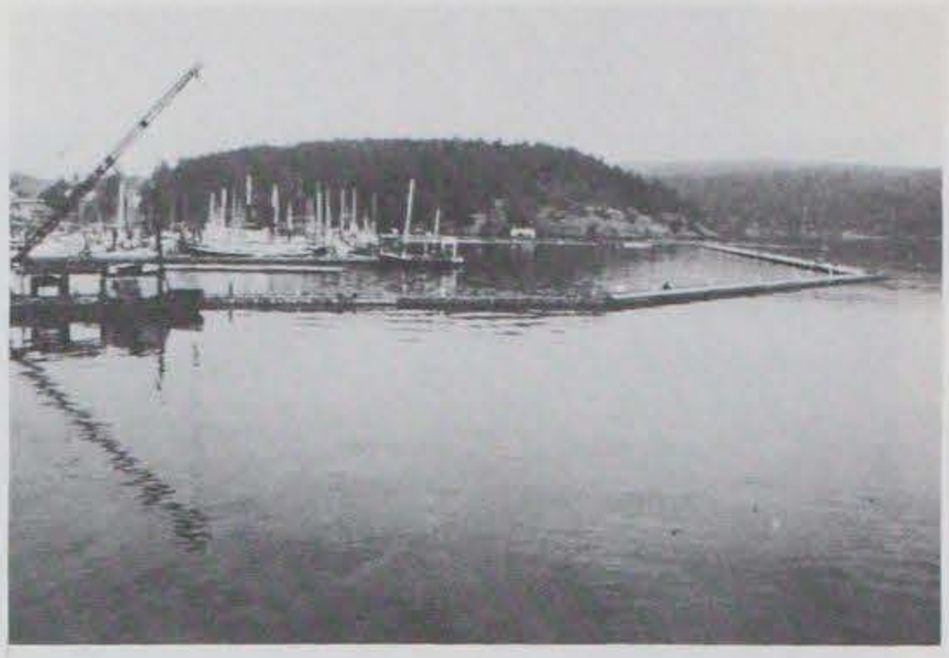

Photo 26. Test units after being connected to the floating breakwater at Friday Harbor, Washington.

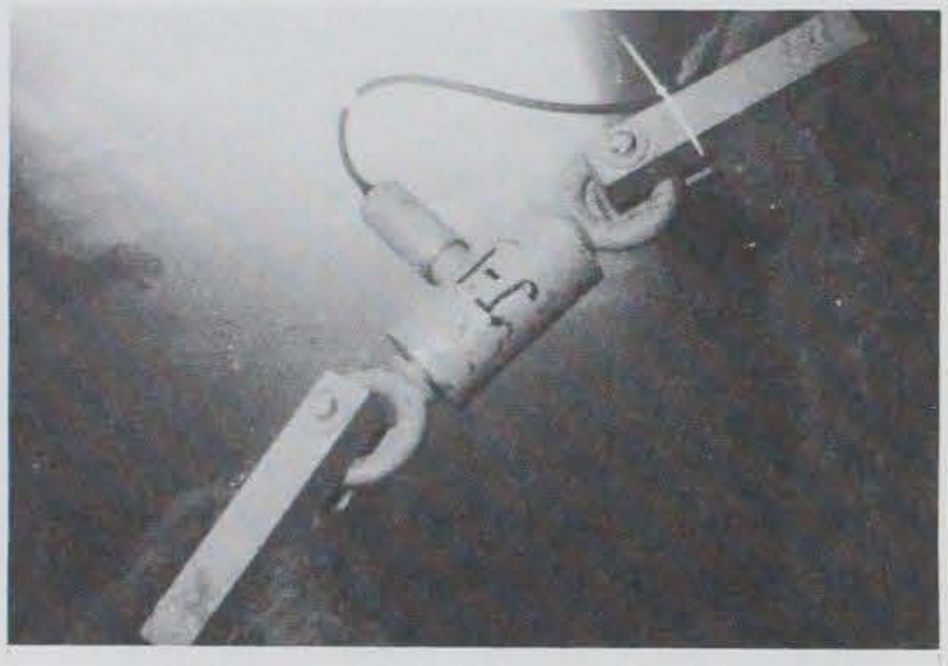

Photo 27. Underwater photo depicting upper load cell in anchor line.

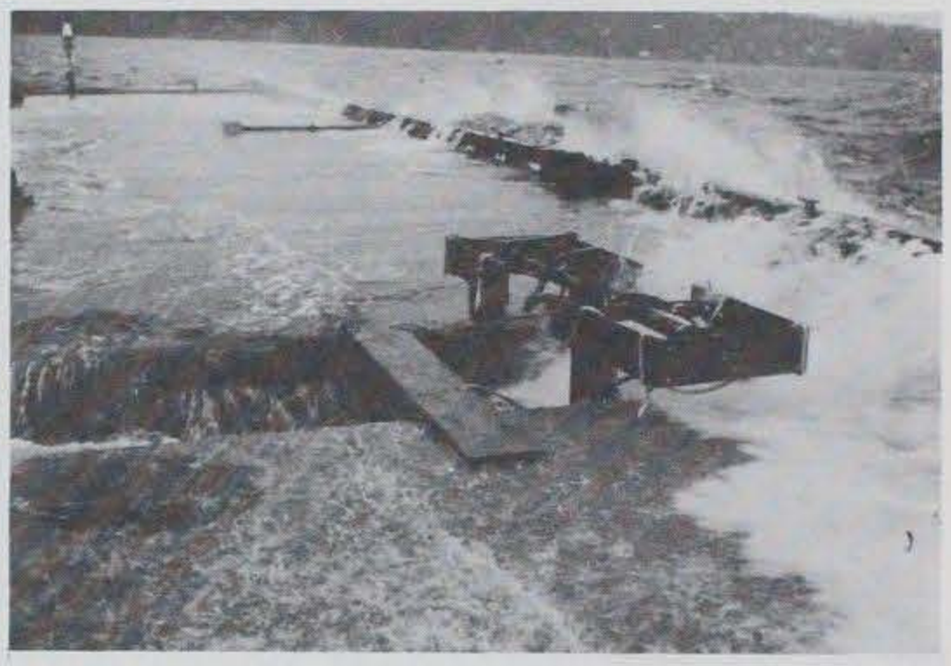

Photo 28. Relative motion sensor being used during test of flexible connector.

Photo 29. Photo showing the deckhouse that protected equipment from the elements (wave buoy in foreground).

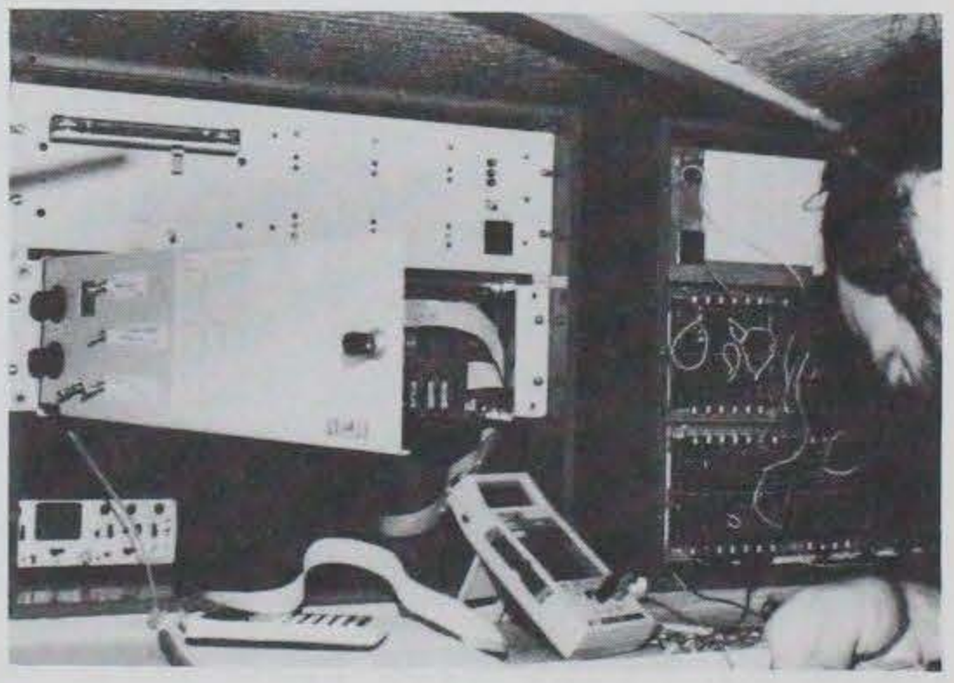

Photo 30. Photo showing two hermetically sealed cases that housed the on-board computer.

APPENDIX A

CONCRETE BREAKWATER: DESIGN, CONSTRUCTION, OPERATION, AND MAINTENANCE

1.0 Design.

1.01 Wave Analysis. Prior to the designing of the prototype test structures, wave heights at the West Point test site were estimated using methods outlined in the Shore Protection Manual (SPM) (reference A-1). The test site location, effective fetch lengths, hydrographic data, and wind data are shown in figures A-1 through A-6. Wave estimates are listed in table A-1. The design wave with a height, H_S, of 6 ft and a period of 5 sec, was estimated to be equal to the significant wave calculated for the maximum storm condition on record (24 years). During the 18-month test period, storm conditions, with winds over 20 mph, occurred on more than 40 days. A maximum wind speed of 70 mph and a maximum wave height of 4 ft (4-sec period) were recorded. On one occasion, the wind speed continuously exceeded 35 mph for 24 hr.

1.02 Tides. Tides at West Point are typical of the Pacific coast of North America. Tides are of the mixed type, with two unequal highs and lows each day. The diurnal tide range at the site was 11.3 ft, and the extreme range was 19.4 ft. Tidal datums for the West Point vicinity, as published by the National Ocean Service, are shown in figure A-3.

1.03 Tidal Currents. In the vicinity of West Point, tidal currents flow in a southwesterly direction on the floodtide and in a northwesterly direction on the ebb, with flood and ebb surface velocities about equal. Maximum current speed predicted by the National Oceanic and Atmospheric Administration (NOAA) is 1.3 knots (2.2 fps), with average daily maximum speeds of 0.7 knots (1.2 fps). A site-specific field study was performed by U. S. Army Engineer District, Seattle, on 20 April 1981. During this study, current speeds of approximately 1.5 fps were measured during both ebbtide and floodtide. NOAA-predicted currents for the time of the study, in the general vicinity of West Point, were 0.9 fps on both the floodtide and ebbtide. Based on this information, the maximum tidal current speed at the test site was estimated to be 3.7 fps, and the average daily maximum speed was estimated to be 2 fps.

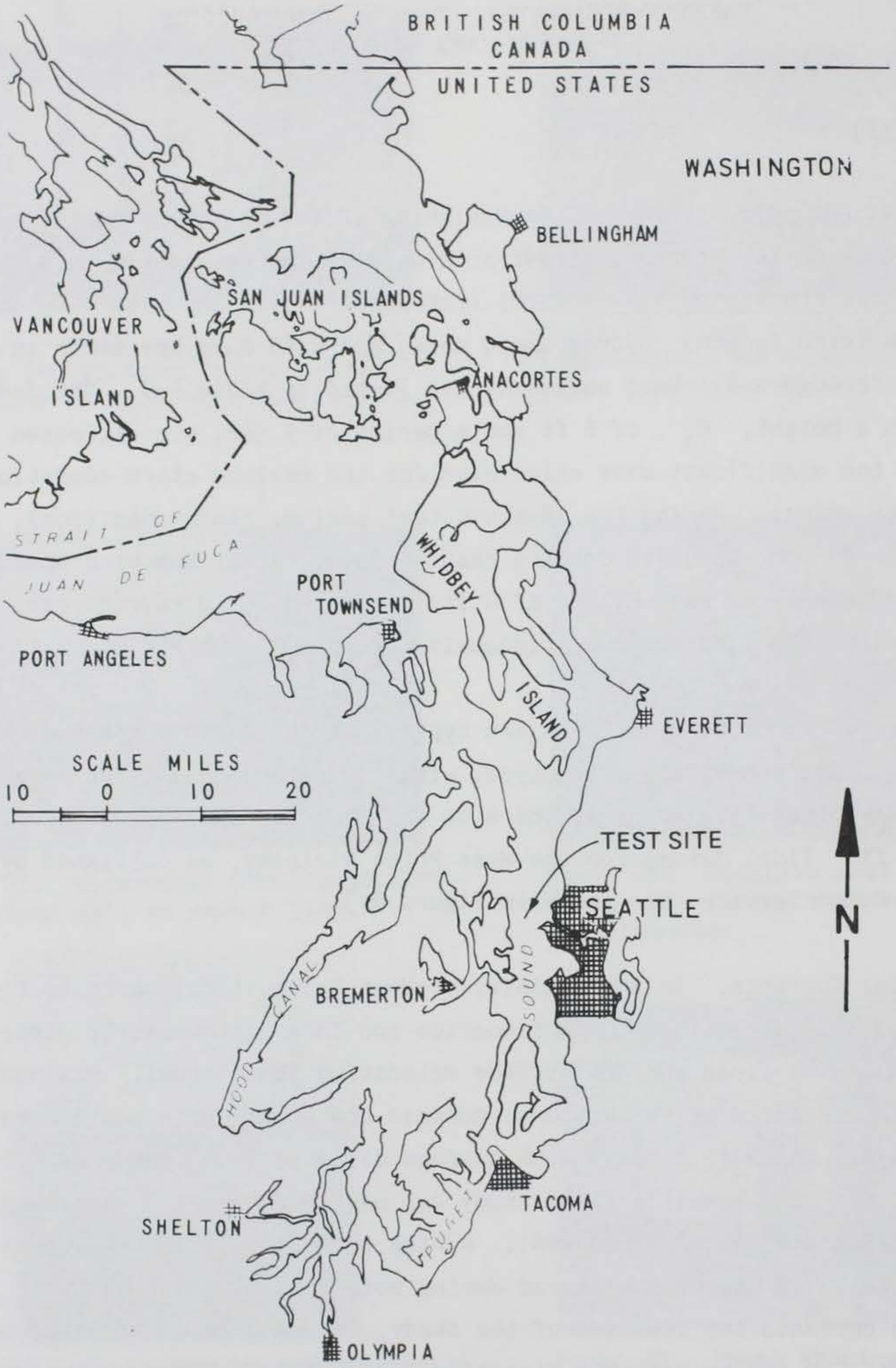

FIGURE A-1. Test Site Location

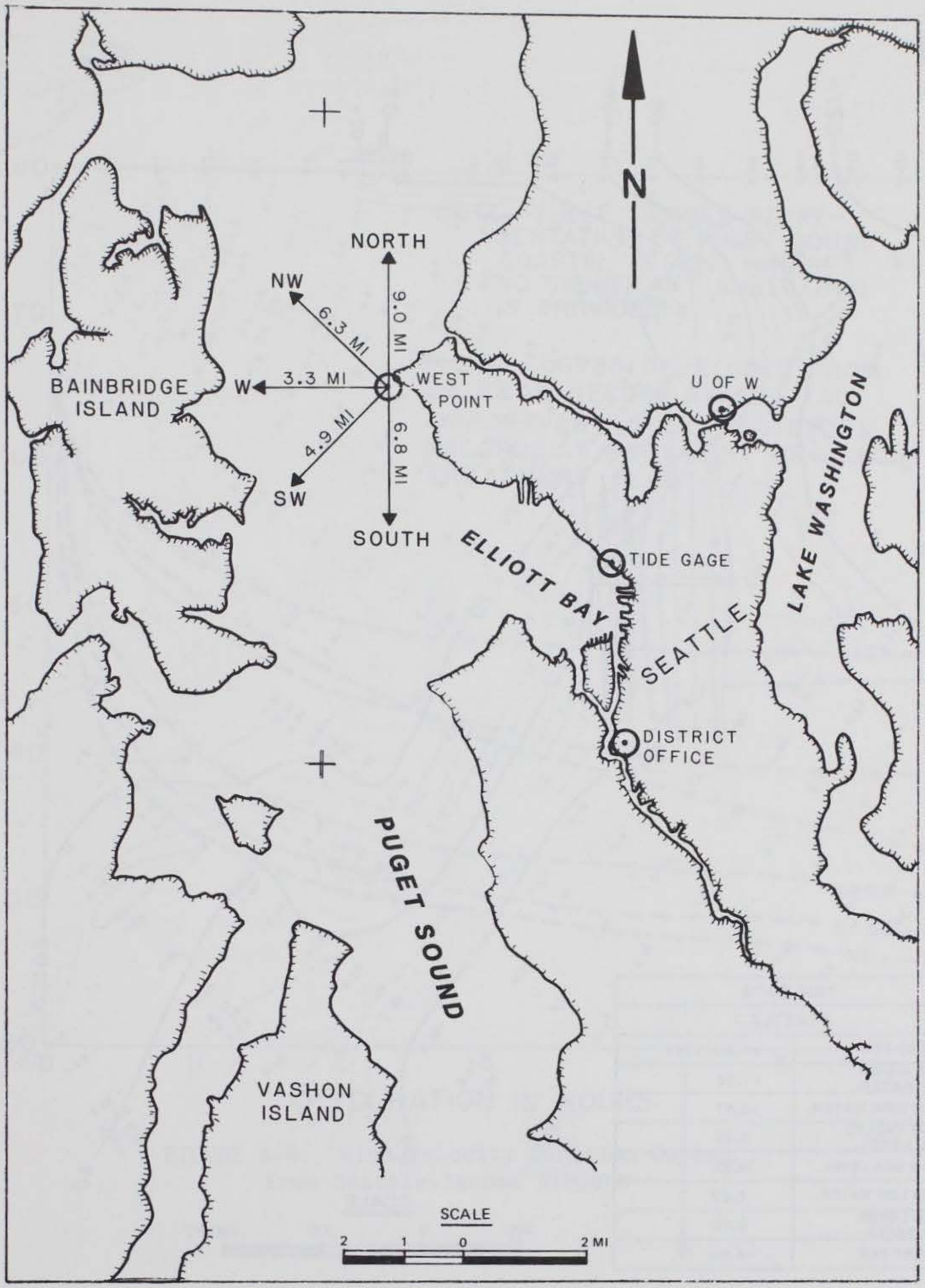

FIGURE A-2. Effective Fetch Lengths

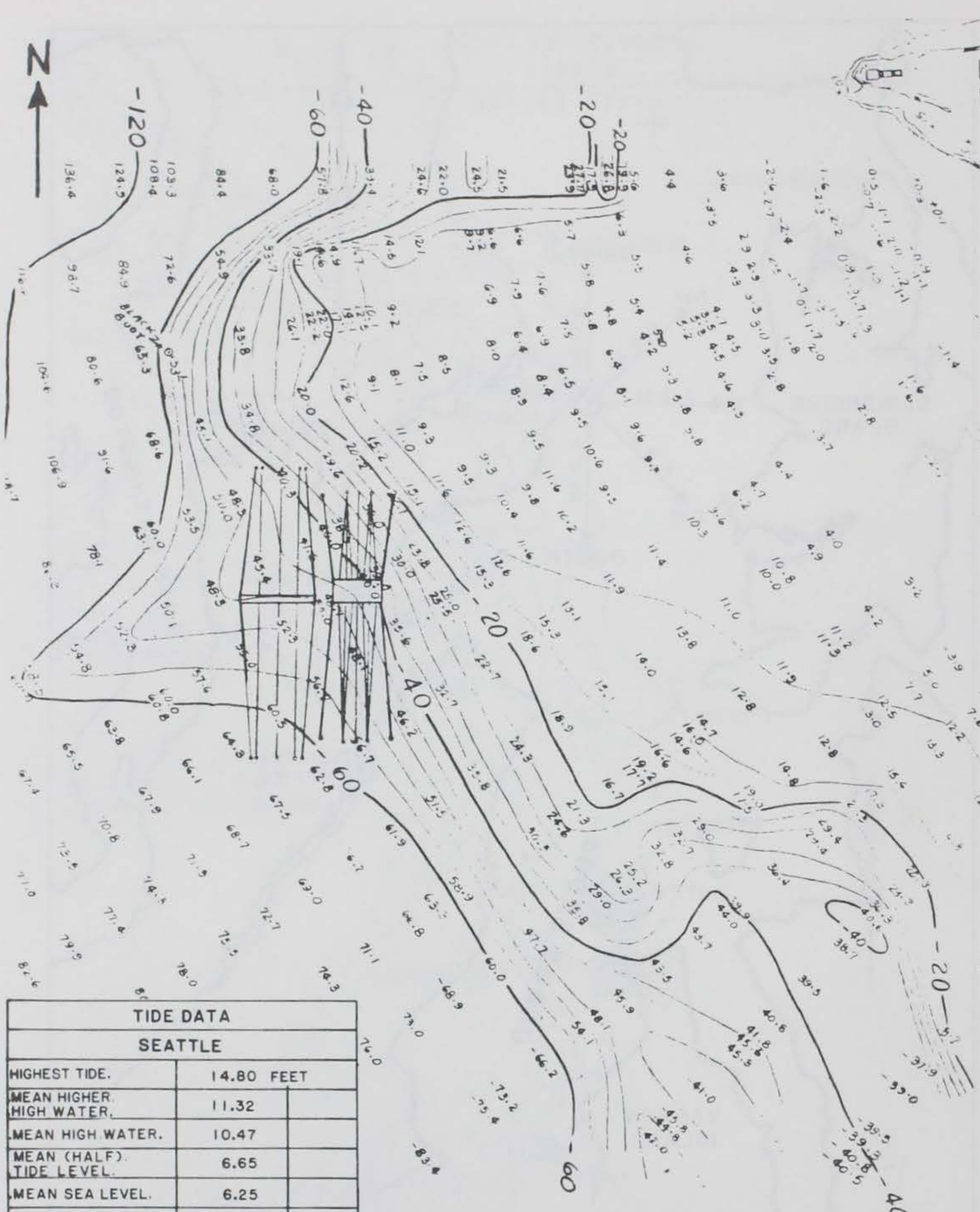

TIDE DATA		
SEATTLE		
HIGHEST TIDE.	14.80 FEET	
MEAN HIGHER HIGH WATER.	11.32	
MEAN HIGH WATER.	10.47	
MEAN (HALF) TIDE LEVEL.	6.65	
MEAN SEA LEVEL.	6.25	
MEAN LOW WATER.	2.82	
MEAN LOWER LOW WATER.	0.00	
LOWEST TIDE.	-4.60	

FIGURE A-3. Hydrographic Survey Map

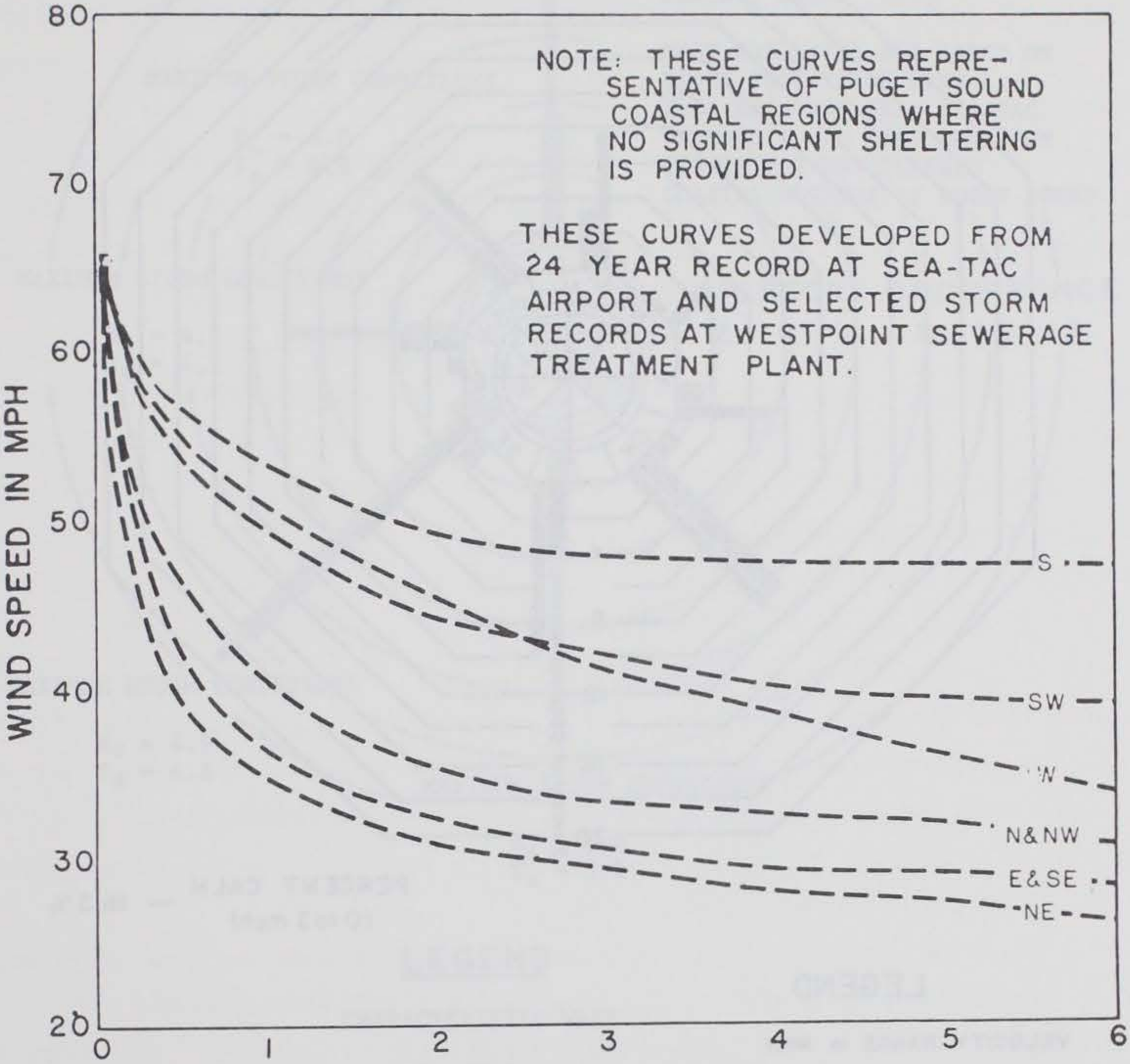

FIGURE A-4. Wind Velocity Duration Curves from Seattle-Tacoma Airport

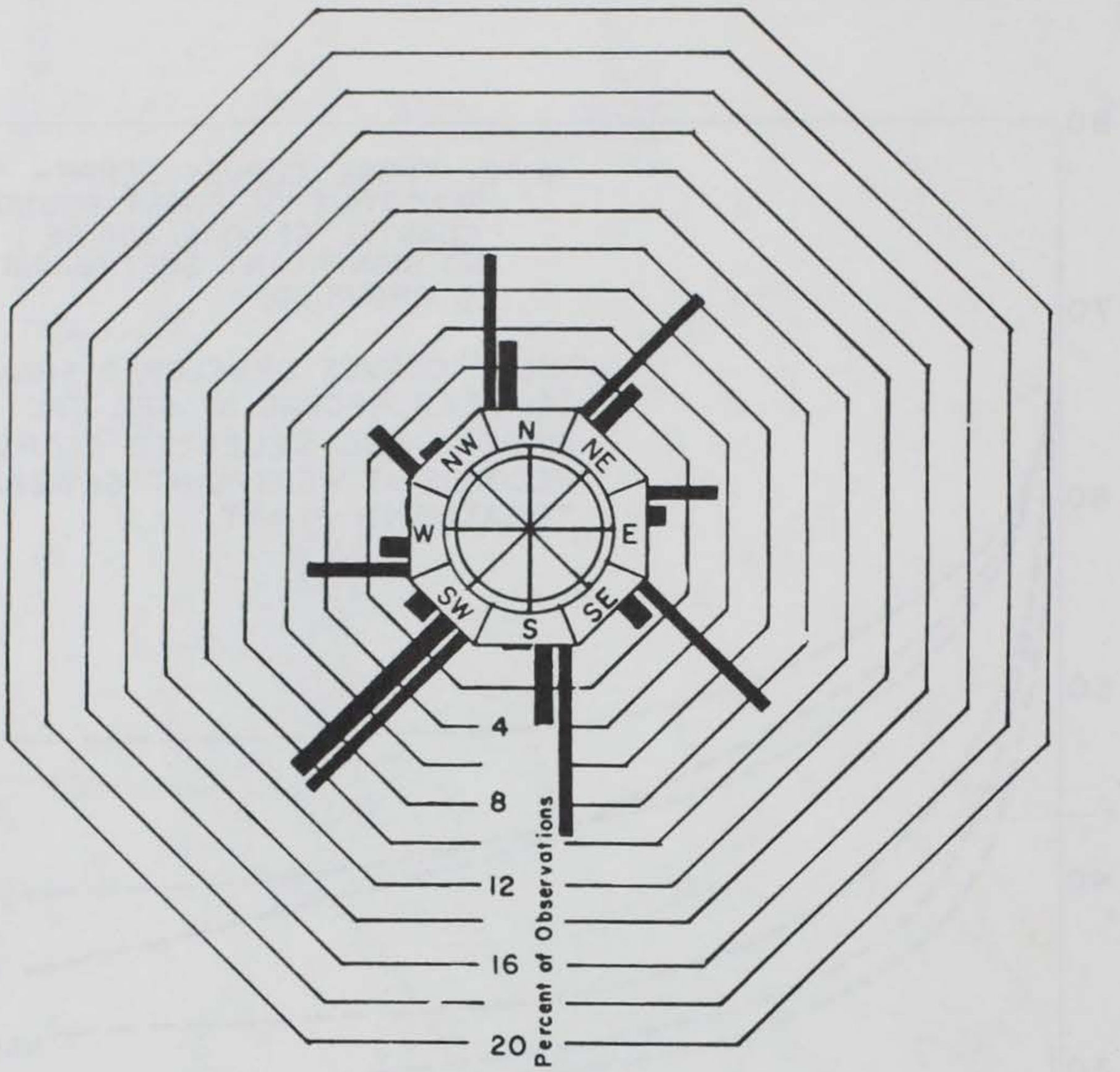

PERCENT CALM — 16.3%
(0 to 3 mph)

LEGEND

VELOCITY RANGE in MPH

OVER 3 TO 12
OVER 12 TO 24
OVER 24

FIGURE A-5. Wind Rose from Seattle-Tacoma Airport (1948-1969)

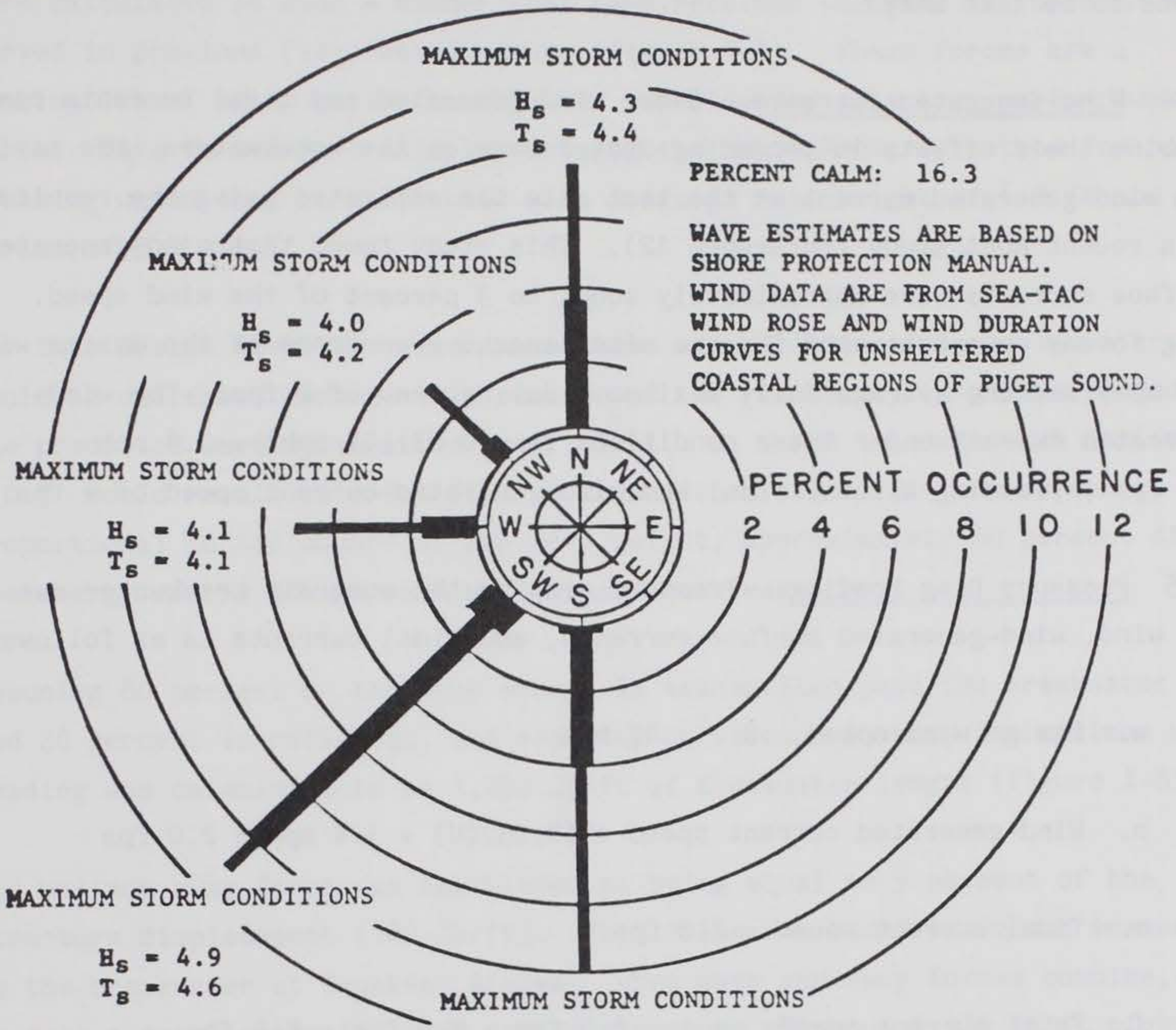

LEGEND

CHARACTERISTIC WAVE

H_s (FT)
T_s (SEC)

UP TO H_s = 1.0, T_s = 2.0

H_s = 1.0, T_s = 2.0 TO H_s = 2.5, T_s = 3.5

OVER H_s = 2.5, T_s = 3.5

FIGURE A-6. Wave Rose for West Point, Washington

During the field test, current speeds were measured using a drogue and were found to be 1 to 2 fps.

1.04 Wind-Generated Currents. Since wind-generated and tidal currents can combine their effects in producing drag forces on the breakwaters, the maximum wind-generated current at the test site was estimated using the results of a recent NOAA study (reference A2). This study found that wind-generated surface currents were approximately equal to 3 percent of the wind speed. Drag forces were estimated for the simultaneous occurrence of the design wind (47 mph) and the average daily maximum tidal current of 2 fps. The wind-generated current under these conditions is (0.03)(47 mph) = 1.4 mph = 2 fps , yielding a total tidal and wind-generated current speed of 4 fps.

1.05 Pressure Drag Loading. Pressure drag on the concrete breakwater due to the wind, wind-generated surface currents, and tidal currents is as follows:

a. Design wind speed, U , = 47 mph

b. Wind-generated current speed = (0.03)(U) = 1.4 mph = 2.0 fps

c. Tidal current speed = 2.0 fps

d. Total current speed, u , = 2.0 fps + 2.0 fps = 4.0 fps

e. Wind pressure drag = negligible

f. Pressure drag coefficient, C_D , = 2.0 (reference A-3)

g. Breakwater draft = 3.5 ft

h. Density of seawater, ρ , = 2 slugs/ft^3

i. Hydraulic pressure drag = $C_D \frac{\rho u^2}{2}$ (Draft) (reference A-3)

= 112 lb/ft of breakwater length

1.06 Estimated Wave and Anchor Loads. Loads on the concrete breakwater were calculated in such a manner that they retained the same features observed in previous field measurements (figure A-7). These forces are a combination of short period wave forces superimposed on a long period sway force. Wave forces were calculated using the Miche-Rundgren method for non-breaking waves on a vertical wall with a design wave height of 6.0 ft and a period of 5.0 sec.

For this design wave, the wave attenuation capabilities of the breakwater would be decreased considerably because of the relatively long wave period. The predicted wave attenuation coefficient, C_t , = H transmitted/H incident = 0.9 would result in a 5.4-ft-high transmitted wave. Since wave energy is proportional to the square of the wave height, approximately 80 percent of the energy of the design wave would pass the breakwater.

Assuming 80 percent of the wave energy is transmitted past the breakwater and 20 percent is reflected, and assuming no viscous losses, the maximum wave loading was calculated to be 1,750 lb/ft of breakwater length (figure A-8).

The maximum sway force was calculated as being equal to 5 percent of the structure displacement (180 lb/ft). This value was based on forces measured on the breakwater at Tenakee, Alaska. When wave and sway forces combine, they produce a total estimated load on the structure of about 1,930 lb/ft of breakwater length for a 16-ft-wide structure with a draft of 3.5 ft (figure A-9).

Available information from model tests and from prototype observations (reference A-4) suggested that only a portion of the wave force, calculated by the Miche-Rundgren method, is ultimately transmitted to the anchor lines. For this reason, the load at the breakwater anchor line connection was set equal to 50 percent of the wave induced force plus 100 percent of the sway force. When the adjusted wave force was combined with the sway force, the total estimated load was 1,055 lb/ft of breakwater, or about 40,000 lb on each anchor, assuming an anchor line spacing of 37.5 ft. Tidal and wind-driven currents contributed an additional pressure drag force of 112 lb/ft of breakwater length for a maximum force on each anchor line of 44,000 lb.

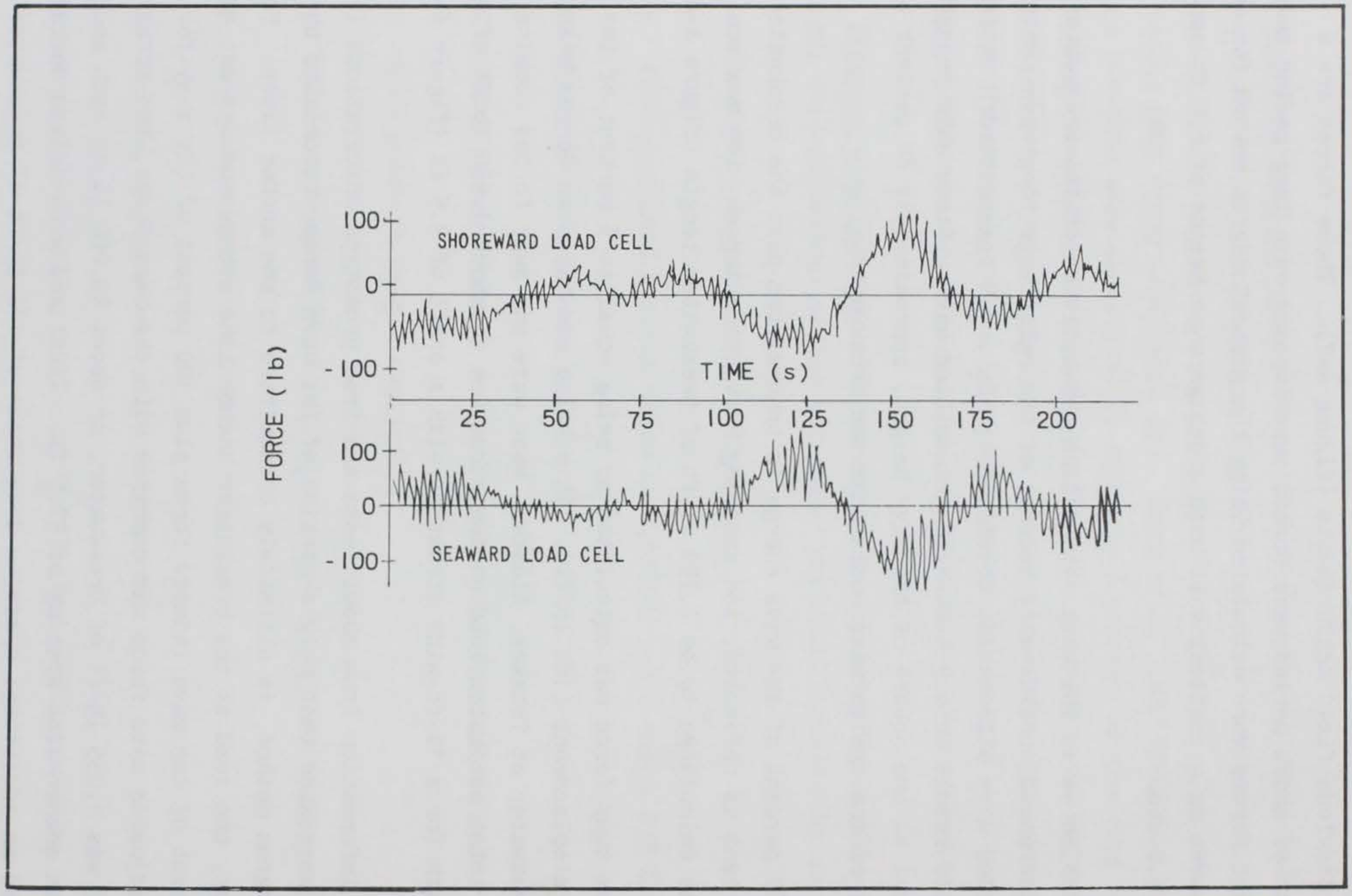

FIGURE A-7. Typical Anchor Force Record from Friday Harbor Floating Breakwater - 1976

WAVE DATA

Height = 6.0 ft

Period = 5.0 sec

Length = 128 ft

Water Depth = 55 ft

BREAKWATER DATA

Width = 16 ft

Freeboard = 1.5 ft

Draft = 3.5 ft

Transmission coefficient = 0.9

ELEVATION, Z (FT)	LANDWARD PRESSURE, P_L (LB/FT^2)	SEAWARD PRESSURE, P_S (LB/FT^2)	LANDWARD FORCE, F_L (LB/FT)	SEAWARD FORCE, F_S (LB/FT)	NET WAVE FORCE, F_{NET} (LB/FT)	SWAY FORCE, F_{SWAY} (LB/FT)
+1.5	210	--	--	--	--	180
0	306	--	--	--	--	--
-3.5	488	78	1,777	31	1,750	--

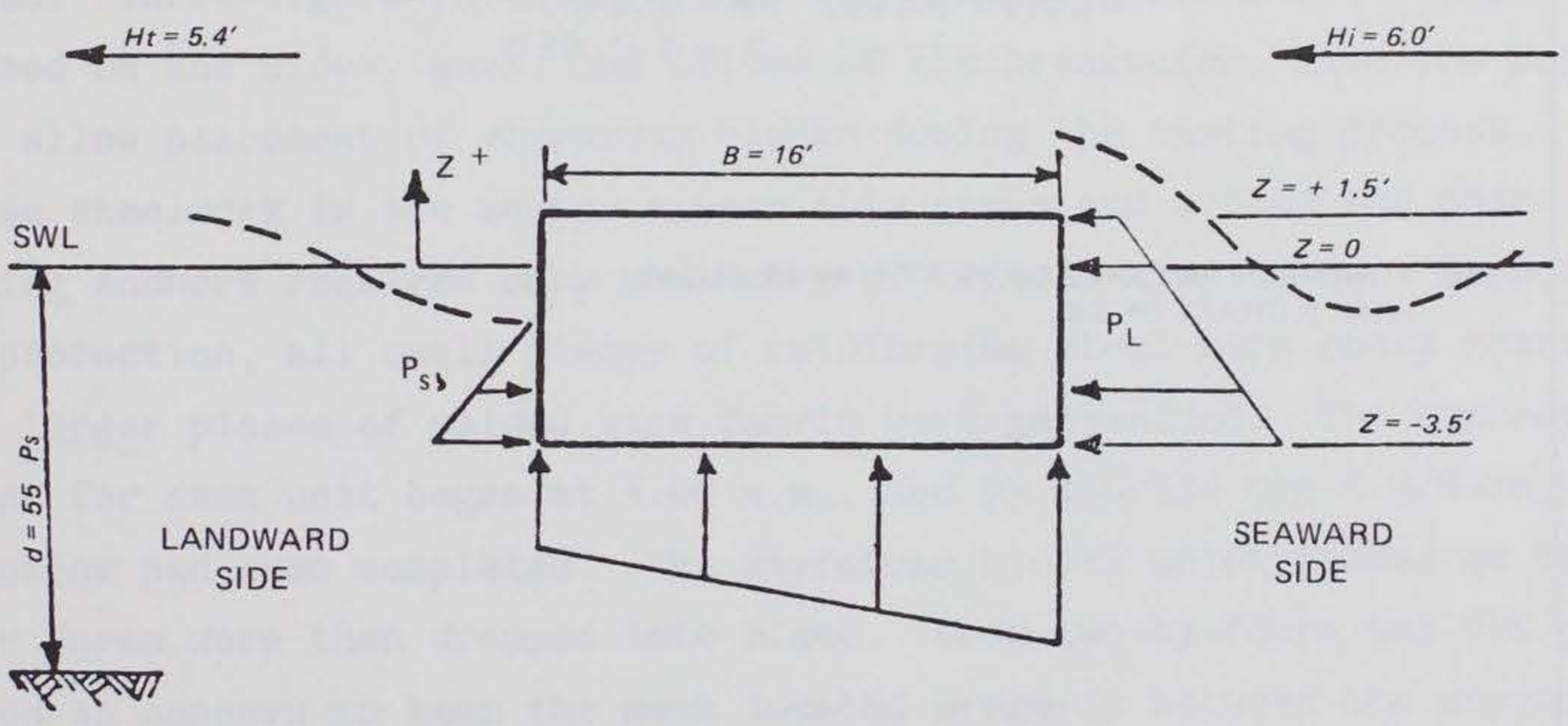

SECTION VIEW

FIGURE A-8. Estimated Wave Pressures and Forces on Concrete Breakwater

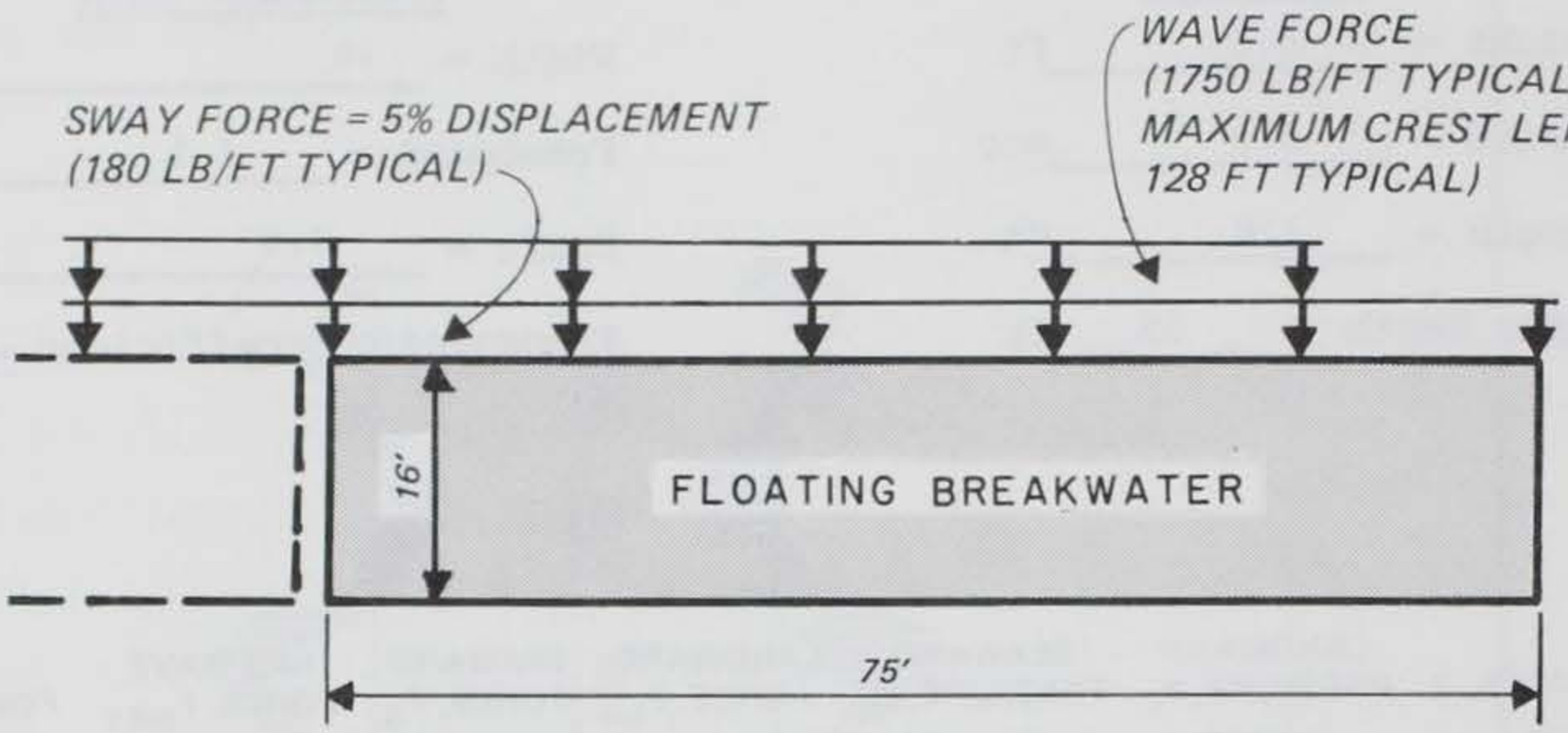

PLAN VIEW, APPLIED WAVE AND SWAY FORCE

ON CONCRETE FLOATING BREAKWATER

NOT TO SCALE

DESIGN WAVE: Hs = 6.0 FT
T = 5.0 SEC

NOTE: FORCES SHOWN ARE FOR 75' BY 5' BY 16' FLOAT WITH A DRAFT OF 3.5'.

FIGURE A-9. Estimated Wave and Sway Force on Concrete Floating Breakwater

1.07 Predicted Wave Attenuation. The basic design of the concrete breakwater was adapted from the structure planned for a Corps of Engineers project at Friday Harbor, Washington, but with modifications to accommodate the more severe wave climate at the West Point test site. The test breakwater consisted of two rectangular units, each unit being 75 ft long and 16 ft wide, with a draft of 3.5 ft and a freeboard of 1.5 ft. The float dimensions were selected to provide a wave transmission coefficient (C_t = Ht/Hi) of 0.4 under design storm conditions for Friday Harbor (H_s = 2.7 ft , T = 2.6 sec). Wave transmission characteristics of the floats were based on 1:10 scale model tests conducted at the U. S. Army Engineer Waterways Experiment Station (WES) (reference 2, main report).

2.0 Construction.

2.01 Construction Sequence. The two 75-ft-long concrete breakwater units were cast in Bellingham, Washington, and towed approximately 90 miles south to the West Point test site. Construction drawings for the concrete breakwater are shown in figures A-10 through A-17. Work on these units began in May 1982 with the erection of the exterior plate steel forms on a special concrete pad. Three-eights-in.-diam welded wire fabric (WWF 12 × 4 - W12 × W12) was placed on the sides, ends, and bottom of the breakwater, with the top left open to allow placement of styrofoam blocks during the casting process. The extensive steelwork in the anchor hawser hole areas and around the post-tensioning anchors required many man-hours of tedious wire tying. For corrosion protection, all small pieces of reinforcing steel were epoxy coated, and the larger pieces of welded wire fabric were galvanized. The concrete placement for each unit began at 5:00 a.m., and by sunrise the 4-3/4-in.-thick bottom had been completed. The styrofoam blocks which served as the interior forms were then dropped into place. Wood two-by-fours and PVC pipe were used as spacers to keep the mesh located properly between the styrofoam blocks and the outer steel plate forms. Steel beams were placed across the deck, and wedges were hammered in between the beams and the foam to keep the foam from floating up as the sides of the float were placed. Some difficulty was encountered in obtaining a satisfactory amount of concrete cover over the steel while keeping wall thickness within tolerances. This problem was particularly pronounced in the transverse bulkheads. Placing of the sides of

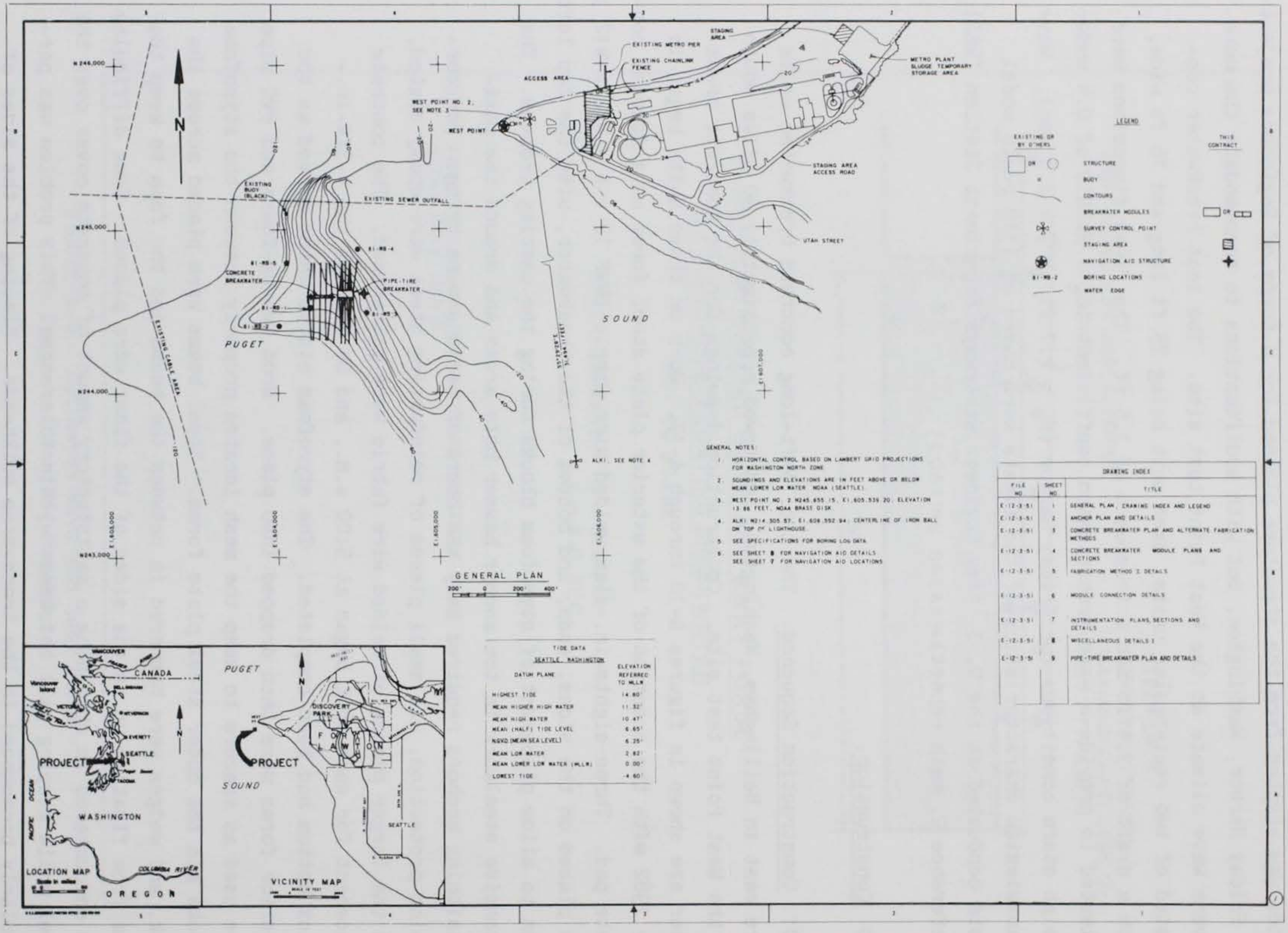

FIGURE A-10. General Plan, Drawing Index and Legend

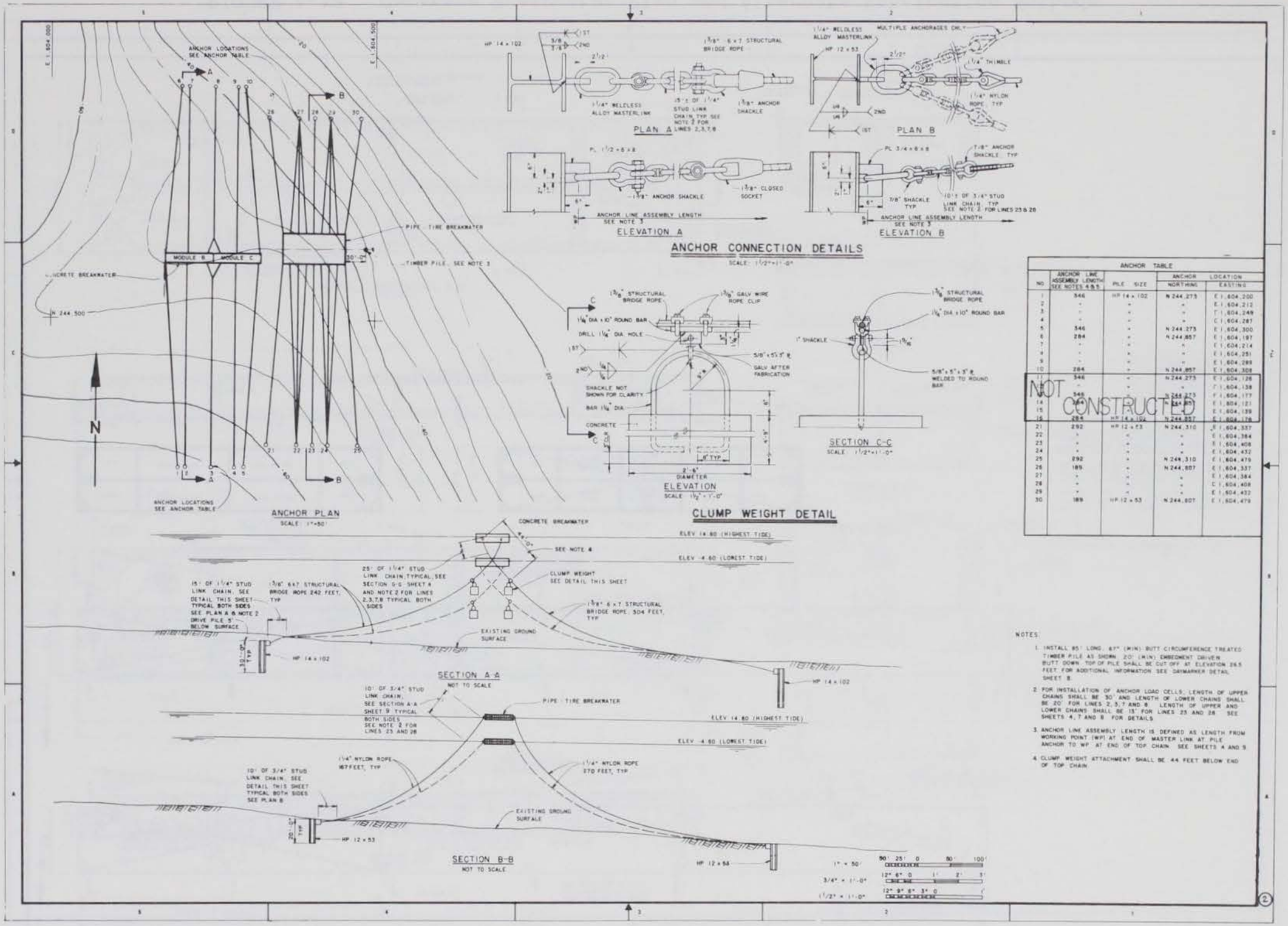

ANCHOR TABLE

NO.	ANCHOR LINE ASSEMBLY LENGTH* SEE NOTES 4 & 5	PILE SIZE	ANCHOR LOCATION NORTHING	ANCHOR LOCATION EASTING
1	546	HP 14 x 102	N 244,273	E 1,604,200
2	"	"	"	E 1,604,212
3	"	"	"	E 1,604,249
4	"	"	"	E 1,604,287
5	546	"	N 244,273	E 1,604,300
6	284	"	N 244,857	E 1,604,197
7	"	"	"	E 1,604,214
8	"	"	"	E 1,604,251
9	"	"	"	E 1,604,289
10	284	"	N 244,857	E 1,604,308
11	546	"	N 244,273	E 1,604,126
12	"	"	"	E 1,604,138
13	546	"	N 244,273	E 1,604,177
14	284	"	N 244,857	E 1,604,121
15	"	"	"	E 1,604,139
16	284	HP 14 x 102	N 244,857	E 1,604,176
21	292	HP 12 x 53	N 244,310	E 1,604,337
22	"	"	"	E 1,604,384
23	"	"	"	E 1,604,408
24	"	"	"	E 1,604,432
25	292	"	N 244,310	E 1,604,479
26	189	"	N 244,807	E 1,604,337
27	"	"	"	E 1,604,384
28	"	"	"	E 1,604,408
29	"	"	"	E 1,604,432
30	189	HP 12 x 53	N 244,807	E 1,604,479

NOT CONSTRUCTED

NOTES:

1. INSTALL 85' LONG, 67" (MIN) BUTT CIRCUMFERENCE TREATED TIMBER PILE AS SHOWN. 20' (MIN) EMBEDMENT DRIVEN BUTT DOWN. TOP OF PILE SHALL BE CUT OFF AT ELEVATION 26.5 FEET. FOR ADDITIONAL INFORMATION SEE DAYMARKER DETAIL SHEET 8.
2. FOR INSTALLATION OF ANCHOR LOAD CELLS, LENGTH OF UPPER CHAINS SHALL BE 30' AND LENGTH OF LOWER CHAINS SHALL BE 20' FOR LINES 2,3,7 AND 8. LENGTH OF UPPER AND LOWER CHAINS SHALL BE 15' FOR LINES 25 AND 28. SEE SHEETS 4, 7 AND 8 FOR DETAILS.
3. ANCHOR LINE ASSEMBLY LENGTH IS DEFINED AS LENGTH FROM WORKING POINT (WP) AT END OF MASTER LINK AT PILE ANCHOR TO WP AT END OF TOP CHAIN. SEE SHEETS 4 AND 5.
4. CLUMP WEIGHT ATTACHMENT SHALL BE 44 FEET BELOW END OF TOP CHAIN.

FIGURE A-11. Anchor Plan and Details

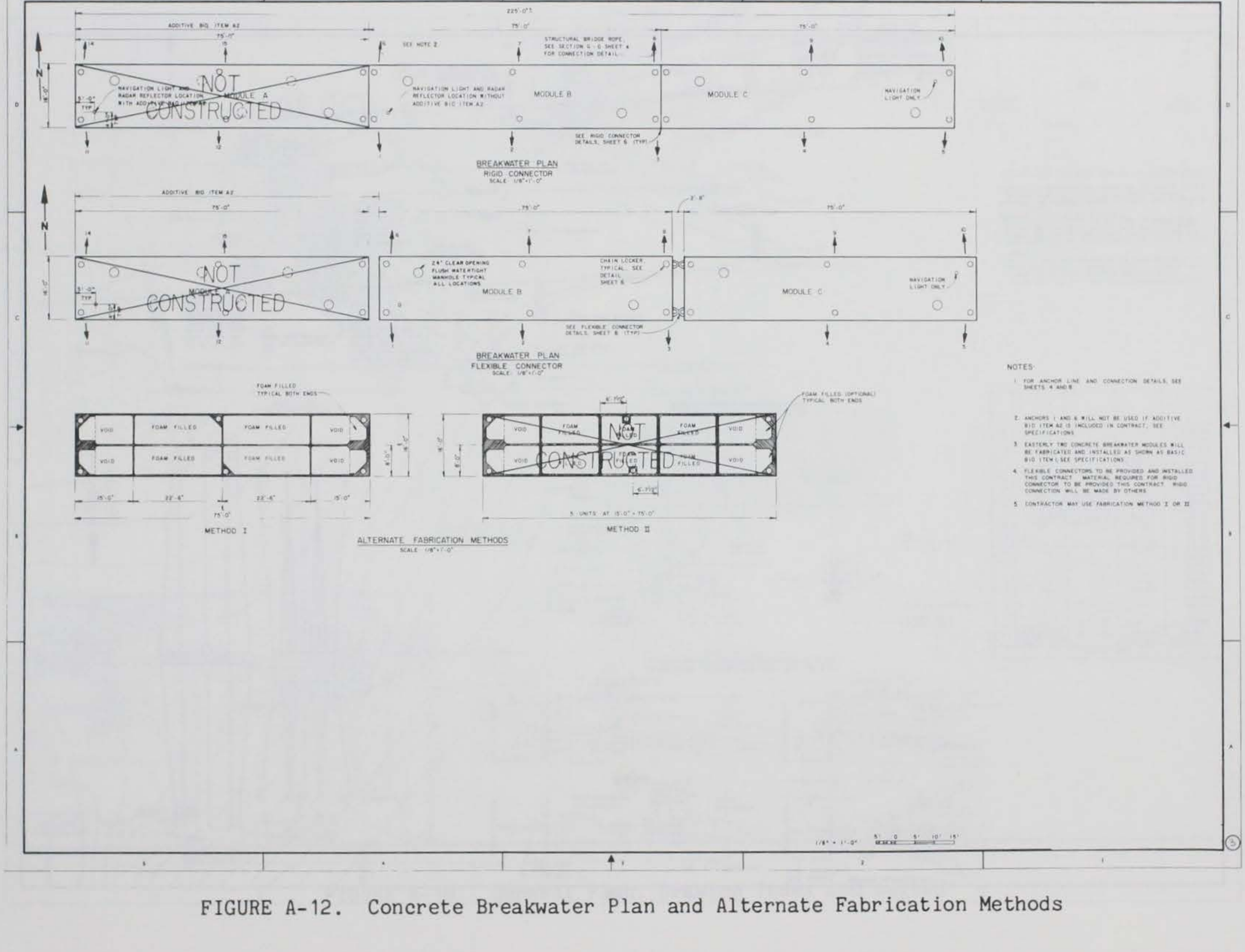

FIGURE A-12. Concrete Breakwater Plan and Alternate Fabrication Methods

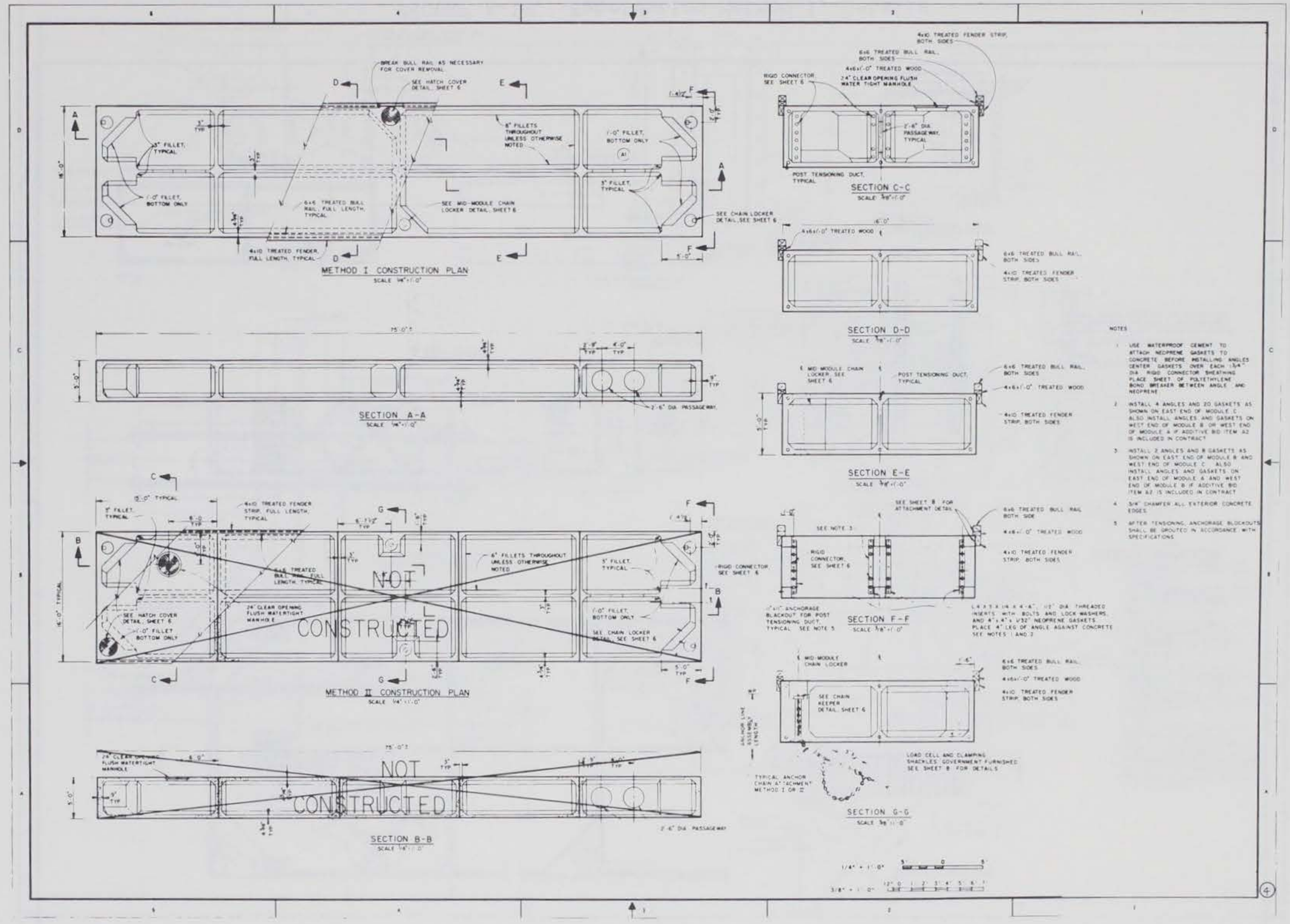

FIGURE A-13. Concrete Breakwater Module, Plans and Sections

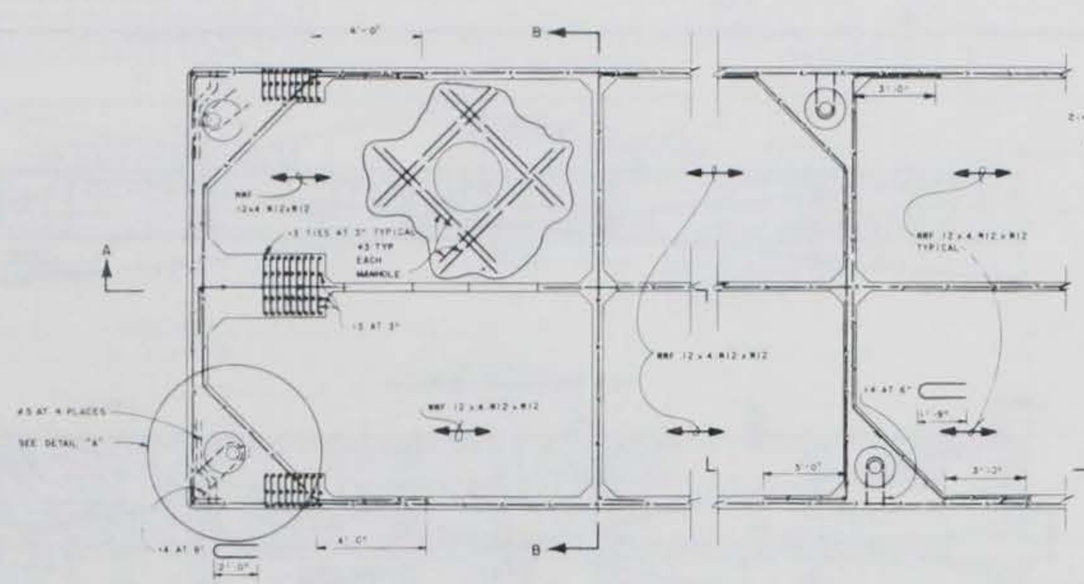

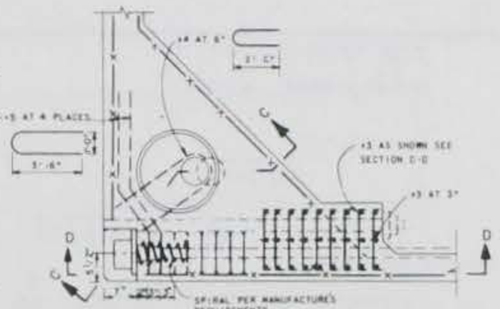

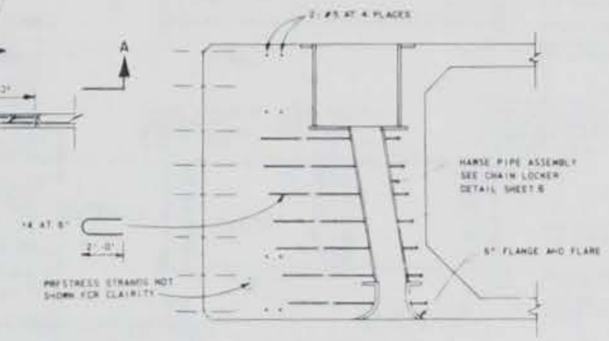

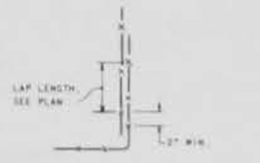

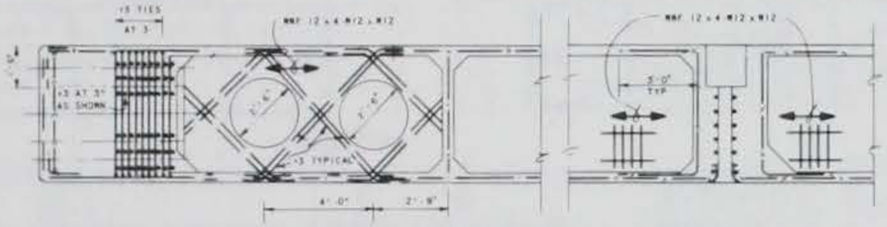

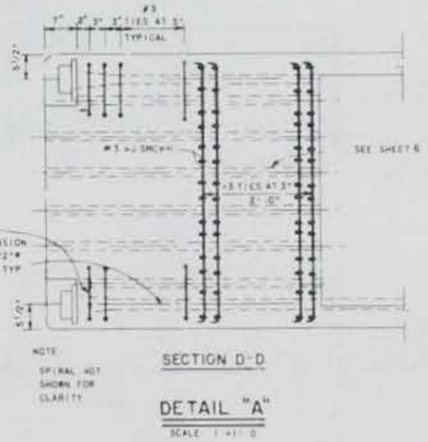

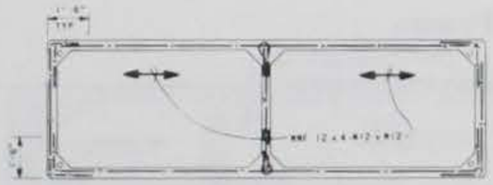

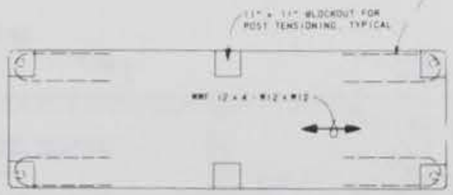

FIGURE A-14. Fabrication Method I, Details

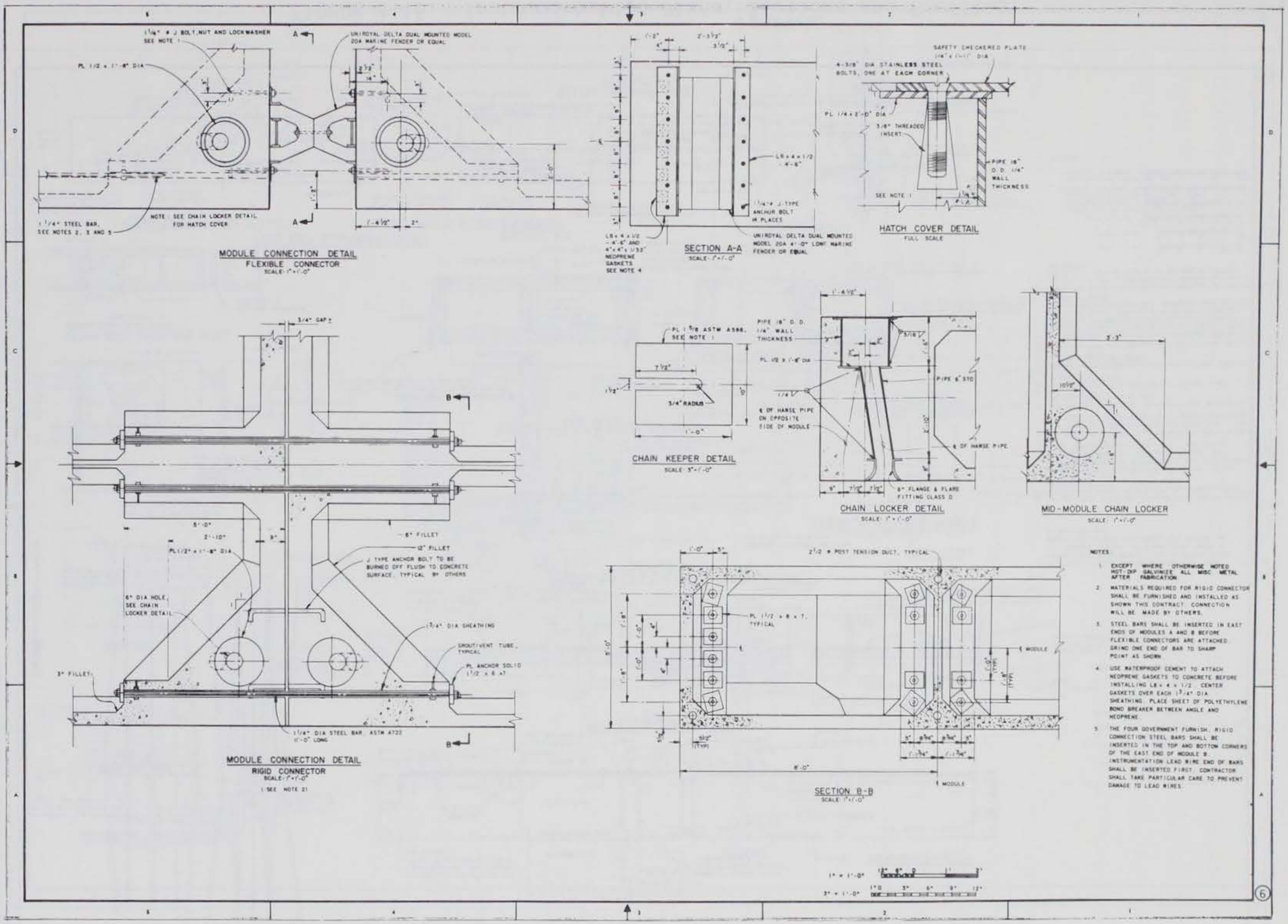

FIGURE A-15. Module Connecting Details

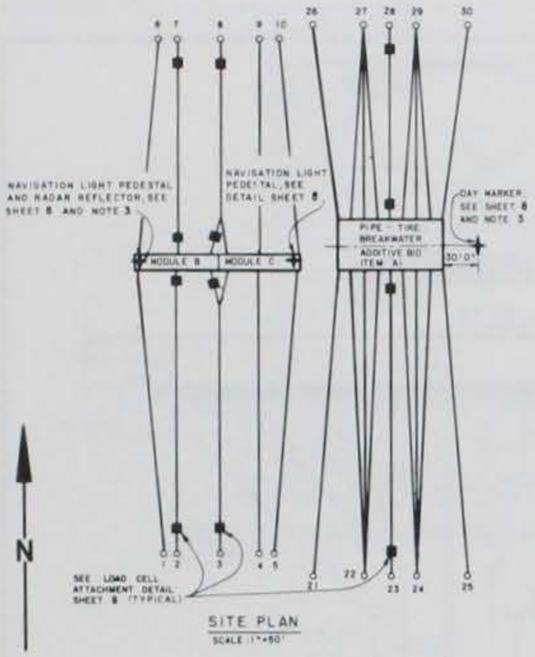

SITE PLAN
SCALE 1"=50'

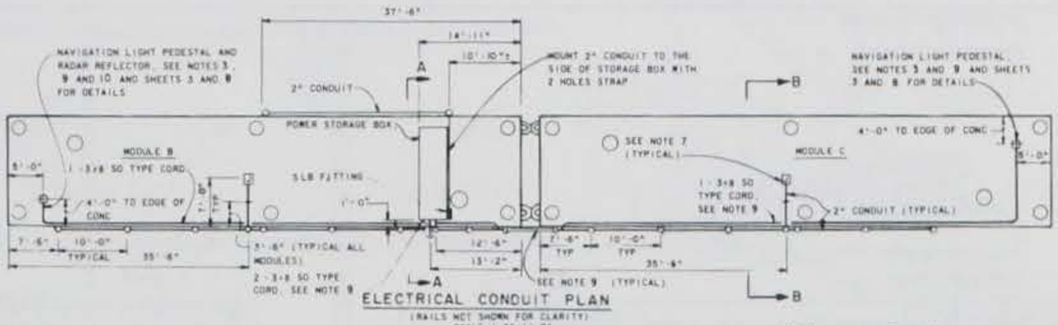

ELECTRICAL CONDUIT PLAN
(RAILS NOT SHOWN FOR CLARITY)
SCALE 1/8"=1'-0"

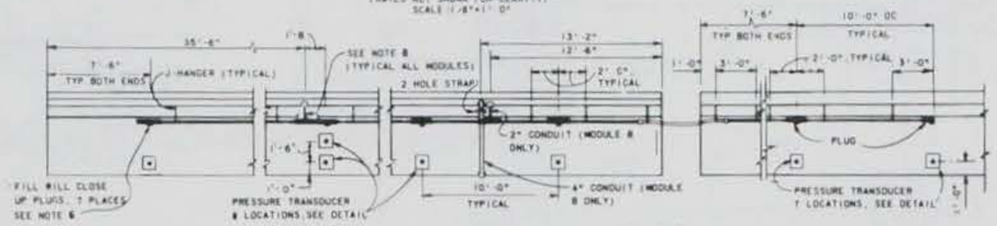

PARTIAL MODULES A, B AND C SOUTH ELEVATION
(FLEXIBLE CONNECTORS NOT SHOWN FOR CLARITY)
SCALE 1/4"=1'-0"

LEGEND

- CONDUIT RISER
- JUNCTION BOX - SEE SPECIFICATIONS
- T - FITTINGS 2"
- LB FITTING 2" UNLESS OTHERWISE NOTED
- EMBEDDED STRAIN GAUGES

NOTES:

1. PROVIDE AND INSTALL CONTINUOUS INSERTS AS SHOWN. TYPICAL FABRICATION METHOD I AND II. INSTALL FLUSH WITH CONCRETE SURFACE. USE P3300 SERIES INSERT AS MANUFACTURED BY UNISTRUT CORPORATION, SEATTLE, WA OR APPROVED EQUAL.
2. USE CARE WHEN INSTALLING STRAIN BOLTS TO PREVENT DAMAGE TO ELECTRICAL LEADS. AFTER INSTALLING, TIGHTEN STRAIN AND CONNECTOR BOLTS TO UNIFORM TORQUE.
3. NAVIGATION LIGHT PEDESTALS, RADAR REFLECTOR, AND DAY MARKER TO BE INSTALLED THIS CONTRACT. LIGHTS BY OTHERS. INSTALL LIGHT PEDESTALS AT LOCATIONS SHOWN. USE 1/2"ø THREADED INSERTS. SEE SHEET FOR DETAILS.
4. EMBEDDED STRAIN GAUGES TO BE INSTALLED IN MODULE B ONLY THIS CONTRACT. LOCATIONS SHOWN ARE APPROXIMATE. FINAL LOCATIONS WILL BE DETERMINED DURING MODULE FABRICATION.
5. INSTRUMENTATION HARDWARE FOR MODULE A WILL BE REQUIRED FOR ADDITIVE BID ITEM A2 ONLY.
6. INSTALL LB FITTING IF ADDITIVE BID ITEM A2 IS NOT INCLUDED IN CONTRACT.
7. TEMPLATE MOUNTING BOLT SIZE AND LOCATION FROM JUNCTION BOX. USE THREADED INSERTS.
8. NOTCH BULL RAIL AND FENDER AS REQUIRED TO CLEAR CONDUIT.
9. USE SINGLE HOLE CLAMP EVERY 5'-0" TO SECURE CORD TO BULL RAIL. ATTACH CORD TO LIQUID TIGHT CONDUIT WITH 5 CABLE TIES. ATTACH CORD TO PEDESTAL WITH 2 STAINLESS STEEL HOSE CLAMPS. PROVIDE 18'-0" "PIGTAIL" FOR EACH CORD INSIDE POWER STORAGE BOX. ELECTRICAL HOOK UP WILL BE MADE BY OTHERS.
10. CORD SHOWN IS FOR NAVIGATION LIGHT INSTALLATION WITHOUT ADDITIVE BID ITEM A2. ROUTE CORD TO NAVIGATION LIGHT ON MODULE A IF ADDITIVE ITEM A2 IS INCLUDED IN CONTRACT. SEE SHEET 3.

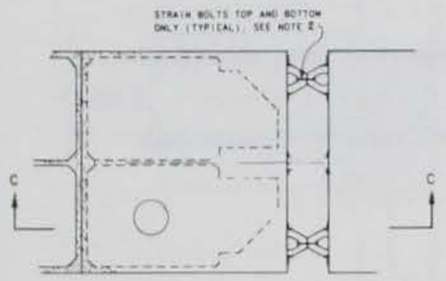

STRAIN BOLT LOCATIONS DETAIL
(BETWEEN MODULES B AND C ONLY)
SCALE 1/4"=1'-0"

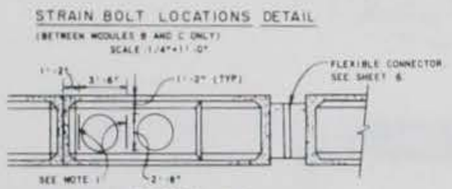

SECTION C-C
SCALE 1/4"=1'-0"

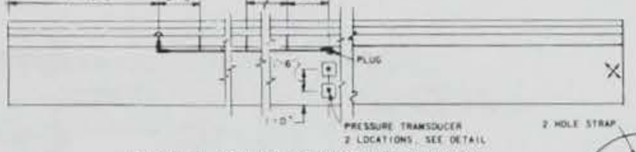

PARTIAL MODULE B NORTH ELEVATION
SCALE 1/4"=1'-0"

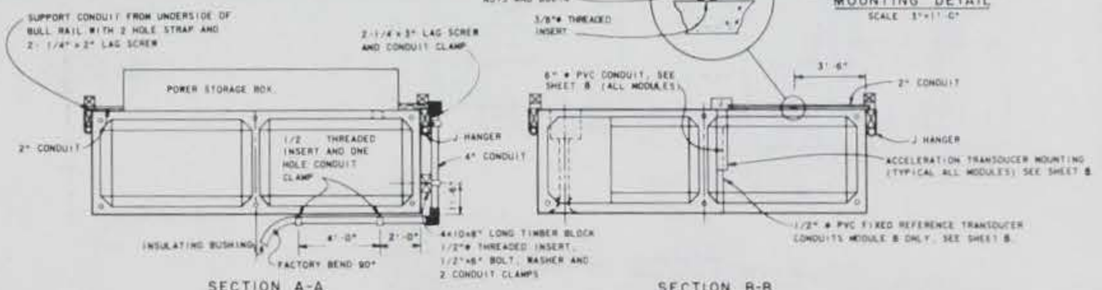

SECTION A-A
SCALE 3/8"=1'-0"

SECTION B-B
SCALE 3/8"=1'-0"

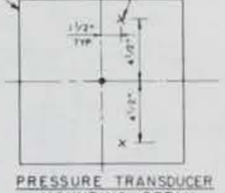

PRESSURE TRANSDUCER MOUNTING DETAIL
SCALE 1"=1'-0"

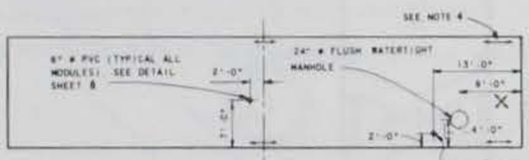

TOP DECK PLAN
SCALE 1/8"=1'-0"

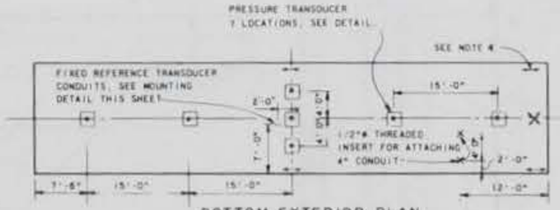

BOTTOM EXTERIOR PLAN
(MODULE B ONLY)
SCALE 1/8"=1'-0"

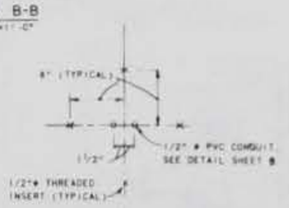

FIXED REFERENCE TRANSDUCER MOUNTING DETAIL
SCALE 1"=1'-0"

1/8" = 1'-0"
1/4" = 1'-0"
3/8" = 1'-0"
1 1/2" = 1'-0"
3" = 1'-0"
1" = 50'

A-20

FIGURE A-16. Instrumentation Plans, Sections and Profiles

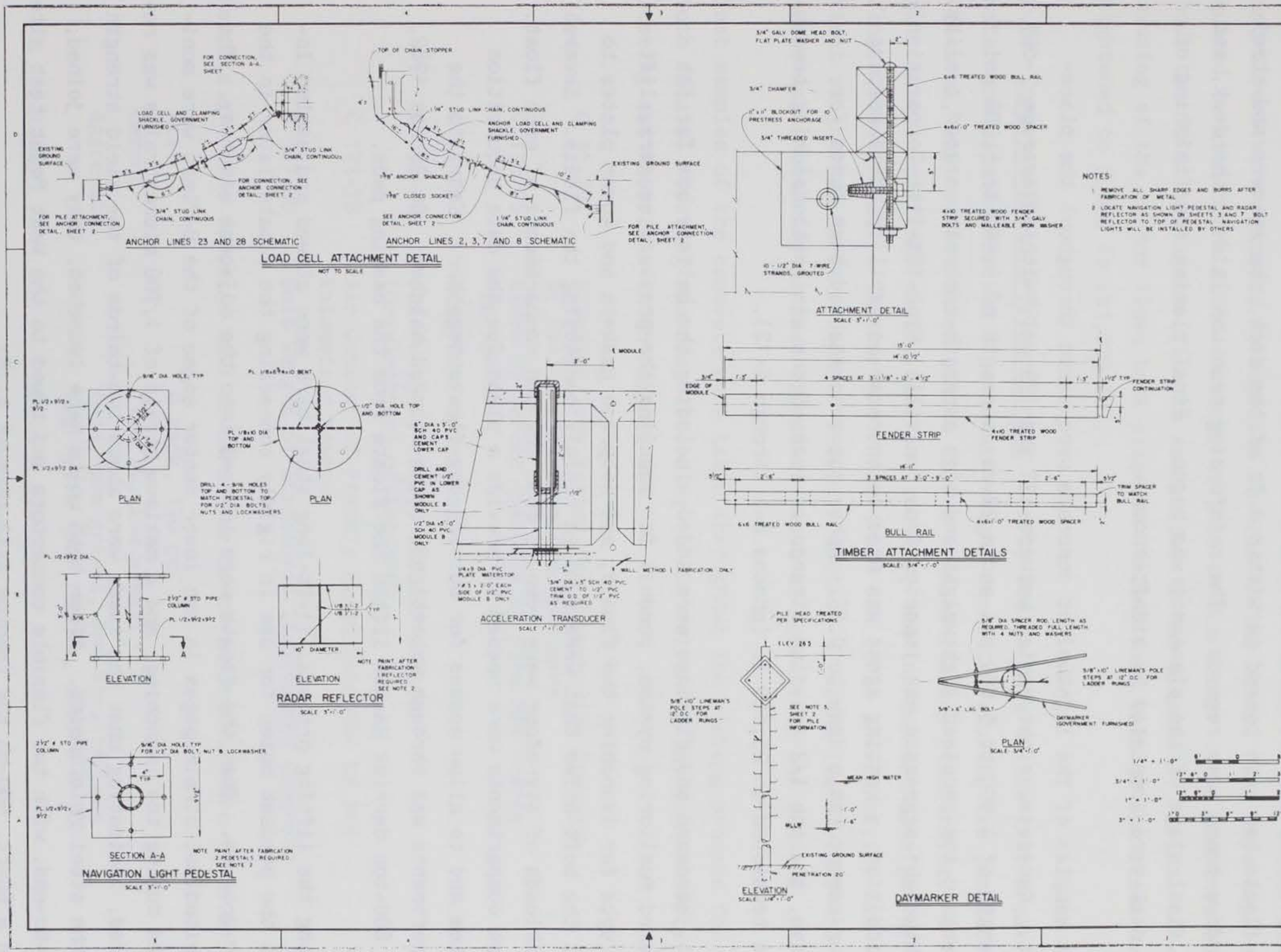

FIGURE A-17. Miscellaneous Details

the float was done in three lifts of about 1 ft each. Handheld electric vibrators were used to reduce the possibility of voids. After the sides of the floats had been poured to within 1 ft of the deck, the spacers and steel holddown beams were removed. The reinforcing mesh was laid on the deck, and the final stage of the placement was begun. Final placing and finishing of the deck were completed by midafternoon.

Test samples of the lightweight concrete were taken throughout the placement. Concrete weight varied between 131 and 134 pcf, with an average 7-day strength of 4,000 to 5,000 psi and a 28-day strength of 5,000 to 6,000 psi. To obtain the required lightweight and high strength concrete, a good quality lightweight aggregate was imported from Coalville, Utah (Utelite Corporation). In addition, a wetting agent was used to increase workability while keeping water-cement ratio down to 0.35. After the concrete had been cured for 7 days, the ten 1/2-in.-diam strands in each of the six posttensioning tendons were tensioned to 25,000 lb (photos A-1 through A-12).

Next, hardware and fittings were added, including the battery box for the onboard monitoring system, conduit for mounting the pressure sensors, lifting eyes for launching the floats, and neoprene gaskets and cover plates to seal the bolt holes that were used in rigidly connecting the floats. Several truckloads of styrofoam were removed from the end compartments of each float. These compartments were needed to provide a place for the data acquisition system and to allow access for bolting the floats together. Entry to the compartments was through watertight, flush-mounted hatches. On 28 May 1982, the 600-ton derrick Haakon lifted the floats from the casting pads.

During the lifting process, 11-ft-long steel bars were stowed and sealed inside the precast holes for use in rigidly connecting the floats later in the test program. Then the floats were lowered into the adjacent waterway. The longitudinal strain gages in the lower center edges of the B-float were monitored during the launching, and a maximum strain of 1,700 microstrains was recorded, indicating that the loads were about two-thirds of the yield strength of the steel reinforcing. After both units were launched, they were joined, end-to-end, with two flexible connectors and towed to the West Point test site with a 60-ft, 500-hp tug (photos A-13 through A-18).

The two concrete breakwater units arrived at the test site on 1 July 1982. Some difficulties were encountered in locating the buoys for the anchor lines, and divers were required to retrieve several of the lines. Ten days was required to attach the 2,000-lb clump weights to the anchor lines and then connect the 10 anchor lines (five on each side) to the breakwater. Final tensioning of the anchor lines took place on 16 July when each of the lines was tightened to 5,000 lb (±1,000 lb).

2.02 Concrete Mixture Proportioning. Early design work on the test breakwater anticipated the use of standard weight concrete. During the job advertisement, last minute calculations showed that additional reinforcing, required because of the severe test environment, had increased the weight of the floats substantially. Either the float draft had to be increased, or the float weight had to be reduced. Weight reduction by using lightweight concrete was chosen as the most expedient means of correcting the problem.

Test samples of the concrete were taken throughout the casting process for both floats. Testing was done according to the following American Society for Testing and Materials (ASTM) standards:

C 39-80	Standard Test Method for Compressive Strength of Cylindrical Concrete Specimens
C 136-76	Sieve or Screen Analysis of Fine and Coarse Aggregates
C 94-80	Ready Mix Concrete
C 138-77	Unit Weight, Yield, and Air Content (Gravimetric) of Concrete
C 173-78	Air Content of Freshly Mixed Concrete by the Volumetric Method
C 567-80	Unit Weight of Structural Lightweight Concrete

Results of these tests as well as other pertinent information are shown below:

Mix	8 sack, 130 pcf
Cement	Type II, low alkali
Aggregate	Sand, pea gravel, and Utelite (see aggregate test report, figure A-18)
Slump	6 to 8 in.

(Continued)

MATERIAL

	BUILDERS	BUILDERS	UTELITE	
% PASSING	# 8 PEA	SAND		
U.S. SLEVE NO.	GRAVEL			
2-1/2 IN.				
2 IN.				
1-1/2 IN.				
1-1/4 IN.				
1 IN.				
3/4 IN.			100	
1/2 IN.	100		90	
3/8 IN.	83		55	
1/4 IN.				
NO. 4	14	100	8	
NO. 8	2	87	1	
NO. 16	0	63		
NO. 30		43		
NO. 50		18		
NO. 100		4		
NO. 200				
F.M.		2.85		
S E OR C V				
SPECIFIC GRAVITY	2.68	2.67		
% ABSORPTION				
L A R LOSS 500 REV				
SOUNDNESS - 5 CYCLES				
MORTAR TEST				
C.A. RODDED UNIT WEIGHT				

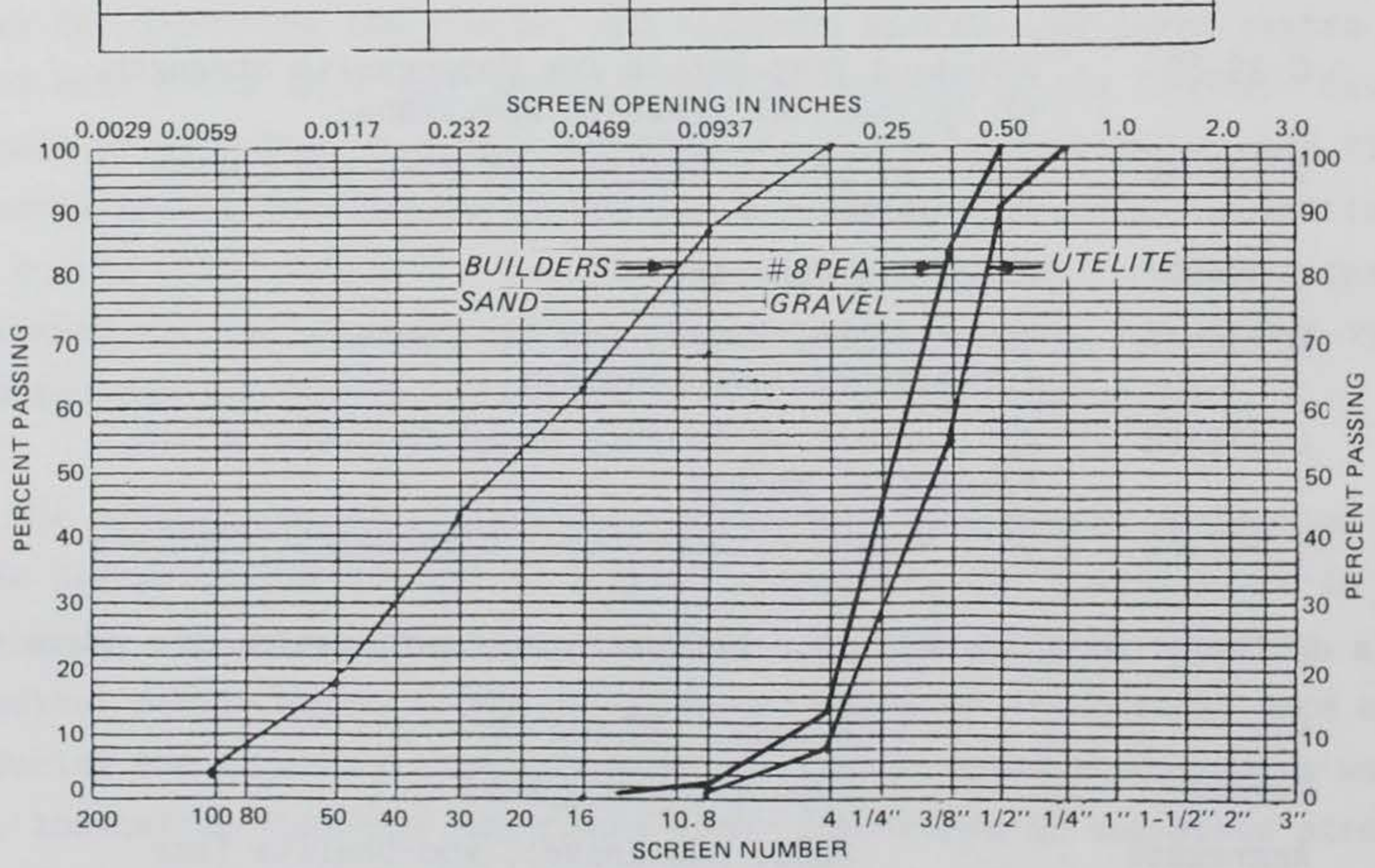

FIGURE A-18. Aggregate Test Report

Air Content	6.1% - 7.3%; 6.6% avg.
Water Cement Ratio	0.35
Admix	Zeecon - H, 7.0 oz/100; MBAE -10, 4.5 oz/cu yd
Unit Weight	131.0 - 134.5 pcf; 132.6 pcf avg.
Weather and Temperature	Clear, 55° - 75° F
Concrete Temperature	62° - 68° F
7-Day Strength	4,060 - 4,930 psi; 4,605 psi, avg.
28-Day Strength	4,846 - 6,540 psi; 5,722 psi, avg.
Post-Tension Grout	2,500 psi at 7 days

2.03 Costs. Costs for the prototype test's concrete breakwater are presented below. Also presented are costs for a longer breakwater (at Friday Harbor) of very similar design.

	Prototype Breakwater 1/ 1981		Friday Harbor Breakwater 2/ 1983	
	Per Foot Cost ($)	Total Cost ($)	Per Foot Cost ($)	Total Cost ($)
Concrete Breakwater	1,913	287,000	1,011	1,618,000
Anchor System (50-ft-Depth)	687	103,000	215	344,000
Total	2,600	390,000	1,226	1,962,000

1/ 150 ft long.
2/ 1,600 ft long.

3.0 Operation and Maintenance.

3.01 Freeboard and Overtopping. The initial freeboard of the floats varied from 15 to 18 in. No additional ballast was required to trim the breakwater. After the anchor lines had been secured, the additional vertical anchor line load lowered the freeboard to 13 in., 5 in. lower than originally desired. The increased draft (and reduced freeboard) may have improved the wave attenuation capabilities slightly, but the reduced freeboard undoubtedly caused an increase in the amount of wave overtopping. Incident waves estimated to

be 2 ft high caused 6-in.-deep water to flow across the deck (photo A-19). This made moving about on the rolling, slippery deck an extremely precarious proposition (photo A-20). On more than one occasion, tools and equipment were swept overboard, and life vests were a standard dress item. In addition, care had to be exercised in mooring the work boat to avoid swamping it with the water which ran off the leeward side of the breakwater (photo A-21).

3.02 Float Motion and Accessibility. The relative motion between the breakwater and workboats which were tied up alongside resulted in some minor damage to the workboats. A 13-ft fiberglass skiff was carried up onto the center of the breakwater by a tugboat wake. Tugboat wakes also swamped a 17-ft aluminum workboat and knocked a 30-ft steel workboat against the breakwater, damaging the boat's wheelhouse. When work was being done on the breakwater in rough water conditions, the workboats had to be watched continuously to avoid damage or swamping (photo A-21). Access to the moving deck of the breakwater from the workboats required careful timing to prevent a person's falling into the water or being caught between the boat and the breakwater. Measurements of relative float motion (with the two breakwater units in the fendered, unconnected configuration) were made during the first of the boat wake tests. The maximum relative displacement was ±9 in. vertically and ±12 in. horizontally. The wake was about 2 ft high with a 2.5-sec period (see Appendix F for details).

3.03 Leakage. Aside from damage done to the various connectors (discussed in Appendix D), the concrete structure survived the test period undamaged; however, water leaking into the end compartment provided a few anxious moments. The leaks occurred at the entrance hatches and at the through-hull Dywidag bolt holes. The hatches were designed to be flush with the deck to facilitate the future use of the floats in the Friday Harbor Marina project. Unfortunately the hatches were the low point of the deck, and faulty seals turned the hatches into drains for overtopping waves. Quick calculations indicated that the floats might be negatively buoyant if the end compartments were filled with water, and on two occasions emergency pumping operations were carried out to avoid field verification of the buoyancy calculations (photos A22 and A-23). Leaks also developed where the neoprene gaskets sealed the twenty 1-3/4-in.-diam bolt holes cast into the end of

each float. Eventually the hatch seals were reworked and made watertight, and the bolt holes were sealed with injected urethane foam and plumbing corks.

3.04 Debris Effects. On several occasions, storms, accompanied by extreme high tides, produced large amounts of floating debris. Logs as large as small automobiles were found on the breakwater deck one day and were gone the next. While the logs took their toll of monitoring instrumentation, no damage to the floats themselves was attributed to debris (photo A-24).

3.05 Structure Durability. A visual inspection of the concrete breakwater, including a diver inspection of the sides and bottom, revealed only minor cracks and chips in the concrete. There were some very small 1-in.-diam chips in the vicinity of hawse pipes on the bottom of the floats, probably a result of the unanchoring and reanchoring exercises carried out at various times in the field test. The wood fenders and bull rails showed considerable wear and tear by the end of the test period and had to be replaced when the breakwater was salvaged for reuse at the Friday Harbor Marina.

3.06. Environmental Effects. When the prototype test program was initiated, no adverse impacts to fish and wildlife were anticipated. The breakwater was expected to have an artificial reef effect and attract various types of marine life. The breakwater did prove to be a popular habitat for many species of marine plants and animals which attached to the bottom and sides of the floats. The cover and food supply provided by the breakwater attracted numerous perch and rock fish. Sea birds, such as gulls, auklets, western grebe, and sandpipers, also took up residence on or around the breakwater. In October 1982, 4 months after the breakwater was first anchored at the test site, a brief biological assessment was made by marine biologists from the Seattle Aquarium. Mussels (Mytilus edulis) were found to cover 20 percent of the bottom and 98 percent of the sides of the floats. Barnacles (Balanus sp.) covered 80 percent of the float bottom but were nearly nonexistent on the sides. Tunicates (Corella willermeriana) were numerous (approximately 5/sq ft) as were hydroids (Obelia longissima) and amphipods (Caprella equilibria). Many nudibranchs (Dorid sp.) also were found. As described earlier, the West Point site is subject to swift currents and

heavy wave action, and the breakwater developed a marine life community representative of many other exposed rocky areas in Puget Sound.

Some additional information on the design, construction, and use of concrete breakwaters is provided in references A-5 and A-6.

APPENDIX A

REFERENCES

A-1. Shore Protection Manual, 4th ed., 2 vols, U. S. Army Engineer Waterways Experiment Station, Coastal Engineering Research Center, U. S. Government Printing Office, Washington, D. C., 1984.

A-2. Holbrook, J. R., Muench, R. D., Kachel, D. G., and Wright, C., "Circulation in the Strait of Juan de Fuca: Recent Oceanographic Observations in the Eastern Basin," Technical Report ERL 412, PMEL 33, National Oceanic and Atmospheric Administration, Washington, D. C., April 1980.

A-3. Olson, R. M., Essentials of Engineering Fluid Mechanics, 2nd ed., International Book Co., Scranton, Pennsylvania, 1966.

A-4. Davidson, D. D., "Wave Transmission and Mooring Force Tests of Floating Breakwaters, Oak Harbor, Washington," Technical Report H-71-3, U. S. Army Engineer Waterways Experiment Station, Vicksburg, Mississippi, April 1971.

A-5. Lorman, W. R., "Concrete Cover in Thin Wall Reinforced Concrete Floating Piers," Technical Note N-1447, Civil Engineering Laboratory, Naval Construction Battalion Center, Port Hueneme, California.

A-6. Western Canada Hydraulic Laboratories Ltd., "Development of a Manual for the Design of Floating Breakwaters," Canadian Manuscript Report of Fisheries and Aquatic Sciences No. 1629, Department of Fisheries and Oceans, Small Craft Harbours Branch, Ottawa, Ontario, November 1981.

TABLE A-1

WAVE ESTIMATES FOR WEST POINT TEST SITE

Direction	Effective Fetch, F_{eff} (mi) 1/	Wind Duration, t_d (hr) 2/	Wind Speed, U (mph) 2/	Wave Height, H_s (ft) 3/	Wave Period, T_s (sec) 3/
North	9.0	1.7	36	4.3	4.4
			35	4.1	4.4
			30	3.5	4.0
			25	2.8	3.6
			20	2.2	3.2
			12	1.2	2.4
South	6.8	1.2	52	6.0	5.0
			50	5.8	4.9
			40	4.2	4.3
			30	3.1	3.7
			25	2.5	3.4
			20	1.9	3.0
			12	1.1	2.2
Southwest	4.9	0.9	50	4.9	4.6
			40	3.8	4.1
			30	2.8	3.5
			25	2.2	3.1
			20	1.7	2.7
			13	1.1	2.2
West	3.3	1.1	50	4.1	4.1
			40	3.3	3.7
			30	2.3	3.2
			25	1.9	2.9
			20	1.5	2.6
			15	1.1	2.2
Northwest	6.3	1.3	38	4.0	4.2
			35	3.7	4.0
			30	3.0	3.7
			25	2.5	3.3
			20	1.9	2.9
			12	1.1	2.2

1/ Effective fetch calculated with an arc width of ±45 deg.

2/ The wind speed duration curves used were developed from Seattle-Tacoma Airport records.

3/ The wave theory used was the Sverdrup-Munk-Bretschneider (SMB) method (reference A-1).

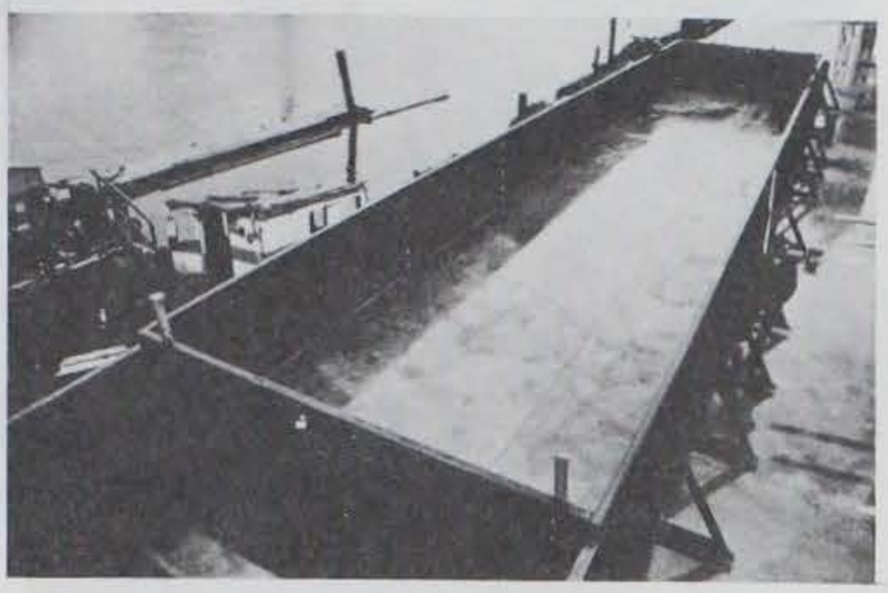

Photo A-1. Forms being erected for casting a 75- by 16- by 5-ft float.

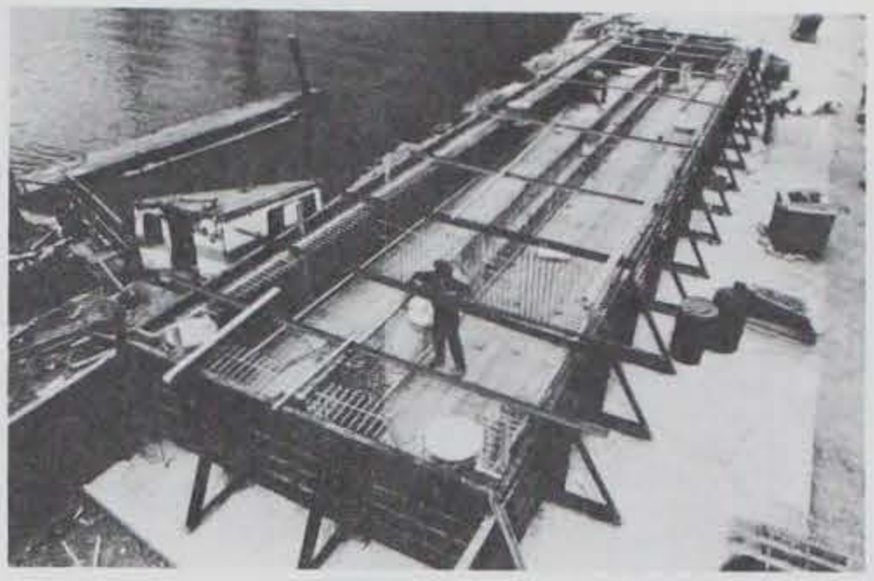

Photo A-2. Reinforcing steel being placed in the forms.

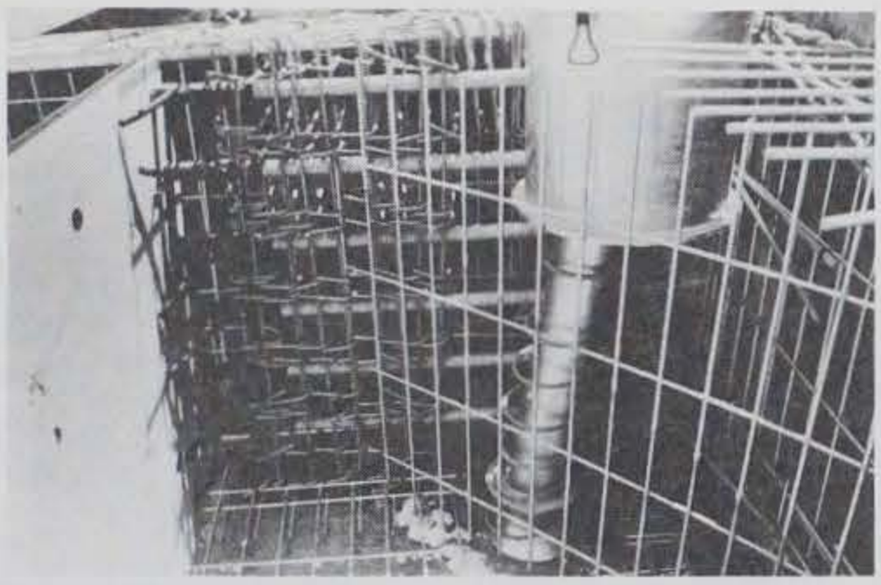

Photo A-3. Reinforcing steel being installed around hawse pipes and chain locker.

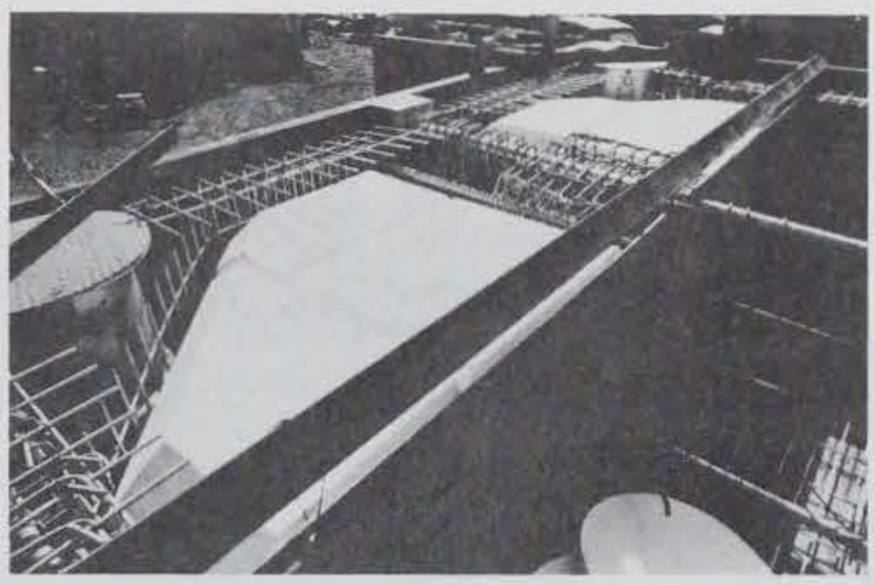

Photo A-4. Blocks of styrofoam being checked for proper fit.

Photo A-5. Styrofoam being lowered after bottom of float was placed.

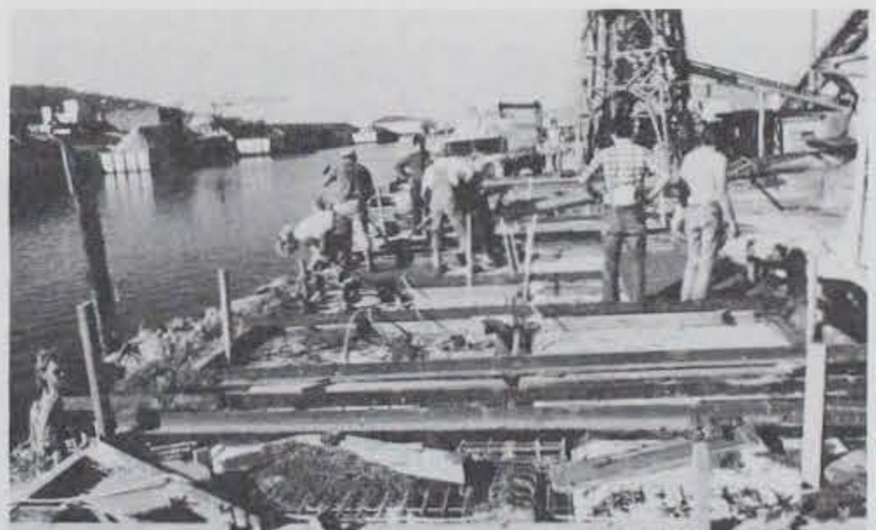

Photo A-6. Steel angles, 2 by 4's, and PVC pipe being used to keep styrofoam located properly.

Photo A-7. 3/8-in. welded wire fabric being laid on the deck.

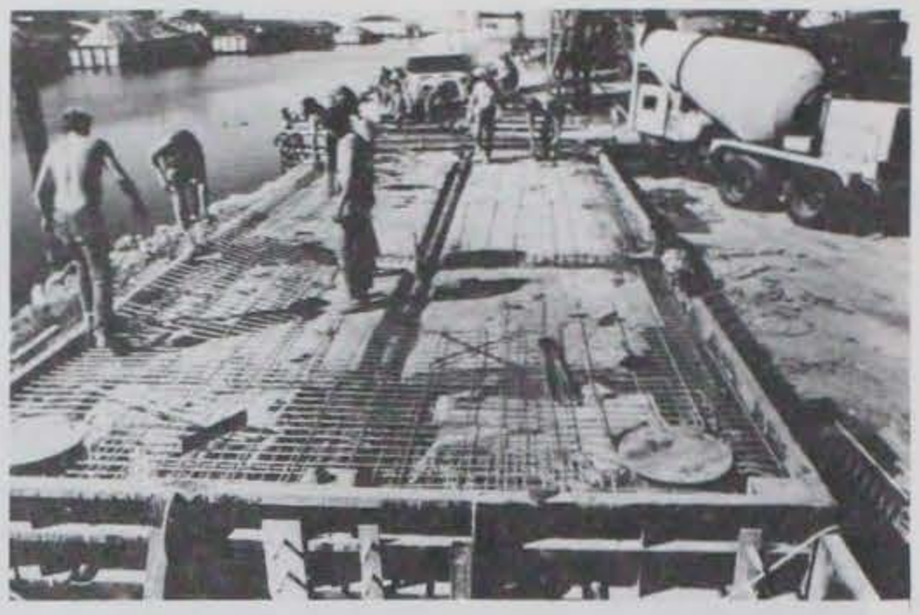

Photo A-8. Fabric being placed carefully in corner areas (crossed rebar strain gages near center of photo).

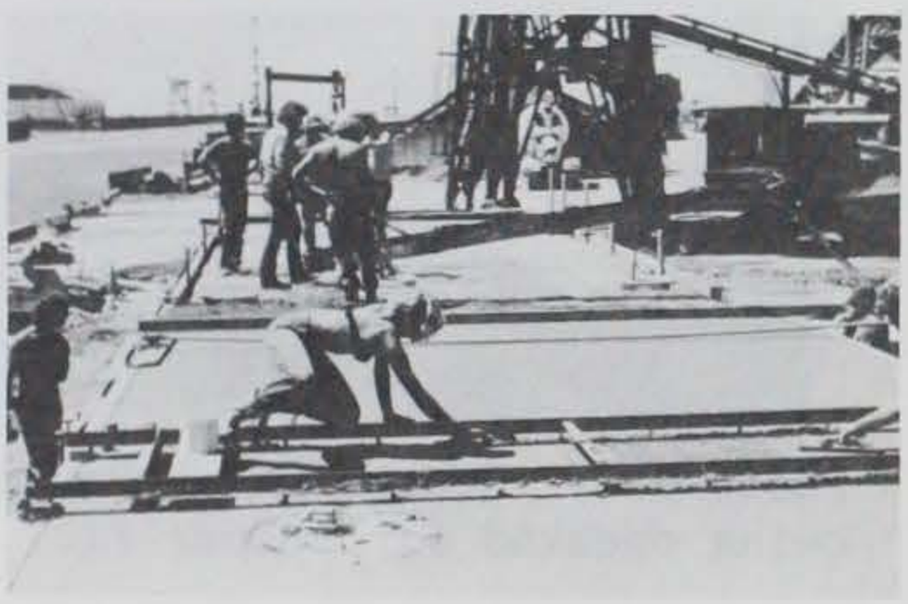

Photo A-9. Placing and finishing the deck.

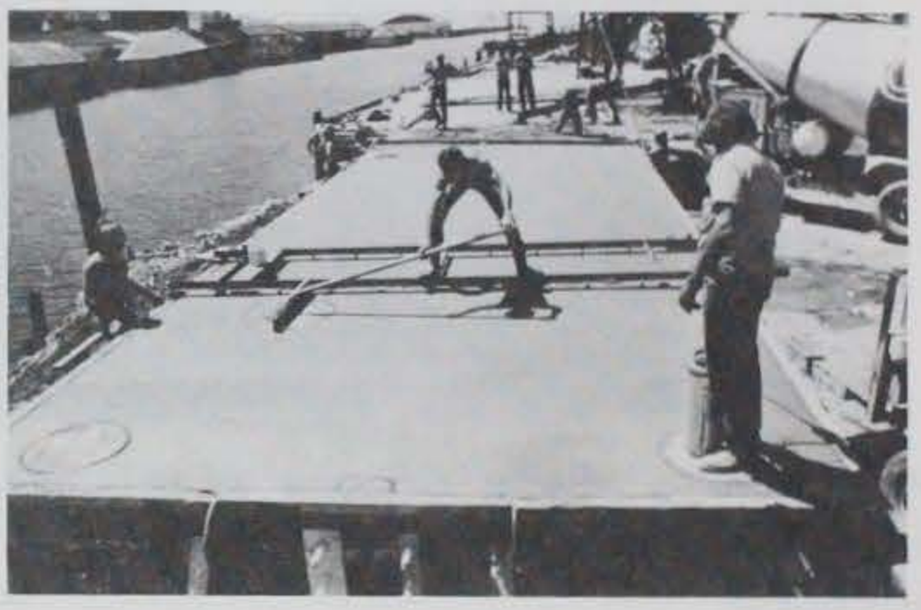

Photo A-10. Using a broom to create a nonskid surface.

Photo A-11. Taking concrete samples (done throughout the placement).

Photo A-12. Preparing for post-tensioning.

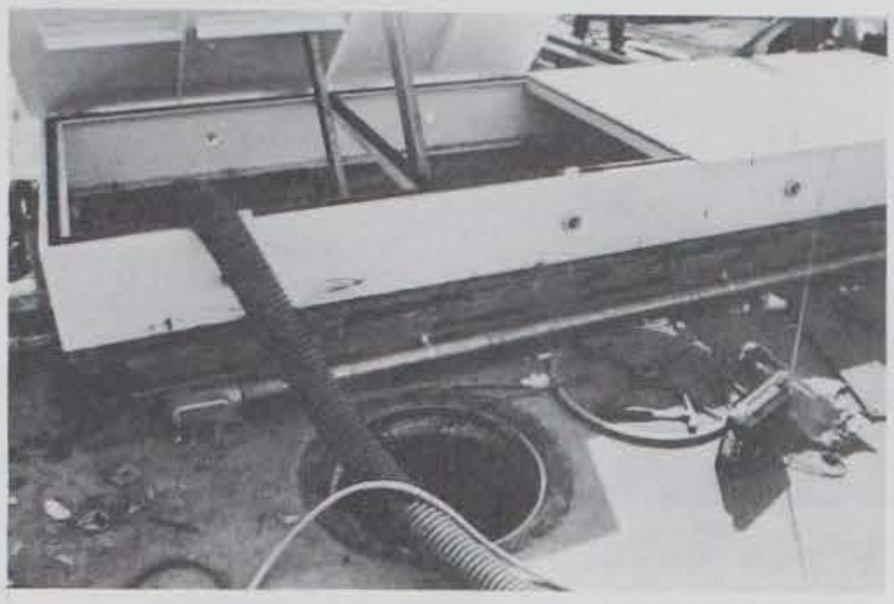

Photo A-13. Photo depicting original battery box and access hatch to equipment compartment.

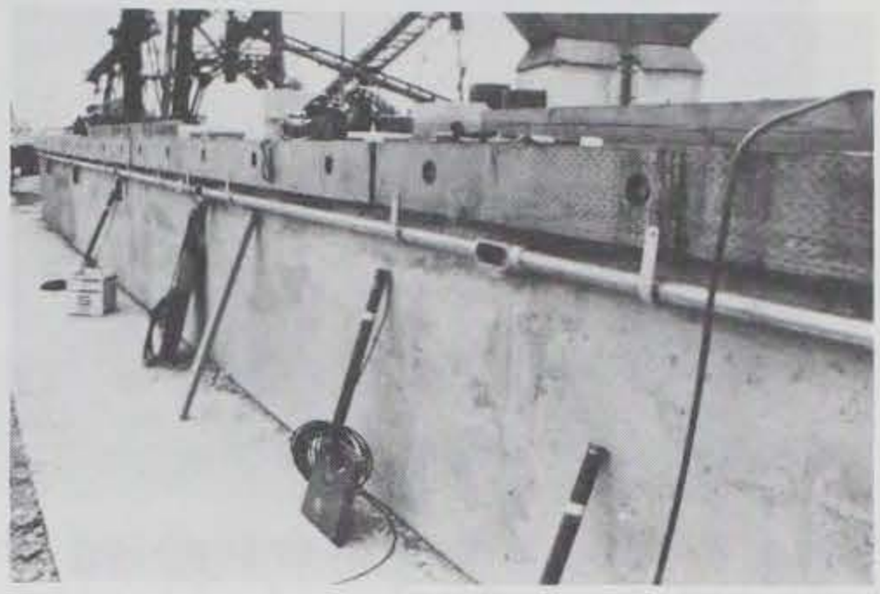

Photo A-14. Pressure transducer mounting locations being verified.

Photo A-15. Photo showing 600 cu ft of styrofoam that was "mined" from the end compartments of each float.

Photo A-16. A large derrick lifting one of the 140-ton floats.

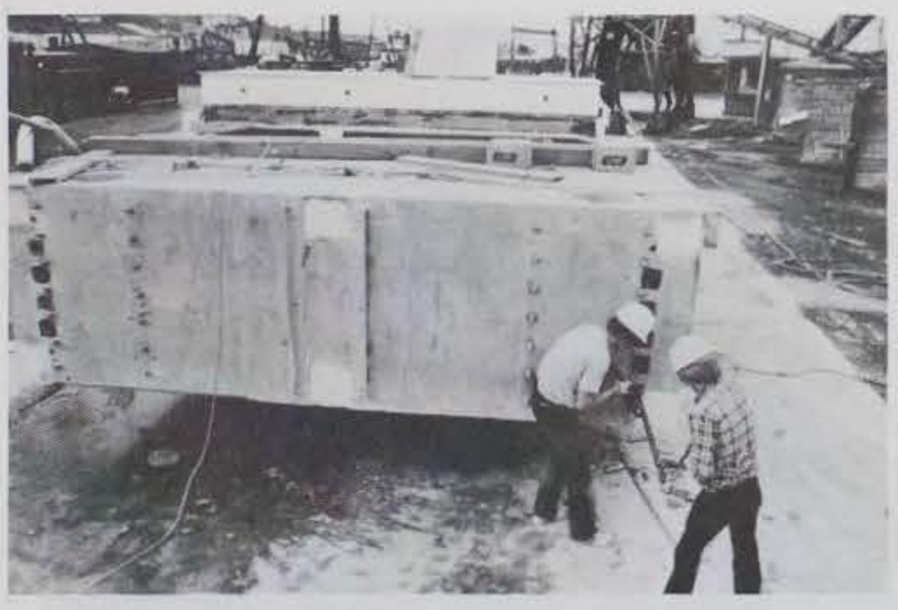

Photo A-17. 11-ft-long bolts being stowed inside one of the floats for later use.

Photo A-18. Rubber patches being glued over the bolt holes (later covered by steel angles).

Photo A-19. Waves overtopping the low deck (13-in.) freeboard allowing considerable wave overtopping.

Photo A-20. Work continuing cautiously on the slippery, rolling deck.

Photo A-21. Overtopping waves swamping a work skiff.

Photo A-22. About 3,000 gallons being pumped from an end compartment after a storm.

Photo A-23. Pumping out another end compartment (the deck is nearly awash).

Photo A-24. Photo showing type of debris which washed across the deck.

APPENDIX B

PIPE-TIRE BREAKWATER: DESIGN, CONSTRUCTION,
OPERATION, AND MAINTENANCE

1.0 Design.

1.01 Waves and Tidal Currents. For design calculations, wave, tide, and wind conditions were assumed to be identical for both the pipe-tire and concrete breakwaters. (See Appendix A, paragraphs 1.01 through 1.04 for a discussion of anticipated design conditions.)

1.02 Pressure Drag Loading. Pressure drag on the pipe-tire breakwater due to the wind, wind-generated surface currents, and tidal currents was calculated as follows:

a. Design wind speed, U , = 47 mph

b. Wind-generated current speed = (0.03)(U) = 1.4 mph = 2.0 fps

c. Tidal current speed = 2.0 fps

d. Total current speed, u , = 2.0 fps + 2.0 fps = 4.0 fps

e. Wind pressure drag = negligible

f. Pressure drag coefficient, C_D , = 0.65 (reference B-1)

g. Breakwater draft = 3.3 ft (40 in.)

h. Density of seawater, ρ , = 2 slugs/ft^3

i. Hydraulic pressure drag = $C_D \frac{\rho u^2}{2}$ (Draft)

= 35 lb/ft of breakwater length
(reference B-2)

1.03 Estimated Wave and Anchor Loads. Mooring loads for the pipe-tire breakwater were calculated for the 6-ft, 5-sec design wave using an empirical equation based on prototype data taken at the US Army Corps of Engineers Coastal Engineering Research Center (CERC) (reference 5, main report). As recommended by the originator of the pipe-tire design, the calculated anchor force was increased by 70 lb/ft as an added safety factor for design purposes. The resulting mooring load, due to waves, was estimated to be about 500 lb/ft of breakwater length (figure B-1). Current drag was estimated to be 35 lb/ft, producing a total of 535 lb/ft of breakwater, or a maximum design load of about 6,000 lb on each of the nine (12 ft on center) anchor lines.

1.04 Buoyancy Calculations. During the design process the buoyancy of the pipe-tire breakwater was calculated from the difference between the total buoyant force and the weight of the breakwater with its mooring system attached plus the vertical component of the load on each anchor line. The styrofoam filled 16-in.-diam pipes contributed approximately 40 lb of buoyant force per linear foot of pipe. The other major source of buoyancy was the urethane foam in the crowns of the tires, anticipated to be 75 lb per tire for 880 tires. The weights used for buoyancy calculations were (1) 15 lb per tire for 1,650 tires (submerged weight), (2) 11 lb per tire for sediment and biofouling, (3) 1,540 lb for submerged anchor lines, and (4) 13,000 lb for total vertical component of anchor load with design wave loading and wind/tidal current force applied. The buoyant force and weights combined to produce a calculated net positive buoyancy of about 16,000 lb.

2.0 Construction.

2.01 Construction Sequence. Construction of the pipe-tire breakwater began in late March 1982 (see figure B-2 for construction drawing). The 1,650 truck tires required for the job were brought to the contractor's workyard where they were arranged into rows and held in a vertical orientation by two 4 by 4's running parallel to the rows. A hole was drilled in each tire to allow the water to drain, after which a two-part urethane foam was sprayed into the crown of 880 tires (see figure B-2 for foam specifications). The tires were assembled into bays on a construction platform located adjacent to a waterway. As each bay was completed, the breakwater was moved (one bay at a time) into

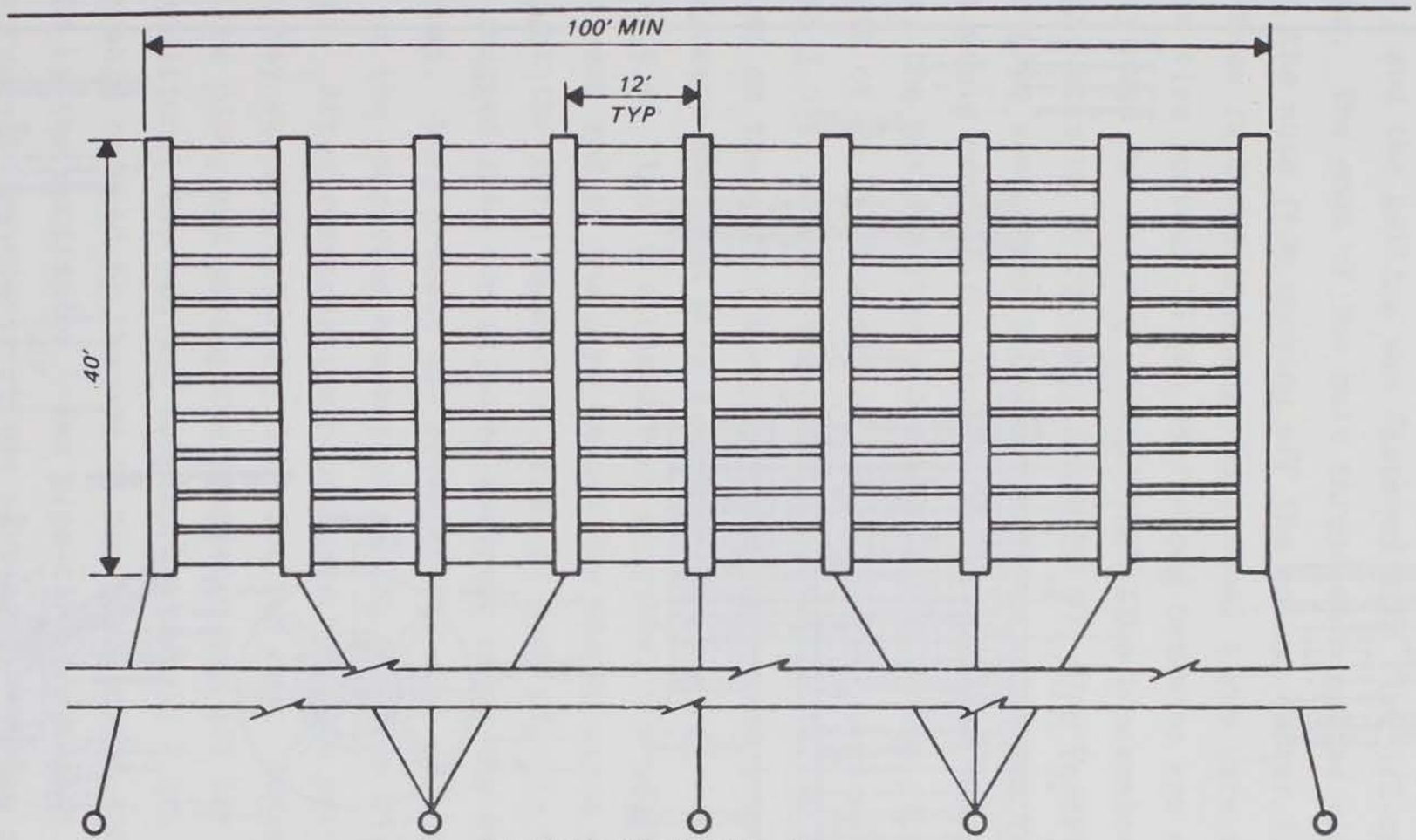

PLAN VIEW PIPE - TIRE BREAKWATER

NOT TO SCALE

FIGURE B-1. Estimated Wave Force on Pipe-Tire Breakwater Anchor Lines

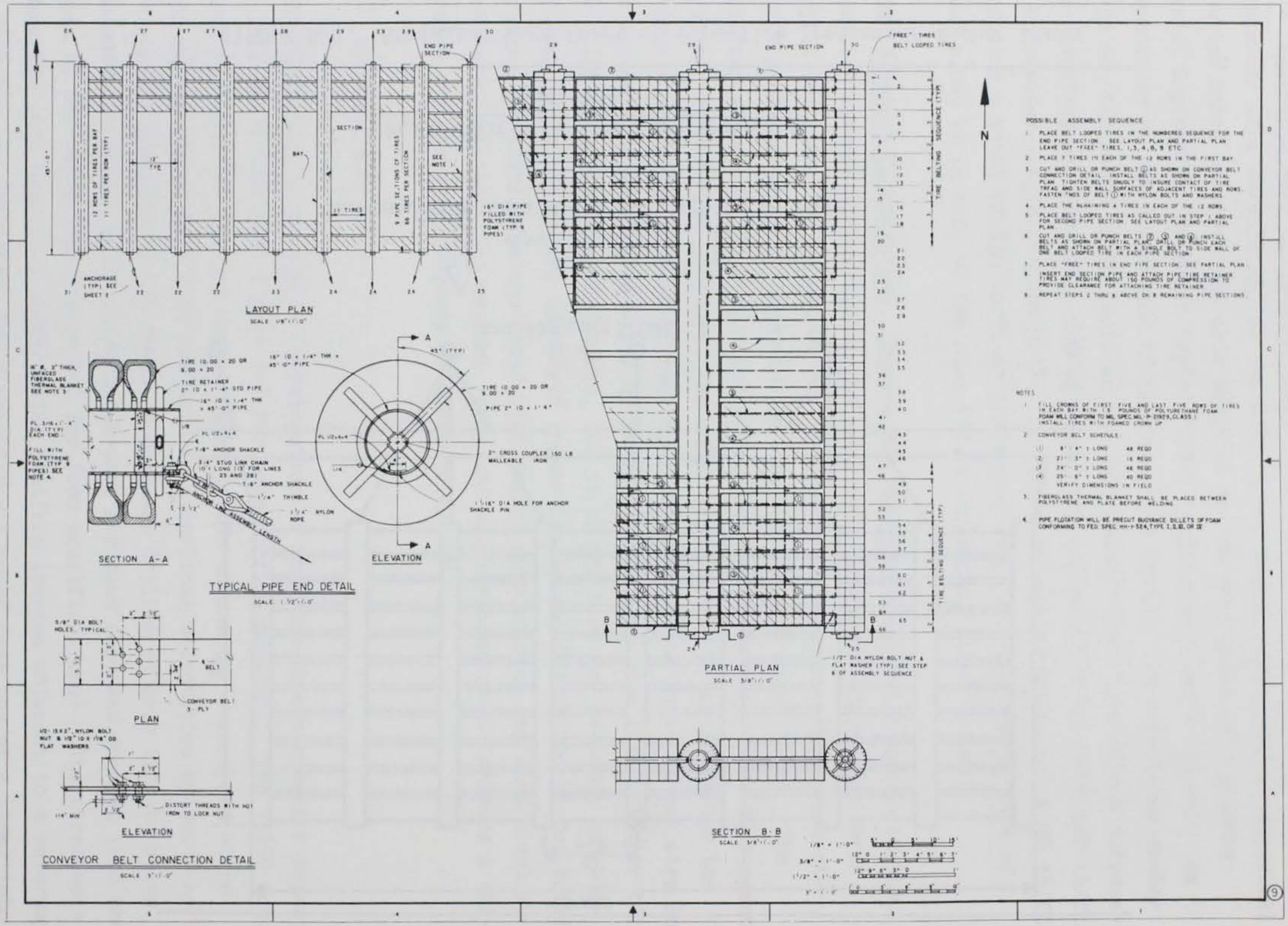

FIGURE B-2. Pipe-Tire Breakwater Plan and Details

the waterway. Construction of the breakwater closely followed the sequence described by Harms (reference 5, main report). A forklift brought the tires to the assembly platform where they were bound by loops of 5-1/2-in.-wide, 3-ply conveyor belting. A special tool fabricated from a car jack was used to tighten the belting. Holes were cut in the belting with another special tool, and the belting was fastened with five 1/2-in.-diam by 2-in.-long nylon bolts. The ends of the bolt thread were melted with a welding torch to prevent the nuts from working off the bolts. After 12 rows of 11 tires each had been fastened together, additional tires were forced into the open spaces (free tire spaces) in the 45-ft-long beamwise row of tires using a device normally used for driving sheetpiling. The breakwater was then ready to have a 16-in.-diam by 45-ft-long, schedule 40, pipe inserted into the beamwise row. This pipe was chosen because the 16-in.-diam was the largest standard size that would readily fit inside the 20-in.-diam rim of the truck tires. However, the maximum standard length of this size pipe is 40 ft. The specified length of 45 ft resulted in structural failures which are discussed in paragraph 3.01. Because the tires were not perfectly aligned, a nose cone was placed on the end of the pipe which was moved into place using a large overhead crane and then shoved through the row of tires with the forklift. To produce as tight a structure as possible, one additional tire was compressed onto each end of the pipe before the keeper pipes were installed. (This brought the total number of tires on each pipe to 66.) The completed bay was dragged into the adjacent waterway using the overhead crane and a small tugboat. This process was repeated for each of the eight bays, with launching of the completed breakwater taking place on 29 April 1982 (photos B-1 to B-21). After construction procedures had been perfected, assembly time for each bay was approximately 8 hr for two men. Adding the free tires, inserting the pipe, and moving the completed bay off the assembly platform required an additional two men and took approximately 4 hr. Construction time was considerably reduced by the use of heavy equipment and the special tools fabricated by the contractor. The pipe-tire breakwater was the first of the test structures to be moored at the test site. Hookup of the anchor lines was relatively simple and was completed on 21 June 1982 (photo B-22).

2.02 Costs. Costs for the prototype test's pipe-tire breakwater are presented below:

	Cost per Linear Foot ($)	Total Cost ($)
Pipe-Tire Breakwater (100 ft)	930	93,000
Anchor System	640	64,000
Total 1/	1,570	157,000

1/ Cost per square foot was $35.00.

3.0 Operation and Maintenance.

3.01 Field Observations. After only 3 days at the test site, five of the tire retaining keeper pipe assemblies on the end of the 45-ft-long pipes had worked loose. A close examination revealed that wave action was causing the tires on the steel pipe to roll back and forth around the axis of the pipe. The end tires rubbed against the keeper pipes and eventually unscrewed the pipes from the cross couplers. By the time repairs were made, over 20 individual keeper pipes were missing, but because the tires were held together by the conveyor belting and since each pipe had an anchor line which prevented the tires from escaping, the structure was not in danger of failing (or losing tires) in the relatively light summer winds. The solution to the problem was to lift the ends of the 16-in. pipes out of the water, to replace the 2-in. keeper pipes and cross couplers, and then to weld the keeper pipes in place. Throughout the winter of 1982 the performance and durability of the pipe-tire breakwater were observed closely. Wave attenuation appeared to be similar to that of the concrete breakwater (photos B-23 and B-24). Wave action tended to compress the tires on the pipes, somewhat reducing the effective width of the breakwater (photo B-25), and diffraction around the ends of the breakwater was obvious, particularly in aerial photographs of the test site. The low profile of the tires made visibility of the breakwater very difficult from a distance. Often the large amount of debris that collected on top of the tires was the most visible part of the structure (photo B-26). While the visual aesthetics of the tire breakwater were debated, marine life in the area did not seem to object to its presence. Harbor seals and sea birds readily appropriated the above water portion of the breakwater as a convenient refuge, while the tires provided a habitat for mussels, barnacles, and numerous species of fish underwater. A dense growth of kelp (Nereocystis luetkeana) attached to the nylon

anchor lines. The upper portion of the anchor lines became heavily covered with diatoms, hydroids, mussels (Mylitis edulis), and the red alga (Neoagardhiella). Pile perch (Rhacochilus vacca) and striped surfperch (Embiotoca lateralis) resided near the surface by the tire reef. There were both adult and young of the year of these species present. The undersides of many tires were heavily covered with barnacles (Balanus glandula), but the mussels seemed to be mainly on the tire beads (the inner rims). Inside the casings, some barnacles grew along with the jingle shell (Pododesmus cepio) and a translucent tunicate (Corella wilmeriana) (photos B-27, B-28, and B-29).

Even though the breakwater had hundreds of bolted connections that were being flexed continuously, the only maintenance performed during the winter storm period was to one keeper pipe assembly. This repair lasted through the winter, but by April 1983 the keeper pipe was completely gone; and the tires began falling off the end of the pipe and sliding down the anchor line. A switch in wind direction caused most of the tires to work their way back onto the pipe, and a makeshift repair was made (photo B-30).

Up to this point, all of the damage was relatively minor and could be repaired onsite. The first serious damage occurred during a storm on 9-10 June 1983. This storm caused one of the 16-in.-diam pipes to break at a point approximately 5 ft from one end (photo B-31). The short 5-ft section sank, but the long 40-ft section was recovered. Both sections remained attached to their respective anchor lines. An inspection of the break revealed an edge that had been prepared for welding but which had been only partially welded. The weld failed, and the pipe sections parted. On 12 July 1983, a second pipe broke, lost its styrofoam flotation, and sank before it could be recovered. On 19 July 1983, the tire keeper pipes on the north side of the center pipe failed, and the pipe was protruding approximately 20 ft to the south (photo B-32). The 45-ft-long pipe was still intact, and both anchor lines were holding.

The two 45-ft-long pipes which broke were located adjacent to each other on the west end of the tire breakwater. This situation permitted a considerable amount of wave transmission through the gap between the concrete float and the

tire breakwater; consequently, any wave attenuation data collection while the breakwater was in this condition was suspect. Also, since only the center pipe anchor lines were instrumented with anchor load cells, failure of the retaining pipe on the north side of the center pipe complicated interpretation of anchor force readings. The high probability that no meaningful data were being collected prompted a decision to remove the breakwater to prevent further deterioration.

On 5 August 1983, after 414 days of testing, the pipe-tire breakwater was removed from the West Point test site. Four Corps personnel disconnected the breakwater in approximately 3 hr. The breakwater was towed 3 miles from the test site to the Lake Washington Ship Canal by a Corps workboat (31 ft, 300 hp). The tow required 6 hr, even though tidal currents were relatively minor (photo B-33).

3.02 Posttest Inspection. On 12 August 1983 an inspection of the tire breakwater was conducted.

The short 5-ft sections of the two broken 16-in.-diam pipes were recovered. Both showed evidence of a complete, but poor, ring weld (photo B-34). The 45-ft pipe was found to have been constructed from two pieces of pipe (40 and 5 ft). Corrosion and continual flexing led to eventual failure. While the breakwater was being removed from the test site, the application of minor lateral loads inadvertently broke three more 16-in.-diam pipes. All the breaks occurred at exactly the same welded joint, 5 ft from the end of the pipe.

Ten conveyor belt connections were inspected. Eight of the connections, which use five 1/2- by 2-in. nylon bolts, had one or more broken bolts. Only those connections on the perimeter of the breakwater were accessible for inspection. Two bolt patterns were used in fastening the belting together, but no conclusions regarding their relative performance could be drawn (photos B-14 and B-15).

One conveyor belt section showed evidence of heavy wear, with approximately 25 percent of the material worn away. Otherwise the conveyor belting was in excellent condition (photo B-35).

The beads of many of the tires that encircled the pipes had worn down to the wire reinforcing. The loose wire was found wrapped tightly around the 16-in. pipes. The wear on the beads did not appear to weaken the tires significantly. The surface of the 16-in. pipe was pitted, but corrosion was not severe enough to compromise the structural integrity. The reinforced portion of the pipe where the anchor line connection was made showed very little wear.

None of the cotter keys that secured the anchor line clevises were made of stainless steel. All were corroded and could often be broken off by hand. Some pitting of the clevises was noted.

Of the 14 keeper pipes on the seven remaining 16-in. pipes, four had partly failed, and two had failed completely. Several of the 2-in.-diam keeper pipes were badly corroded, particularly in the vicinity of the threads at the cross coupler.

The urethane foam flotation was removed from four tires. The samples were weighed immediately and then dried for several months and reweighed (photo B-36). The displaced volume of each sample was then measured to allow a calculation of foam density. Foam flotation data are presented in the table below.

Sample Number	Dry Weight (lb)	Wet Weight (lb)	Saltwater Displacement (lb)	Volume (ft^3)	Density (lb/ft^3) Dry	Density (lb/ft^3) Wet
1	1.1	3.4	28.5	0.42	2.7	8.2
2	0.8	1.8	20.5	0.31	2.6	5.9
3	0.8	2.4	18.6	0.28	2.9	8.5
4	1.9	4.3	21.8	0.33	5.7	13.1
Average	1.2	3.0	22.4	0.34	3.5	8.9

Based on this information the actual flotation provided by each foamed tire was far lower than the desired 75 lb. The fact that the breakwater did not appear to have flotation problems can be accounted for by a lack of any siltation (original estimate was 11.0 lb/tire for sediment and biofouling) and much lower than anticipated anchor line forces. (The actual vertical component of the anchor line load was approximately 20 percent of the original design

estimate.) With these two corrections to the buoyancy calculations, the reserve buoyancy of the breakwater was 5,000 to 10,000 lb even if each of the 880 foamed tires provided only an average of 22.4 lb of flotation.

Additional information on the design, construction, and use of floating tire breakwaters is available from references B-3 through B-6.

APPENDIX B

REFERENCES

B-1. Harms, V. W., "Design Criteria for Floating Tire Breakwaters," Journal of the Waterway, Port, Coastal and Ocean Division, ASCE, Vol. 105, No. WW2, Proc. Paper 14570, May 1979.

B-2. Olson, R. M., Essentials of Engineering Fluid Mechanics, 2nd ed., International Textbook Company, Scranton, Pennsylvania, 1966.

B-3. Bishop, C. T., "Drag Tests on Pipe-Tire Floating Breakwaters," National Water Research Institute, Canada Centre for Inland Waters, Burlington, Ontario, Canada, November 1981.

B-4. Bishop, C. T., Harms, V. W., and Westerink, J. J., "Pipe-Tire Breakwater Model Tests Data Report," National Water Research Institute, Canada Centre for Inland Waters, Burlington, Ontario, Canada, March 1982.

B-5. Bishop, C. T., "Floating Tire Breakwater Buoyancy Requirements," National Water Research Institute, Canada Centre for Inland Waters, Burlington, Ontario, Canada, May 1982.

B-6. Cornell University, "Guidelines for the Effective Use of Tire Breakwaters," Bulletin No. 197, Cornell University, Ithaca, New York, 1982.

Photo B1. Truck tires (1,650) being prepared for assembly of the pipe-tire breakwater.

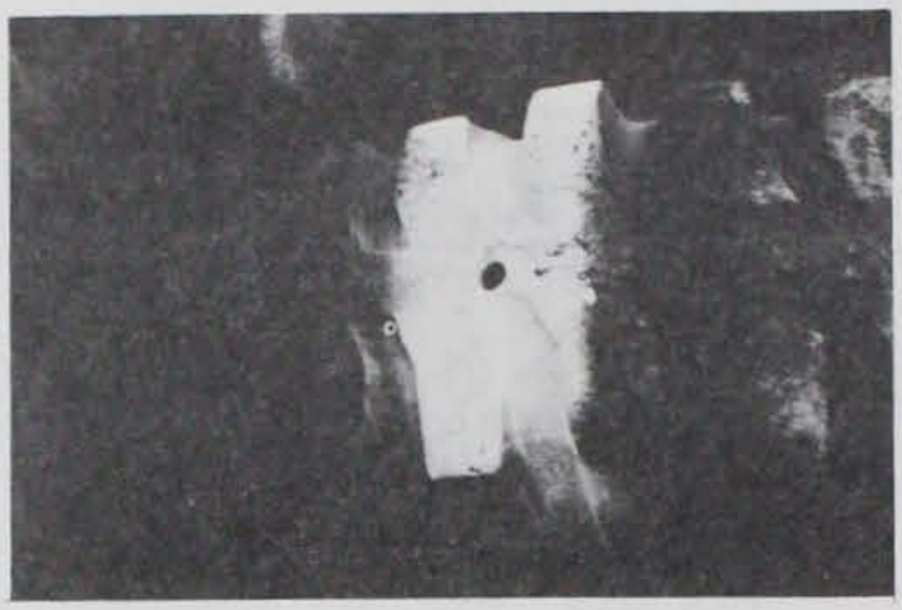

Photo B-2. Closeup showing hole for draining water from tires.

Photo B-3. Photo depicting urethane foam that was sprayed into the tires.

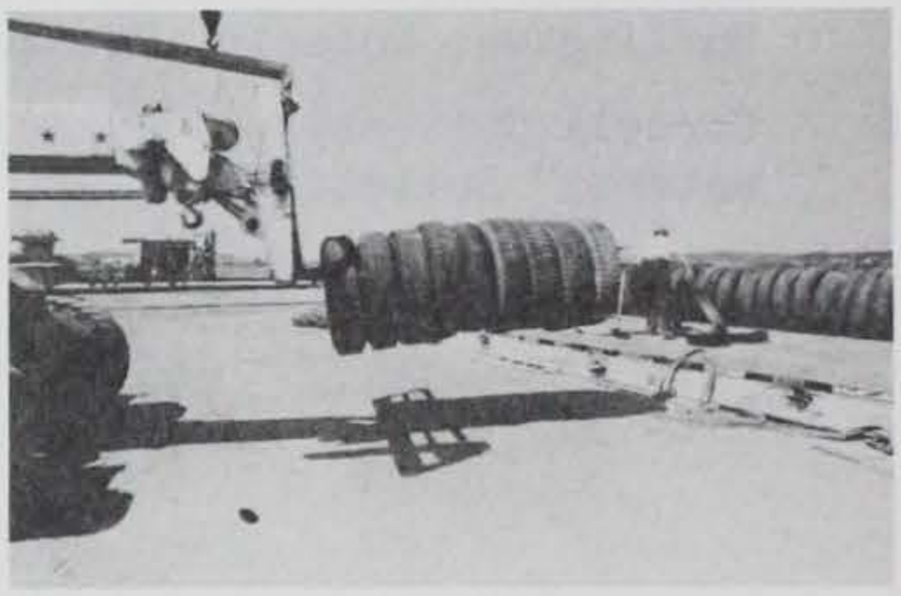

Photo B-4. A fork lift moving tires to the assembly platform.

Photo B-5. Placing the first row of 11 tires (note belting around center 3 tires).

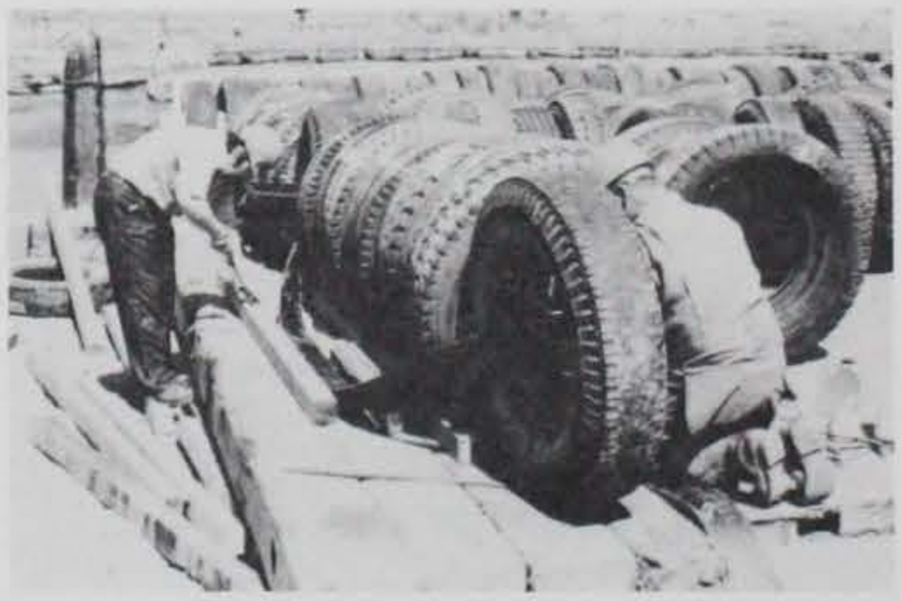

Photo B-6. Belting being placed around the first row of tires.

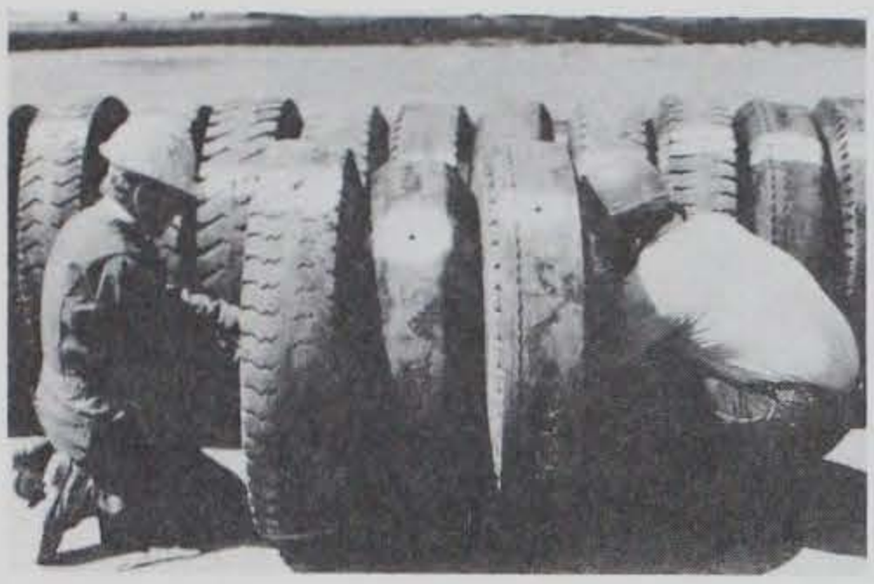

Photo B-7. Center tires of two adjacent rows being joined with belting.

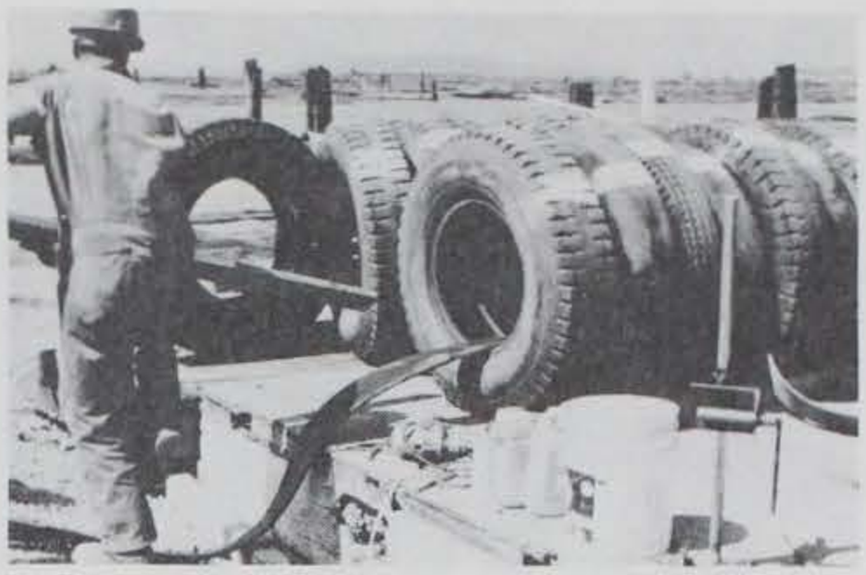

Photo B-8. Belting being shoved through the tire row on a wood plank.

Photo B-9. A device, fashioned from an auto jack, being used to tighten belting.

Photo B-10. Close-up of device for tightening belting.

Photo B-11. Marking the hole pattern on the belting.

Photo B-12. Holes being drilled in belting (locking pliers holding belting in place).

Photo B-13. Closeup showing a punch-shaped bit used to make holes in the tires and belting.

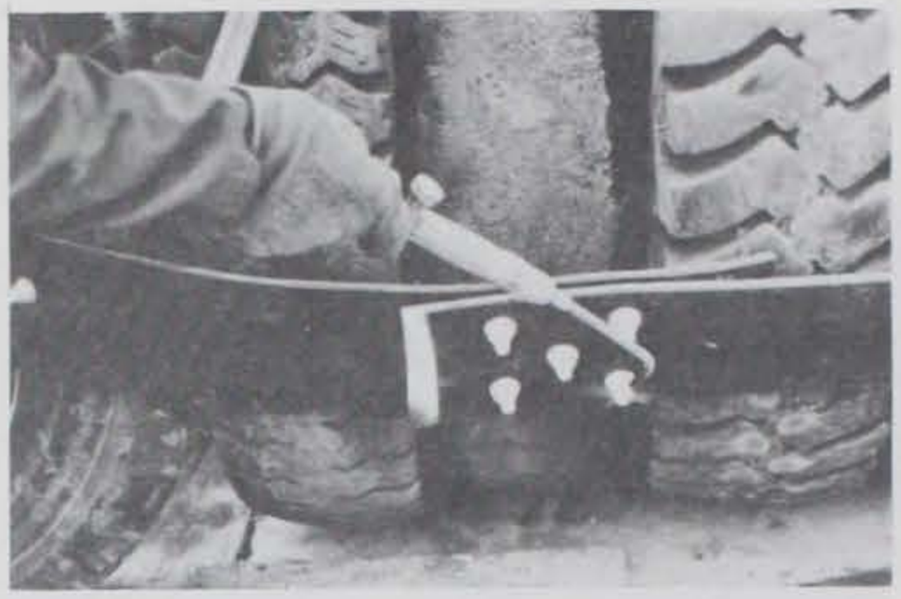

Photo B-14. Melting the ends of the 1/2-in.-diam nylon bolts (note 2-1-2 bolt pattern).

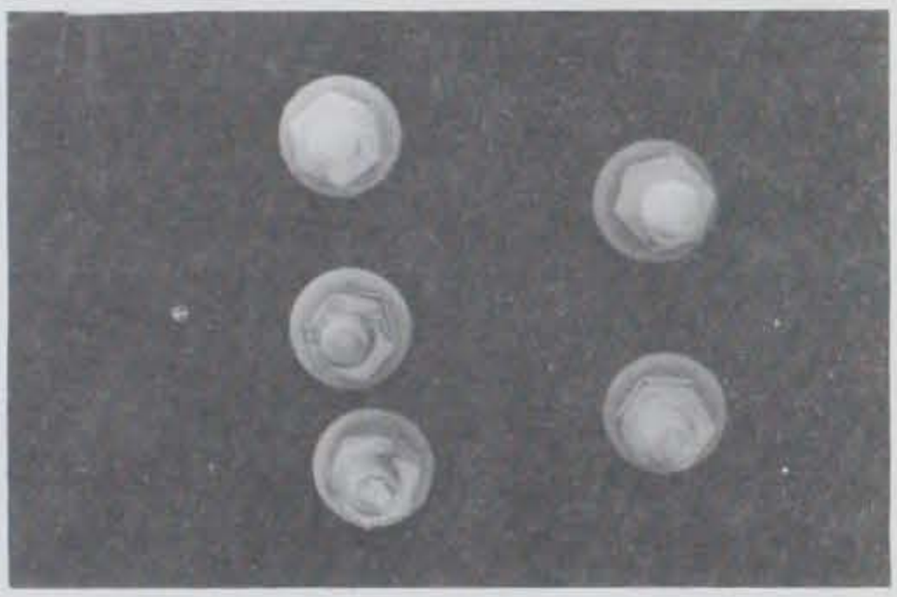

Photo B-15. Photo depicting 3-2 bolt pattern used for the majority of connections.

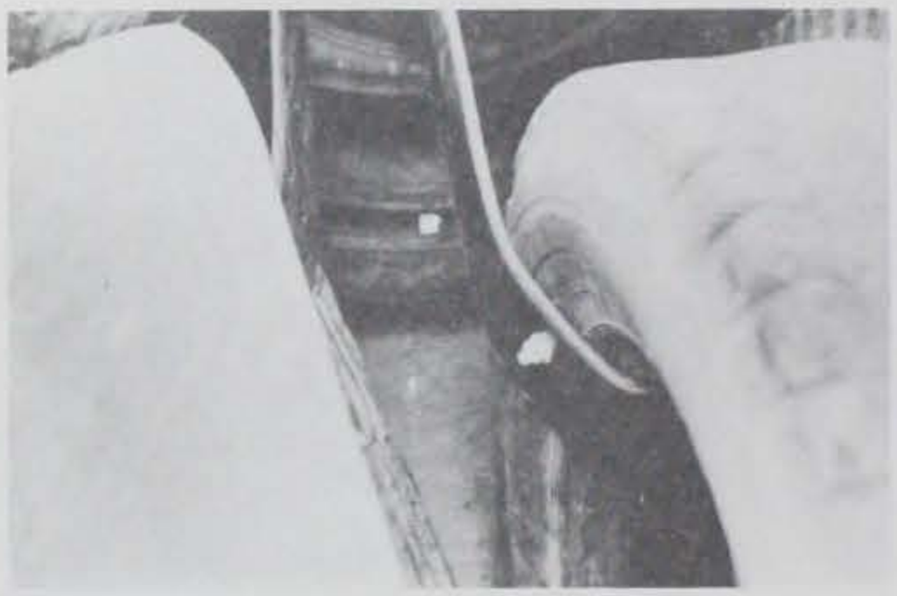

Photo B-16. Closeup showing bolt which fastened the belting to the tires (all such bolts broke, with no adverse consequences).

Photo B-17. Photo showing two bays of tires after being assembled on the platform.

Photo B-18. Free tires being shoved into the beamwise row prior to insertion of the pipe.

Photo B-19. Styrofoam-filled pipe being shoved through a beamwise row of tires.

Photo B-20 Securing the keeper pipes.

Photo B-21. Launching of completed pipe-tire breakwater.

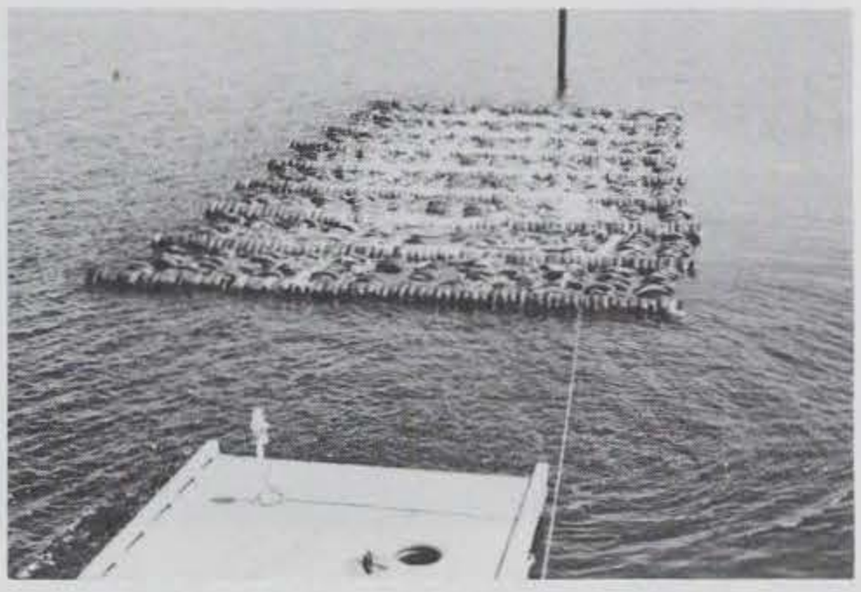

Photo B-22. Pipe-tire breakwater in position at the West Point test site.

Photo B-23. 1.5-ft-high waves washing onto the pipe-tire wave breakwater.

Photo B-24. Photo showing the wave attenuation capabilities of the breakwaters to be equal.

Photo B-25. Wave action compressing the tires on the pipes.

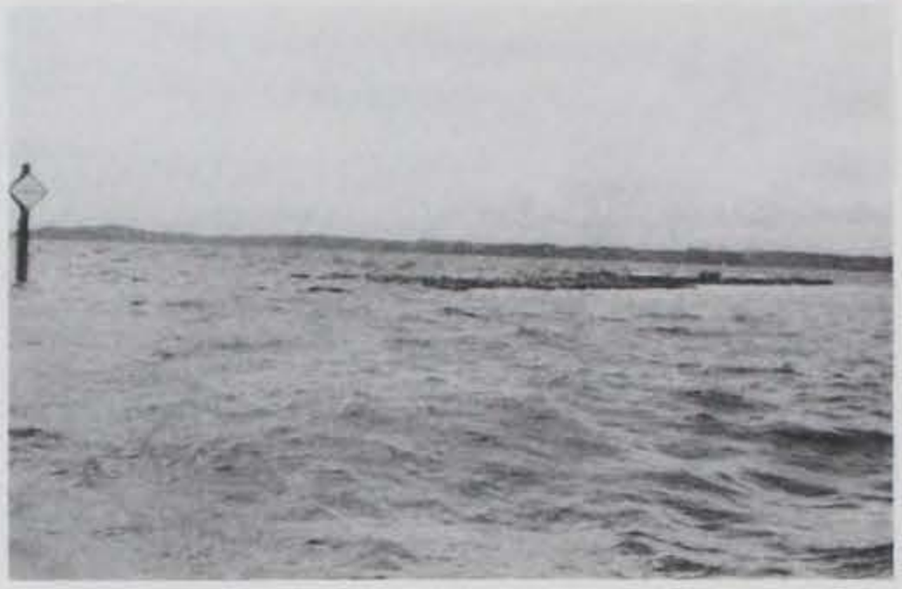

Photo B-26. Photo illustrating low visibility of the pipe-tire breakwater during bad weather.

Photo B-27. Harbor seal resting on the tires (note kelp attached to anchor lines).

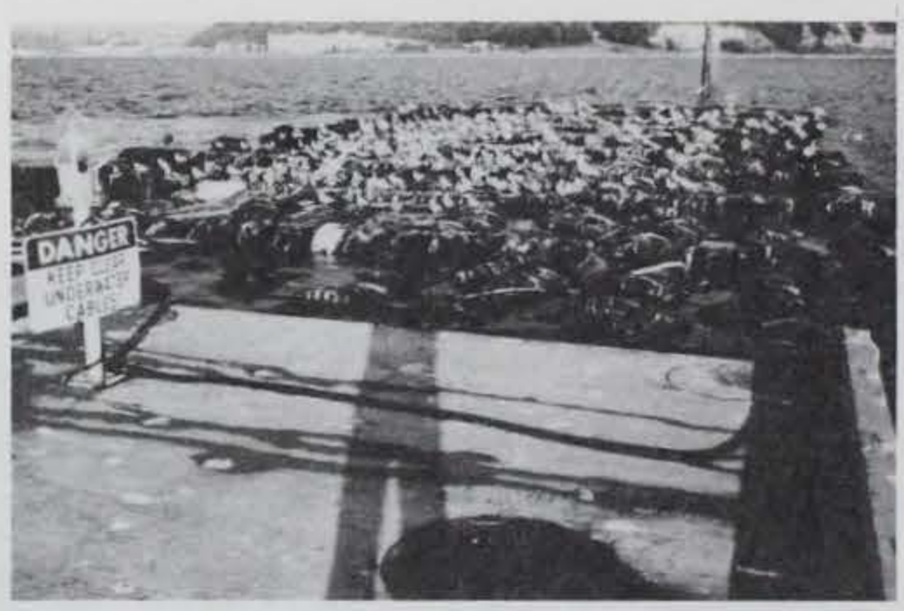

Photo B-28. Birds resting on the pipe-tire breakwater.

Photo B-29. Underwater photo showing how the inside of the tires provided an excellent habitat for mussels.

Photo B-30. Photo showing keeper pipe repair which prevented additional tires from falling off.

Photo B-31. A 45-ft pipe pulling out after breaking at a welded joint.

Photo B-32. The center pipe protruding from the breakwater after failure of keeper pipes.

Photo B-33. The tire breakwater being removed from the test site on 5 August 1983.

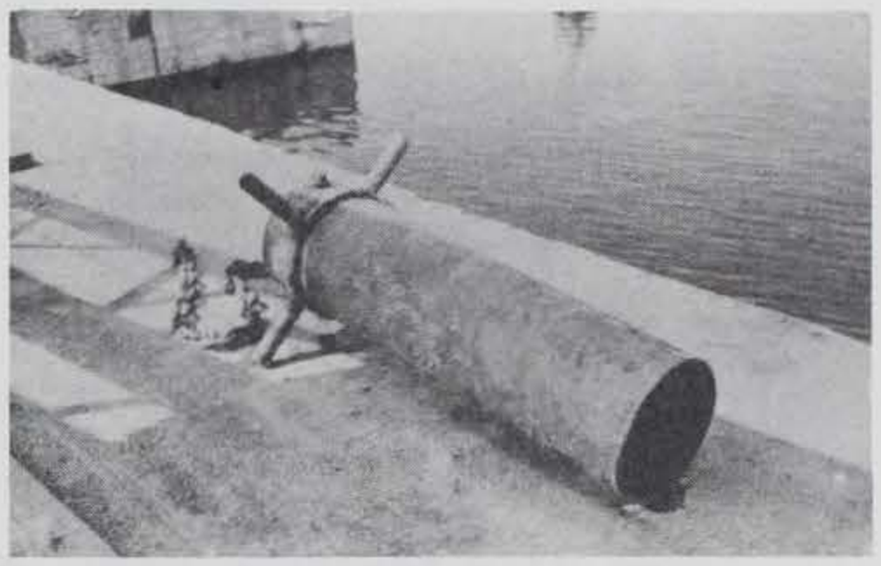

Photo B-34. Photo showing a clearly broken 5-ft section of pipe indicating an incomplete weld.

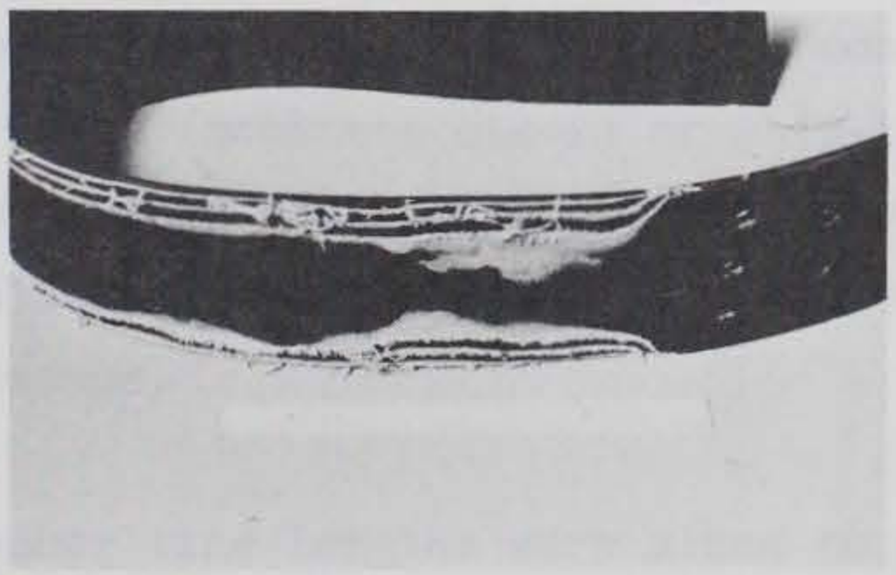

Photo B-35. Photo depicting a loop of worn belting (approximately 20 percent).

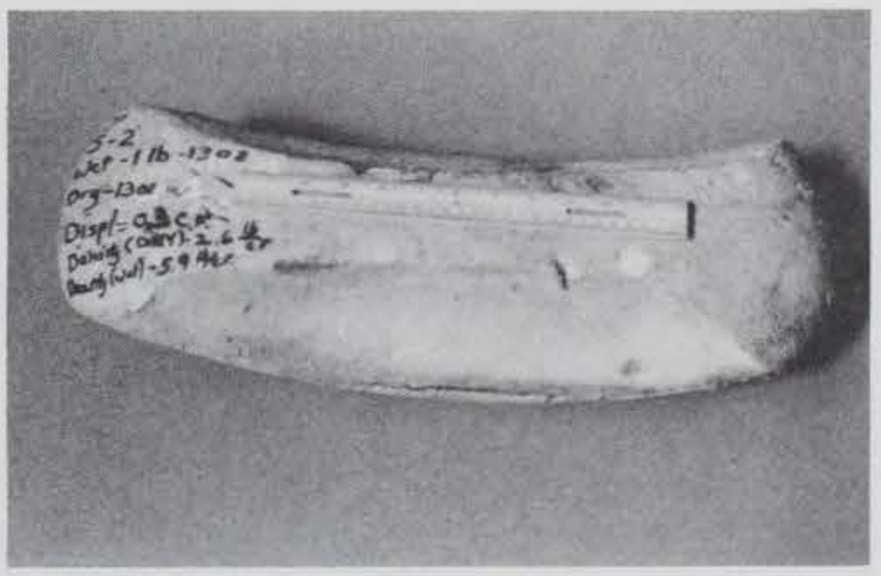

Photo B-36. Urethane foam flotation after being removed from a tire.

APPENDIX C

ANCHOR SYSTEM: DESIGN, CONSTRUCTION, OPERATION, AND MAINTENANCE

1.0 Anchor System Design.

1.01 Original Design Assumptions. Design anchor line loads for both the concrete breakwater and the pipe-tire breakwater were calculated for the design wave condition of H_s = 6 ft , T = 5 sec combined with tidal and wind driven current of 4 fps. The total estimated maximum anchor loads were 44,000 lb per anchor for the concrete breakwater and 6,000 lb per anchor for the pipe-tire breakwater.

1.02 Description of Concrete Breakwater Anchor System. The concrete breakwater was anchored in place by ten 30-ft-long steel H-piles (HP 14 by 102) embedded their full length (photo C-1). Anchor lines consisted of 1-3/8-in.-diam galvanized bridge rope with 15 to 30 ft of 1-1/4-in. stud link chain at each end (photos C-2 and C-3). Details of the concrete breakwater anchor system are shown on the construction drawings in figure A-11.

The bridge rope anchor line was chosen because, when combined with an anodic corrosion protection system, it appeared to be a cost-effective design if maintenance over a 50-yr life is taken into account. The prototype test breakwater anchor lines did not have anodes attached because of the short test duration. For the design conditions, the steel H-piles were considered the most suitable type of anchor for this project because the cost of steel pile anchors was considerably less than alternatives such as gravity (concrete block) or ship-type (stockless) anchors, and the consequences of dragging a gravity or ship-type anchor over either a sewer outfall lying to the north or a cable area to the south were potentially very serious.

Anchor line lengths were sized to provide a scope no steeper than 1 vertical to 4.5 horizontal. Actual catinary measurements of the concrete breakwater's anchor line No. 7 were made by divers during the test program. Results of these measurements are shown in figure C-1. Positioning of the four corner

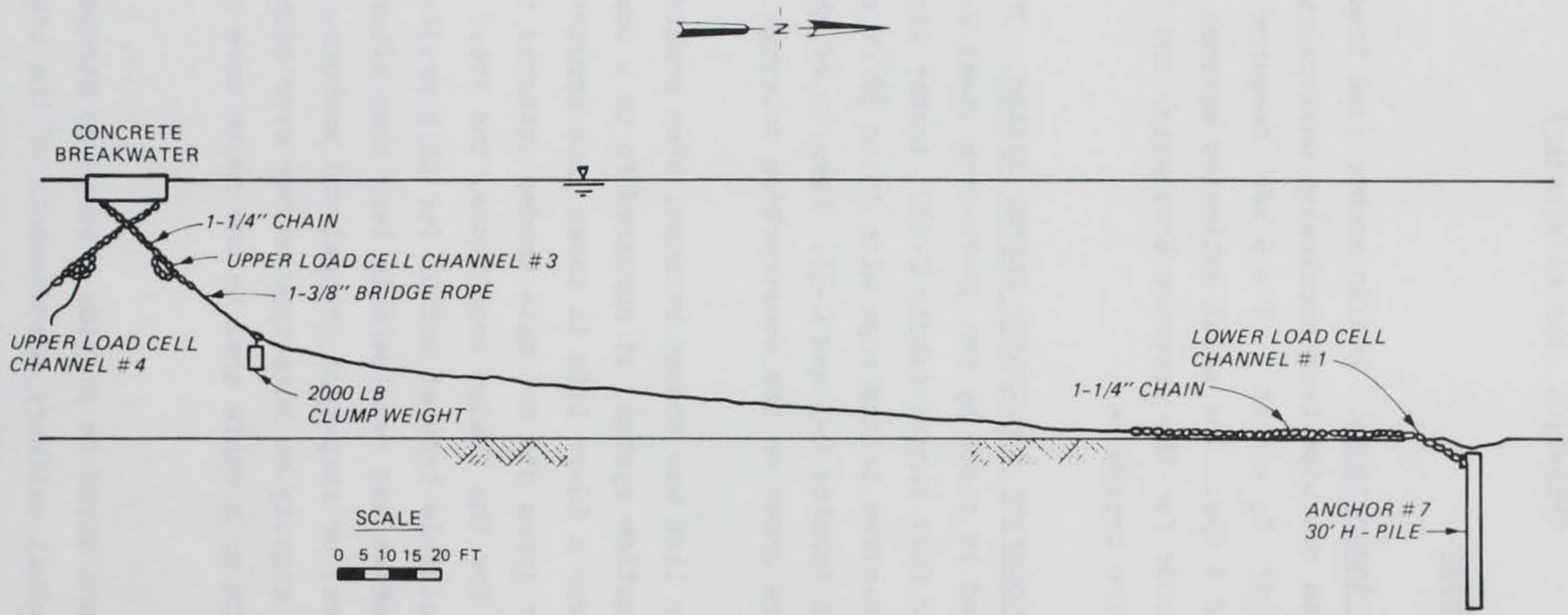

FIGURE C-1. Measured Catinary for Anchor Line No. 7

H-pile anchors at a 5-deg inward angle was designed to provide resistance to longitudinal displacement of the breakwater.

A 2,000-lb (submerged weight) concrete clump weight was attached 44 ft from the upper end of each anchor line. The purpose of this design was to produce a more even anchor line tension over the full range of tides and thereby to reduce the horizontal excursions of the breakwater, particularly at lower tide elevations. Initial anchor line tensions were 5,000 ± 1,000 lb. In September 1983, the clump weights were removed for the last 4 months of testing to determine how their absence would affect float motions, anchor forces, and wave attenuation. Initial (i.e., ambient) anchor line tensions dropped from 5,000 lb to approximately 1,500 lb after removal of the clump weights.

1.03 Description of Pipe-Tire Breakwater Anchor System. The pipe-tire breakwater was anchored alongside the concrete breakwater with ten 20-ft-long steel H-piles (HP 12 by 53). Anchor lines consisting of 1-1/4-in.-diam, three-strand nylon rope with 10 ft of 3/4-in. stud link chain at each end were attached to both ends of each 16-in.-diam pipe (photo C-4). The scope for these anchor lines was no steeper than about 1 vertical to 4 horizontal. The center and end H-piles had one anchor line each, while the remaining four anchor piles were attached to three anchor lines apiece. The four end pilings were offset at an outward angle to counteract the opposing longitudinal component of force from the adjacent anchor lines. Details of the pipe-tire breakwater anchor system are shown on the construction drawing in figure A-11.

1.04 Laboratory Tests of Anchor Lines. Prior to the installation of the breakwaters at the West Point test site, the specified breaking strength of the anchor lines was verified in laboratory tests conducted at the University of Washington's 2.4-million-pound Baldwin testing machine (photo C-5). The 1-3/8-in.-diam steel rope failed in the center of the test specimen (at a load of 204,000 lb), 29,400 lb above its rated strength of 175,000 lb. Elongation of the 10-ft-long test specimen, when the break occurred, was 1.8 percent. The socket that was attached to each end of the test rope was the same type used on the concrete breakwater's anchor lines.

The 1-1/4-in.-diam nylon rope was available in two stiffnesses: soft lay and

hard lay. Ten-foot-long test specimens of each stiffness were tested both dry and wet (1-month soak in fresh water). The table below shows the breaking strength and elongation at failure. Only the hard lay test specimen had a breaking strength greater than the required 37,500 lb (photo C-6). The hard lay breaking strength was nearly 25 percent greater than that for the soft lay for the dry test specimens. Soaking the test specimens in water reduced the breaking strength by 14 percent for the hard lay and 10 percent for the soft lay. In June 1984 an 11-ft-long section of one nylon anchor line was recovered from the test site to determine the effects of wear and aging. This rope was tested by the U. S. Army Engineer Waterways Experiment Station, Structures Laboratory. Two of the three strands broke 3 ft from one end at a load of 27,000 lb, with an elongation of 65 percent at maximum load. The original stiffness of this test specimen (hard or soft) could not be determined. Depending on its original stiffness, the breaking strength of the used anchor line was reduced by either 19 percent (soft lay) or 32 percent (hard lay).

Test Specimen	Maximum Load (lb)	Elongation (%)
Hard Lay, Dry	45,900	44
Hard Lay, Dry	46,600	46
Hard Lay, Wet	39,750	44
Soft Lay, Dry	37,450	40
Soft Lay, Dry	36,800	45
Soft Lay, Wet	33,400	33

2.0 Anchor System Installation.

2.01 Foundation Conditions. Prior to final selection of West Point as the prototype test site, an investigation of the foundation conditions at the site was made. In April 1981, a drill barge was used to take bore samples at five locations near the proposed anchor pile positions (photo C-7). The investigation found that the anchor locations were on a relatively steep (approximately 1 vertical on 6 horizontal) marine slope characterized by a thick mantle of medium dense sand and gravelly sand with the gravel content usually increasing with depth. These materials are probably underlain by very dense glacial deposits at depths greater than 35 ft. Foundation exploration at the anchor

pile extremities was conducted at the locations shown in figure C-2, and boring logs are shown in figure C-3. The borings indicated that stake pile anchors could be driven to depths of 25 to 35 ft.

2.02 Pile Driving. The pilings were driven using a Vulcan 010 hammer with a 10,000-lb ram weight and an 8,000-lb mandrel (photo C-8). A special fitting

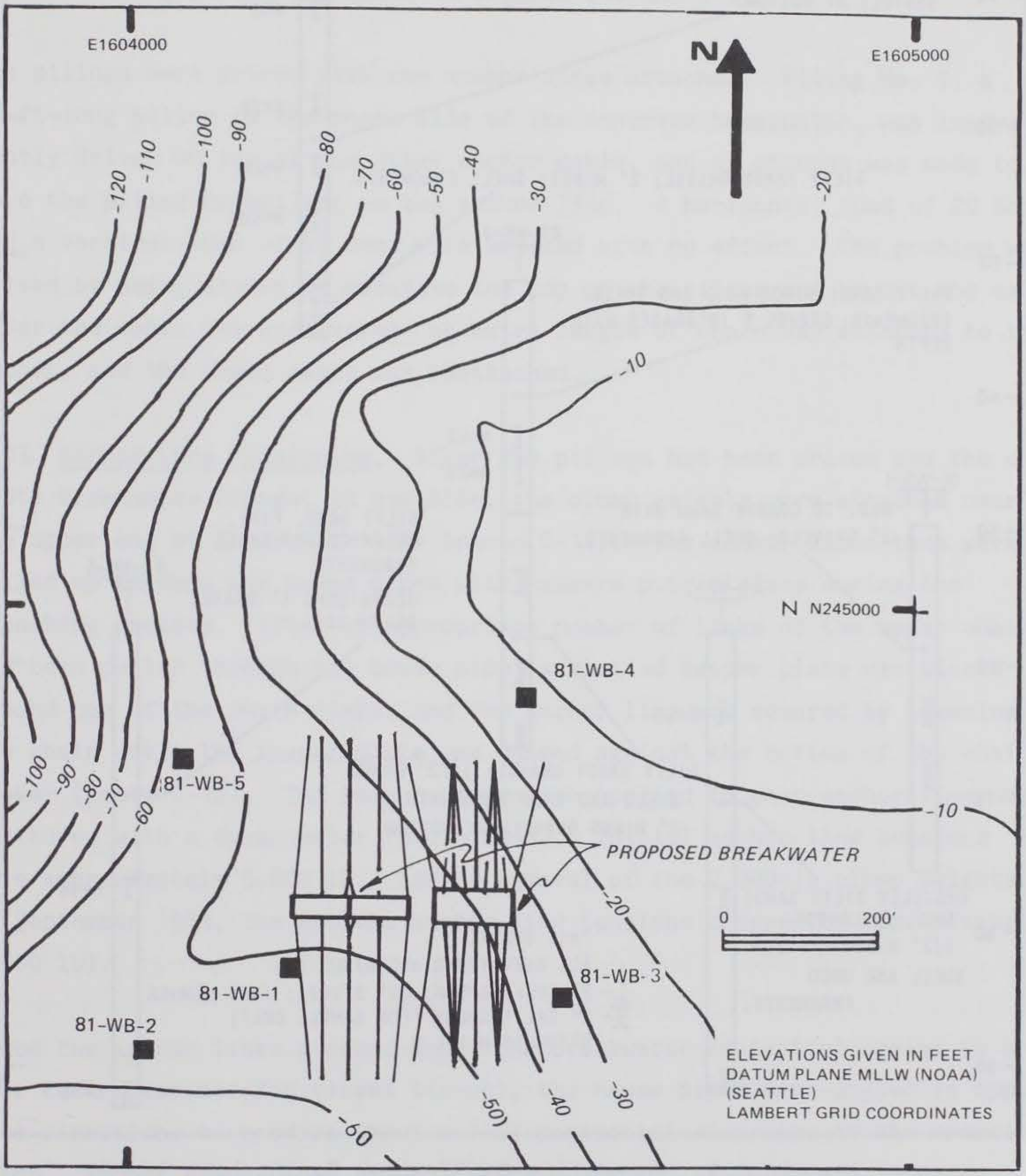

FIGURE C-2. Foundation Exploration Test Hole Locations

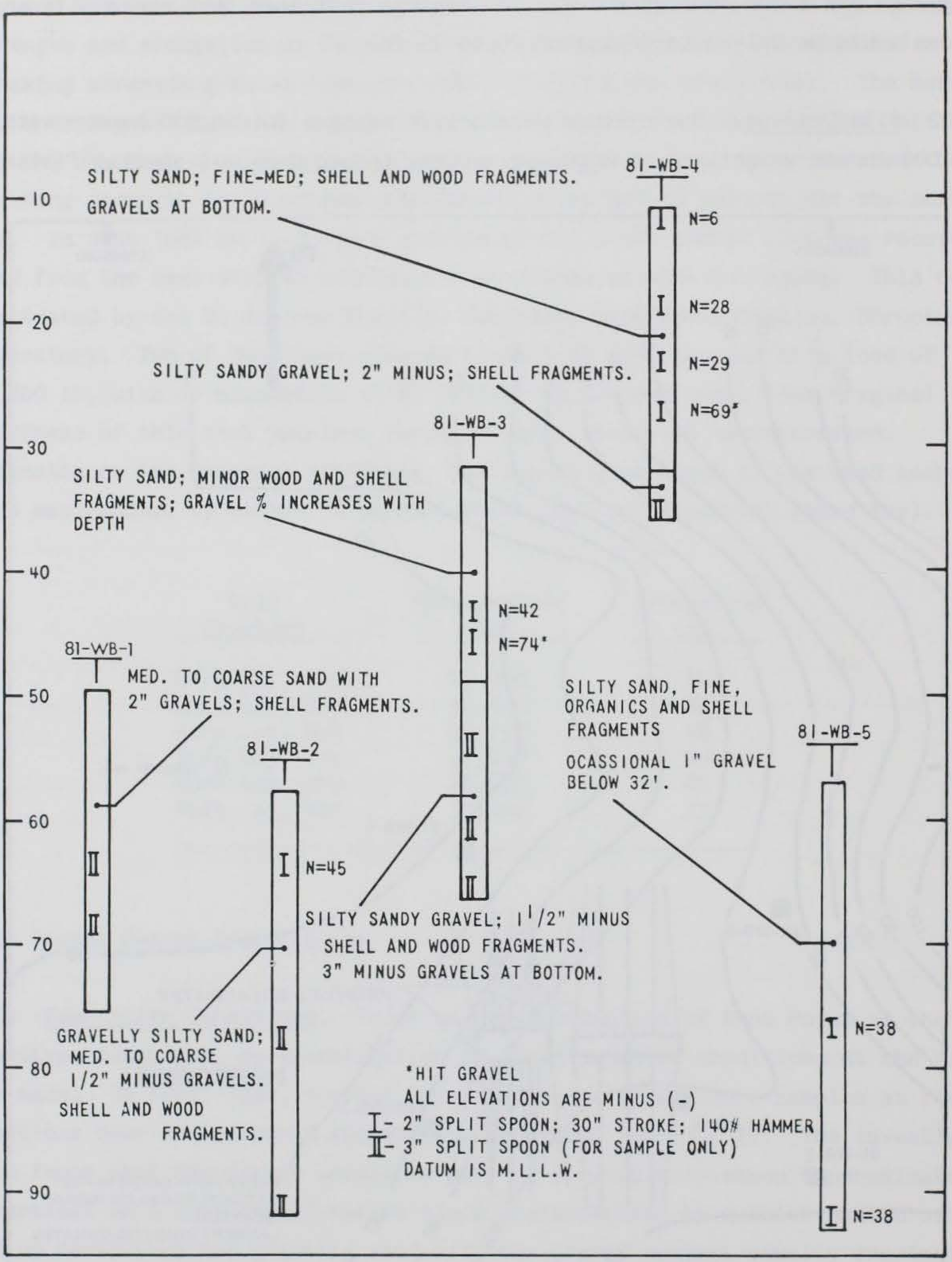

FIGURE C-3. Foundation Exploration Boring Logs

was attached to the mandrel to hold the piling in proper alignment while it was being driven (photo C-9). Two 1/2-in.-diam bolts held the piling and fitting together until the piling was lowered to the bottom. The first blow of the pile driver hammer sheared the bolts, allowing the mandrel to be brought back to the surface after the piling had been driven approximately 3 ft below the mudline (photo C-10). Typical pile driving records for the 30-ft and for the 20-ft-long piling are shown in figures C-4 and C-5.

The pilings were driven with the anchor lines attached. Piling No. 7, a 30-ft-long piling on the north side of the concrete breakwater, was inadvertently driven on top of the steel anchor cable, and an attempt was made to remove the piling by pulling on the anchor line. A horizontal load of 20 tons and a vertical load of 50 tons were applied with no effect. The problem was solved by using divers to excavate the top of the piling and to cut the cable. After the cable was resocketed, an extra length of chain was attached to the anchor, and the steel cable was reattached.

2.03 Anchor Line Tensioning. After the pilings had been driven and the concrete breakwater brought in position, the clump weights were attached near the upper end of the anchor line (photo C-11). The anchor lines then were pulled up through the hawse pipes with hawsers put in place during the launching process. After an appropriate number of links of the upper chain had been pulled through the hawse pipe, a slotted keeper plate was placed around one of the chain links, and the anchor line was secured by lowering the chain until the keeper plate was jammed against the bottom of the chain locker (photo C-12). The amount of tension applied to each anchor line was monitored with a dynamometer (photo C-13). Initial anchor line tensions were approximately 5,000 lb. (After removal of the 2,000-lb clump weights in September 1983, the ambient anchor line tensions dropped to approximately 1,500 lb).

Since the anchor lines crossed under the breakwater (a typical design to provide keel clearance for vessel tie-up), the hawse pipes were angled in opposite directions to produce about a 1-ft horizontal clearance at the crossing point. Anchor lines (Nos. 1 and 6) were pulled up in the wrong sequence, and they rubbed against each other. By the time an underwater inspection

PILE PLACEMENT LOG

Date Apr 29, 1982 Sheet 8 of 21

Floating Breakwater Prototype Test Program
West Point, Seattle, Washington
Contract No. DACW67-81-C-0208

American Construction Co., Inc.
411-13th Street
Everett, WA 98201
Job No. 50-81

Pile: Type HP 12 x 53
Length 20'

Hammer: Make & Mod. Vulcan 010
Stroke 39"
Ram Weight 10,000 lb

Penetration calculation:

Before pile is driven and with pile tip resting on the bottom:

Sounding 57-

Water line reading on mandrel	____'	
+ pile length	____'	
= tip to water line	____'	
- tide reading	-0.6'	
= bottom elevation	52.4'	

After pile is driven:

Water line reading on mandrel	57'	
- Tide reading	-0.6'	
= Top of pile elev.		-57.6'

Mandrel: Material 24" Steel Pipe
Weight 8000 lbs
Length 93'

Driving: Finish Time 1503
Start Time 1458
Driving Time ____

Coordinates:
Calculated: N 244,310.00
E 1,604,908.00
Final: N SAME
E

Remarks: Attached Load cell to lower chain

Ft	Blows	Pile No. 23					
0							
		Ft	Blows	Ft	Blows	Ft	Blows
1		11	5	21		31	
2	V	12	5	22		32	
3	1	13	5	23		33	
4	1	14	4	24		34	
5	2	15	5	25		35	
6	2	16	5	26		36	
7	2	17	6	27		37	
8	2	18	6	28		38	
9	3	19	8	29		39	
10	3	20	12	30		40	

Recorder L O Knutson

FIGURE C-4. Pile Placement Log I

PILE PLACEMENT LOG

Date May 3, 1982 sheet 14 of 21

Floating Breakwater Prototype Test Program
West Point, Seattle, Washington
Contract No. DACW67-81-C-0208

American Construction Co., Inc.
411-13th Street
Everett, WA 98201
Job No. 50-81

Pile: Type HP 14x102
Length 30'

Hammer: Make & Mod. Vulcan 010
Stroke 39"
Ram Weight 10,000

Mandrel: Material 24" Steel Pipe
Weight 8,000 lbs
Length 93'

Driving: Finish Time 1529
Start Time 1517
Driving Time

Penetration calculation:

Before pile is driven and with pile tip resting on the bottom:

Water line reading on mandrel Soynding 72 '
+ pile length '
= tip to water line '
- tide reading 8± '
= bottom elevation 63± '

After pile is driven:

Water line reading on mandrel 77 '
- Tide reading 8± '
= Top of pile elev. -68± '

Coordinates:
Calculated: N 244,273.00
E 1,604,212
Final: N SAME
E

Remarks: Installed load cell "E" on lower chain

Ft	Blows	Pile No. 2					
0							
		Ft	Blows	Ft	Blows	Ft	Blows
1		11	4	21	7	31	11
2		12	4	22	9	32	14
3	V	13	5	23	8	33	13
4	1	14	6	24	8	34	12
5	2	15	7	25	8	35	22
6	3	16	8	26	8	36	
7	2	17	8	27	9	37	
8	2	18	8	28	10	38	
9	3	19	8	29	11	39	
10	5	20	8	30	12	40	

Recorder L S Knudson

FIGURE C-5. Pile Placement Log II

discovered the problem 3 months later, several tenths-of-an-inch of the steel anchor chain had been worn away (photo C-14). Anchor line No. 6 was replaced with the aid of commercial hard-hat divers and US Army Corps of Engineers (Corps) equipment and personnel (photo C-15).

Emergency operations such as this, which required the use of commercial

divers, a large Corps floating plant, and six to eight deck personnel (in addition to a four-man dive team) cost approximately $3,000 per day of work. The exposed location of the test site added the complication of uncertain weather. On several occasions, scheduled repair work had to be canceled because of high winds. Cancellations of this sort cost between $500 and $1,000 each.

2.04 Anchor Line Stiffness Test (Pull Test). On 18 August 1983, a marine tugboat was used to pull on the concrete breakwater with varying loads while surveying instruments measured horizontal displacements of the breakwater, and load cells monitored anchor line forces and tow line loads (photos C-16 and C-17). This test was conducted to obtain simultaneous measurements of breakwater lateral displacement and the resisting anchor force. Results of the test are shown on the plot of anchor line force versus horizontal displacement (figure C-6). The anchor stiffness (slope of this line at any point) varied

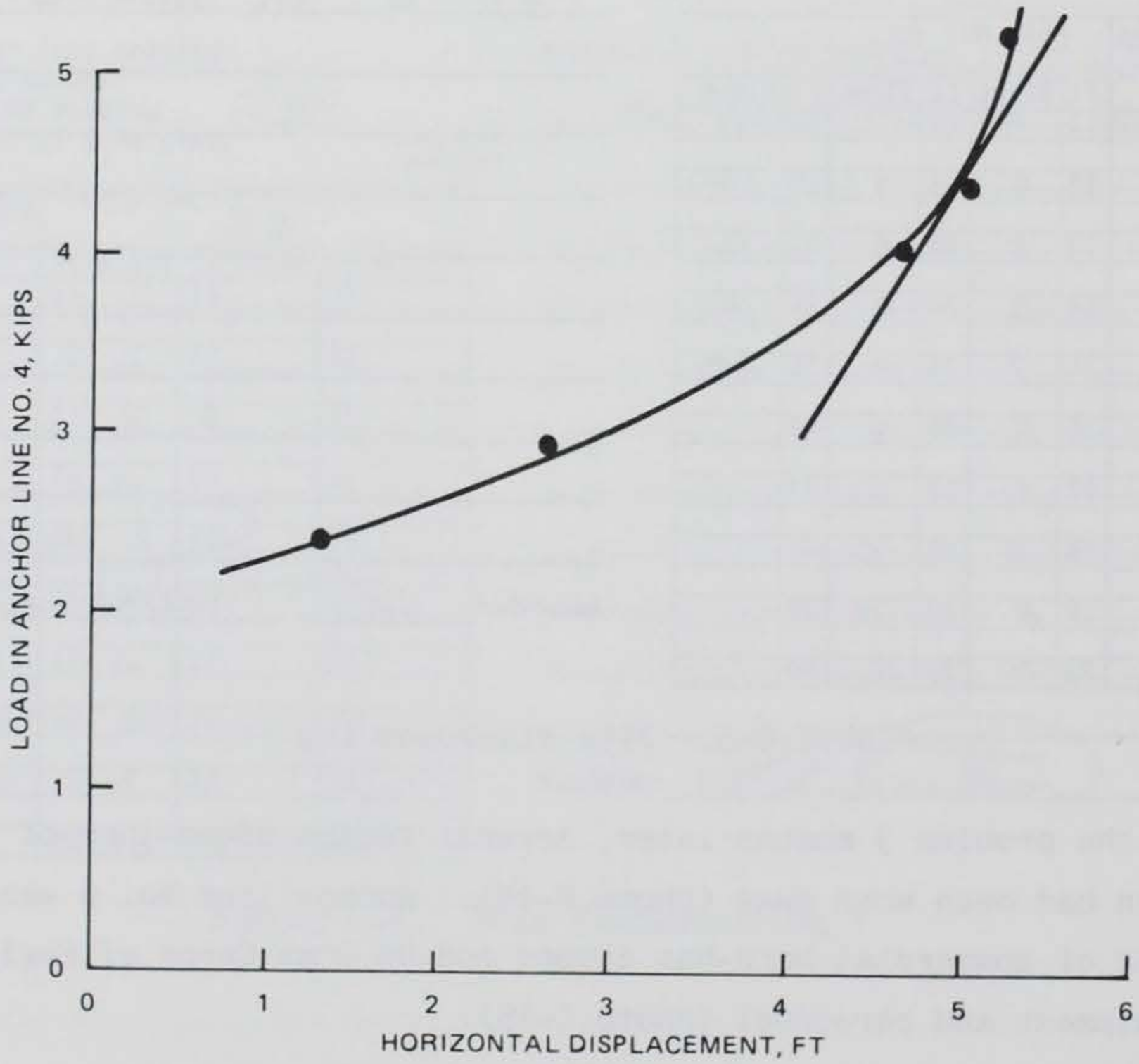

FIGURE C-6. Concrete Breakwater Anchor Line Pull Test: Anchor Line Load versus Horizontal Displacement

from 300 lb/ft, when the load in the anchor line was 2,000 lb above ambient, to 1,700 lb/ft at a load of 5,000 lb above ambient. The rapidly increasing anchor stiffness measured in this test explains why visual observations of the concrete breakwater did not detect a measurable lateral displacement even in fast currents or high waves (photo C-18).

At the time of the pull test, the two concrete floats were rigidly bolted together, and the clump weights were still attached to the anchor lines. The ends of a Y-shaped pulling line were attached to the breakwater at the lifting eyes located 15 ft in from each end of the floats. The pulling hawser from the tug was attached to a snatch block which was allowed to move freely on the cable running between the two lifting eyes. This arrangement was used to assure that the same pulling load was applied to each end of the breakwater. Load cells were placed in both ends of the pulling line near each lifting eye.

The tugboat had considerable difficulty pulling exactly at a right angle to the breakwater. Since the anchor system was fairly compliant along the longitudinal axis, large excursions were measured when the tug pulled to one side or the other. Longitudinal movements of up to 34 ft were measured; so care was taken during the analysis of the pull test data to select only those measurements that were made when the tug was pulling perpendicular to the breakwater (i.e., minimal excursions in the longitudinal east and west directions).

3.0 Operation and Maintenance.

3.01 Wear and Corrosion. Except for the installation difficulties discussed previously in this appendix, no problems at all were experienced with the anchor systems of the test breakwaters. On the concrete breakwater anchor line, very little wear was observed on the keeper plates, chain, shackles, and sockets in the anchor line itself (photo C-19). The only significant wear point appeared at the shackle that attached the clump weights to the anchor lines (photo C-20). The shackles that attached the clump weights to the anchor lines of the south side of the breakwater were worn considerably more than those on the north side. The predominant wave approach was from the south, but exactly why this should cause a marked difference in the wear of the clump weight shackles can only be surmised. Corrosion of the concrete

breakwater anchor line hardware did not appear to be significant; however, the galvanizing was completely gone from the steel bridge rope, and all the individual strands of the bridge rope that were examined were noticeably rusted (photo C-21). Several strands in the vicinity of the clump weight attachment clamp had broken. Some algae attached to the upper chains of the concrete breakwater anchor lines. Virtually no marine growth took hold on the galvanized anchor lines, but mussels, tunicates, and anemones had begun to attach to the clump weights by the time these weights were removed in October 1983 (photo C-22).

The pipe-tire breakwater anchor line showed only minor wear at the attachment points. The eye splices, shackles, and chain were in excellent condition after 1 yr of hard use. However, the cotter keys that secured the shackle nuts were obviously not made of corrosion resistant material and were nearly destroyed by the time testing of the pipe-tire breakwater was complete (photo C-23). (All cotter keys on the concrete breakwater were stainless steel and were not corroded.) The pipe-tire breakwater anchor lines proved to be an excellent substrate for marine growth (photo C-24). Because the anchor lines descended at a shallow angle, kelp attached to them and grew to the water surface in an area 50 ft to either side of the breakwater. The kelp was an additional attraction for the artificial reef community that was establishing itself in, on, and around the breakwater.

3.02 Anchoring and Unanchoring Procedures. After the initial anchoring of the test breakwaters, the concrete breakwater was removed three times and re-anchored twice. The pipe-tire breakwater was not removed until the end of its test period.

The first time the concrete breakwater was unanchored, the Corps' debris boat, Puget, was used to lower each anchor line to the bottom with a 70-ft-long, 1/2-in.-diam steel rope (photo C-25). The reanchoring plan called for retrieving the anchor lines without using divers; consequently, surface floats and 100-ft-long lengths of 3/4-in.-diam polypropylene rope were fastened to each of the 1/2-in. steel ropes. When the breakwater was brought back to the test site by the Puget for the first reanchoring, divers were hired to stand by in case the original plan failed. Soon after the Puget arrived at the

site, the complexity of the situation became evident. The divers reported that all the retrieving lines were severely tangled. Several hours of work by hard-hat divers were required to straighten the retrieving lines and reanchor the breakwater (photos C-26 and C-27).

Another method of unanchoring and reanchoring was tried when the breakwater was removed for the second time. Large polypropylene hawsers were attached to the clump weight shackle on the four corner anchors by divers. Then the anchor lines were lowered to the bottom with a double length of 3/4-in. poly line which was retrieved after the anchor line was resting on the bottom (photos C-28 and C-29). Care had to be exercised in choosing the dropping order to avoid applying a twisting torque to the breakwater. Upon returning to the test site, the divers temporarily moored the breakwater to the four corner hawsers which had been left floating free during the breakwater's absence. A diver then attached a lifting rope to each of the anchor lines which were laid out on the bottom in perfect order (photo C-30). This time, the reanchoring process went very smoothly and was completed in less than 1 hr of diving time (photos C-31 and C-32).

The final unanchoring was the easiest of all. After the breakwater had been secured to the four large hawsers (still attached to the clump weight shackles), the Puget's crane raised the anchor chains in the hawse pipe; and the keeper plate was removed. A Peck and Hall quick-release hook was used to connect the lifting line to the anchor chain. After the keeper plate had been removed, the release hook was tripped, and the anchor line was dropped to the bottom (photos C-33 through C-36).

Unanchoring the pipe-tire breakwater was less dramatic. The nylon anchor lines were fished to the surface with a grappling hook, the shackle holding the upper chain to the rope was unfastened, and the rope was released. All work was done by hand from small skiffs.

Additional information on anchor system design is available in references C-1 through C-5.

APPENDIX C

REFERENCES

C-1. Bitting, K. R., "Fatigue Failure in Nylon Rope," Marine Technology Society Journal, November 1980.

C-2. Boivin, M. J., "The Effects of Mooring Cable Connecting Location on the Operating Characteristics of a Twin Pontoon Floating Breakwater," Master of Science Thesis, University of Washington Department of Civil Engineering, Seattle, Washington, November 1970.

C-3. Atturio, J. M., Valent, P. J., and Taylor, R. J., "Preliminary Selection of Anchor Systems for OTEC," Technical Report R853, Naval Civil Engineering Laboratory, Port Hueneme, California, March 1977.

C-4. Olsen, O. A., Kvalstad, T., Lereim, J., Lohne, P. W., and Namork, J., "Deepwater Operations Demand Safe, Stable Anchoring," Petroleum Engineer International, May 1982.

C-5. Berteaux, H. O., "Design of Deep Sea Mooring Lines," American Society of Civil Engineers Preprint 1199, ASCE National Structural Engineering Meeting, Portland, Oregon, April 1970.

Photo C-1. Photo depicting steel H-piles.

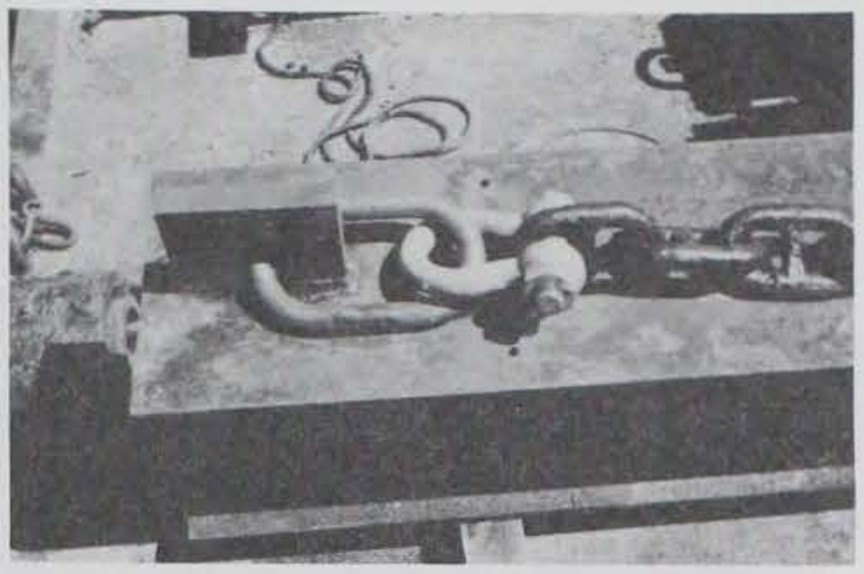

Photo C-2. Photo showing attachment of lower chain to H-pile.

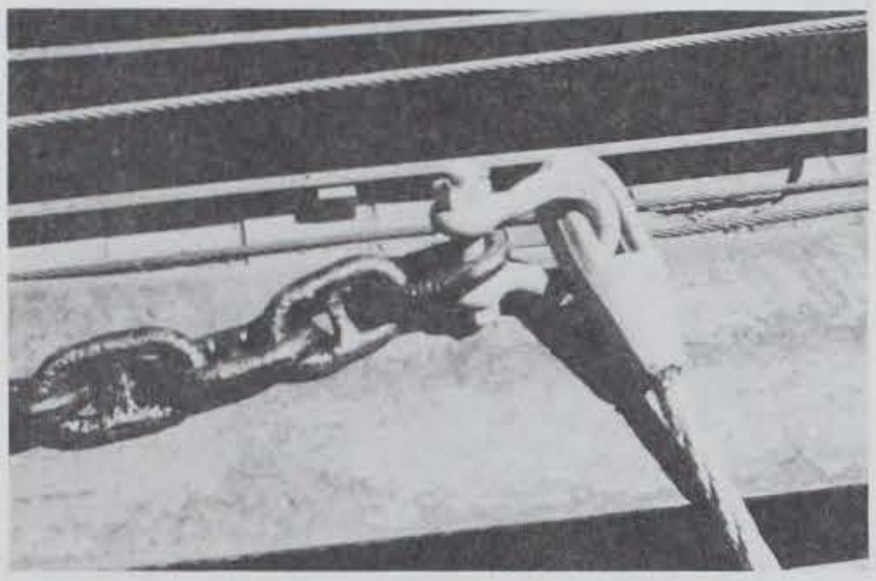

Photo C-3. Photo showing attachment of lower chain to steel bridge rope.

Photo C-4. Photo showing eye of splice and thimble in pipe-tire breakwater anchor line.

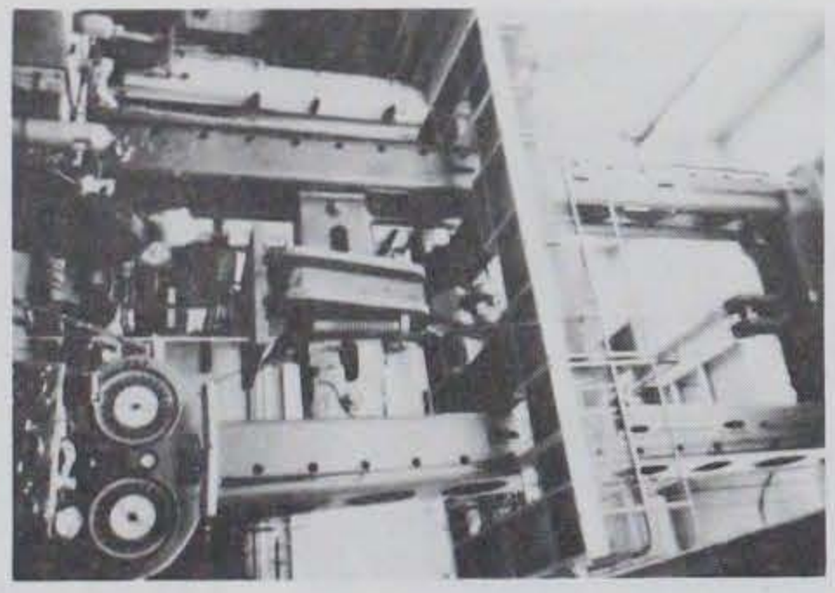

Photo C-5. Determining anchor line breaking strengths.

Photo C-6. Photo depicting nylon rope after failure.

Photo C-7. Drill barge taking bore samples at the test site.

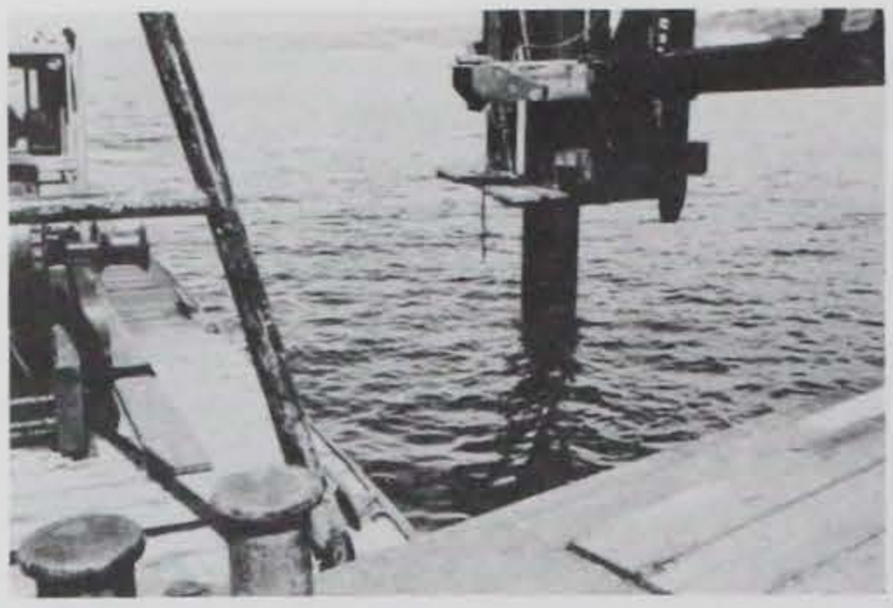

Photo C-8. Piling being driven.

Photo C-9. Photo showing special fitting used to hold H-piles in proper alignment for driving.

Photo C-10. Close-up of fitting used to drive H-piles.

Photo C-11. Attaching clump weights to the concrete breakwater's anchor lines.

Photo C-12. Upper chain being placed in slotted keeper plate on concrete breakwater.

Photo C-13. Monitoring anchor line tension.

Photo C-14. Underwater photo of anchor lines rubbing against each other.

Photo C-15. A new anchor chain being readied for installation.

Photo C-16. Tugboat pulling to determine anchor line stiffness.

Photo C-17. The concrete breakwater tipping in response to the tug's pull.

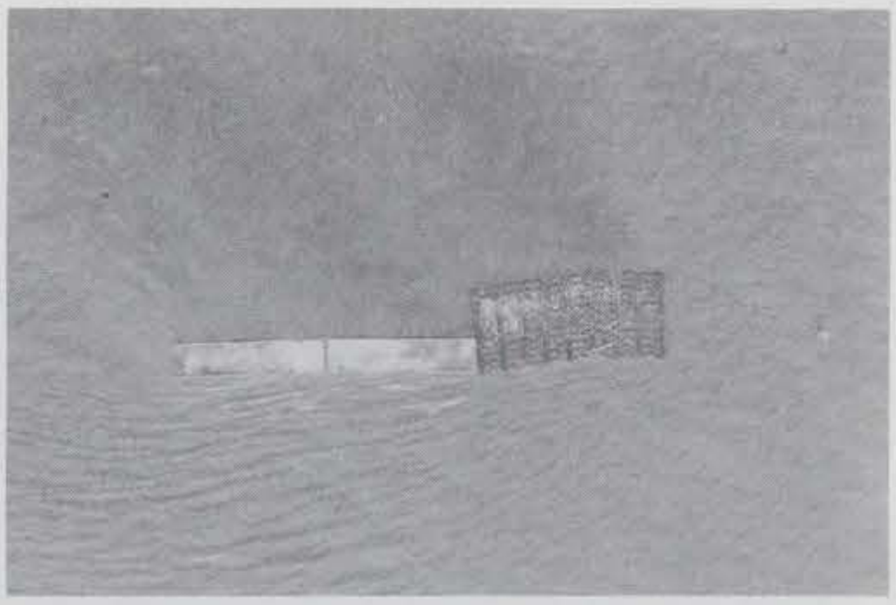

Photo C-18. Vertical photo of fast currents running past the breakwaters (note current generated waves).

Photo C-19. Photo depicting good condition of anchor line hardware at test completion.

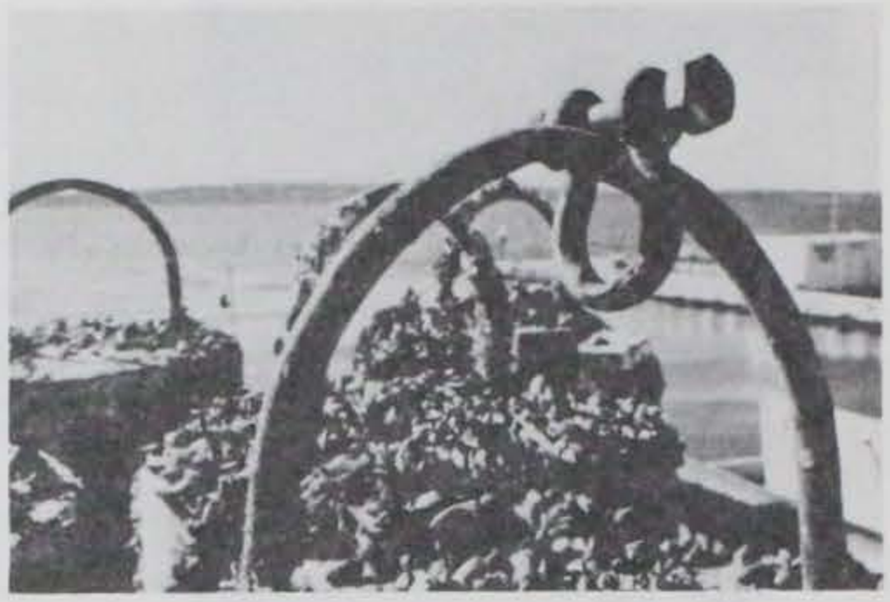

Photo C-20. Photo depicting shackles that attached clump weights to worn anchor lines.

Photo C-21. Photo depicting clump weight attachment hardware (note corroded steel bridge rope anchor line).

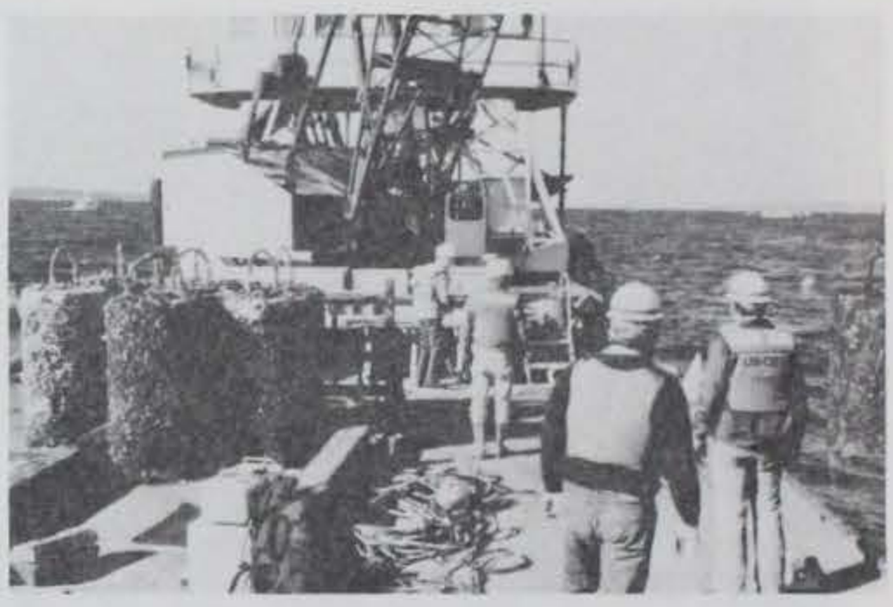

Photo C-22. Removing clump weights (note numerous marine organisms attached to the weights).

Photo C-23. Photo depicting corrosion of the mild steel cotter key in a shackle bolt.

Photo C-24. Photo of marine growth covering the nylon anchor line.

Photo C-25. Photo depicting the debris boat, Puget, which was used extensively throughout the test program.

Photo C-26. Encountering some difficulties during the first reanchoring operation.

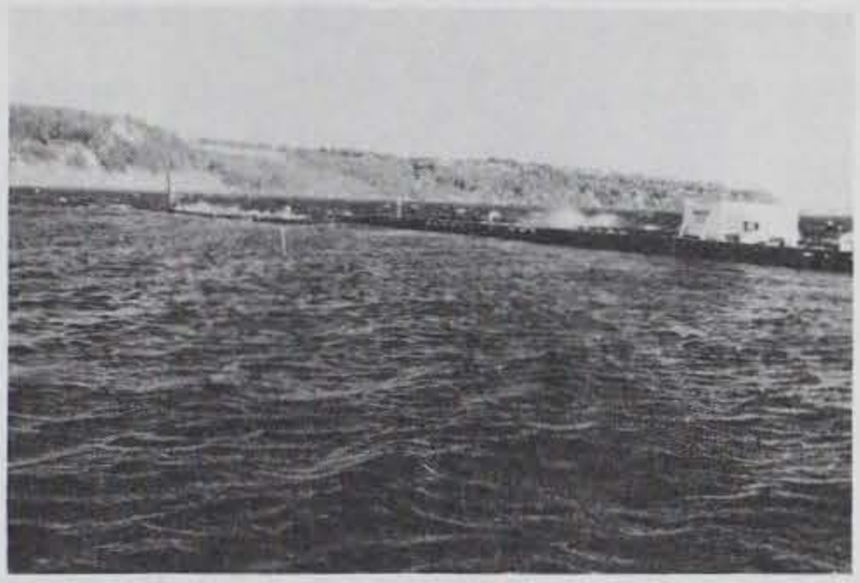

Photo C-27. Resuming data collection after reanchoring of the concrete breakwater.

Photo C-28. Unanchoring the concrete breakwater for the second time (keeper plate on deck).

Photo C-29. Anchor line tension being measured during the unanchoring procedure.

Photo C-30. Utilizing divers to simplify the second reanchoring.

Photo C-31. Raising of an anchor line after it was connected to a lifting cable by divers.

Photo C-32. Resuming monitoring of the second reanchoring.

Photo C-33. A quick-release hook being used for the third and final unanchoring.

Photo C-34. Removing the keeper plate prior to dropping the anchor line.

Photo C-35. Anchor line falling away after tripping release hook.

Photo C-36. Towing the breakwater from the test site for the final time.

APPENDIX D

CONNECTOR TESTING

1.0 Introduction. One of the major goals of the test program was to investigate various methods of connecting (or fendering) the two 140-ton concrete floats. Four different connection methods were tested. The first two methods involved two types of flexible connections. The third method involved complete disconnection (with fendering), and the fourth involved rigidly bolting the units together. The rigid connection and the fendering (with one modification) were successful, but neither of the flexible connector designs survived their test period undamaged.

2.0 Vertical Fender Connector. Both types of flexible connectors using commercially available butyl rubber marine fenders were of the same basic design, except that the fenders were oriented vertically in the original connector and horizontally in the second. Each of the vertical connectors was composed of two 4-ft, 11-in.-high fenders bolted nose-to-nose with 1-in.-diam bolts (photo D-1). The fenders were secured to 5-ft-long steel angles by 10-3/4-in.-diam by 1-ft 6-in.-long bolts (see construction drawings, figures A-12 and A-15). After the connectors were assembled, the angles were fastened to the ends of the east float by six 1-in.-diam threaded anchors which were embedded in the concrete (photo D-2). After both floats were launched, the connector was bolted to the west float, and the connection process was completed.

Within 5 days after the breakwater arrived at West Point, wave action had loosened the nuts from the 1-in. bolts which held the butyl rubber fenders together (photo D-3). With considerable difficulty, the nuts were reinstalled. The bolts were then double nutted, and an attempt was made to deform the exposed threads. This repair transferred the problem to the 3/4-in. bolts which fastened the fenders onto each float. A number of these bolts sheared, and eventually all were replaced with 3/4-in., high-strength steel pins. The nuts continued to slip off the 1-in. bolts, and eventually only four bolts were holding the two units together. A means of holding the fenders together was required, but the difficult working conditions and a reluctance to expose the floats to possible damage by removing the fenders at the

test site limited the options available. Connecting each pair of fenders with a U-shaped bracket was the eventual choice. The bracket was fabricated from 5-ft-long by 4-in.-diam extra strong pipes welded to a 24- by 12-in. plate of 3/4-in.-thick steel (photo D-4). It was installed by lowering the bracket below the fenders and raising the pipes through the large vertical opening in each fender. A second plate was then placed over the pipes and pinned in place (photo D-5). This connection method lasted for 7 weeks, from late August to mid-October. By mid-October 1982, wave action caused by two storms had deformed the pipes and broken one of the 3/4-in. steel plates (photo D-6). To prevent further damage, the fenders were disconnected from each other, and testing of the fendering alternative was begun.

3.0 Fendering. The fendered float configuration that evolved as a result of emergency field modifications to keep the floats from colliding was not anticipated in the original test plan. For this reason, the large rubber fenders were removed from the east float, and wood fenders were attached to the steel angles which had held the rubber fenders in place. (The angles could not be removed because they sealed the twenty 1-3/4-in.-diam bolt holes which were to be used when rigidly connecting the floats.) Large lag bolts were used to fasten bumper plates to the angles, and 3- by 12-in. timbers were bolted horizontally between the two bumper plates (photos D-7 and D-8). The rubber fenders were left in place on the west float.

At the beginning of the test program, the center anchor lines (Nos. 3 and 8) were attached only to the west float. The connector was intended to transfer loads from the east float to the anchor lines through the west float. When the floats were disconnected from each other to test the fender system, lateral support for the end of the east float was provided by adding a 25-ft length of 1-1/4-in. chain between the upper end of each center anchor line and the east float. This Y-shaped anchor connection prevented excessive relative displacements between the floats while avoiding the problems associated with using the connector to restrain the motions of the 140-ton structures (see figure A-11 and photo D-9).

The two horizontal timbers were torn off during the next storm, leaving only the wood bumper plates. Signs of wear on both the bumper plates and the

rubber fenders began to appear. Within 2 months the bumper plates had been worn enough to expose the lag bolts. The next storm dislodged it completely (photos D-10 and D-11). Just before the arrival of yet another storm system, emergency repairs were carried out to fasten new rubber fenders and new bumper plates made of iron bark (photo D-12). This combination survived the next month (4 storms) with no sign of wear, and 7 months of modification and testing had finally yielded a viable connection method. On 8 February 1983, the concrete breakwater was unanchored and towed 3 miles to the protected waters of the Seattle District (NPS) work yard at the Hiram M. Chittenden Locks to make the rigid connection between the two floats.

4.0 Rigid Connection. To allow work on the connection to be done in a dry environment, NPS personnel designed and constructed a wood cofferdam. The dam was placed under the end of each float and pumped dry. Next the rubber fenders, wood bumper plates, and angles were removed. After the embedded bolts were cut off, the concrete surface was ground smooth. A 15/64-in.-thick high density rubber pad was placed between the two floats to accommodate any unevenness in the surfaces, and the twenty 1-1/2-in.-diam by 11-ft-long high-strength bolts, which had been stored in the float ends for the first 7 months of the test, were shoved through from one float to the other (photos D-13 through D-18). The cofferdam was flooded and the floats were drawn together. Each of the 20 bolts was tensioned to 135,000 lb, and on 1 February 1983, the breakwater was towed back to the test site to continue the test (photos D-19 through D-24). Sixteen working days (approximately 450 man-hours) were required to make the rigid connection which did not require any maintenance or modification during the next 9 months of testing.

5.0 Horizontal Fender Connector. In July 1983, the test program was extended by 1 year to allow additional testing of flexible connectors. The new connector again used large rubber fenders, but this time they were fastened to the floats in a horizontal orientation. On 1 November 1983, the concrete breakwater was removed from the test site again to make this last modification. The cofferdam was pulled into place at the connection, and the 20 connection bolts were detensioned using a hydraulic jack. The floats were parted about 18 in. with wedges and a small hydraulic jack. After the cofferdam was pumped dry, the connecting bolts were cut in half and removed. A careful inspection

of the surfaces of the two floats was made, and no spalling or cracking was found. The rubber pad had 4-in.-square tears around several bolts in the two lower corners and in the upper center. Otherwise the materials used in rigidly connecting the floats showed no evidence of damage or wear.

Additional bolt holes were drilled in the concrete for fastening the new connector brackets to the floats, and sixteen 1-in.-diam bolts were cemented into place with epoxy grout. Each bracket was bolted in place with sixteen 3/4-in.-diam bolts (in addition to eight grouted bolts). Finally, the rubber fenders were lowered into place and fastened to the brackets with 2-in.-diam by 2-ft-long bolts (figure D-1). The cofferdam was flooded and removed, and on 1 December 1983 the breakwater was reanchored at the test site (photos D-25 through D-35). The concrete clump weights were not reattached to the anchor lines for the test of the horizontal fender connector.

This connector proved to be much more durable than the first (vertical fender) configuration. Until a posttest inspection, the connector appeared to be undamaged after 2 months (December and January), but a close inspection found that three of the vertical bolts had been pulled through the rubber fender on the north side of the breakwater (photo D-36). This damage appeared to be progressive, and continued testing probably would have resulted in additional damage.

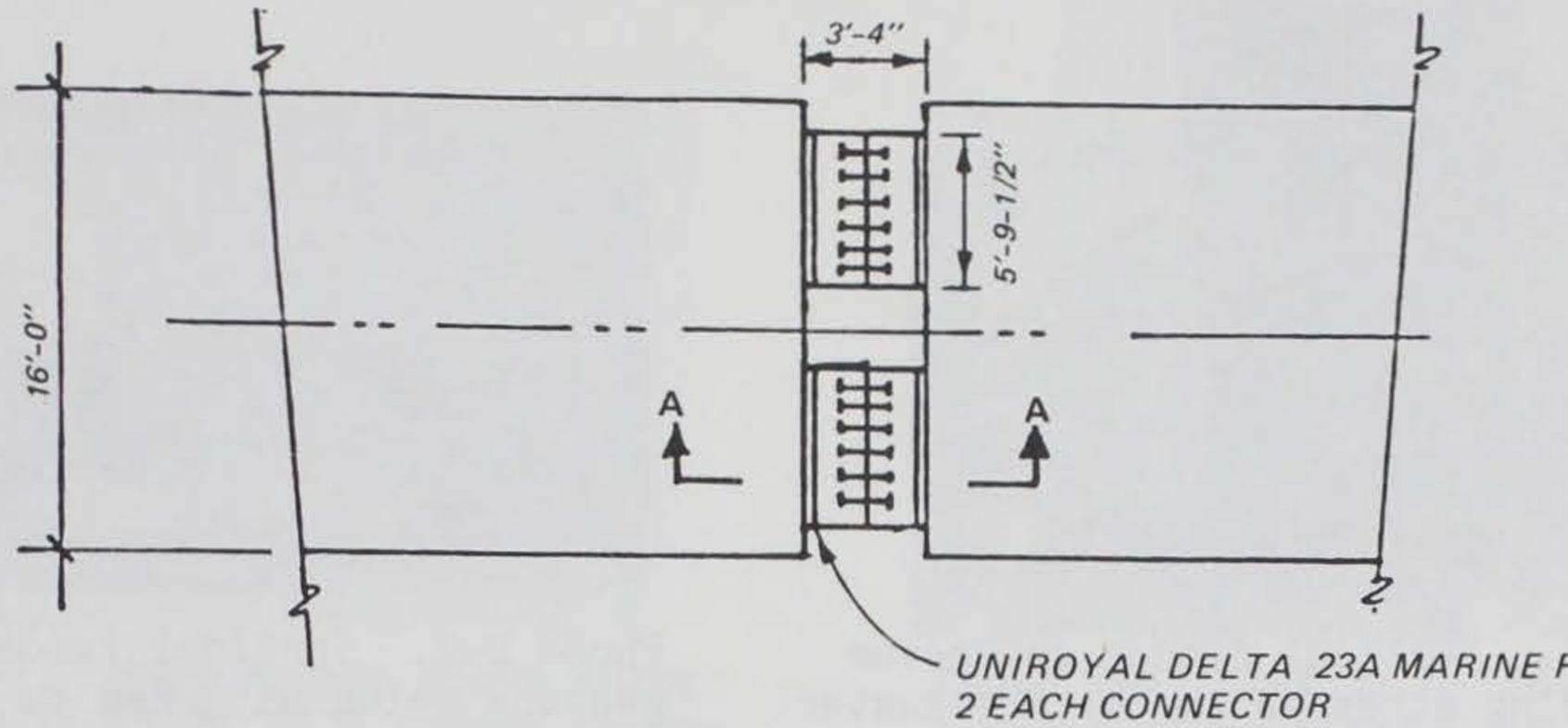

PLAN VIEW

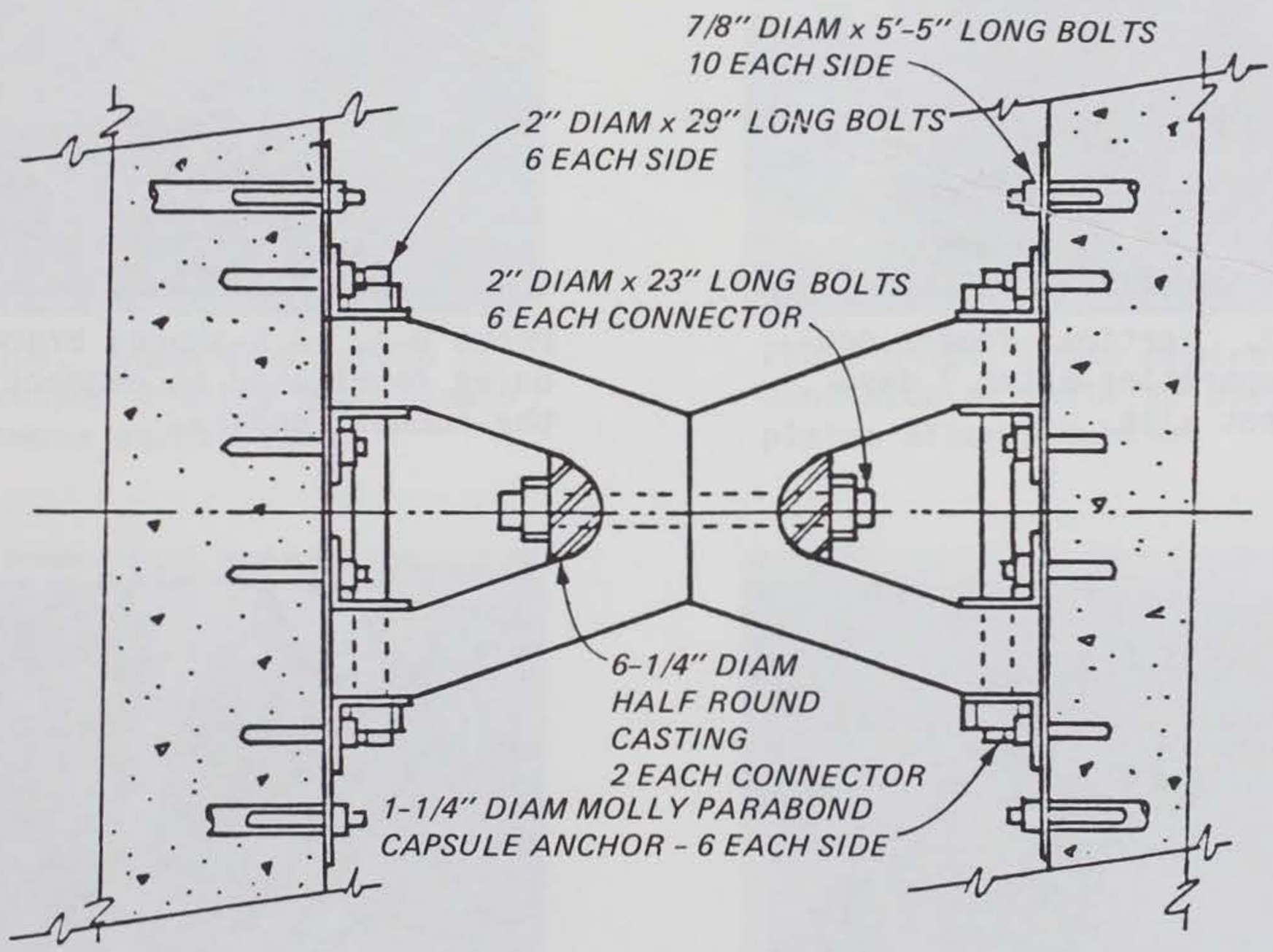

SECTION A-A

FIGURE D-1. Horizontal Fender Connector

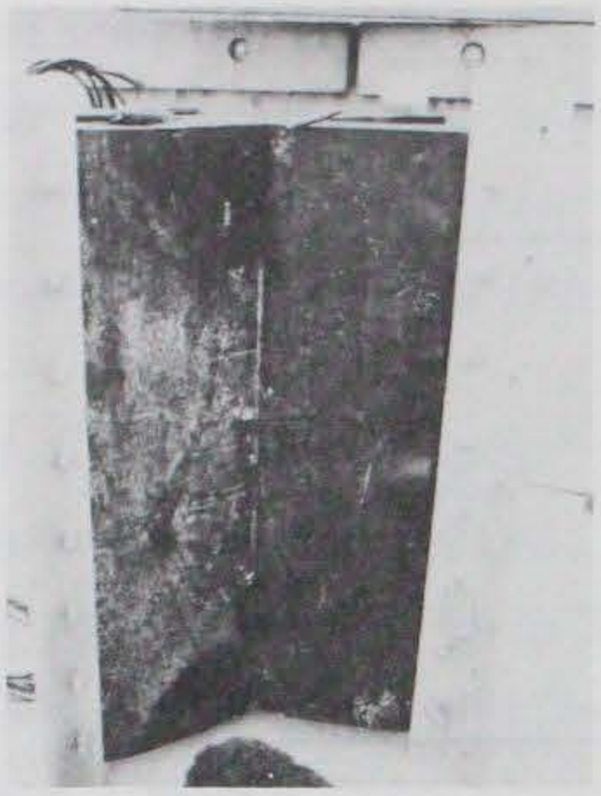

Photo D-1. Vertical fender connector before being attached to the breakwater.

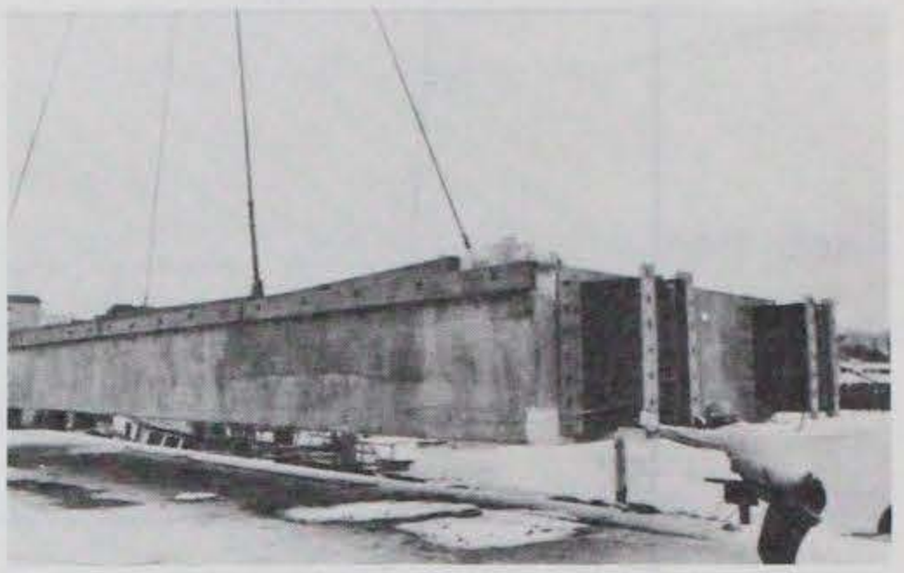

Photo D-2. Vertical fender connectors being attached to one float.

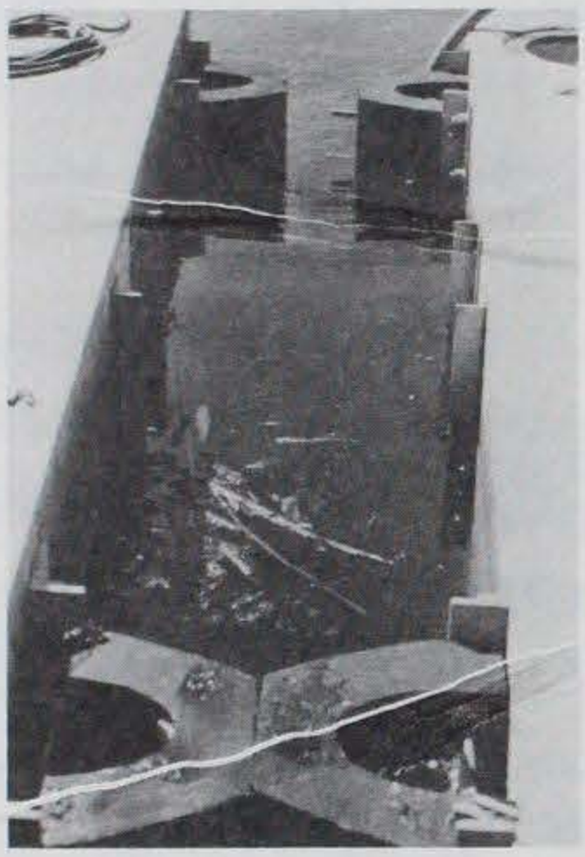

Photo D-3. Vertical fender connector separating after 3 days at the test site.

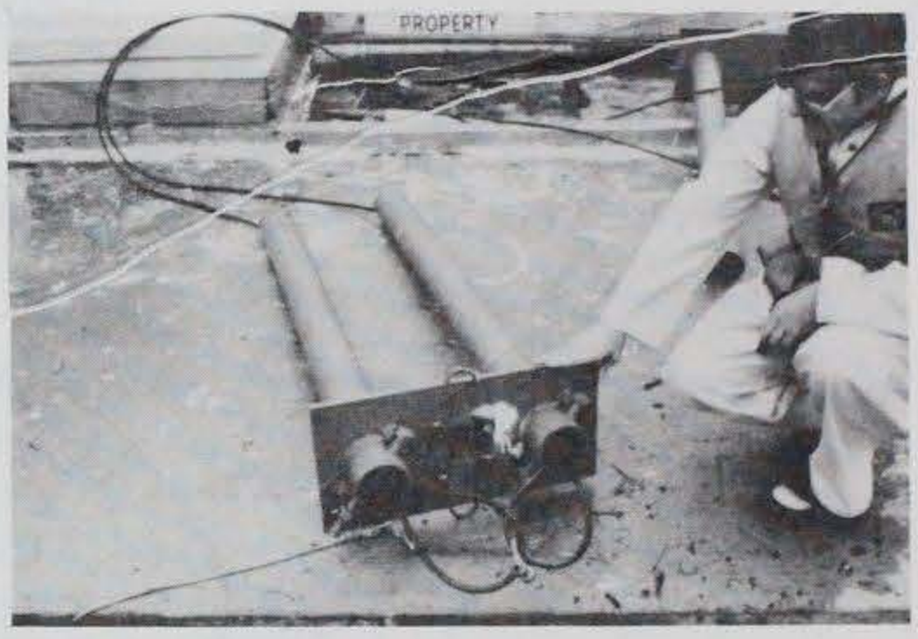

Photo D-4. A U-shaped bracket being fabricated to connect the rubber fenders.

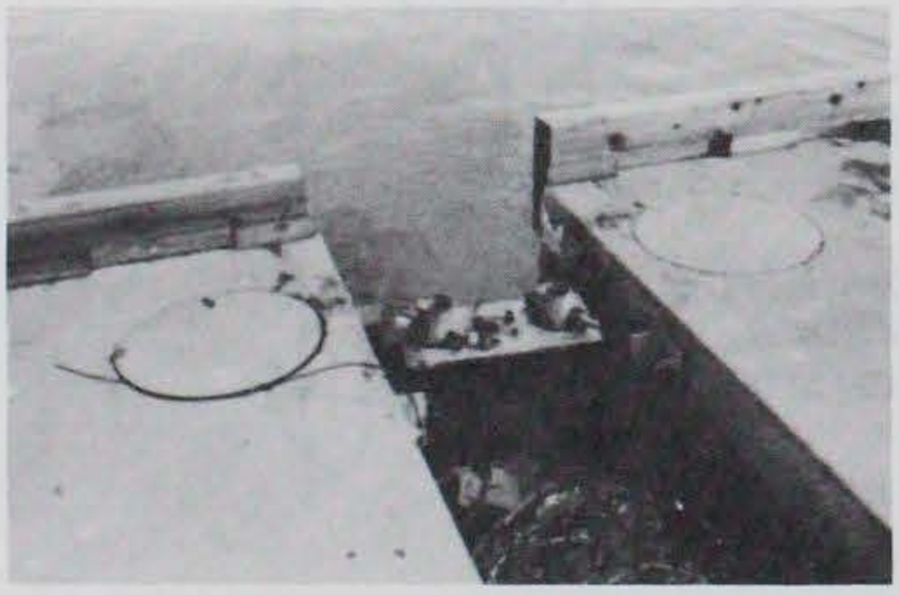

Photo D-5. Photo depicting U-shaped bracket in place.

Photo D-6. Photo depicting failure of U-shaped brackets after 7 weeks.

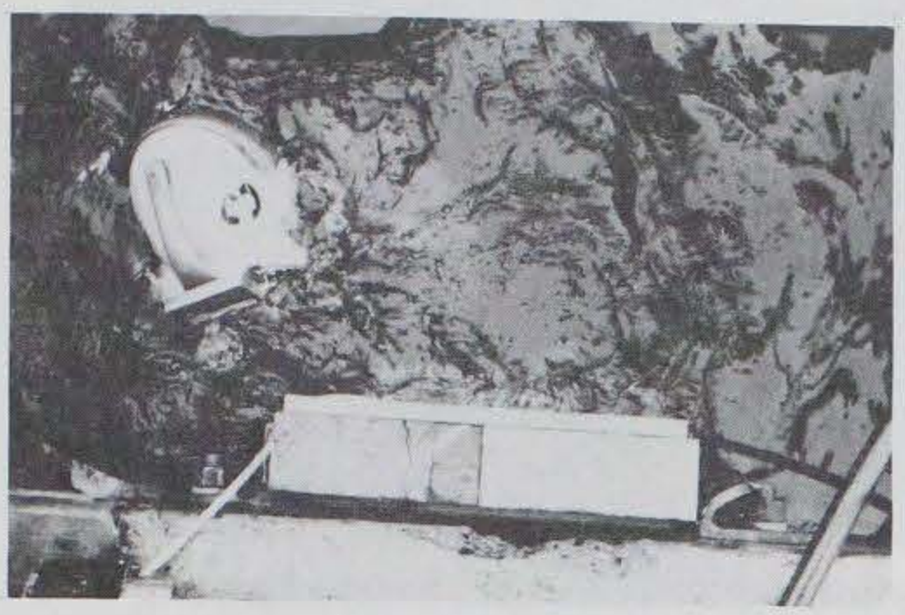

Photo D-7. Wood bumper plate being fastened in place of a rubber fender.

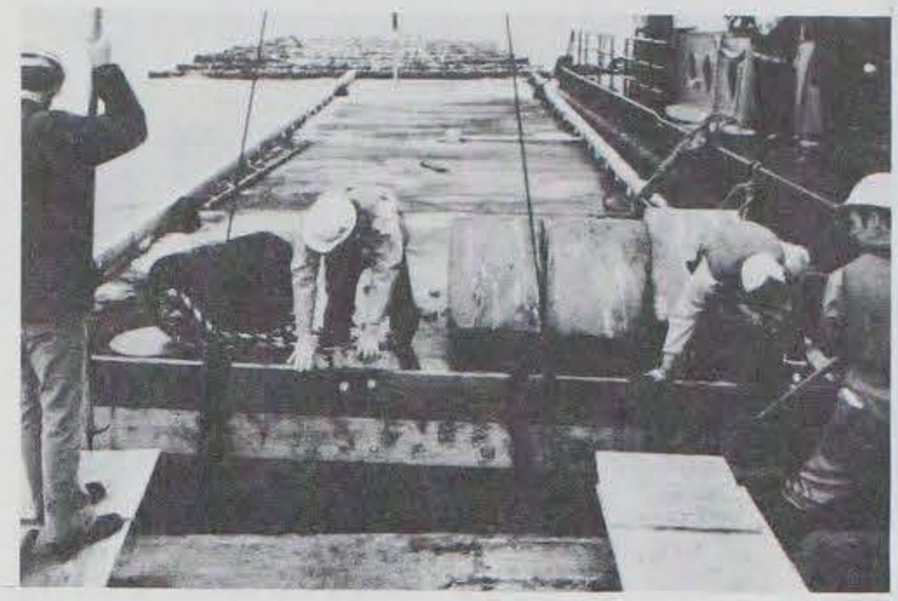

Photo D-8. Two 3- by 12-in. timbers being bolted between the bumper plates.

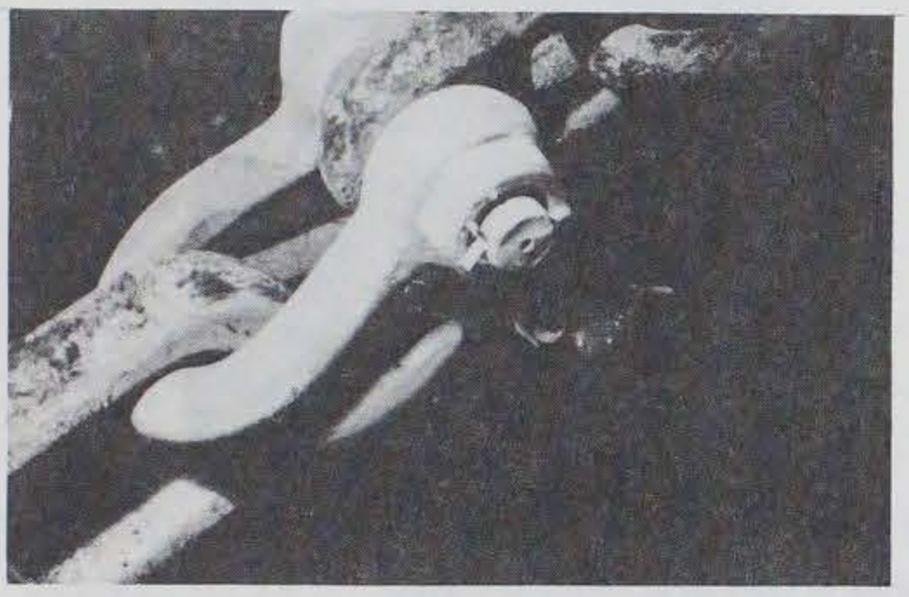

Photo D-9. Underwater photo of Y-connection joining both floats to a common anchor line.

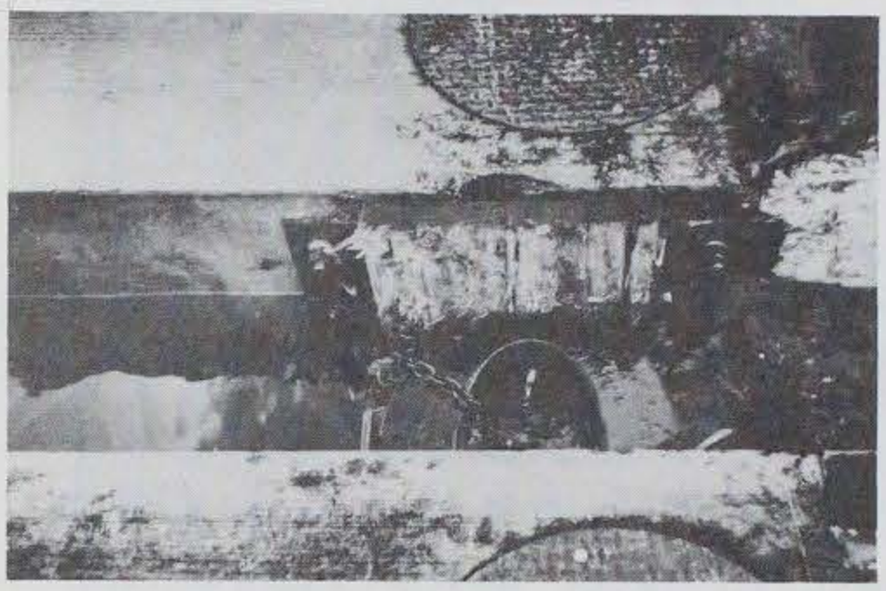

Photo D-10. Photo depicting worn condition of soft fir bumper plates after 2 months.

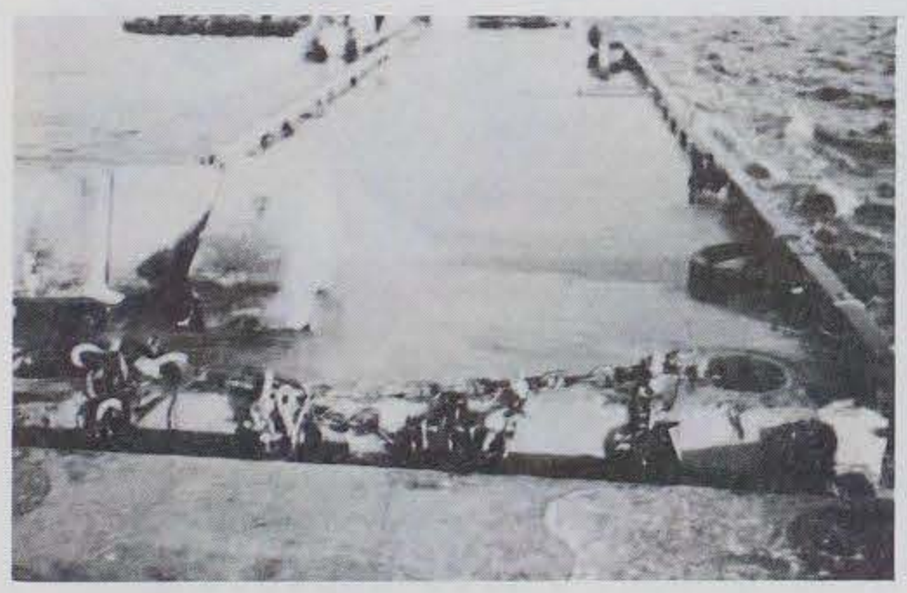

Photo D-11. Ship fenders being hung between the floats after dislodging of damaged plate.

Photo D-12. Photo depicting the new ironwood bumper plate which proved to be more durable.

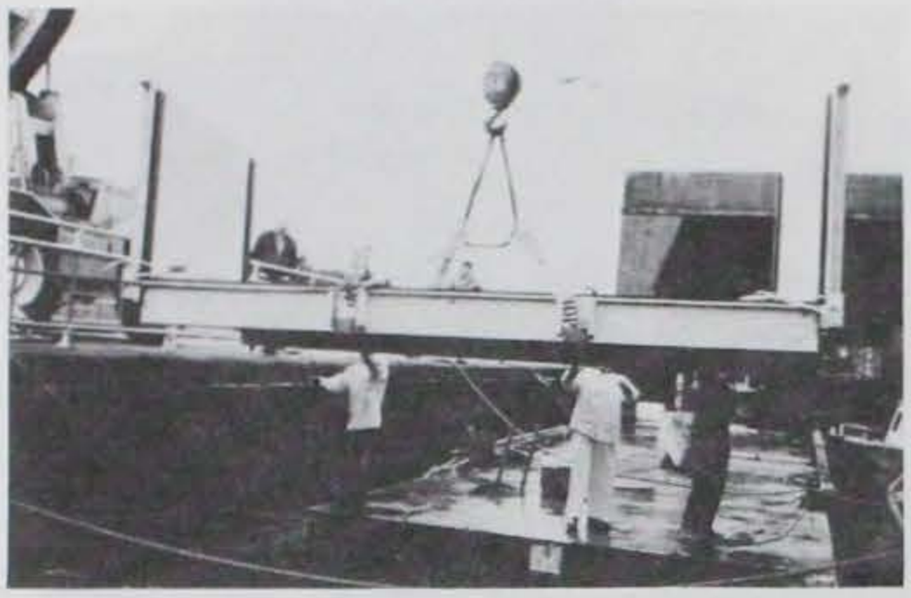

Photo D-13. A wood cofferdam being placed to allow work to be done in a dry environment.

Photo D-14. Cofferdam being lowered between the floats.

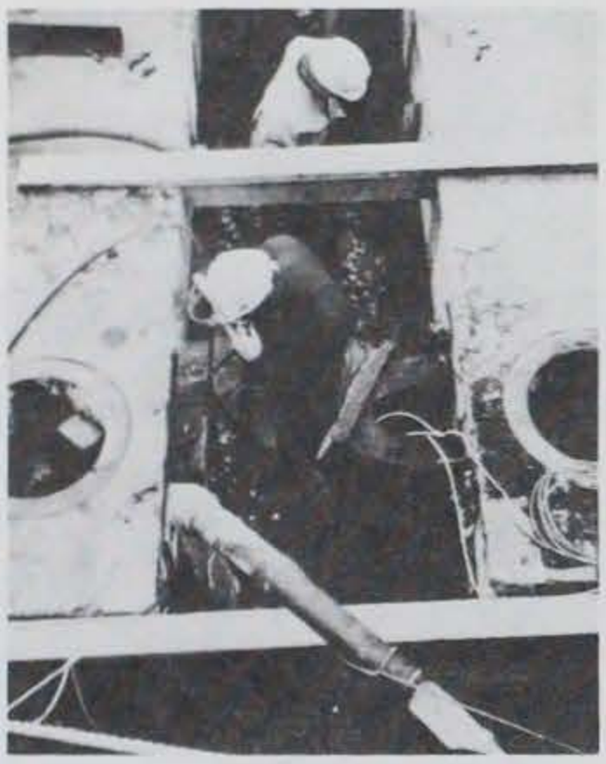

Photo D-15. The cofferdam being dewatered after being secured.

Photo D-16. Fender system hardware being removed.

Photo D-17. Photo showing the end of the float after being cleaned and ground smooth.

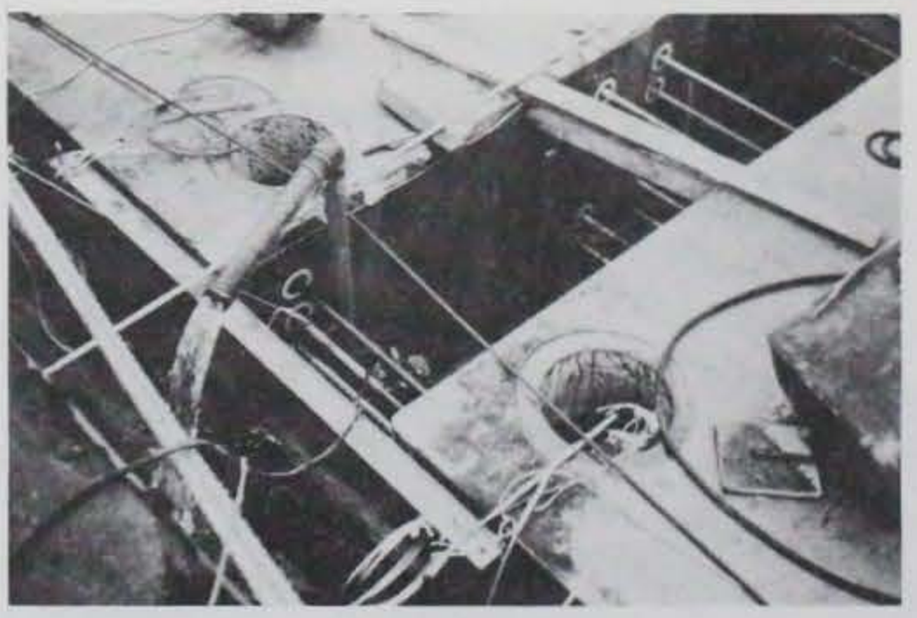

Photo D-18. Photo depicting Dywidag 1-1/4-in.-diam. steel bars and 1/4-in.-thick Fabrieka rubber pad in place.

Photo D-19. Photo depicting inside of float with four tensioned bars near center line.

Photo D-20. Photo depicting inside of float with six tensioned bars near sidewall.

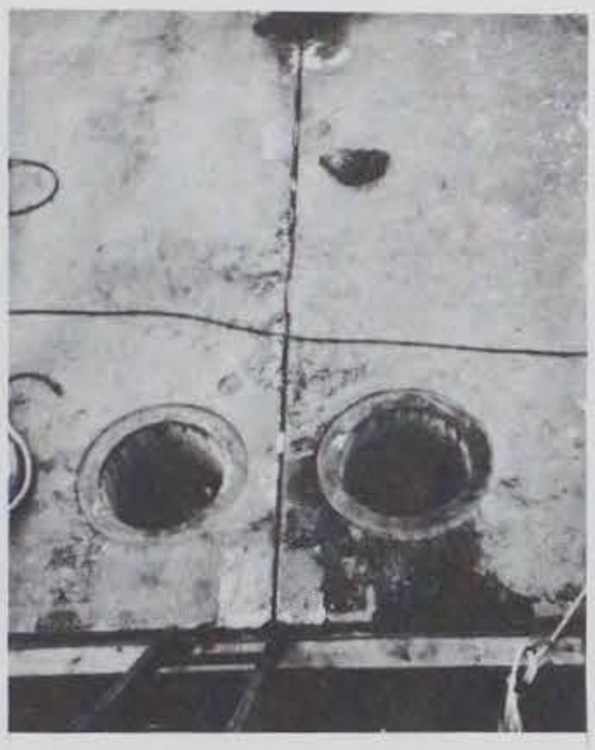

Photo D-21. Photo depicting joint between rigidly connected floats.

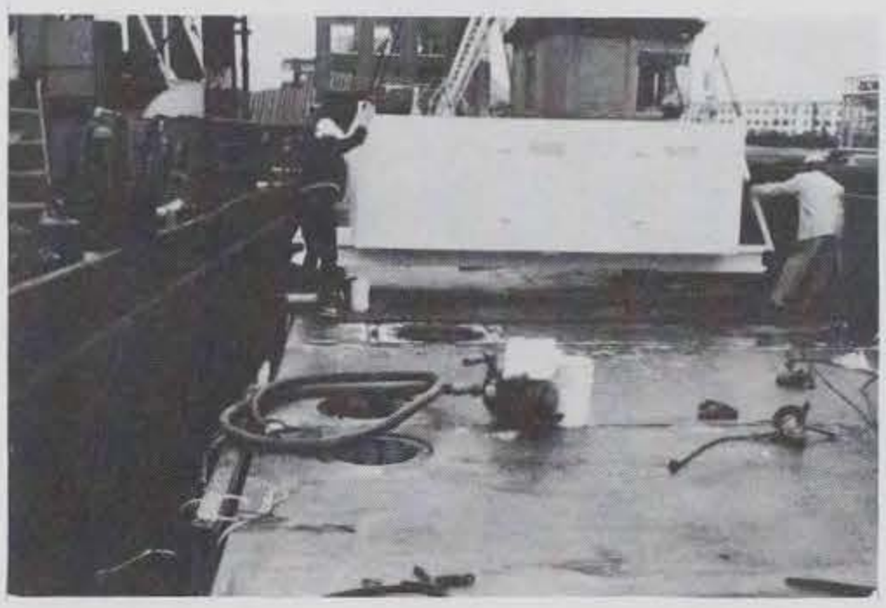

Photo D-22. New deckhouse being lowered into place.

Photo D-23. Returning to the test site.

Photo D-24. Resuming monitoring of rigidly connected breakwater.

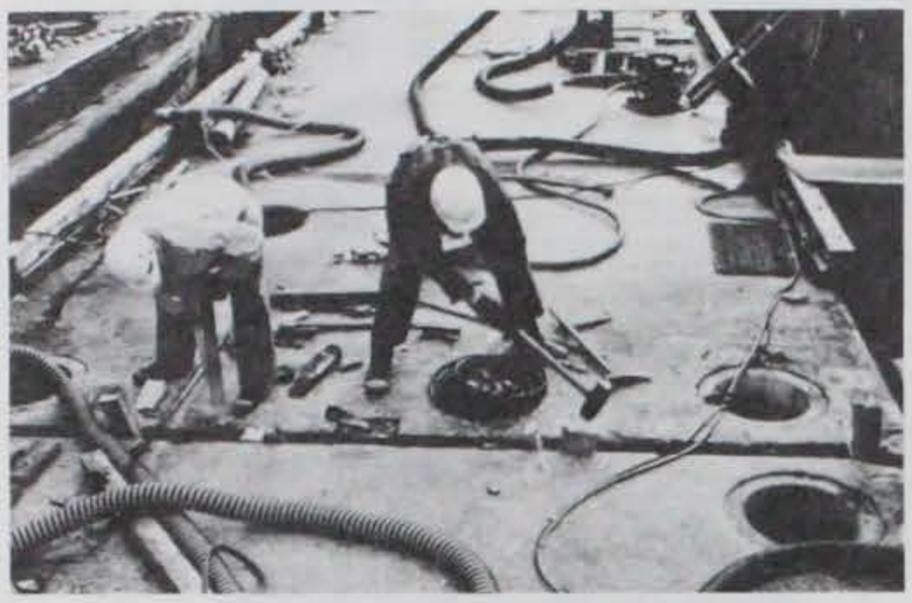

Photo D-25. Floats being parted after rigid connection bars have been detensioned.

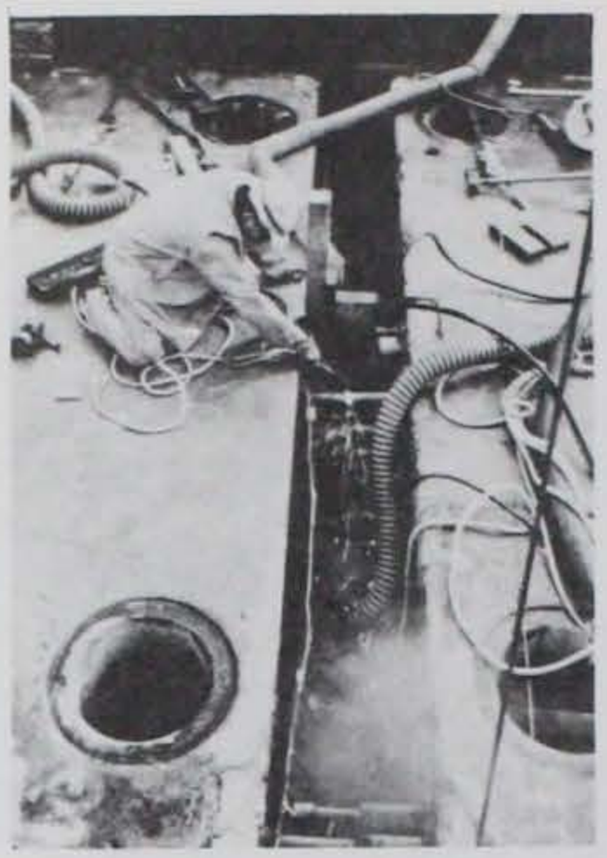

Photo D-26. Connection bars being cut after cofferdam is in place and dewatered.

Photo D-27. Additional bolt holes being drilled in floats.

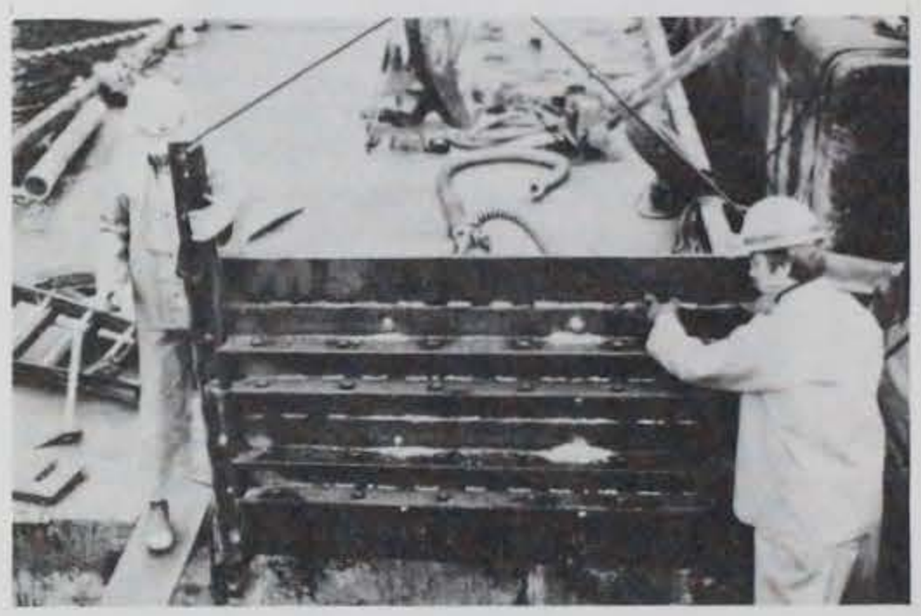

Photo D-28. Lowering connector anchoring plates into position.

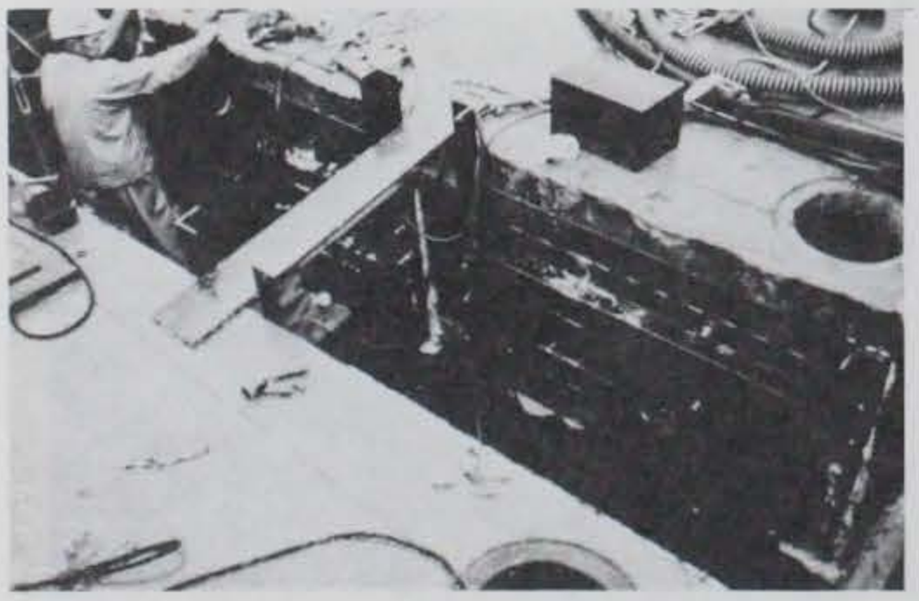

Photo D-29. Anchoring plates being bolted in place (water activated sealant oozes from bolt holes).

Photo D-30. Horizontal connector being lowered between the floats.

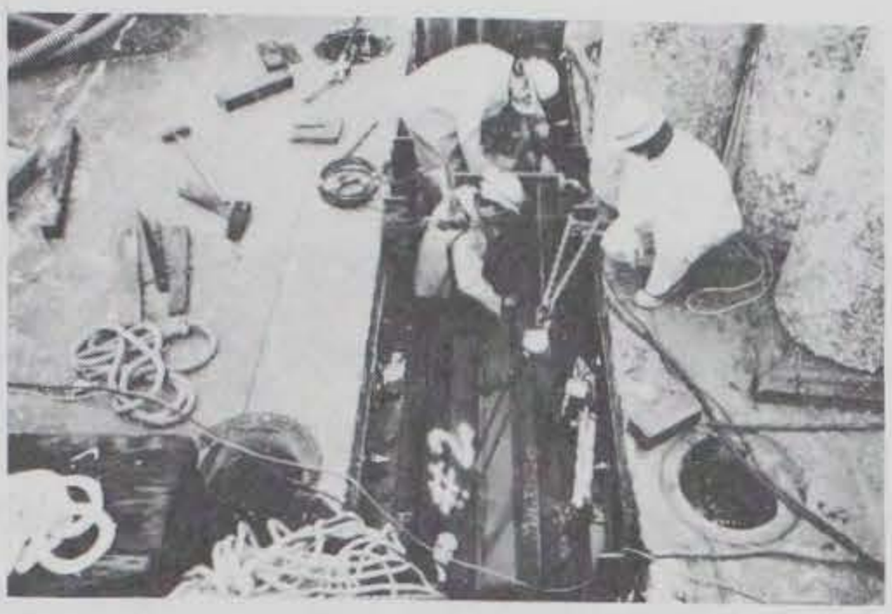

Photo D-31. New flexible connectors being "coaxed" into position.

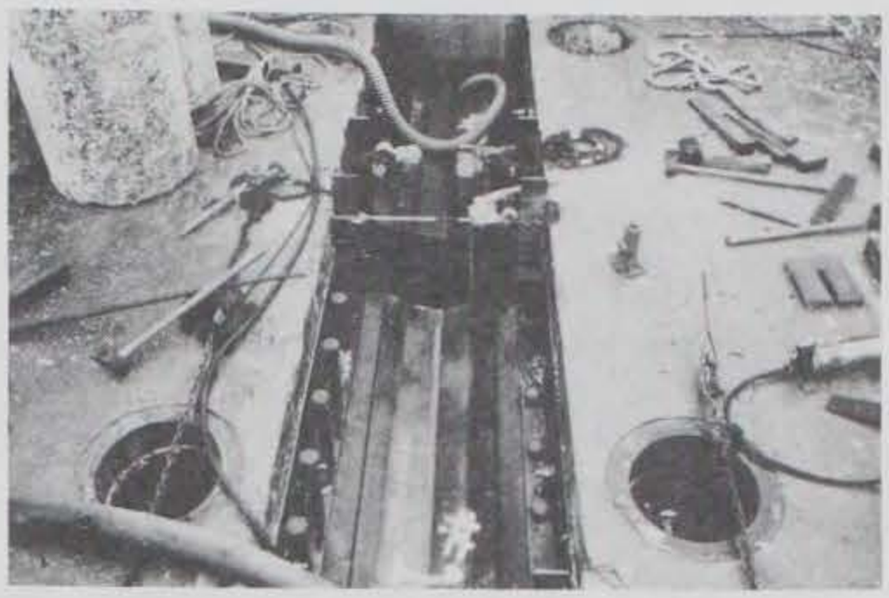

Photo D-32. Flexible connectors being bolted to the anchoring plates with 2.5-ft-long, 2-in.-diam bolts.

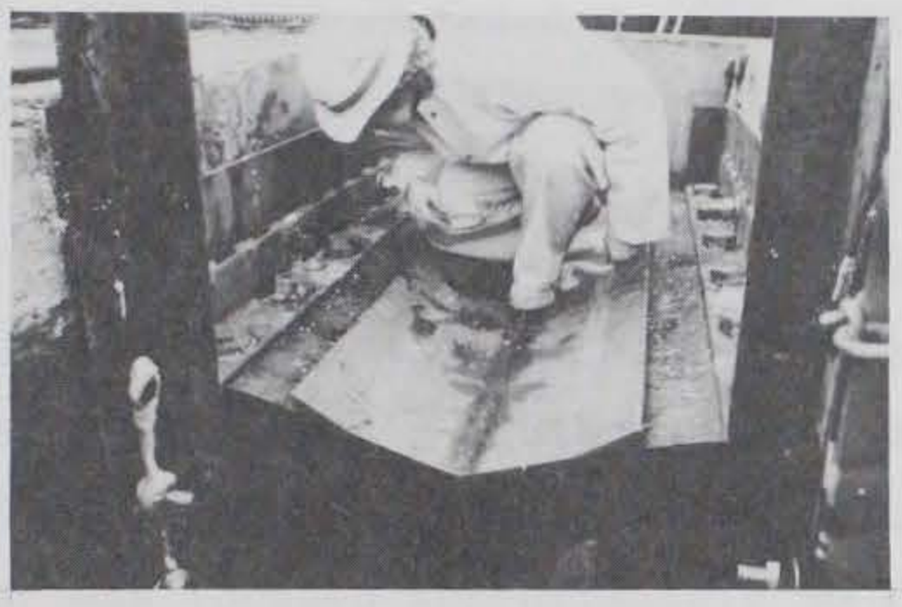

Photo D-33. Horizontal flexible connector being inspected.

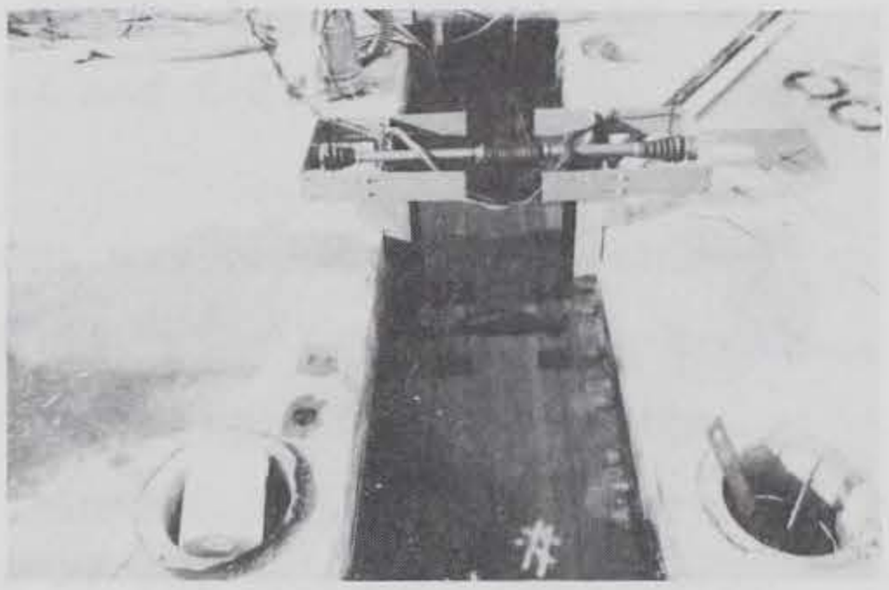

Photo D-34. Photo depicting completed flexible connection (note relative motion sensor between floats).

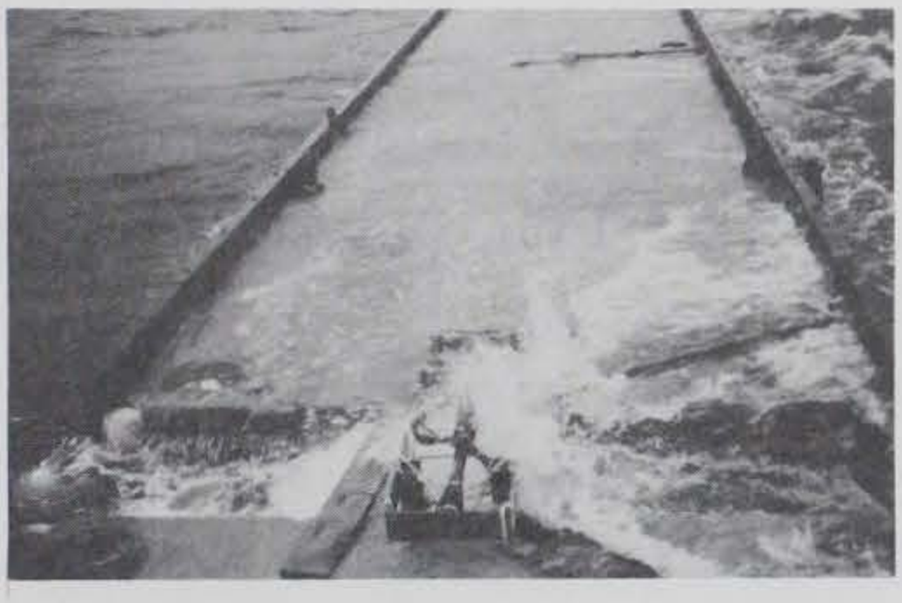

Photo D-35. Waves washing over new flexible connection.

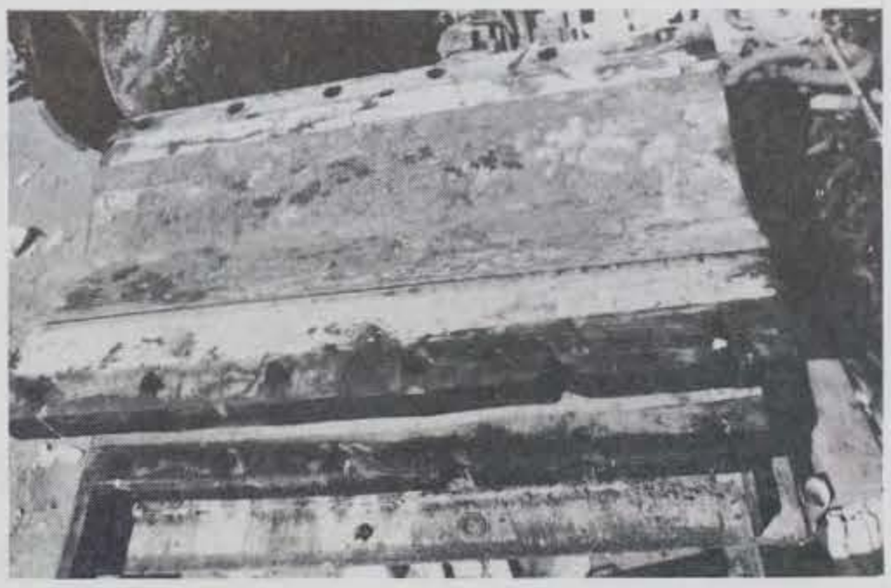

Photo D-36. Photo depicting the area where the 2-in.-diam bolts tore out of the three outermost holes of the north connector.

APPENDIX E

BOAT WAKE TESTING

1.0 Introduction. Because most floating breakwater applications are in semiprotected coastal waters, lakes, and reservoirs where wind wave energy is limited, boat wakes can be as large as the design wind waves. The size of the boat wakes, therefore, becomes another design consideration. To obtain additional design data on boat wake attenuation characteristics of floating breakwaters, four boat wake tests were conducted at various times during the prototype test program. The first two tests, conducted on 31 January 1983 and 22 April 1983, used a 41-ft Coast Guard cutter to generate waves. The third test, conducted 18 August 1983, used a 110-ft marine tug. The last test, conducted 29 October 1983, used a 73-ft harbor tug. Details of the boat wake tests are discussed in references E-1 and E-2.

2.0 Test Description. The first boat wake test was conducted 31 January 1983 using a 41-ft Coast Guard cutter (photo E-1). The two concrete breakwater units were in a disconnected but fendered configuration, with the 2,000-lb clump weights in place on the anchor lines. The pipe-tire breakwater was located approximately 30 ft due east of the concrete breakwater. After the test had been completed, the data acquisition system was found to have been malfunctioning, and no transmission data were obtained. However, an 8mm movie camera mounted on the west float was used to film a target on the east float (photo E-2). An analysis of the movies indicated that the maximum excursion of one float relative to the other was approximately ±1 ft horizontally and ±9 in. vertically. The wakes were estimated to be about 2.5 ft high with a period of 2.5 sec.

The second boat wake test, conducted 22 April 1983, used the same Coast Guard cutter. The sailing lines alternated from parallel to the breakwater to an angle of 45 deg with respect to the breakwater (photos E-3 and E-4). The distance from the sailing line to the breakwater varied from 50 to 250 ft. Vertical aerial photographs documented details such as the distance from the sailing line to the breakwater, wave approach angle, wave lengths, and diffraction of waves around the breakwaters (photos E-5 and E-6). The concrete

breakwater connection had been modified to the rigid configuration that joined the two floats into a continuous 150-ft-long unit. No changes had been made to the concrete breakwater anchor system (i.e., the clump weights were still attached), and the pipe-tire breakwater was still in position. This time the data acquisition system did record data on incident and transmitted waves as well as anchor forces for both breakwaters and internal strains and wave pressures on the concrete breakwater.

The third boat wake test was conducted 18 August 1983 using a 110-ft-long marine tug (photo E-7). The size of this vessel was determined by requirement of the anchor line pull test which was conducted on the same day (see Appendix C). By the time this test was conducted, the pipe-tire breakwater had been removed. The concrete breakwater was still in the rigidly connected configuration, and the clump weights remained attached to the anchor lines. To make attenuation measurements, an attempt was made to orient the tug's sailing line so that the wake crests would be parallel with the length of the breakwater (photos E-8 and E-9). In addition, several wakes were generated so that their crests were perpendicular to the long axis of the breakwater (photos E-10 and E-11). This was done in an attempt to induce large bending moments in the structure.

The fourth and final boat wake test was conducted 29 October 1983 with a 73-ft harbor tug being used to generate wakes (photo E-12). The clump weights had been removed from the anchor lines of the concrete breakwater, but the floats remained rigidly connected. An eight-buoy wave array was anchored where the pipe-tire breakwater had been located. Shortly after the test started, the gage that measured transmitted waves was found to be malfunctioning. For this reason, no wave attenuation data were recorded, but some information on wave pressures, internal concrete strains, and float motions was obtained. In addition, 8mm motion pictures were taken from the fixed wave gage piling at the east end of the test site. A rough estimate of transmitted wave heights was made from these films.

3.0 Test Results. Analysis of the boat wake test data indicated that neither breakwater attenuated boat wakes as well as it did wind waves of comparable periods. Transmission coefficients, C_t = H transmitted/H incident , varied

between 0.3 and 0.7 for the pipe-tire breakwater with an average of 0.5. For the concrete breakwater, which performed slightly better, C_t varied between 0.2 and 0.6, with an overall average of 0.45. The maximum anchor loads measured were 72 lb/ft for the concrete breakwater and 134 lb/ft for the pipe-tire breakwater. Visual observations of the incident and transmitted wakes estimated incident heights at 2 to 3 ft and transmitted heights between 6 in. and 1 ft. The individual waves in each boat wake were far from uniform, and the breakwater response was difficult to correlate with any particular height. In addition, wave diffraction around the relatively short structures, background noise created by passing boats, and varying approach angles of the incident waves were all complicating factors when the boat wake data were analyzed.

APPENDIX E

REFERENCES

E-1. Skjelbreia, N. K., "Boat Wake Transmission Tests of a Floating Breakwater," Master's Thesis, University of Washington, Seattle, Washington, 1984.

E-2. Nece, R. E., and Skjelbreia, N. K., "Ship-Wake Attenuation Tests of a Prototype Floating Breakwater," 19th International Conference on Coastal Engineering, Houston, Texas, 1984.

Photo E-1. 41-ft Coast Guard cutter being used in boat wake tests Nos. 1 and 2.

Photo E-2. A movie camera and target being used to record relative heave and sway motions.

Photo E-3. The cutter traveling on a line parallel to the breakwater.

Photo E-4. The cutter traveling on a line at a 45-deg angle with respect to the breakwater.

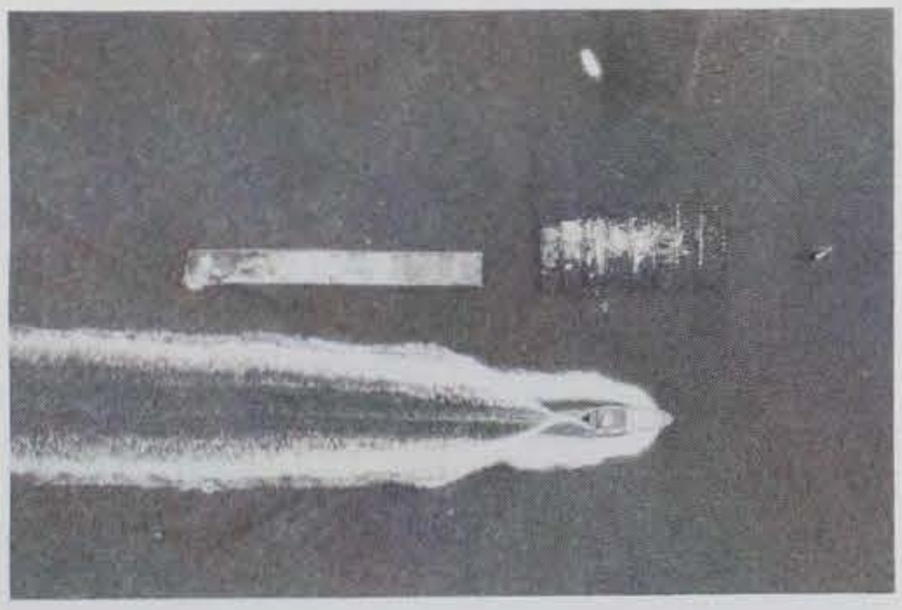

Photo E-5. Aerial photo depicting cutter on parallel sailing line.

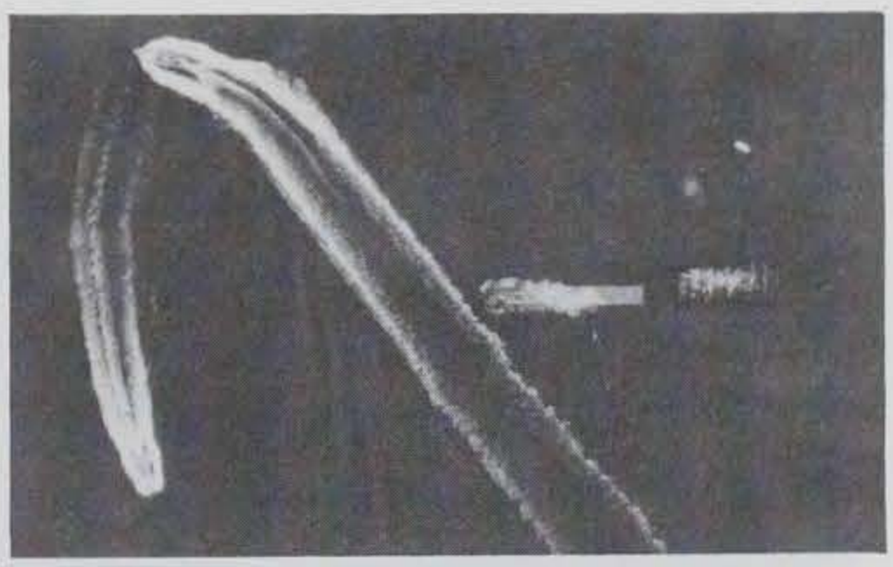

Photo E-6. Aerial photo depicting cutter on 45-deg sailing line (other boat wakes complicated data analysis).

Photo E-7. The 110-ft tug being used for boat wake test No. 3.

Photo E-8. Tug generating wake with crest nearly parallel to breakwater.

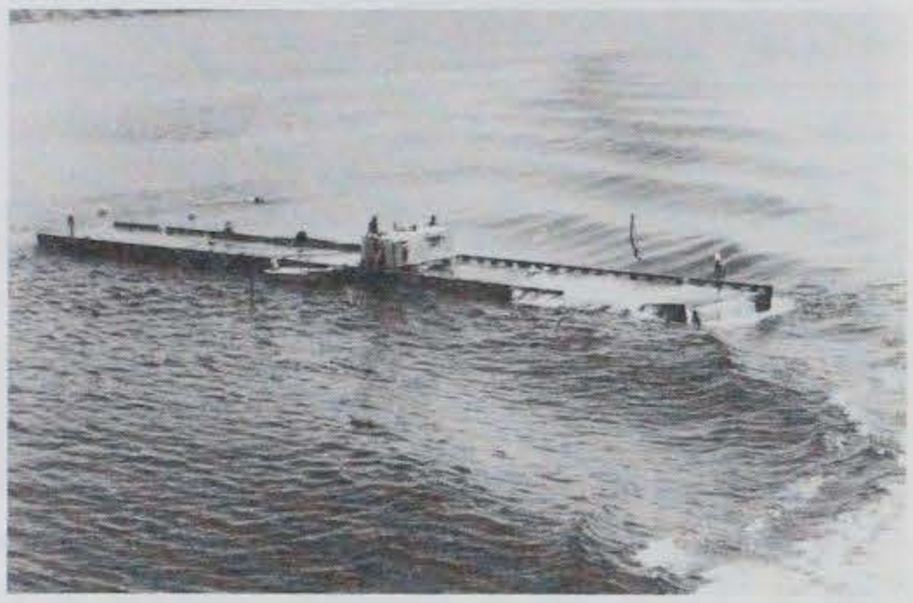

Photo E-9. Wake crests approaching parallel to breakwater (note diffraction around end).

Photo E-10. Tug generating wake with crest perpendicular to breakwater.

Photo E-11. Perpendicular wake traveling down breakwater.

Photo E-12. 73-ft tug generating wake for test No. 4.

APPENDIX F

MONITORING PROGRAM

1.0 System Description. The monitoring program for the prototype test was conducted by the Civil Engineering Department of the University of Washington under contract with the US Army Corps of Engineers (Corps). The purpose of the monitoring program was to collect data that would serve as a basis for establishing and evaluating the fundamental behavior of the two breakwater types under study. The University designed a system to measure and record pertinent environmental and structural variables that were involved in the design and mathematical modeling of the test breakwaters and similar structures. The parameters that were measured included incident and transmitted waves, wind speed and direction, anchor line and connector forces, stresses in the concrete units, relative float motion, rotational and linear accelerations, pressure distribution on the concrete breakwater, water and air temperatures, and tidal current data. The table below lists the parameters, the channel on which the data were recorded, and the transducer range.

Parameters	Channel Number	Transducer Range
Anchor Forces - Concrete	1-8	0-50 kips
Anchor Forces - Tire	10-12	0-10 kips
Wave and Tide Gage	16	0-25 ft
Wave Buoys	17-21	0-8 ft
Dynamic Pressures	22-44	0-5 psi
Concrete Strains	45-60	0-3,000 μs
Accelerometers	61-66	0-1 g
Relative Motions	67-72	0-8 in.
Wind Speed	73-74	0-100 mph
Wind Direction	75-76	0-360 deg
Current Velocity	76-77	0-5 knots
Unused	79-82	
Voltages	83-88	As required
Temperatures	89-92	0-100° C
Wave Array	9-12	0-8 ft
Wave Array	17, 19, 21, 22	0-8 ft
Rubber Connector Forces	23, 28, 29, 43	0-50 kips
Rigid Connector Forces	71, 72	0-100 kips

In addition to the transducers for measuring these parameters, the monitoring system included an onboard data logger and equipment for processing the retrieved data tapes. (See figures F-1 and F-2 for an instrumentation layout and system diagram.) Detailed information on the monitoring system hardware and software is provided in the University's final report on the monitoring program (reference F-1).

Design criteria for the monitoring system placed the following requirements on the recording instrumentation:

a. Automatic recording of data from 74 input channels.

b. Low-power consumption to allow battery operation.

c. Retrievable data storage medium.

d. Automatic hourly observations of selected parameters.

e. System activation if a preset threshold valve of selected parameters was exceeded.

f. Packaging to allow mounting recorder inside an end compartment of the concrete breakwater (i.e., fit through 23-in.-diam hatch).

As a result of these constraints, combined with a modest budget and a lack of suitable off-the-shelf instrumentation, the University designed and fabricated much of the monitoring equipment in-house.

Work on the monitoring system began in October 1981. Special purpose electronics, such as signal conditioning cards, were built specifically for this project. Throughout the winter, work progressed on the manufacture of 16 embedded strain gages, 8 wave measuring spar buoys, 14 anchor force cells, 23 pressure sensor housings, and a relative motion sensor. The pressure sensors, anemometer, current meter, and accelerometers were the only instruments for which suitable transducers were commercially available.

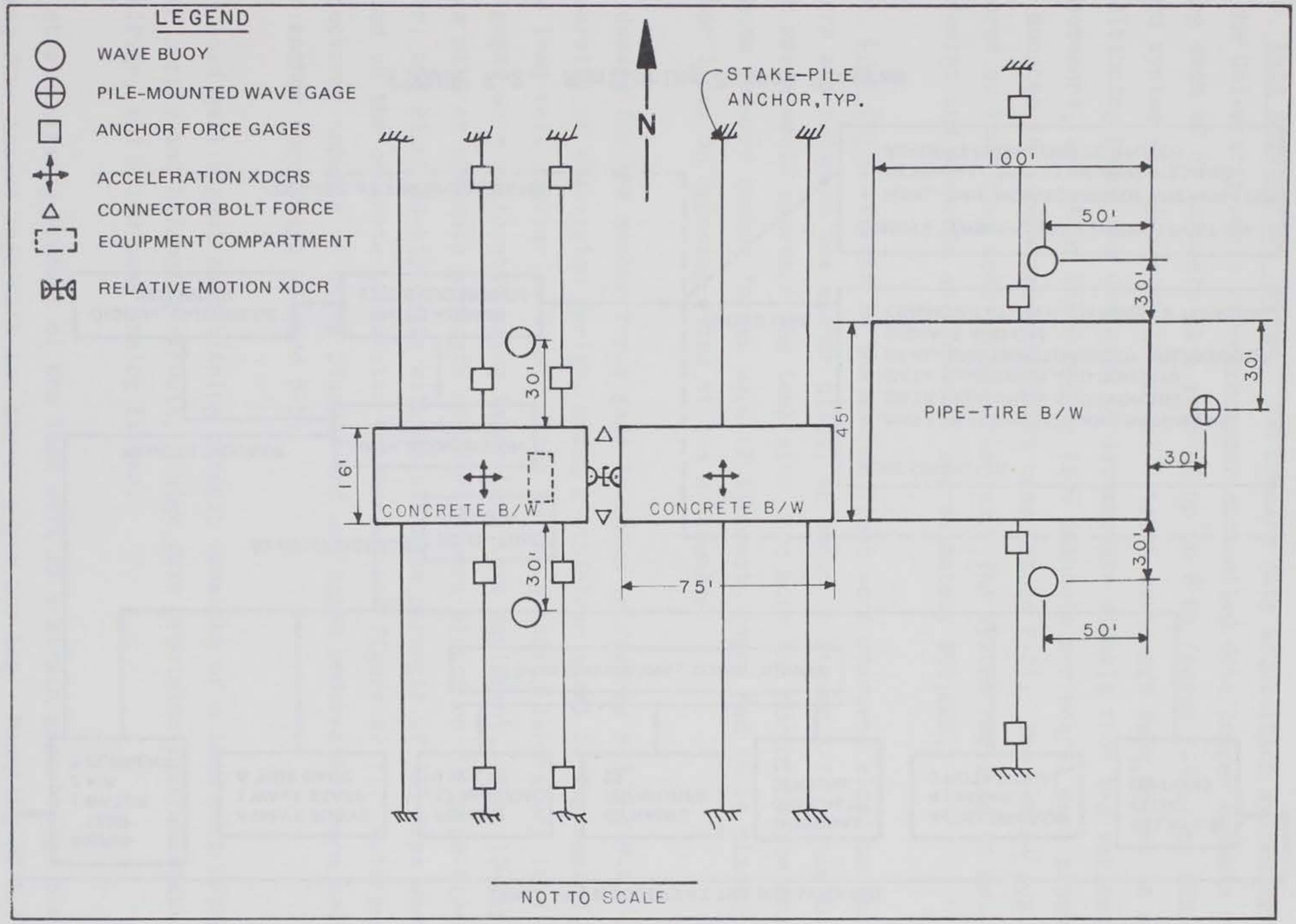

FIGURE F-1. Project Layout

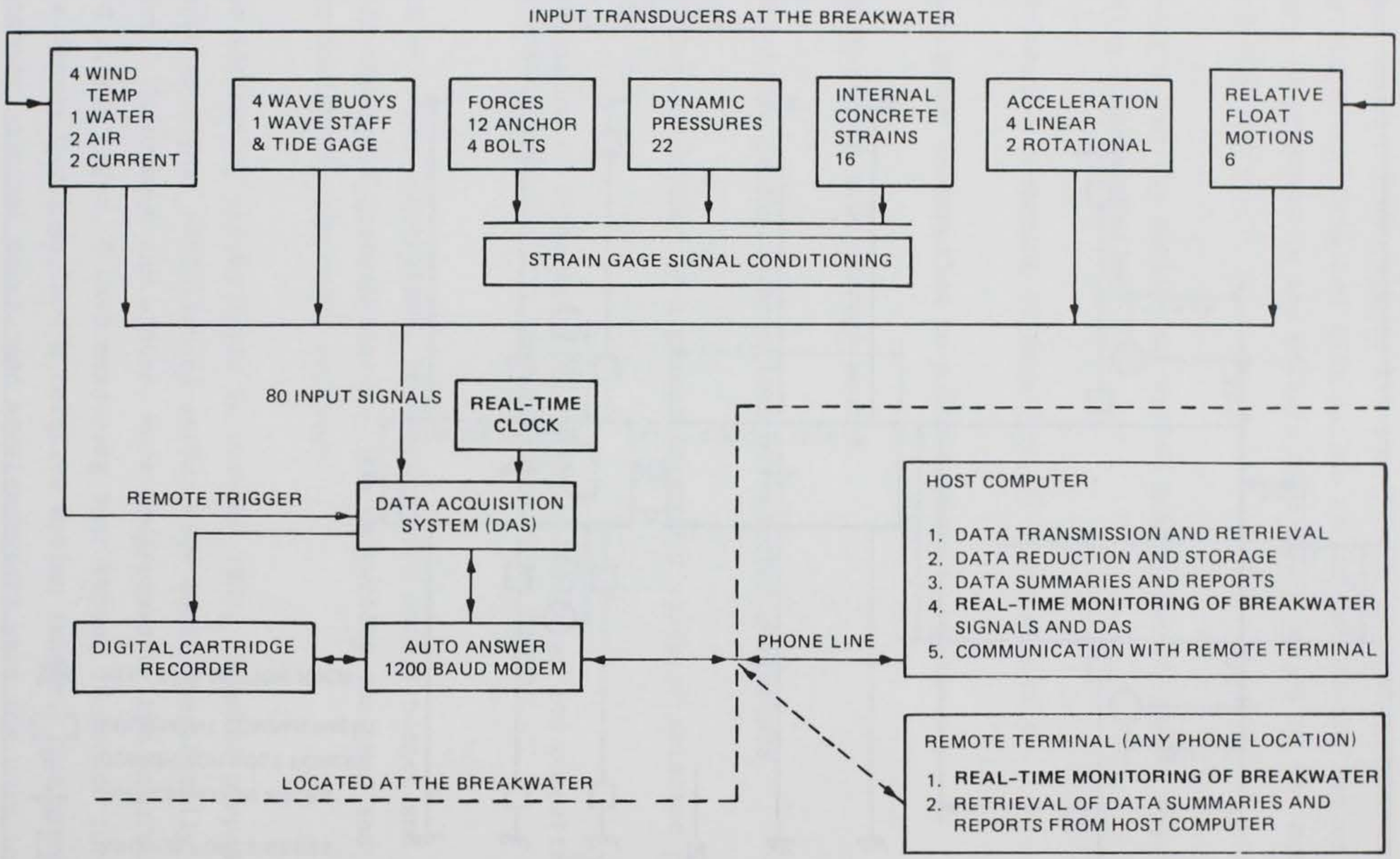

FIGURE F-2. Monitoring System Diagram

2.0 Equipment Description.

2.01 Data Acquisition System. The onboard data acquisition system developed by the University was a microprocessor controlled data logger capable of sampling each of 80 channels at a rate of up to 8 Hz (photo F-1). An RCA microboard system was used with a Quantex 4-track cartridge tape drive. A signal conditioning board was designed to accommodate signals from the various input transducers, and 45 of these boards (two channels per board) were assembled and mounted in a separate watertight case (photo F-2). The entire system was powered by four lead acid truck batteries. The system required 10 man-months to design and assemble at a cost of approximately $50,000.

2.02 Load Cell. Forces in the anchor lines were measured close to the breakwaters and close to the anchor piles, as shown in figure F-1. Since the incident waves would approach the test site from both the north and the south and because leeward anchor forces were of interest, gages had to be placed in the anchor lines on opposing sides of the breakwater.

The design for the anchor force gage is shown in figures F-3 and F-4. It is a University of Washington design, using a stainless steel O-ring sealed strain gage load cell similar in construction to the standard laboratory load cell. The gages were calibrated using laboratory test equipment. Four 10-kip load cells with an ultimate strength of 25 kips were placed on the pipe-tire breakwater, and eight 50-kip cells with an ultimate strength of 125 kips were placed on the concrete breakwater (photo F-3 and figure A-17). Waterproof connectors, capable of being plugged and unplugged underwater, were used on each anchor force gage (figure F-5).

Each load cell signal conditioning circuit consists of a load cell bridge power supply and balancing circuit, a high gain precision instrumentation amplifier, and a low pass analog filter.

The strain sensing element of the load cell is a strain gage bridge circuit having four active legs with two strain gages per leg. Mounting of the strain gages in the load cell is illustrated in photo F-4 and figure F-6. The stress concentration at the edge of the hole is assumed to be a factor of three over

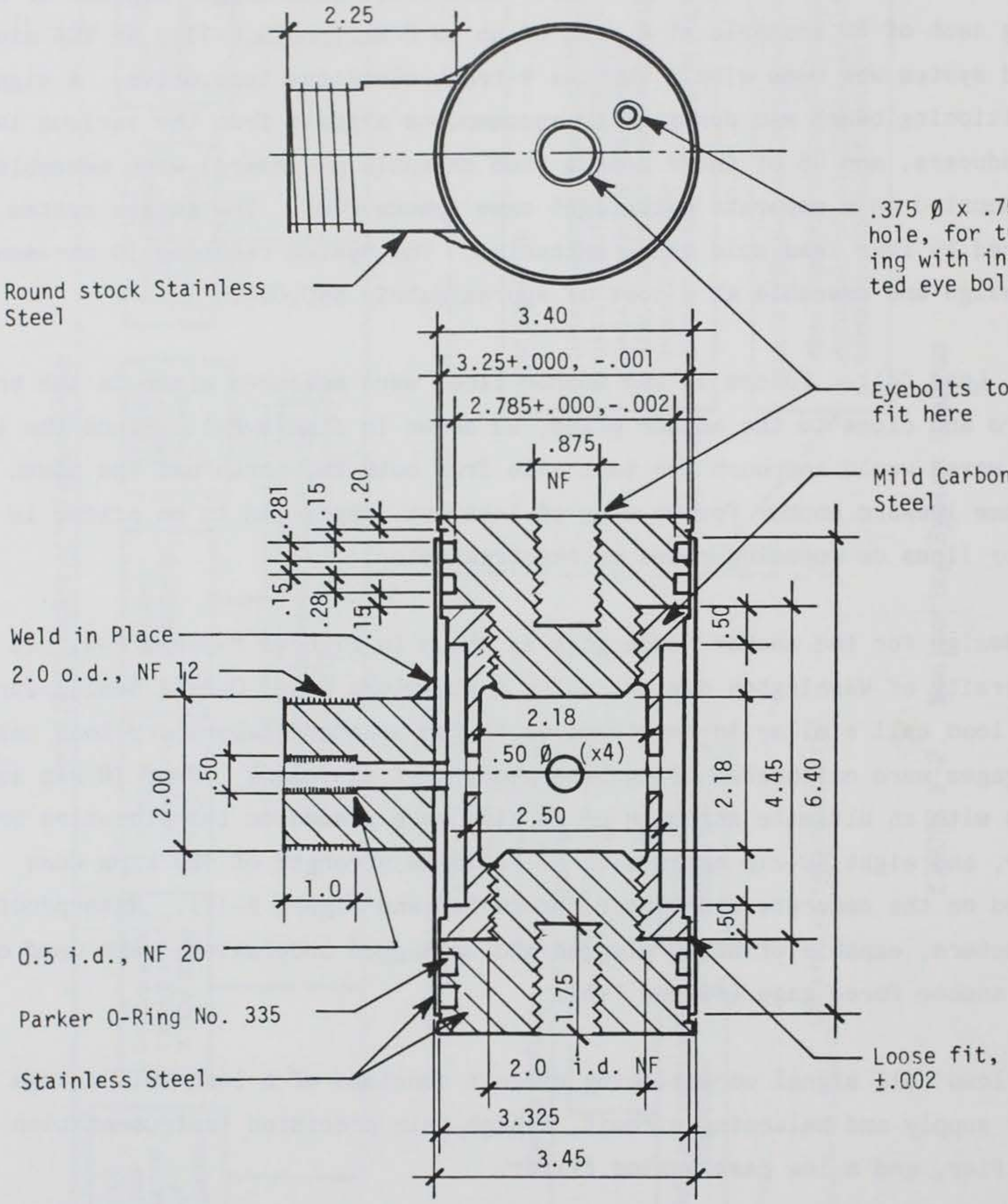

FIGURE F-3. Ten-Kip Load Cell Schematic

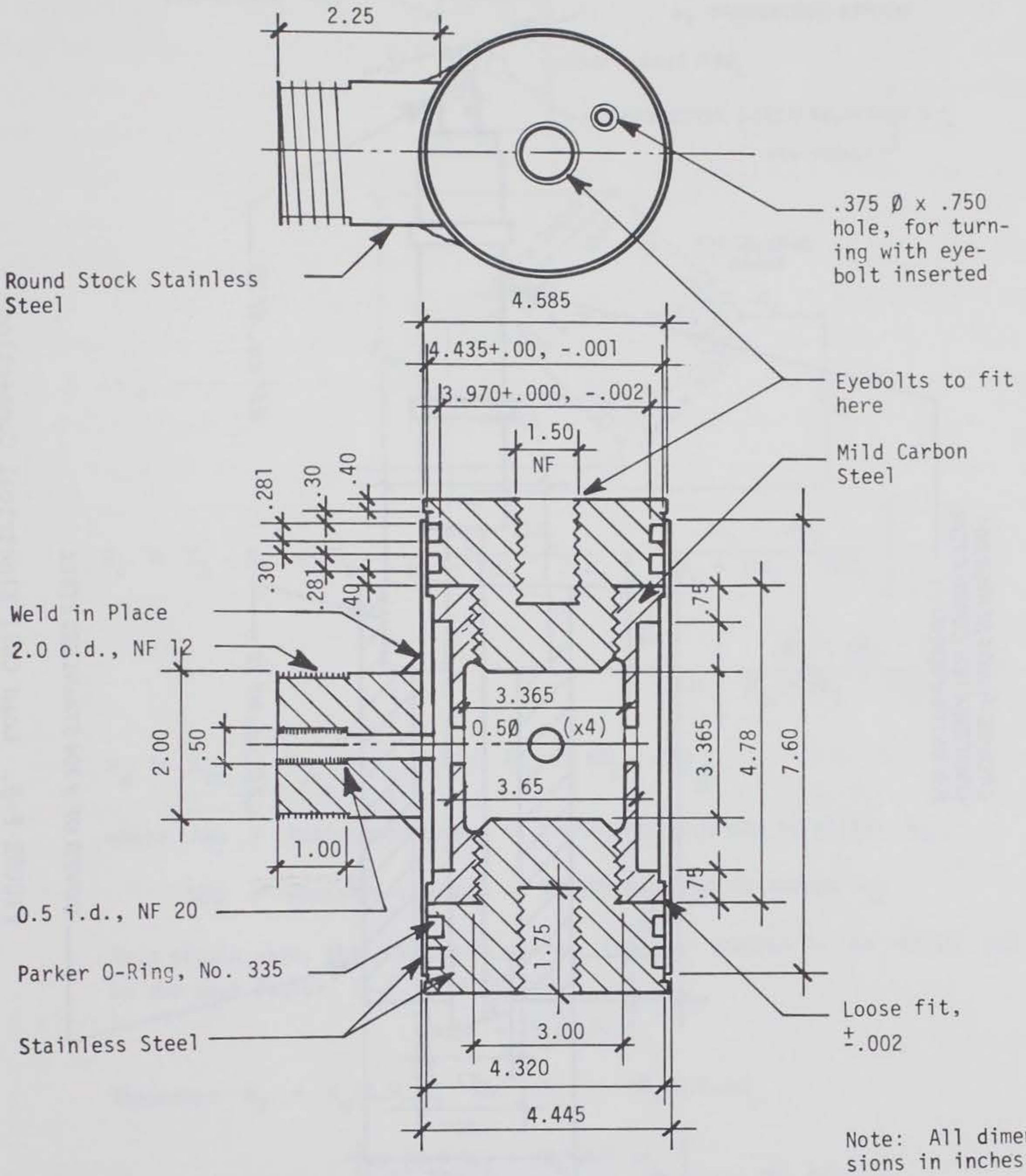

Note: All dimensions in inches

FIGURE F-4. Fifty-Kip Load Cell Schematic

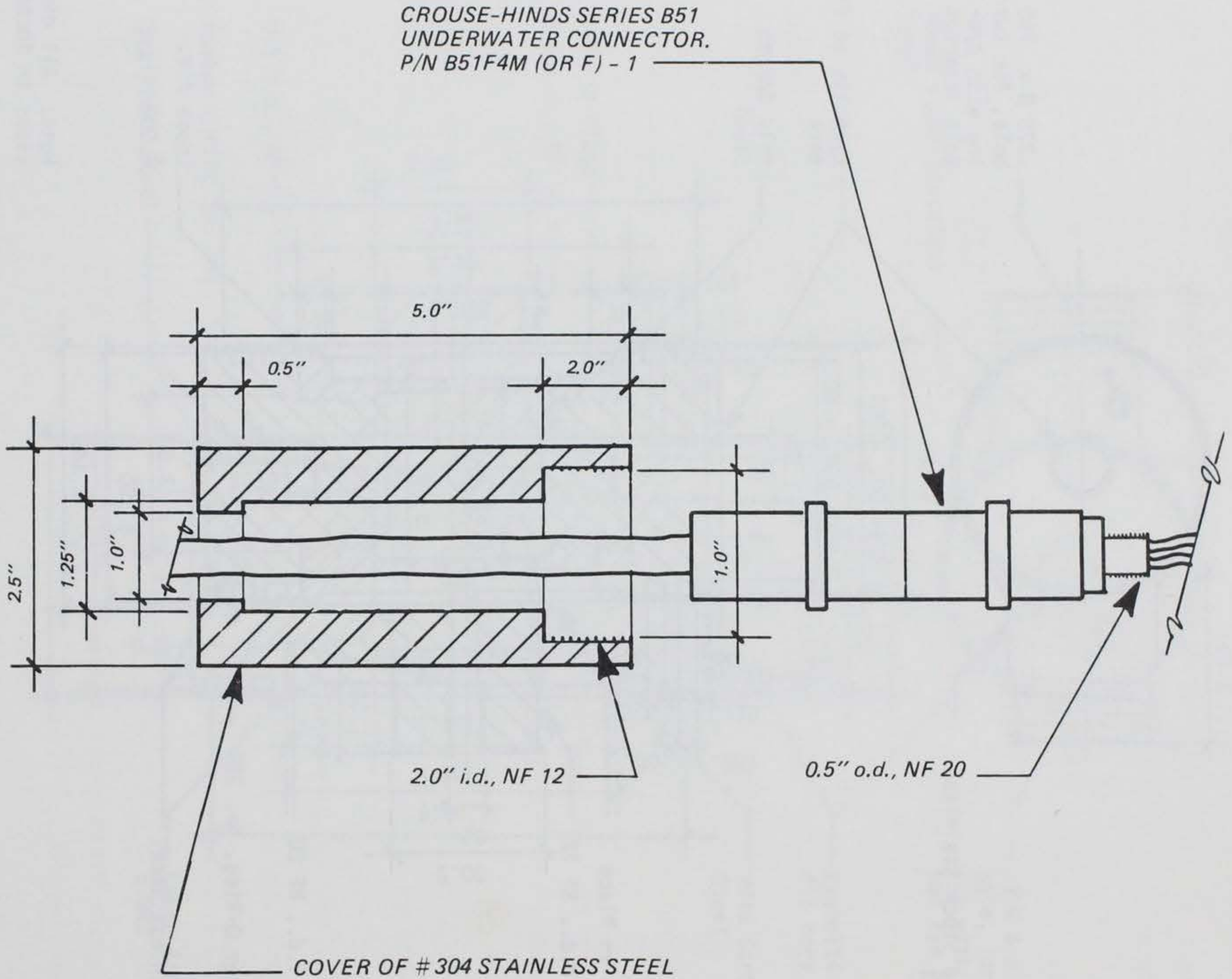

FIGURE F-5. Load Cell Electrical Connection

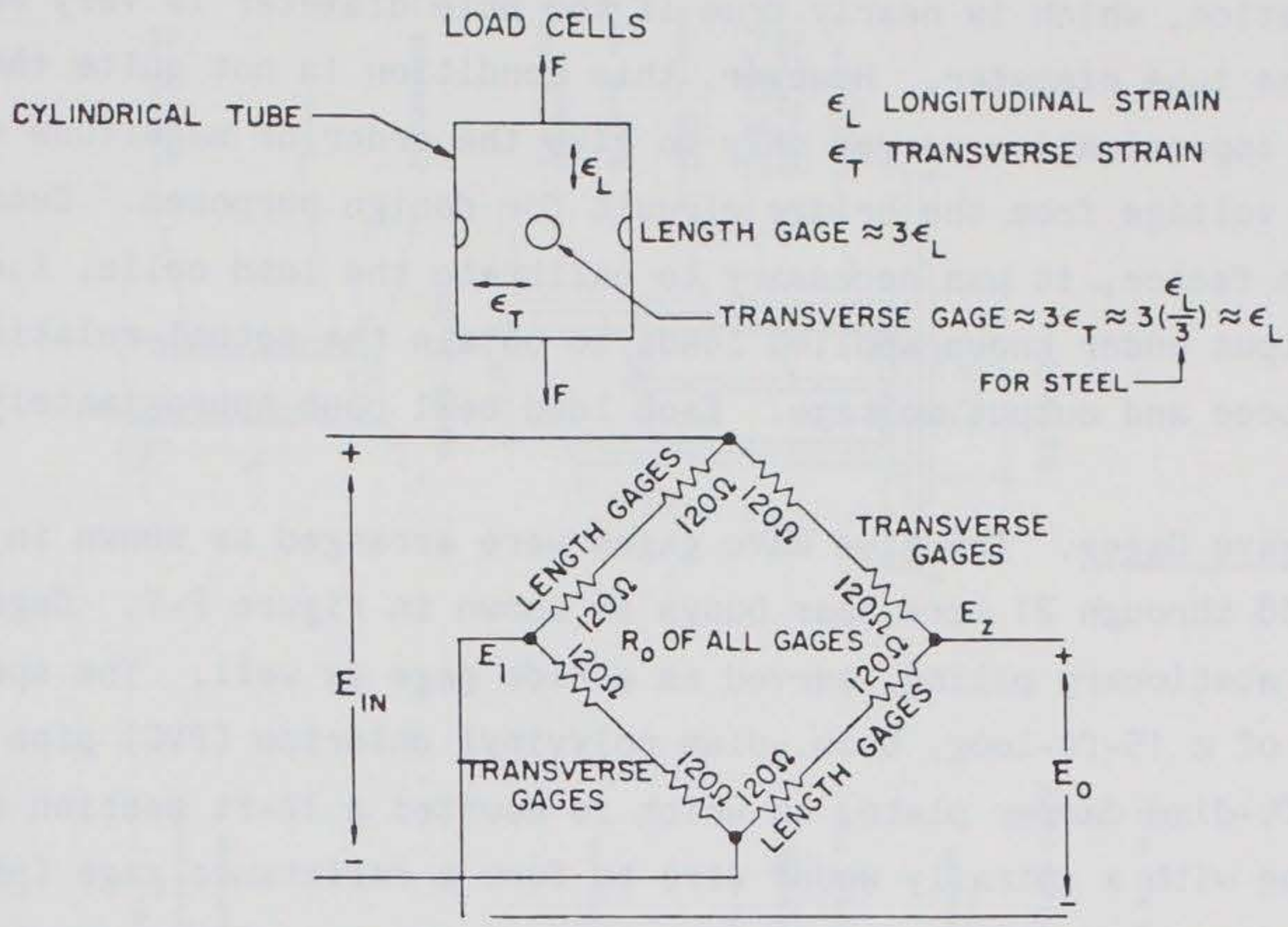

$$E_o = E_2 - E_1 = E_{in}\left[\frac{2R_o + 2\Delta R_L}{4R_o + 2\Delta R_L - 2\Delta R_T} - \frac{2R_o - 2\Delta R_T}{4R_o + 2\Delta R_L - 2\Delta R_T}\right]$$

$$= E_{in}\left[\frac{\Delta R_L + \Delta R_T}{2R_o + \Delta R_L - \Delta R_T}\right]$$

$$E_o \approx E_{in}\left[\frac{\Delta R_L + \Delta R_T}{2R_o}\right] \quad \text{since } 2R_o >> \Delta R_L - \Delta R_T$$

where ΔR_T = Resistance change of transverse gage due to strain ϵ_T

ΔR_L = Resistance change of length gage due to strain ϵ_L

In a strain gage, the resistance change (ΔR) is related to the strain (ϵ) by the gage factor (G.F.) as follows:

$$\Delta R = R_o(G.F.)\epsilon$$

Therefore $R_T = R_o(G.F.)\epsilon_L$ and $\Delta R_L = 3R_o(G.F.)\epsilon_L$

$$\text{and} \quad E_o \approx E_{in}\left[\frac{R_o(G.F.)\epsilon_L + 3R_o(G.F.)\epsilon_L}{2R_o}\right] = 2E_{in}(G.F.)\epsilon_L$$

FIGURE F-6. Strain Gage Layout and Output Calculation

the average stress in the corresponding direction. This is only a rough approximation, which is nearly true if the hole diameter is very small compared with the tube diameter. However, this condition is not quite the case here; so the approximation serves only to give the order of magnitude values for the output voltage from the bridge circuit for design purposes. Because of this unknown factor, it was necessary to calibrate the load cells, i.e., measure the output under known applied loads to obtain the actual relationship between load force and output voltage. Each load cell cost approximately $3,000.

2.03 Wave Gages. The five wave gages were arranged as shown in figure F-1. Gages 18 through 21 were spar buoys as shown in figure F-7. Gage 16, mounted on the stationary piling, served as a tide gage as well. The spar buoys consisted of a 15-ft-long, 6-in.-diam polyvinyl chloride (PVC) pipe with a 2-1/2-ft-diam damper plate, on which is mounted a 12-ft section of 3-1/2-in. PVC pipe with a spirally wound wire to form a resistance gage (photo F-5). The necessary electronics were installed in the top of the upper section. Gage 16 was a 25-ft-long 3/4-in.-diam PVC pipe attached to a steel cage that was bolted to the piling. This gage served as both a wave gage and a tide gage, and, therefore, extended from -5 ft mean lower low water (MLLW) to +20 ft MLLW (figure F-8).

Between mid-October 1983 and late January 1984 when the breakwater was removed, the eight-gage linear wave buoy array was anchored where the rubber tire breakwater was originally located. These gages were at a 5-ft spacing and located 67 ft due west of the tide gage. The longitudinal alignment of the array was parallel with the breakwater (figure F-9).

2.04 Wave Staff Design. A block diagram of the wave staff and associated electronic circuits is shown below:

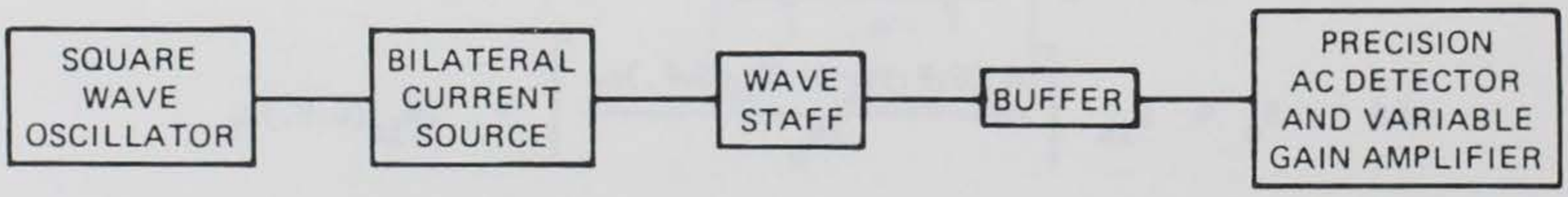

The wave staff itself consists of a length of PVC tubing that is spirally wound with a resistance wire such that when it is immersed in seawater, the

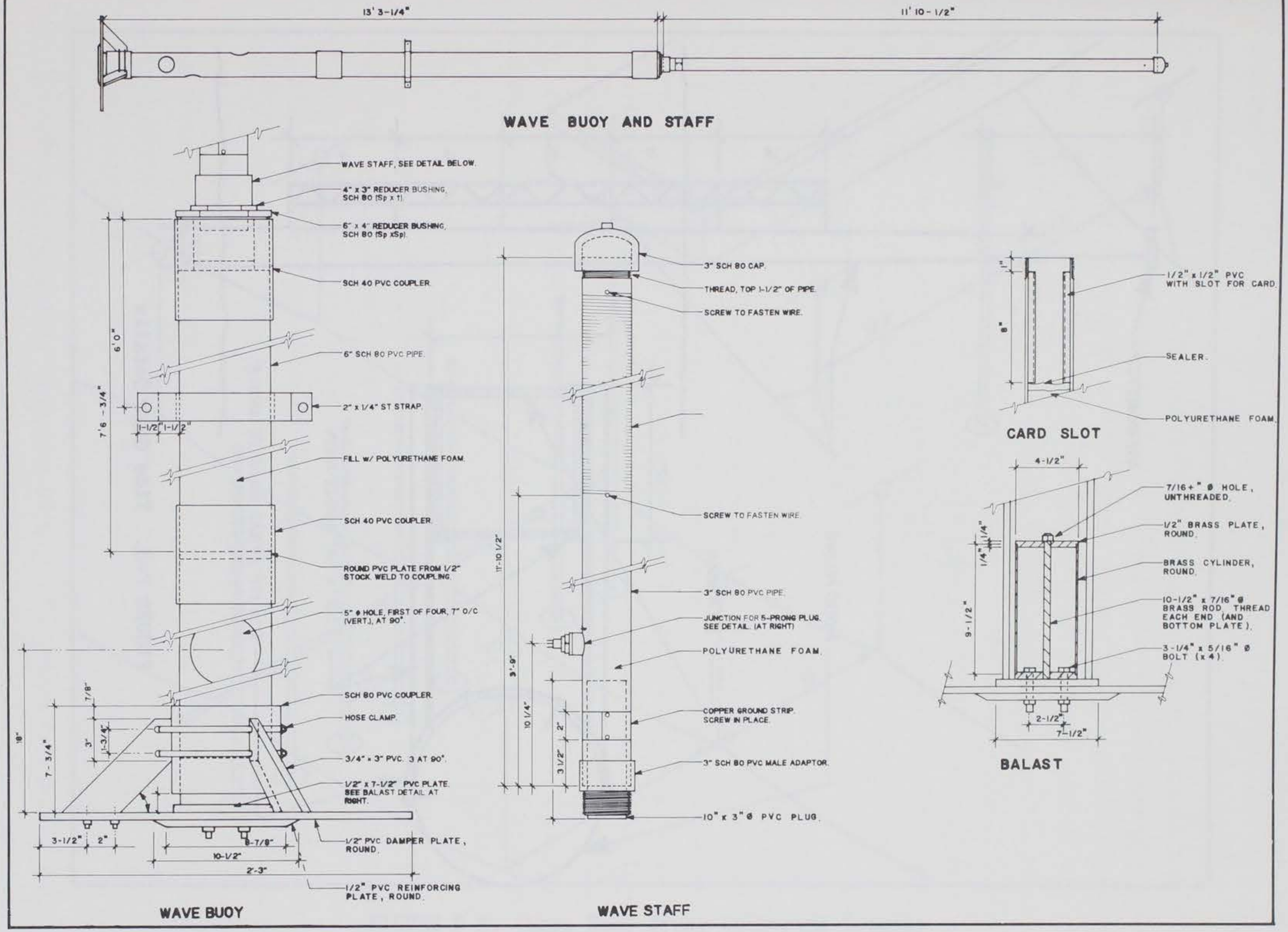

FIGURE F-7. Wave Buoy and Staff Schematic

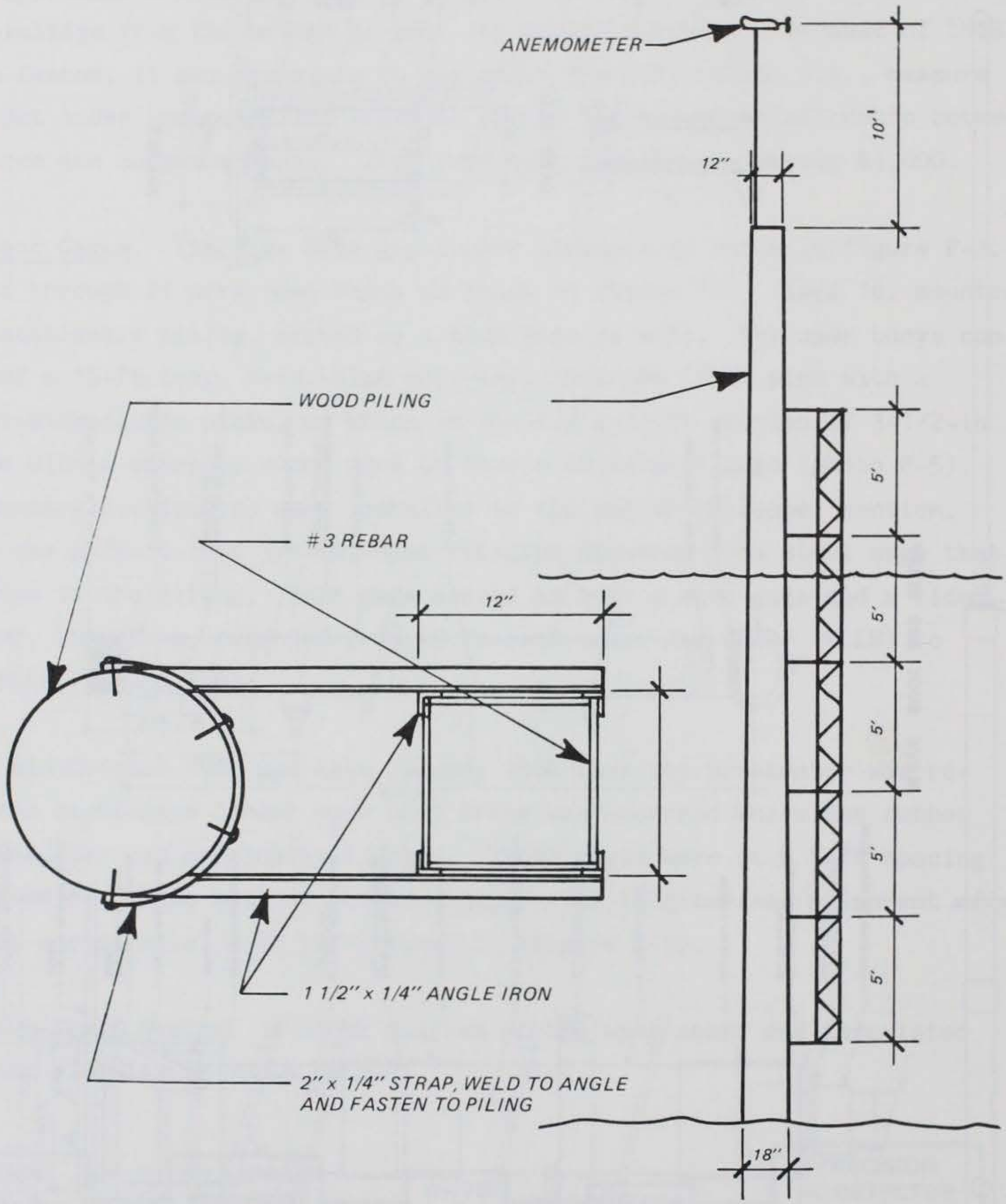

FIGURE F-8. Tide Gage Details

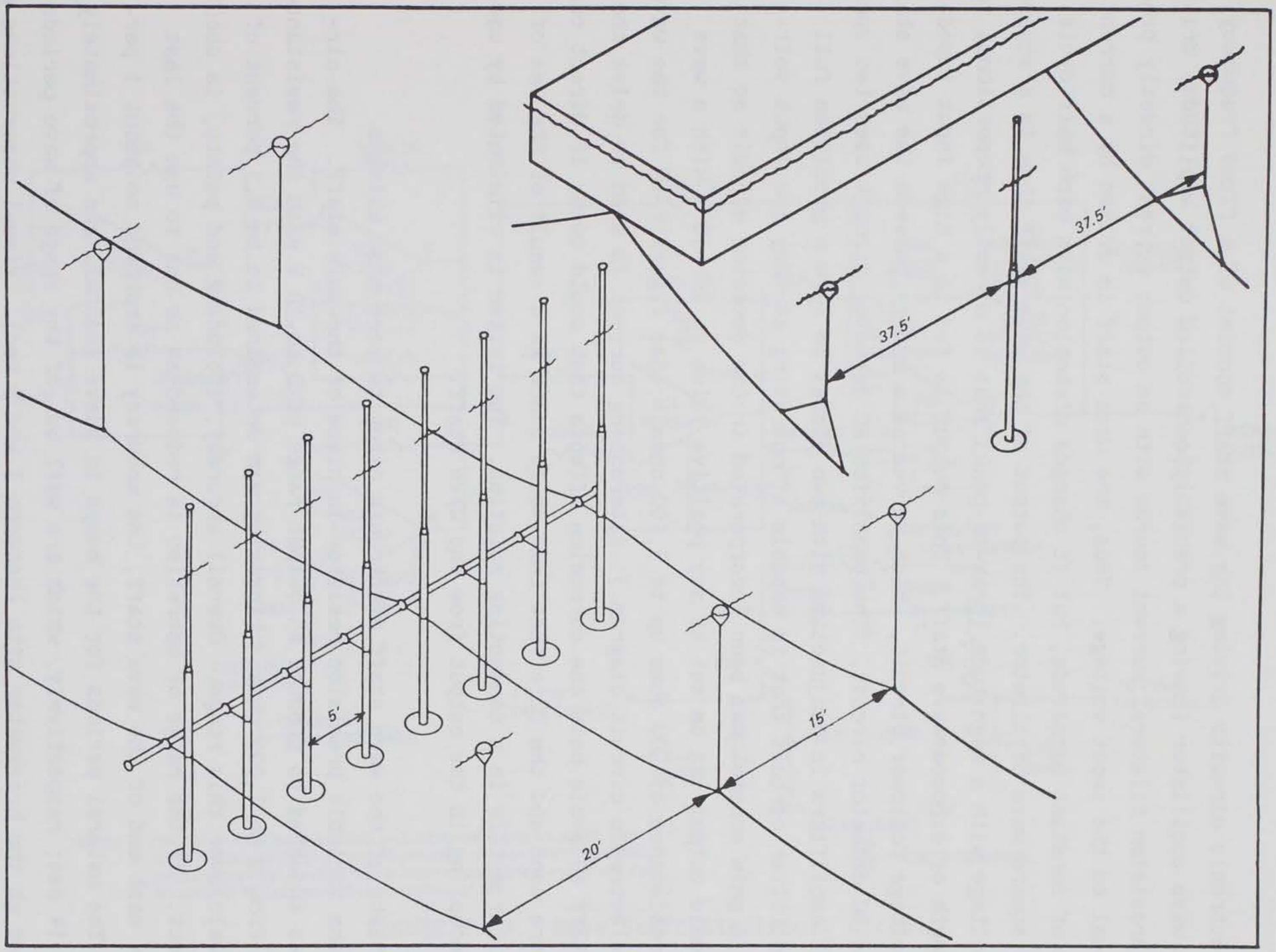

FIGURE F-9. Wave Buoy Array Anchoring Details

electrical resistance varies in direct proportion to the length of the exposed staff.

The electronic circuits driving the wave staff consist of a fixed frequency square wave oscillator (having a precisely controlled output amplitude) driving a precision bilateral current source with an output current directly proportional to the input voltage. Thus, the wave staff is driven by a current source of constant magnitude, but it changes direction with each half cycle of the square wave oscillator. The output of the wave staff then is a square wave voltage with a magnitude (peak-to-peak) that is directly proportional to the length of exposed wave staff. This output is fed to a high input impedance voltage follower circuit, which serves as a buffer between the wave staff and the AC detector circuit. The precision AC detector circuit uses two operational amplifiers in conjunction with two diodes to form a precision full wave rectifier circuit that is capable of operating at very low input voltages. A gain control has been incorporated in the detector circuit so that full scale output can be set at any positive value up to +10 V with a wave staff resistance of 300 ohms up to 3,000 ohms. (See figure F-10 for the wave staff electronic circuit diagram.) Alternating current is used to drive the wave staff to avoid both the corrosion effects that would occur if direct current were used and the DC offset that would occur as a result of the use of dissimilar metals in a conducting solution. The latter is eliminated by use of AC coupling in the output from the wave staff.

Bench tests of the wave staff electronic circuits were made using a 1,000-ohm variable precision resistor in place of the wave staff. The circuit was adjusted to produce an output range of 0 to 10 V with the resistance varied from 0 to 1,000 ohms. Linearity was determined to be 0.1 percent of full scale over this range. Overall accuracy, including end points, is about 3 percent. If the range of operation is reduced so as not to use the last 1 ft on each end of the wave staff, the accuracy is improved to about 1 percent. The natural periods for the buoys in heave and roll are approximately 18 and 14 sec, respectively, which are well out of the range of wave periods expected at the breakwater site (between 3 and 5 sec). Visual observations of the buoy in waves in excess of 1-1/2 ft indicated little heave or roll motion, but some yaw about the anchor line was caused by the current and wind. See

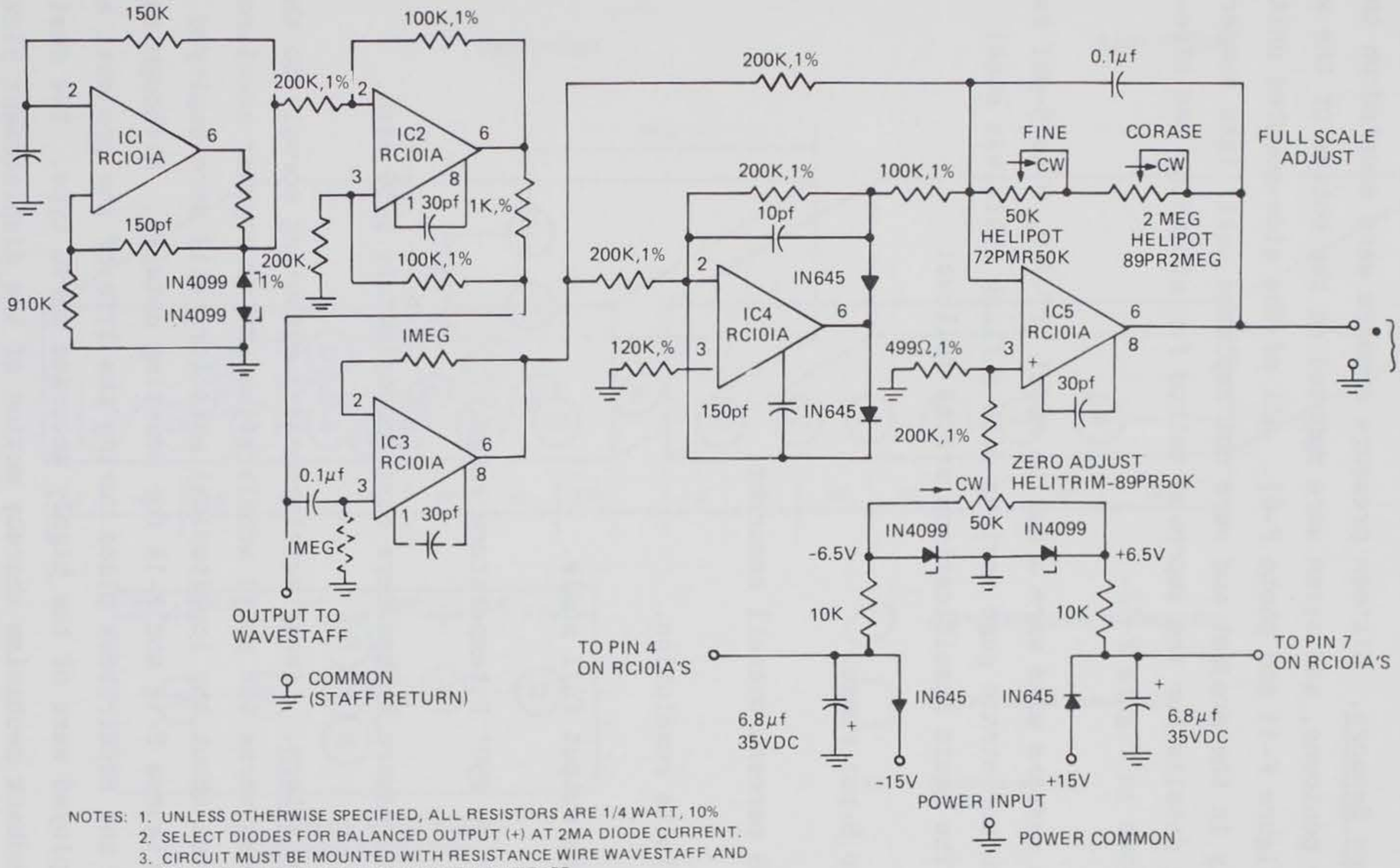

NOTES:
1. UNLESS OTHERWISE SPECIFIED, ALL RESISTORS ARE 1/4 WATT, 10%
2. SELECT DIODES FOR BALANCED OUTPUT (+) AT 2MA DIODE CURRENT.
3. CIRCUIT MUST BE MOUNTED WITH RESISTANCE WIRE WAVESTAFF AND GROUNDED TO SALT WATER AT THE WAVESTAFF.

FIGURE F-10. Wave Staff Electronic Circuit

paragraphs 3.0 and 4.02 of this appendix for a further description of installation and maintenance of the wave gages. Cost of the spar buoy wave gages was approximately $3,000 each.

2.05 Pressure Sensors. Sixteen pressure sensors were mounted on the sides of the concrete pontoons, and seven were mounted on the bottom of the west pontoon only (figure F-11 and photo F-6). All of the side-mounted units were damaged early in the project and were not replaced until late summer 1983. The mounting details for the improved method for attaching the side-mounted gages are shown in figure F-12.

The pressure sensors used were a Kulite Model IPT-750, 0 to 5-psi range. They are semiconductor strain gage devices with a flush stainless steel diaphragm. The basic specifications are as follows:

a. 0 to 5-psi range.

b. 0.85 percent overall accuracy.

c. Infinite resolution.

d. 75-mv output full scale.

e. -40° to 250° F temperature range.

The original pressure transducers cost approximately $450 each.

2.06 Accelerometers. Linear accelerometers measuring normal (to the deck, or heave) and transverse (or sway) acceleration and an angular accelerometer measuring rotation about the longitudinal axis (or roll) were employed on each float. See figures F-13 and F-14 for mounting details. Although some change of equipment and repair took place during the life of the project, all accelerometers employed were of the highly accurate servo type. The design incorporates a feedback mechanism whereby motion of the displacement pickoff produces a countering force (or moment) that accelerates the seismic mass so that it undergoes only a minute displacement from the applied input motion. This

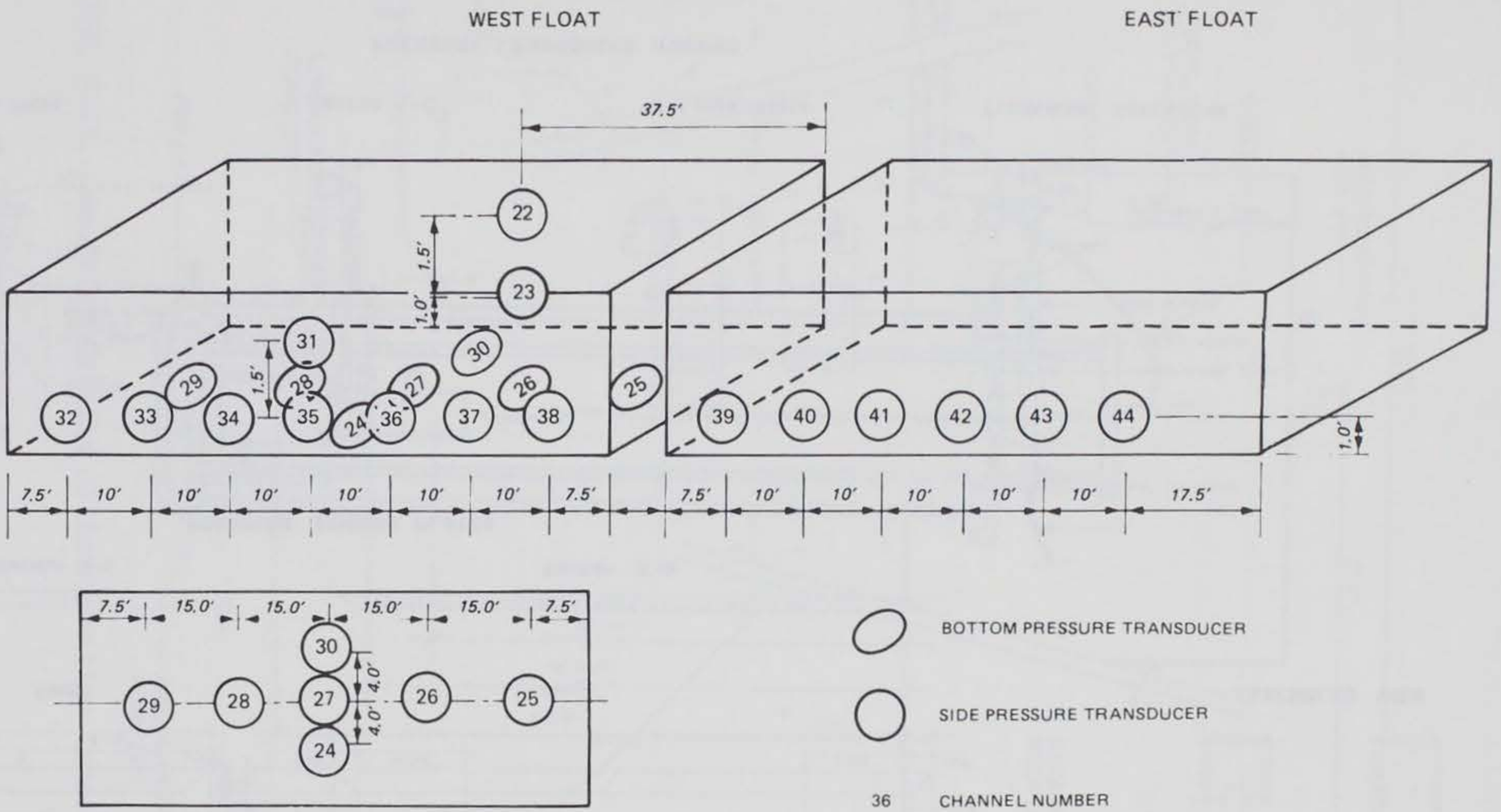

FIGURE F-11. Pressure Transducer Layout

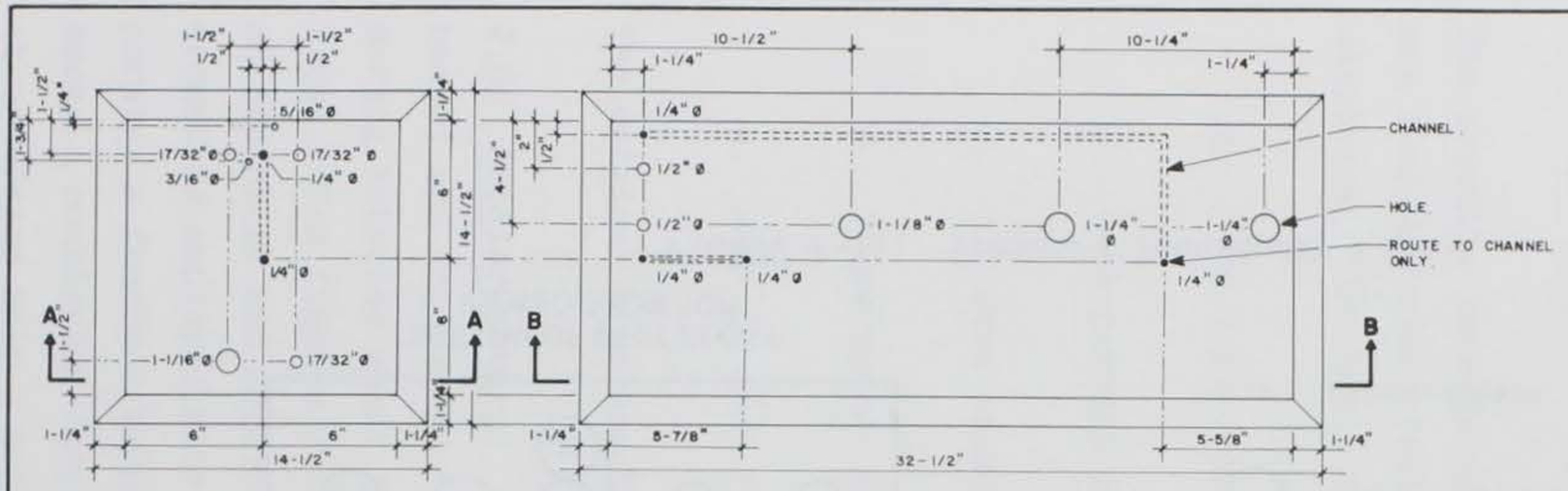

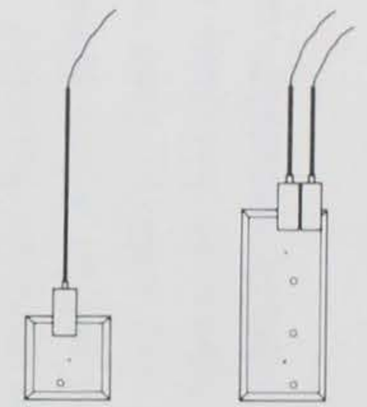

ASSEMBLED VIEW

Section A-A

Section B-B

PRESSURE SENSING PLATES

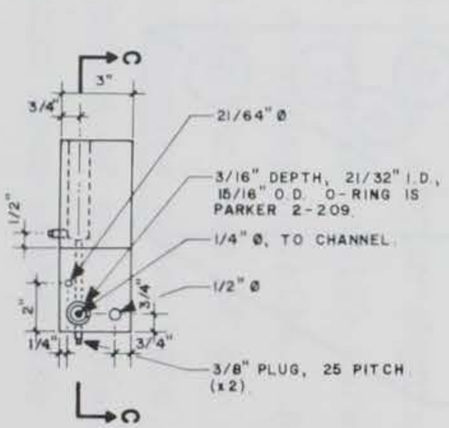

to Small Plate

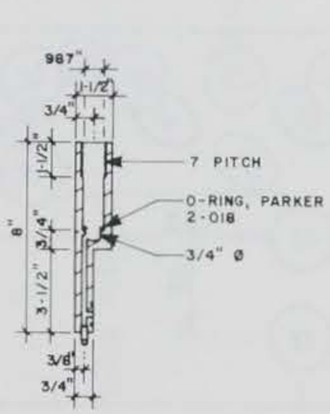

Section C-C

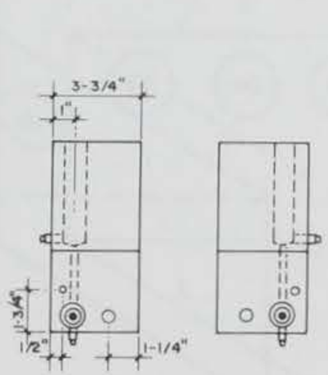

to Large Plate

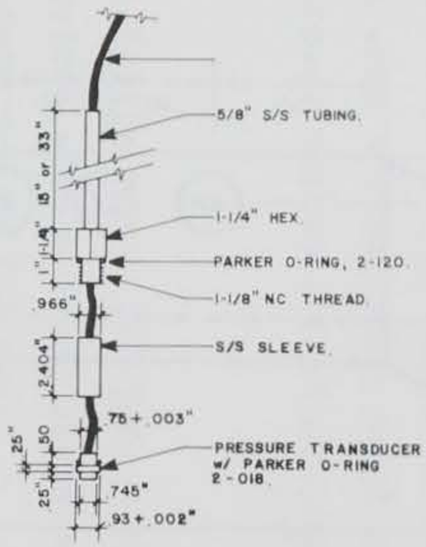

Transducer Connection

PRESSURE TRANSDUCER HOUSING

NOTE:
HOUSINGS TO LARGE PLATE ARE MIRROR IMAGES. DIMENSIONS NOT SHOWN ARE THE SAME AS ON HOUSING TO SMALL PLATE. SECTION C-C IS SAME ON ALL HOUSINGS.

Figure F-12. Mounting Details of Side Pressure Transducers

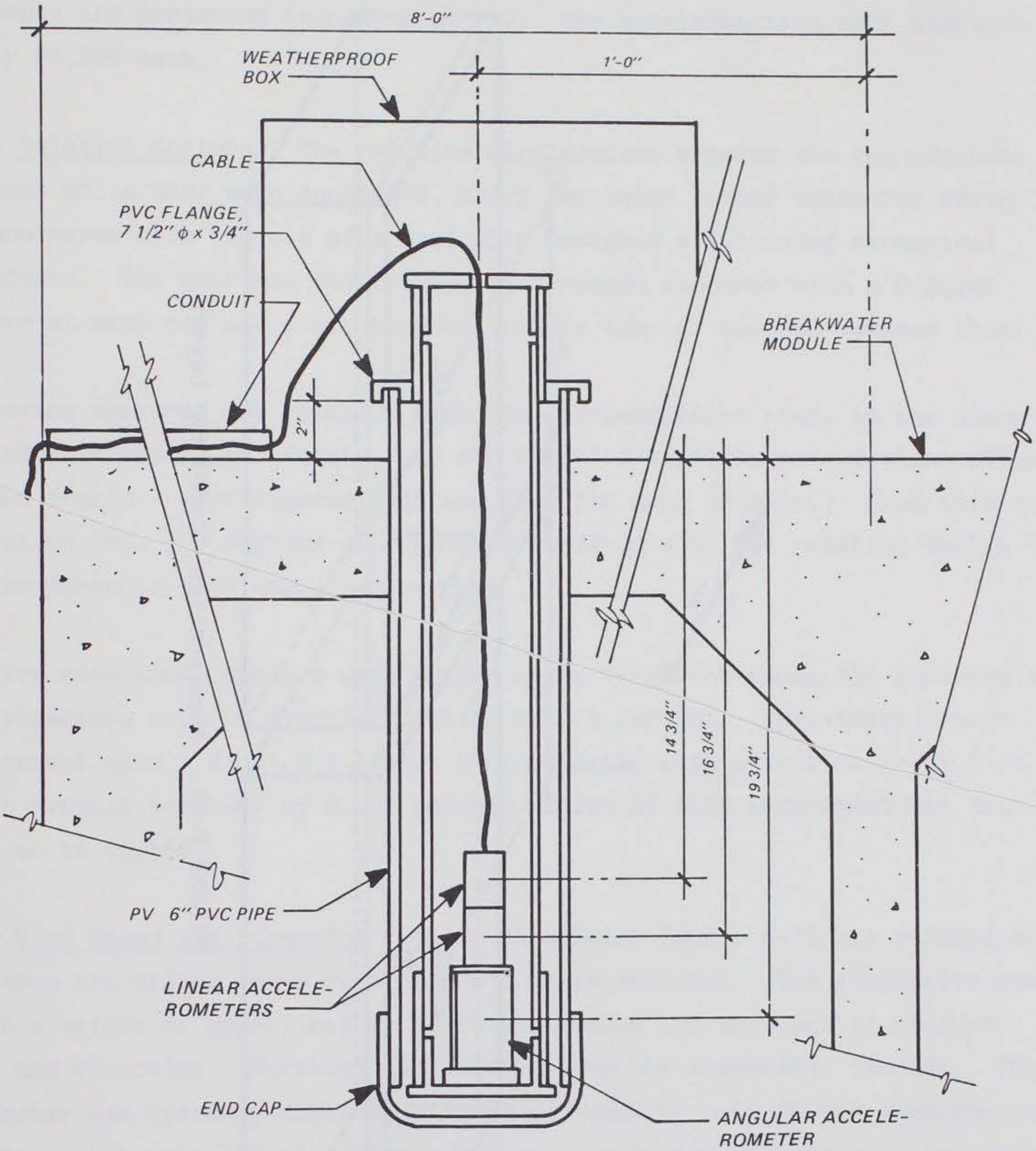

FIGURE F-13. Mounting Details of Acceleration Transducers

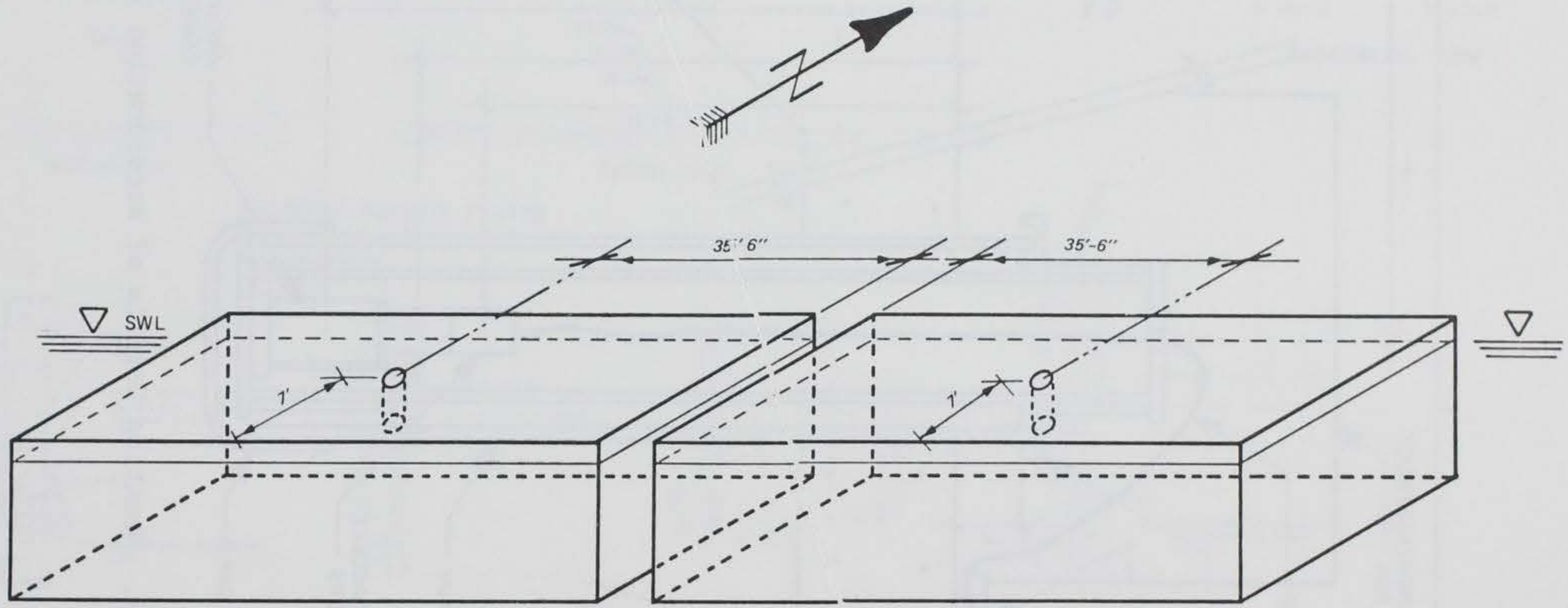

FIGURE F-14. Acceleration Transducer Layout

feature, combined with a flexural suspension system, provided for accurate acceleration measurement with minimal nonlinearities and negligible hysteresis. Internal filtering mechanisms provided very clean data; therefore, no additional filtering or detrending was required. Some results of the motion measurements are presented in reference F-2. The accelerometers cost approximately $1,200 each.

2.07 Relative Motions. The relative displacement between the two concrete pontoons while they were connected, using the later rubber connector design, was monitored with the use of a specially designed articulated mechanical transducer. The unit was constructed of anodized aluminum with a U-joint fixture at each end and a rotating extendable tubular section between them.

The device measured the rotation about the perpendicular axes, in the plane of the end sections of the floats, and the relative distance and rotation between the two floats. (See figures F-15 and F-16 for more details.) From this configuration, all six degrees of freedom associated with the relative motion of the two pontoons were computed.

The five rotational motions were sensed using Vernitech Model 106 Sine-Cosine potentiometers with an overall accuracy of 0.3 percent. The single linear measurement used a Model-111 linear potentiometer with a full range of 8 in. and an overall accuracy of 0.015 percent. Cost of this instrument was estimated to be $5,500.

2.08 Wind Speed and Direction. A cup anemometer (photo F-7) was mounted on a pole atop the piling where wave gage No. 5 was attached. The anemometer was set at a height of approximately 30 ft above MLLW and was used to measure speed and direction. Duration was deduced from the anemometer records. The anemometer was operated continuously and was used to turn on the complete monitoring system when the wind speed reached a preselected speed duration level. The cost of the anemometers was $450 each.

2.09 Concrete Strain. Measurements of internal concrete strains were made at 12 locations on the west module using rebar strain gages (figures F-17 through F-25). The gages, which were built at the University, were constructed using

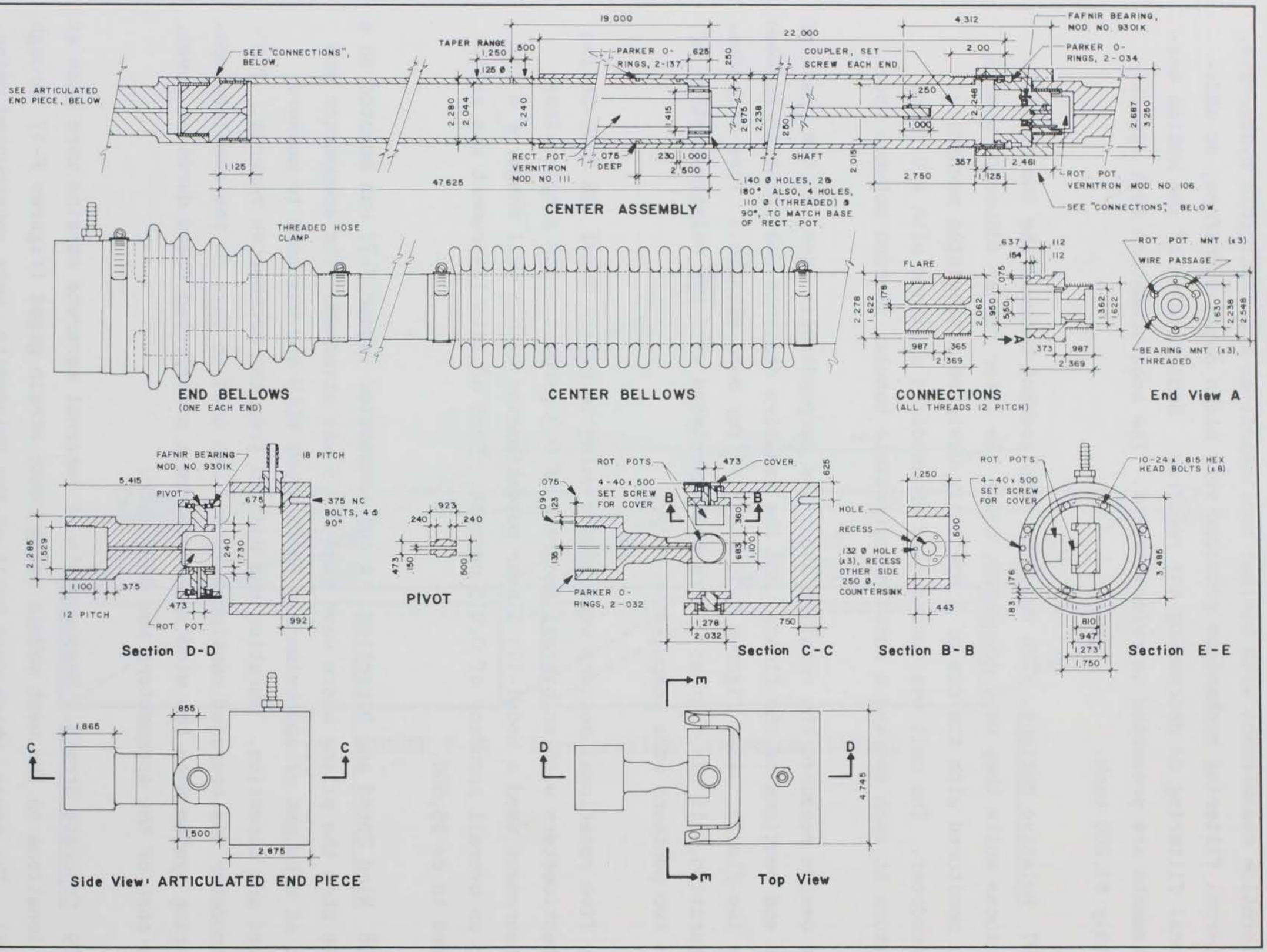

FIGURE F-15. Relative Motion Device Schematic

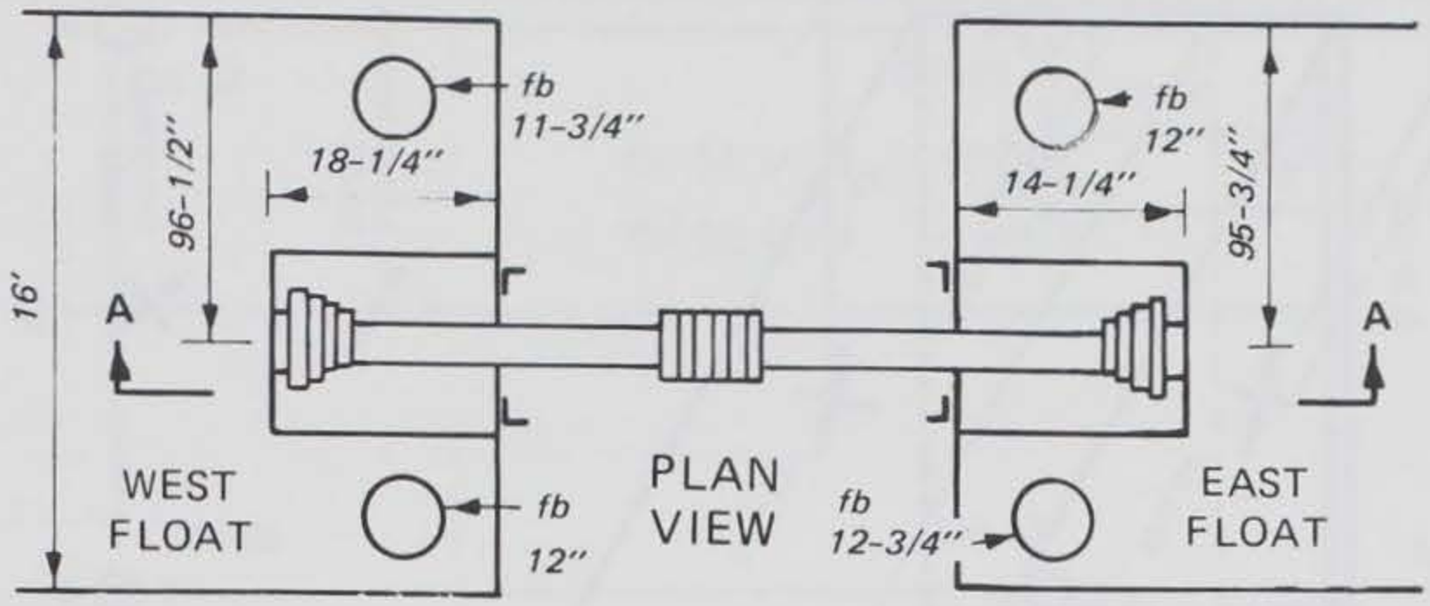

fb = FREEBOARD

NOT TO SCALE

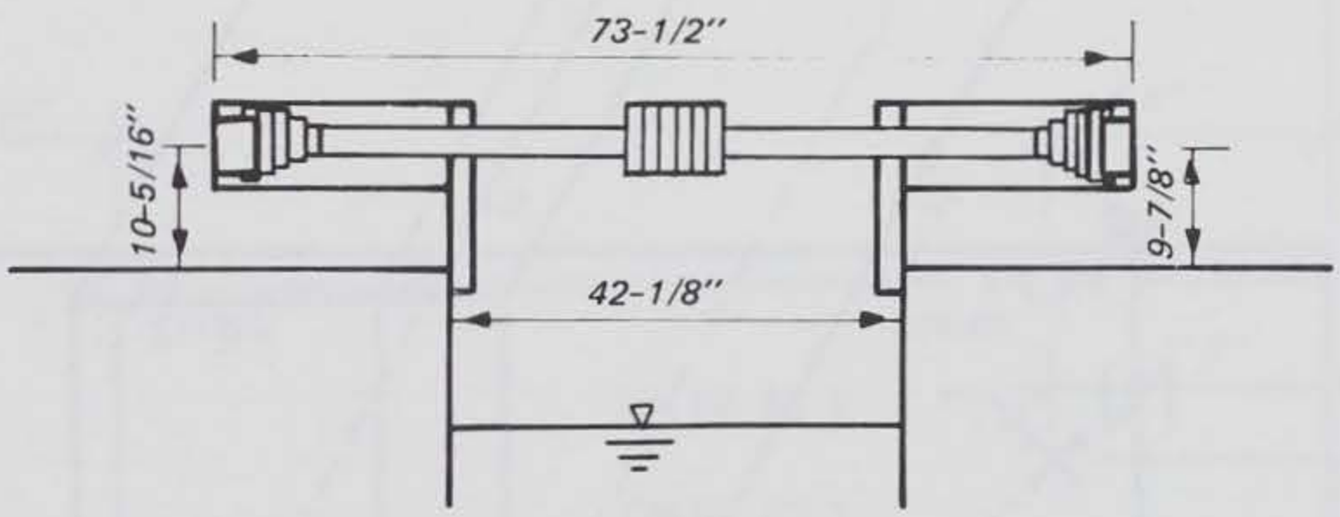

SECTION A-A

FIGURE F-16. Relative Motion Device Location Details

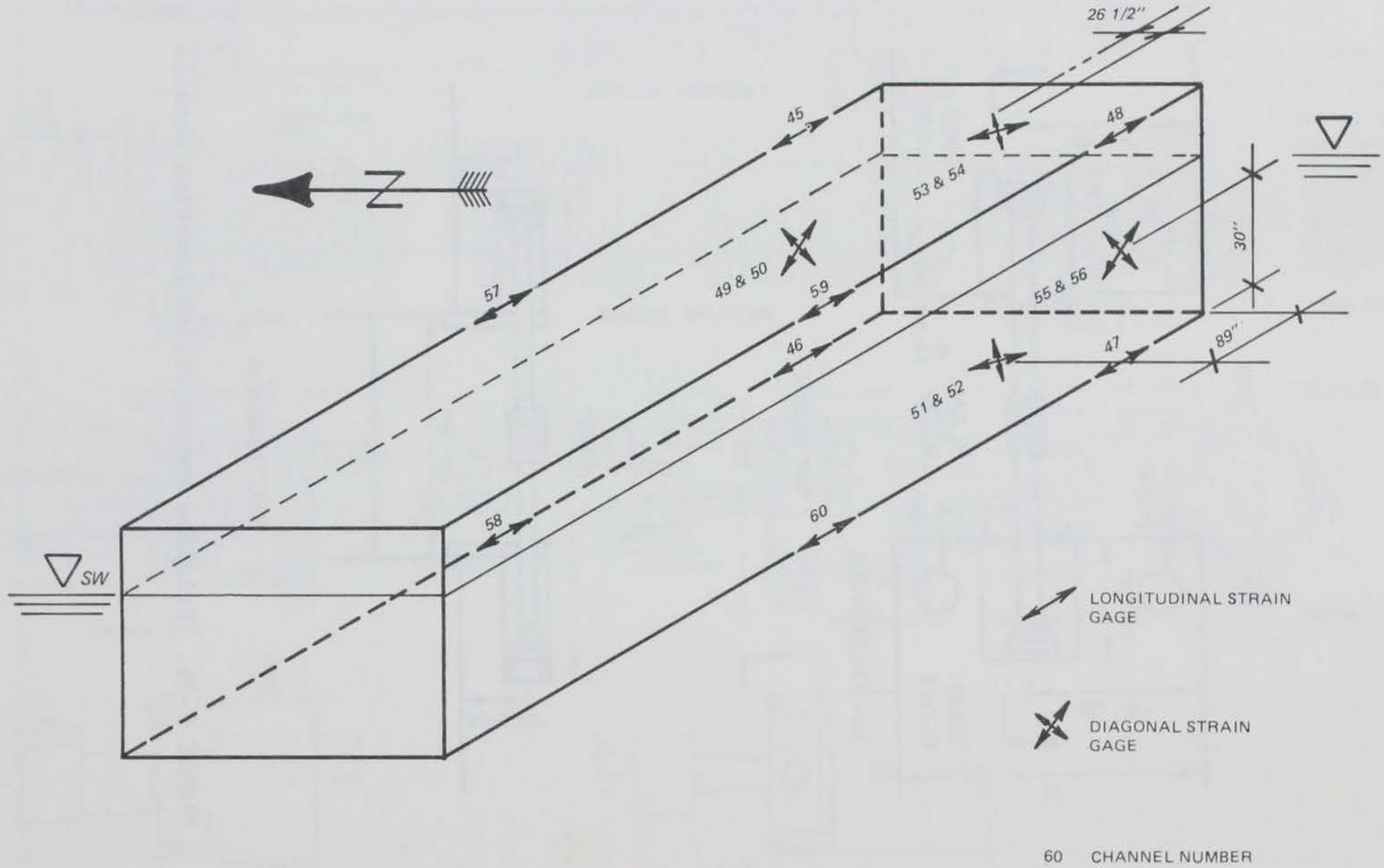

FIGURE F-17. Concrete Strain Gage Locations

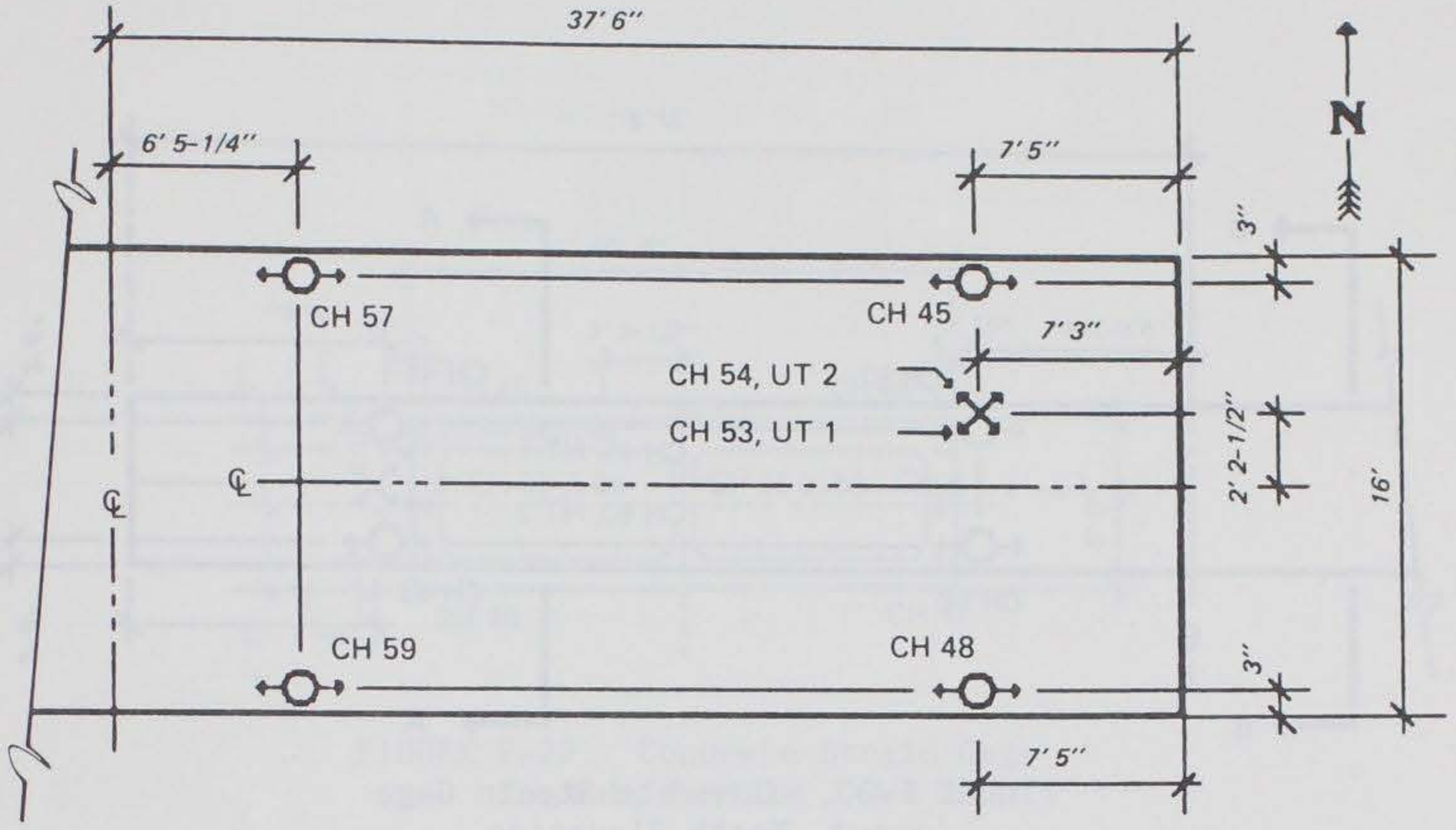

FIGURE F-18. Concrete Strain Gage Layout, Top Plan

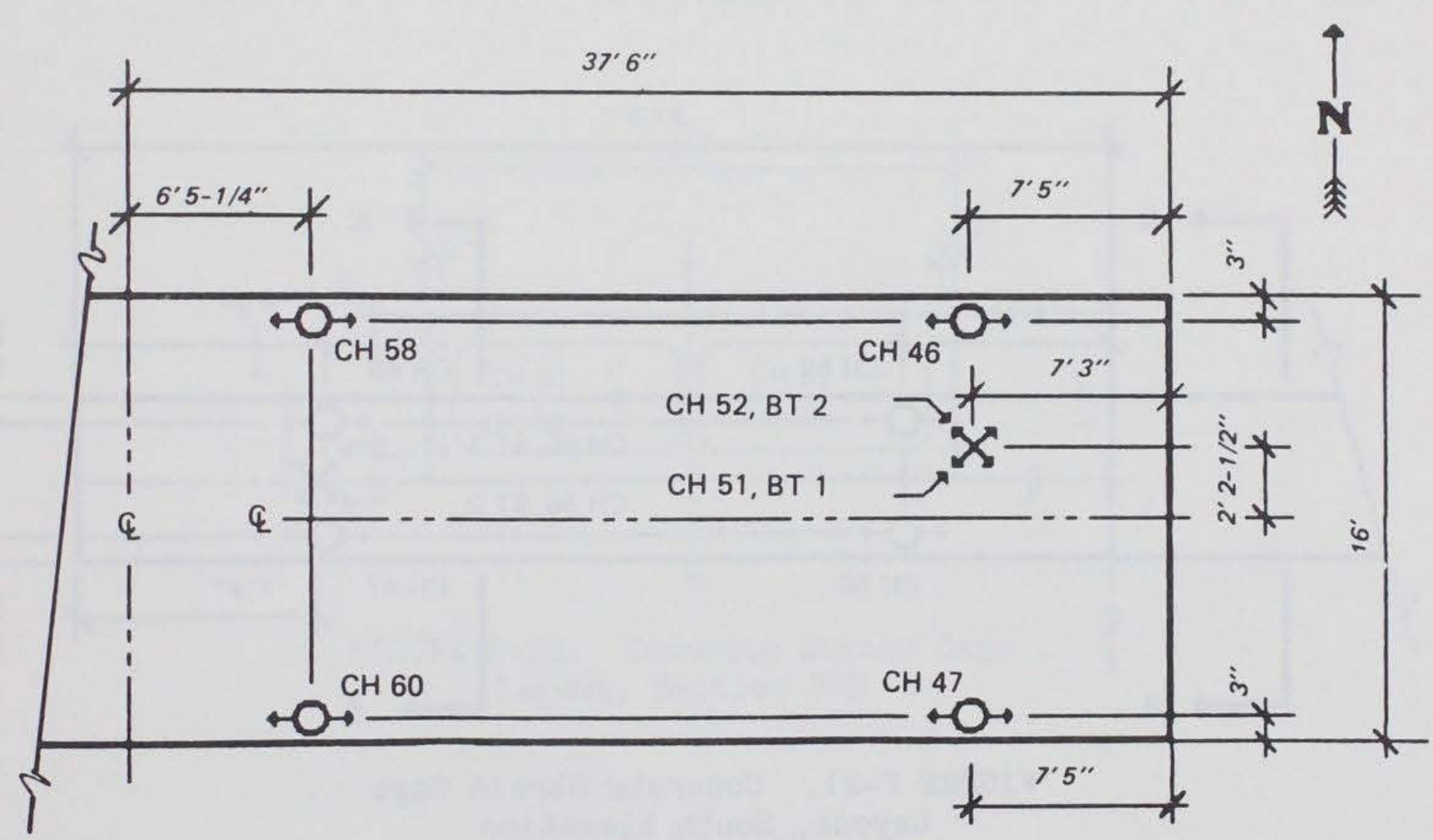

FIGURE F-19. Concrete Strain Gage Layout, Bottom Plan

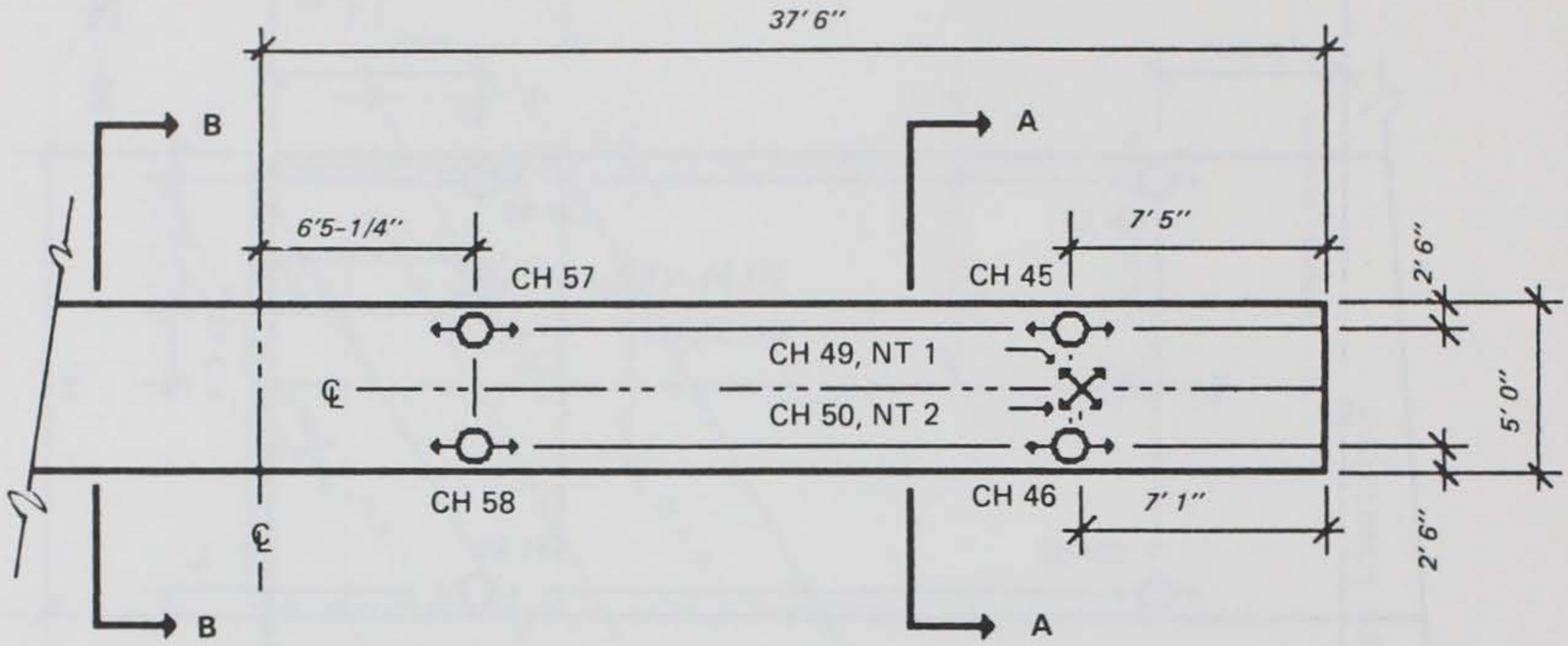

FIGURE F-20. Concrete Strain Gage Layout, North Elevation

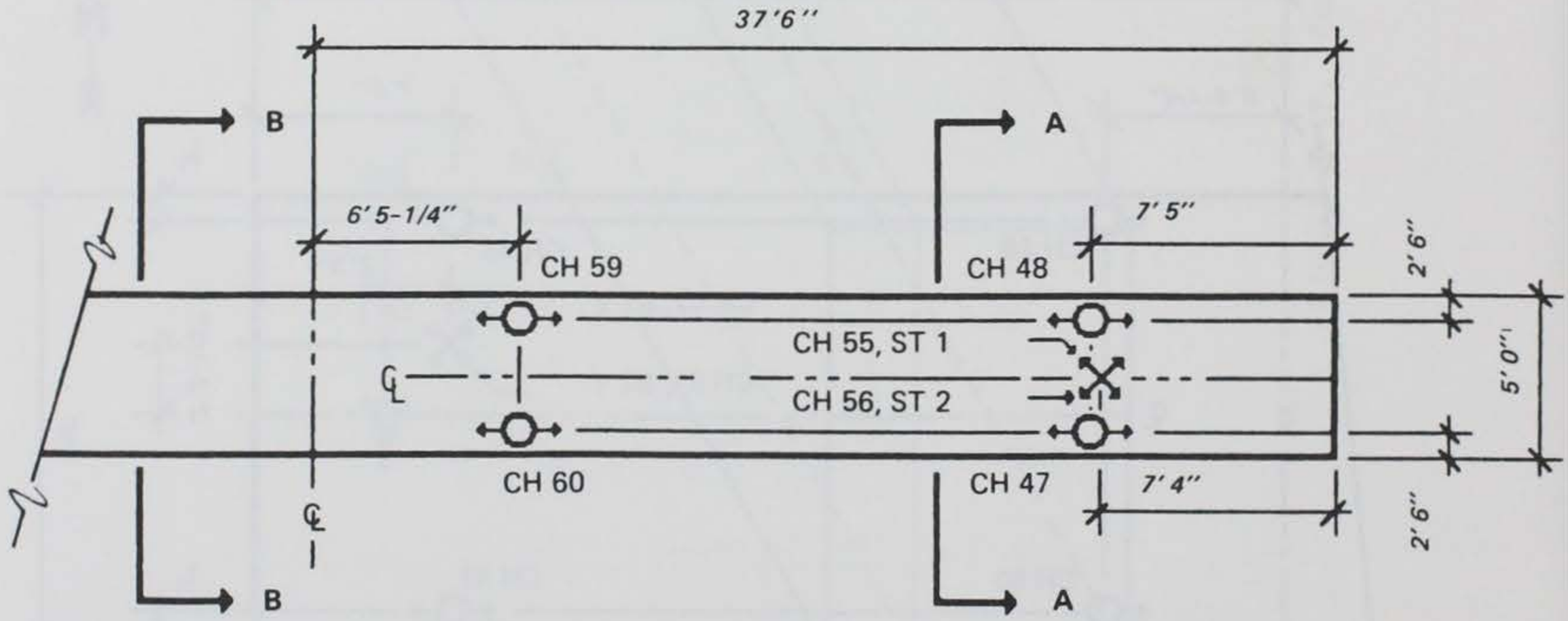

FIGURE F-21. Concrete Strain Gage Layout, South Elevation

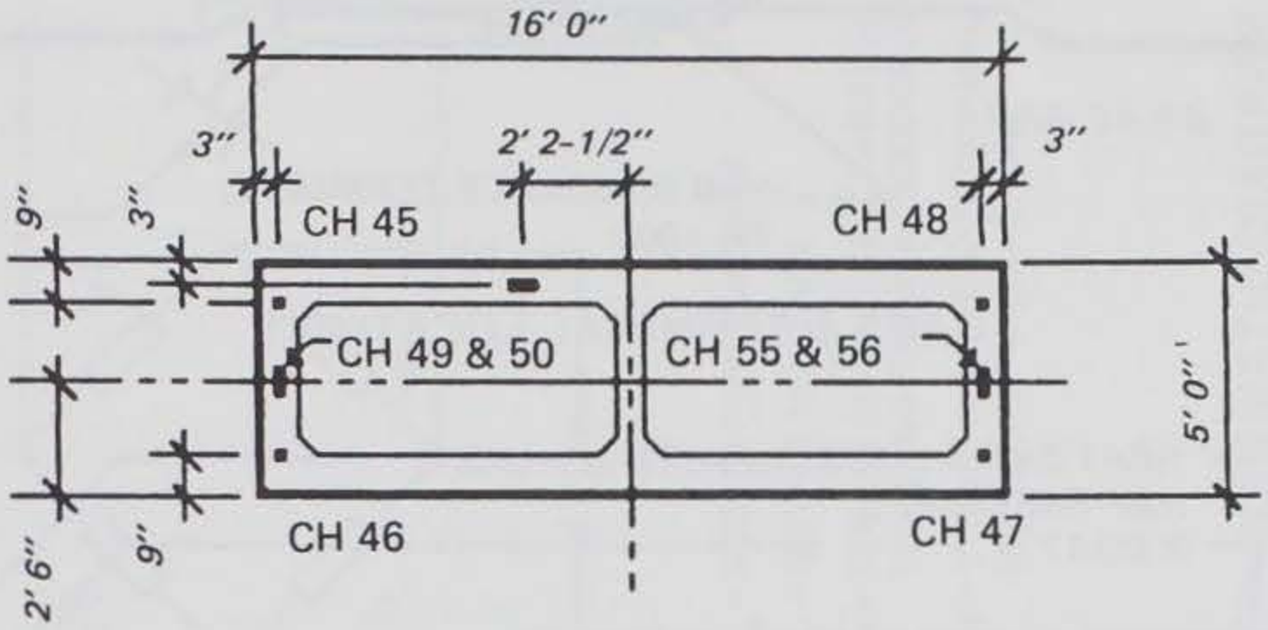

FIGURE F-22. Concrete Strain Gage Layout, Section A-A

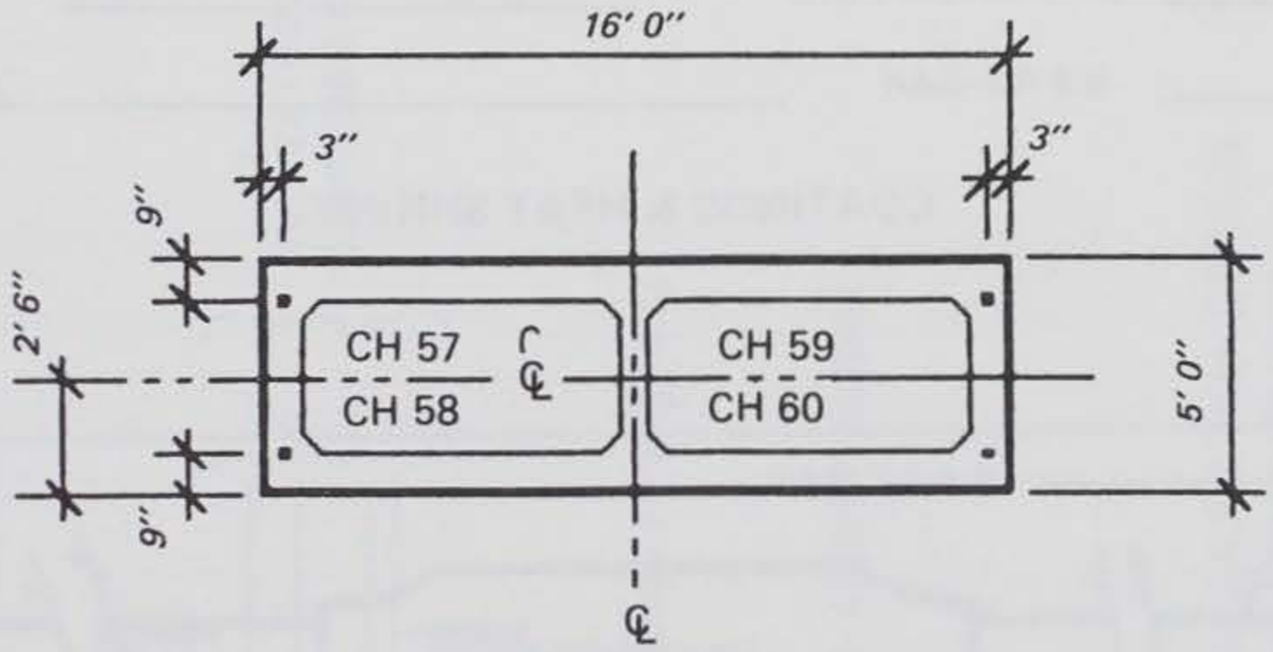

FIGURE F-23. Concrete Strain Gage Layout, Section B-B

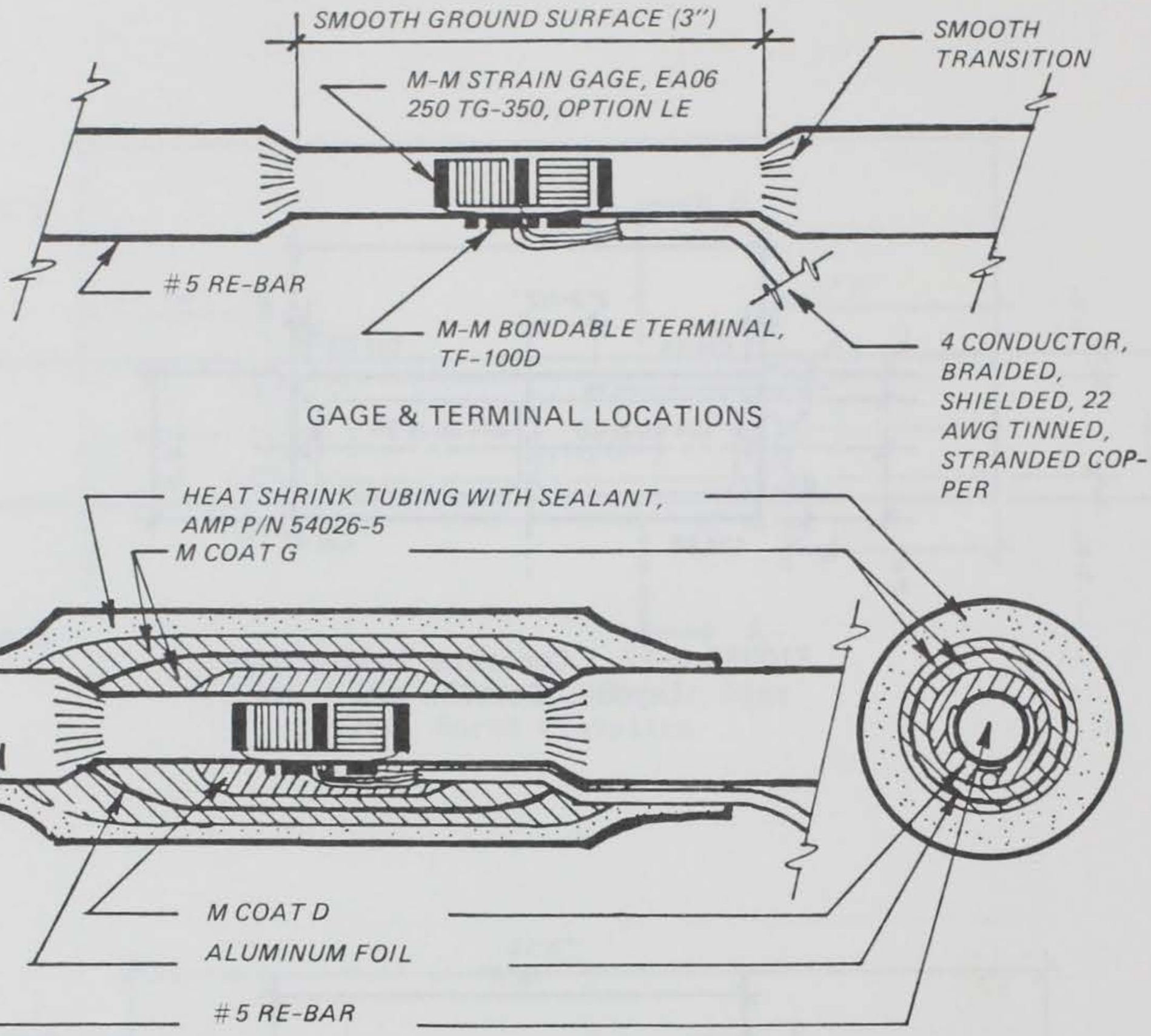

GAGE & TERMINAL LOCATIONS

COATINGS & HEAT SHRINK

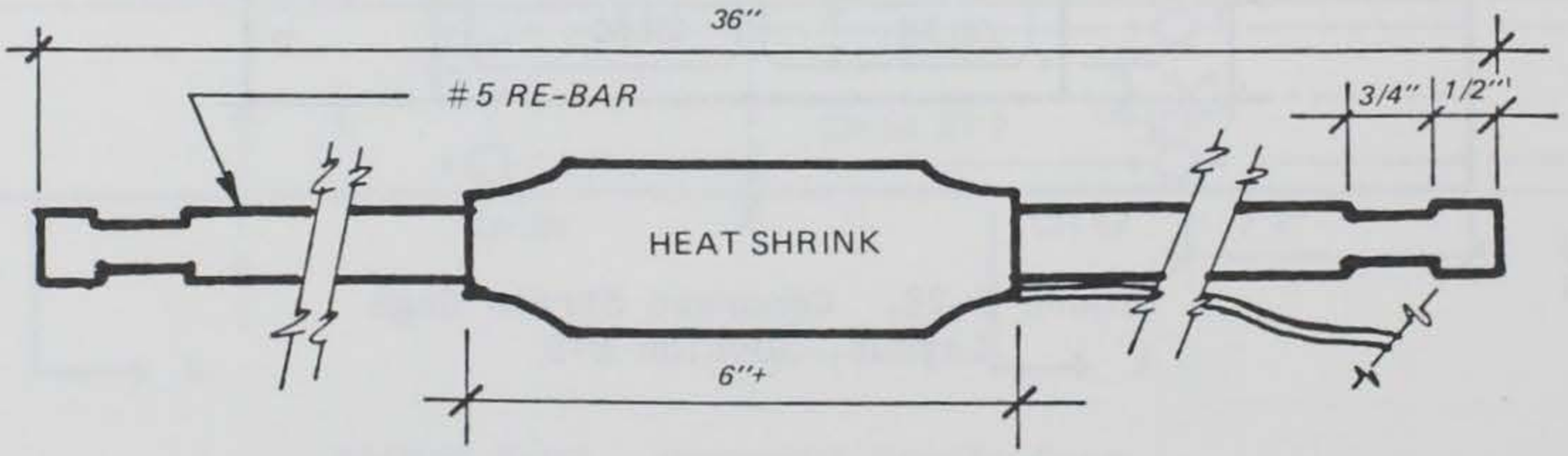

COMPLETED ASSEMBLY

FIGURE F-24. Concrete Strain Gage, Mechanical Detail

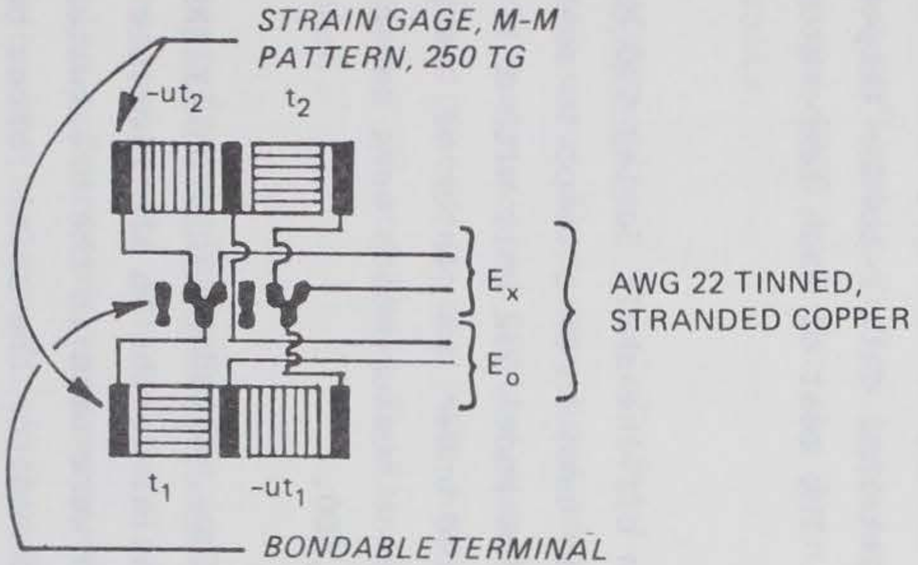

WIRING DIAGRAM FOR STRAIN MEASURING DEVICE

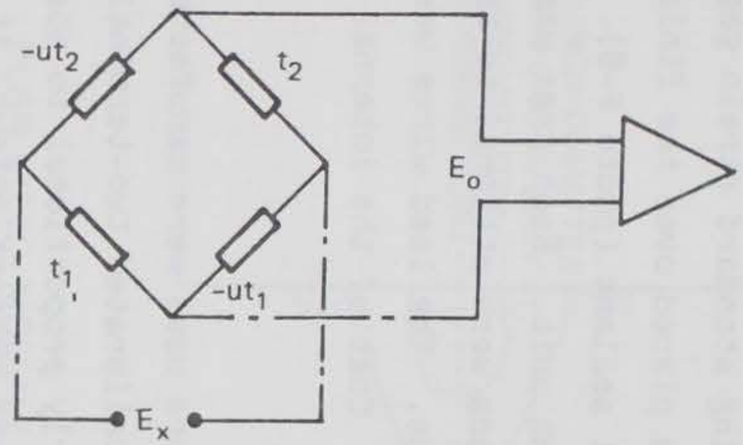

SCHEMATIC DIAGRAM FOR STRAIN MEASURING DEVICE

FIGURE F-25. Concrete Strain Gage, Electronic Detail

a 3-ft piece of No. 5 rebar machined to 1/2-in. diam over a 6-in. section at the center. Four strain gages were attached and wired into a complete bridge circuit. The gages were then sealed, using standard strain gage sealants; then a self-adhesive heat shrink tube was placed over the finished unit for both mechanical protection and as a final sealant (photo F-8). Two sets of gages and lead wires were attached to each unit. Each gage was checked (calibrated) and the gages and electrical leads were attached to the breakwater reinforcing steel using standard wire ties. The lead wires were routed along the rebar to the instrument compartment. Cost of the internal concrete strain gages is estimated to be $450 each.

2.10 Temperature. The temperature sensors used were manufactured by Analog Devices (Model AC2626). They are laser-calibrated two-terminal transducers. The electrical output is a current linearly proportional to absolute temperature. Because of the unit's high impedence current output, it is insensitive to voltage drops over long lines, thus enabling remote monitoring with no need for costly transmitters or special wire. The unit is also insensitive to supply voltage changes above 3 V, thus allowing for battery operation. The units used were housed in a stainless steel tube 3/16 in. by 3 in. Measurements were made of surface water, air, and internal data recorder temperatures. The overall accuracy of each was ±0.8° C. The cost of each temperature sensor was $20.

2.11 Current Speed and Direction. An off-the-shelf Series 500 Marsh McBirney electromagnetic water current meter was used in an attempt to measure the x and y components of water velocity. The Model 512 unit with a 1-1/2-in. probe was used. The current probe was mounted under the center of the pontoon. For a number of reasons, satisfactory current measurements were never obtained. The cost of this current meter was $4,500.

2.12 Rubber Connector. Strainsert, Inc., standard internally gaged hex head steel bolts were used to measure the axial forces on the flexible connectors (photo F-9). Two different connectors were used in the breakwater experiment. In both cases, four bolts were used to monitor the axial forces between the rubber sections (figures F-26 and F27). The bolts were instrumented by drilling a 0.15-in. hole in the end of the bolt approximately 3 to 4 bolt diam

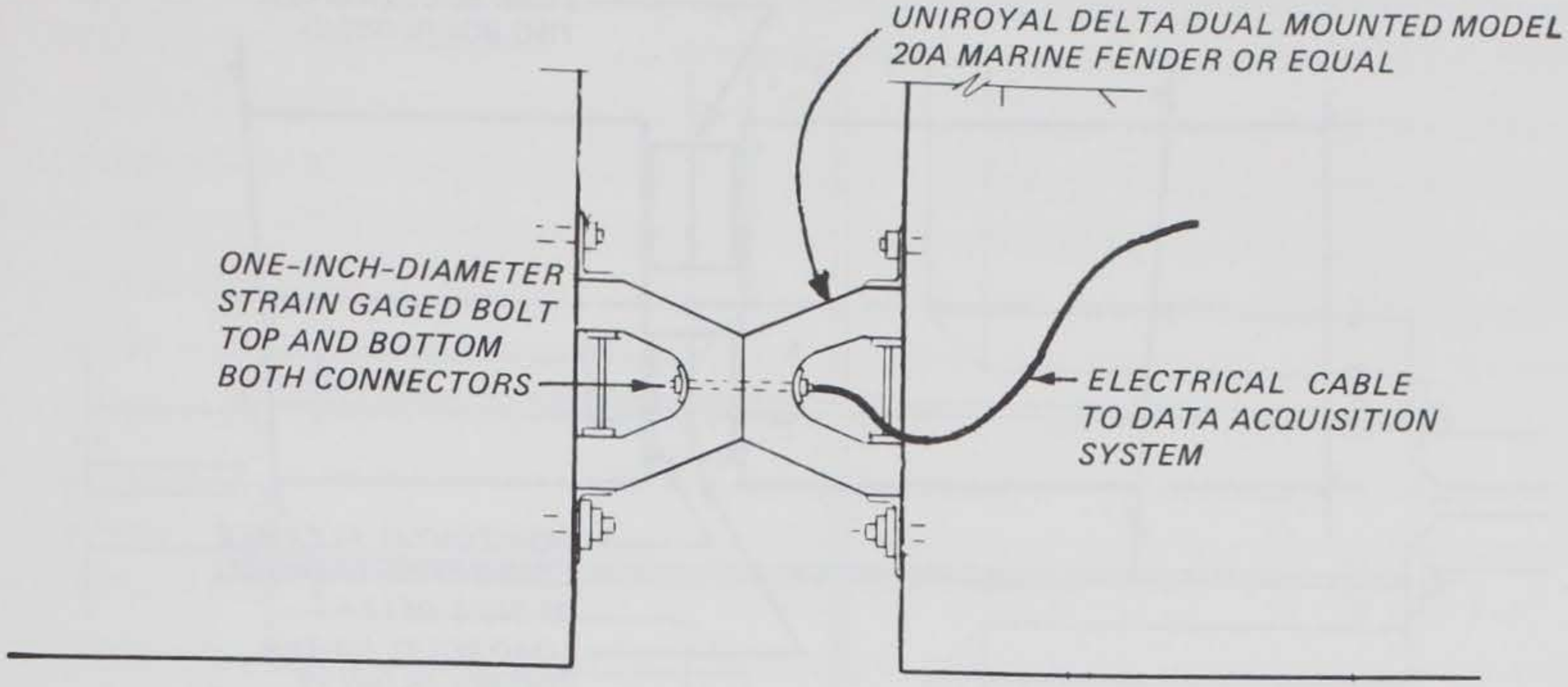

PLAN VIEW - MODULE CONNECTION DETAIL
FLEXIBLE CONNECTOR

FIGURE F-26. Vertical Fender Connector,
Load Sensing Bolt Locations

deep. A complete strain gage bridge was then mounted at the bottom of the hole using an inflatable Teflon tube and special adhesives techniques. Cost of the bolts was $400 each for the 1-in.-diam bolts and $700 each for the 2-in.-diam bolts.

2.13 Rigid Connection. Four of the 1-1/4-in.-diam, 11-ft-long, high-strength steel bars, that were used to bolt the two concrete floats together rigidly, were instrumented in the same manner as the rubber connector bolts. These bars were placed in the four outer corner positions in the rigid connection (figure F-28 and photo F-10). The cost for instrumenting the bars was $1,200 each.

3.0 Monitoring System Installation and Operation. Strain gages for measuring internal concrete strains were the first of the monitoring instruments to be installed. Fourteen gages were attached to the reinforcing steel at 11 locations on the western float the day before the concrete was placed (photo F-11). Two more (crossed) gages were mounted in the deck reinforcing steel while the concrete was being placed (photo F-12). Eight of the gages

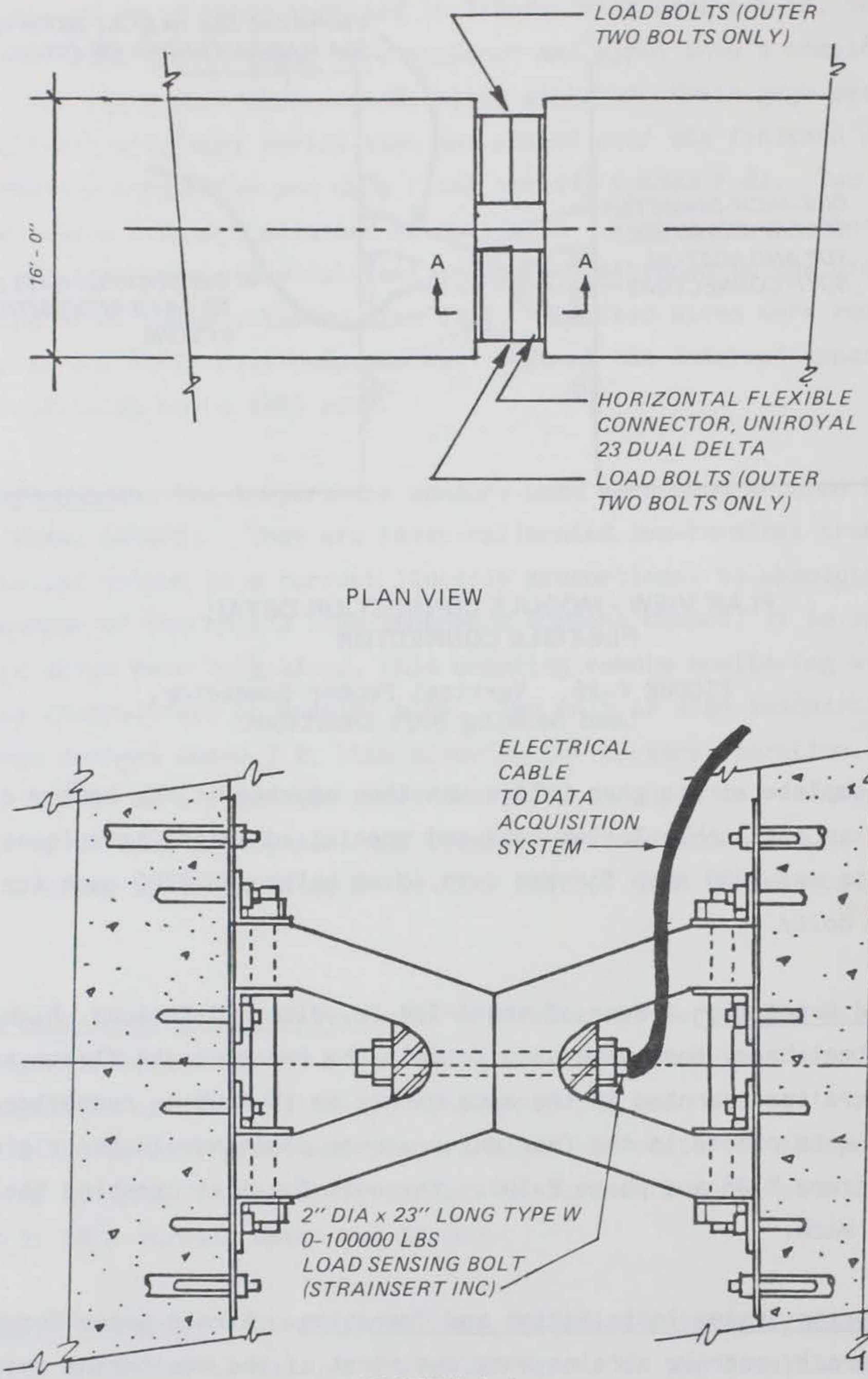

FIGURE F-27. Horizontal Fender Connector,
Load Sensing Bolt Locations

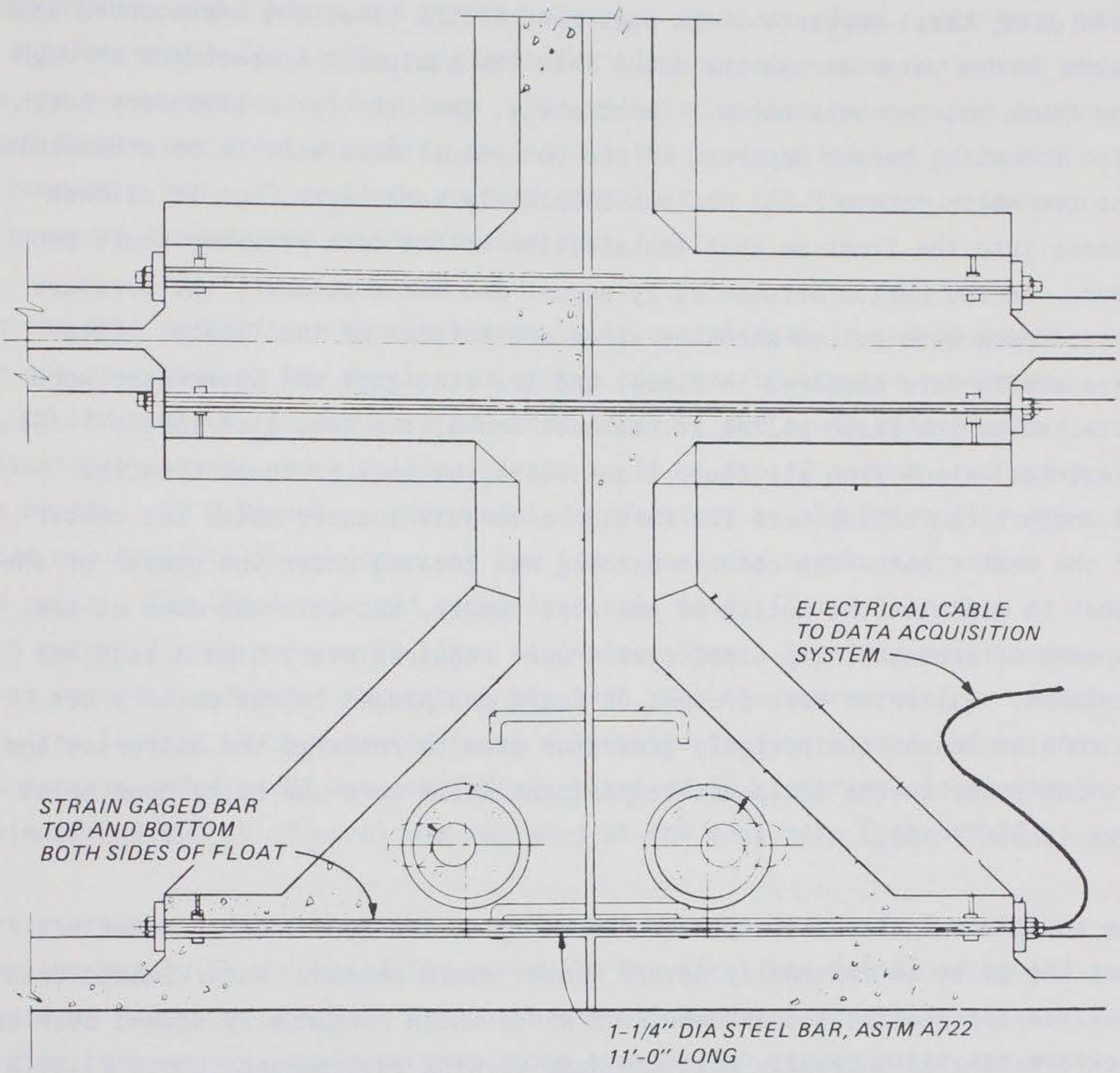

PLAN VIEW - MODULE CONNECTION DETAIL
RIGID CONNECTOR

FIGURE F-28. Rigid Connector, Load Sensing Bolt (Bar) Locations

measured longitudinal strains at the top and bottom edges of the float, while the remaining eight gages were installed in pairs to measure shear strains in the four float surfaces. Leads for the gages were routed through the reinforcing steelwork to the area that would eventually become the hollowed out end compartment housing the data acquisition system.

Final anchoring of the concrete breakwater was completed on 16 July 1982. Then, installation of the monitoring equipment began. Working conditions

at the West Point test site were fairly difficult (photo F-13). Even in a dead calm, tidal currents swept past much of the time; and unannounced ship wakes poured water across the decks into the equipment compartment through the flush mounted deck hatch. Immediately, the need for a secondary hatch with a combing became apparent if the end compartment were to be accessible. The new hatch (photo F-14) was not completely watertight, but it allowed access into the float so that installation of the data recorder could proceed. In the period between early August and mid-September, the pressure transducers were bolted onto the sides and bottoms of the floats. Five wave staffs were anchored in place, and the tide gage and anemometer were attached to the fixed piling at the east end of the test site (photo F-15). Electrical leads from all these transducers, as well as those from the 12 anchor load cells, were fed through a conduit located under the center of the west float. The conduit opening was located under the center of the float to minimize the motion of the wire bundle, but this was done at the expense of accessibility since divers were required every time a lead was replaced. Batteries were brought on board and placed in the battery box which also housed the portable generator used to recharge the batteries and provide power to the equipment compartment while work was being done below deck (photo F-16).

The equipment installation process was complicated by the early onset of what was to be an abnormally severe winter storm season. Water leaked into the interior storage compartment from waves which continually washed over the deck creating an unusually cold and damp working environment (photo F-17). Shortly after being anchored in place, three of the spar buoys were found broken. All the buoys were broken where the 8-ft-long staff joined to the main body of the buoy. A third buoy was missing completely. The probable cause of the damage was fast tidal currents and/or waves. The opening of the gillnet fishing season caused additional problems. Although the test site location had been well publicized to all mariners, particularly local fishermen, 600 ft of gill net became entangled in the breakwater and broke one of the two remaining wave staffs. Two new buoys were deployed; but, within a week, one buoy had broken and another had been torn out by a large wave-borne log (photo F-18). By the end of the first week in October 1982, seven spar buoys had been damaged or destroyed (photo F-19). By mid-October,

the attempt to repair the flexible connectors between the two concrete floats was abandoned, and fenders and bumpers were put in their place. All four of the strain-gaged bolts in the original flexible connector were destroyed before any measurements could be made. The relative motion between the disconnected floats was great enough to pull apart the leads which had to bridge the connector gap. These leads carried signals from all the accelerometers and pressure transducers mounted on the east float.

When the data acquisition system became fully operational in mid-November, only one spar buoy on the north side of the concrete breakwater remained. Most of the pressure transducers had been torn off the south side of the breakwater by waves, and electrical leads to 10 of the 12 anchor load cells were broken. On 9 December, commercial divers hired by the University connected new leads to three upper and two lower concrete breakwater anchor load cells. The three repaired upper load cell leads lasted less than a month before divers were again hired to replace them. The load cells themselves remained undamaged throughout the test, but the unarmored four conductor wires leading to them proved to be vulnerable to damage; and before the test program ended on 31 January 1983, a total of 18 electrical leads (approximately 2,500 ft of wire) was replaced at the test site (photo F-20).

Shortly after the data acquisition system was brought on board, a second generator had to be purchased for use while the first was being overhauled because of saltwater damage. Even with a new generator, very little battery charging time was available between storm systems; so backup batteries were charged on shore and then taken to the breakwater at about 2-week intervals. Each of the four large batteries required to operate the system weighed over 100 lb. Their replacement was a difficult and time consuming task. Several times the batteries were not replaced soon enough, and the system turned off. Such was the case when the worst storm of the entire test program occurred on 21 December 1982.

Even though the unusually stormy weather showed no sign of easing, success in the collection of data improved as the winter wore on. After the replacement of seven wave buoy staffs, reinforced staffs and modified buoy moorings nearly eliminated the breakage problem. With the frequent use of divers, a majority

of the anchor load cells were kept operating. The anemometer and incident (piling mounted) wave/tide gage proved to be reliable. By the time the concrete breakwater was removed from the test site on 7 February 1983 for the purpose of making the rigid connection between the modules, approximately 20 tapes of data had been collected.

Addition of the steel deckhouse during the rigid connection work was a major improvement (photo F-21). The deckhouse provided a dry storage area for the electronic components, two complete sets of lead acid batteries, and the generator. At the test site, work on the system could continue even during relatively rough conditions, dramatically increasing the amount of time that the breakwater data acquisition system was accessible for making repairs and adjustments.

Throughout the early spring of 1983, considerable progress was made in reinstalling wave buoys and reconnecting anchor load cells. Four spar buoys were securely anchored in place (one on the north and south side of each breakwater), 10 of the 12 anchor load cells were successfully reconnected, and a backup anemometer was mounted on top of the new deckhouse. By the end of June, 11 pressure transducers had been salvaged by divers and remounted on the side of the breakwater using an improved attachment method.

After the pipe-tire breakwater was removed from the test site in August, a spar buoy was anchored in the vacated spot to serve as a backup to the incident wave gage mounted on the piling. Eventually, an eight-buoy directional wave array was anchored in this location (photo F-22). See reference F-3 for details of the directional array study.

In November 1983 the concrete breakwater was removed from the test site. The two rigidly connected floats were parted, and the redesigned flexible connectors were fastened between them. A relative motion sensor mounted between the two floats and four strain gaged bolts (located in the outer edges of each connector) completed the monitoring program's large complement of instrumentation (photo F-23). The breakwater was reanchored at the test site on 1 December 1983, and the wave and anchor force transducer leads were reconnected to the data acquisition system. A week later, a Waverider wave

measuring buoy was anchored 600 ft south of the incident (piling mounted) wave gage to allow a comparison of records from the two types of wave measuring devices (photo F-24). At this time, 13 wave gages were connected to the data acquisition system (1 piling mounted, 8 spar buoys in the array, 2 spar buoys on the north side of the breakwater, 1 on the south side, and the Waverider buoy).

The deckhouse addition, increased experience, and a return to a more normal weather pattern all contributed to a continual improvement in the data collection success rate. By the end of the monitoring program on 31 January 1984, 121 data tapes containing approximately 1,000, 8-min time series of 80 input channels each had been obtained.

4.0 Equipment Evaluation.

4.01 Data Acquisition System. Of approximately 8,000 hr that the data acquisition system could have been collecting data on board the breakwater, it was operational for 4,500 hr or 56 percent of the time. Time spent adjusting the system or recharging the batteries on board the breakwater is not included in either the hours available for data collection or hours operational. After initial installation problems were solved, the system was removed from the breakwater six times for repairs and was entirely absent from the test site approximately 750 hr, exclusive of the time the concrete breakwater itself spent removed from the test site for connector modifications.

No single part in the system appeared to be particularly prone to failure. Component failures occurred on the transducer signal conditioning cards, on the serial cards, on the analog to digital cards (A to D cards), and in the tape drive electronics. Some programming errors had to be corrected in the software that controlled the system, and several electrical connector problems occurred.

Power supply problems were the major source of system downtime. For a number of reasons, the amount of power required was higher than originally anticipated. For several weeks, near the start of the monitoring program, persistent high winds caused an 8-min time series of all 80 channels to be made each

hour. More power was required to record the unanticipated abundance of data. Also, because the tape was continuous, storm data, in at least one instance, were written over before the tape could be removed. Additionally, short circuits caused by broken transducer leads were believed to be a source of power drain, but the most serious problem developed when one of the power supply's DC to DC converters failed. The converter was not a standard item and had about a 4-month delivery time. A spare had been purchased and was on hand, but the specification plate had been mislabeled at the factory. The replacement unit was not usable, and a simple removal and replacement job turned into a complicated problem. A temporary power supply was assembled from available components, but problems with the system, related to the power supply, continued until a new converter was installed 4 months later. The increased power requirements and the difficulties involved in keeping the batteries charged combined to shutdown the system several times, particularly during the first winter of monitoring.

By the end of the monitoring program, the data acquisition system had become a well used piece of equipment. Even the capability for system interrogation via telephone lines for transducer monitoring and data transmission was utilized for a short period of time. A 2,000-ft-long electrical cable was laid from the breakwater to shore, and some data transmission was accomplished, but waves and tidal currents soon broke the connection. A second cable was laid with similar results, and no further attempts to provide remote access to the system were made.

4.02 Wave Buoys. Overall performance of the wave measuring buoys was good considering the conditions under which they had to operate. The buoys appeared to be stable in all observed wave conditions, except for a slight low-frequency horizontal (sway) oscillation. The buoys were relatively easy to transport and install, and their modular design made repair or replacement of parts a simple task.

After the upper portion of the buoys was reinforced to solve the initial problem with breakage, the buoys proved to be very durable. Arriving at a satisfactory method for anchoring the buoys in place was a more difficult problem. Initially each wave buoy was tethered between two taut-line floats, which were

anchored with 250-lb concrete anchors. When tidal current speeds exceeded one knot, the buoys were pulled under the surface or were displaced laterally from the desired wave measurement location. To solve the mooring problem, the buoys were tied into the breakwater anchor systems as shown in figure F-9. This modification, combined with adjustment of the vertical location of the attachment collar, finally produced an acceptable anchoring arrangement.

A number of other problems with the wave gages were encountered, but they were considered routine maintenance. The electrical leads running from the buoys to the data acquisition system were damaged and had to be replaced several times. Also, after several months of use, the stainless steel resistance wire on the staffs tended to break, either because of corrosion or debris impact damage; and on one occasion a small brass screw retaining the upper end of the resistance wire corroded and caused electrical problems. Although not a common problem, some of the circuit boards inside the wave staffs did fail and had to be replaced. Finally, some of the buoys slowly lost buoyancy, and empty Clorox bottles were tied on to raise them to the proper height.

4.03 Piling-Mounted Wave Gage. The operating principal of the piling-mounted wave/tide gage was identical to that of the wave buoys, and exactly the same electronics were used in both instruments. An open framework galvanized steel cage protected the gage from debris damage. The original gage operated for 6 months before numerous breaks in the stainless steel resistance wire caused it to fail. A backup gage was installed in April 1983. The gage electronics failed once during the second winter of testing, and a spare circuit card had to be used during the last several months of testing. Breakage of the resistance wire was a problem common to both the piling mounted and buoy mounted staffs. Some form of corrosion in the vicinity of an epoxy bead that held the wire in place is suspected as a cause of the problem.

4.04 Anchor Force Load Cells. The anchor force load cells were the most difficult transducers to maintain because of the vulnerability of the electrical leads. Divers were used six times to lay new wires, and several other

attempts were aborted because of bad weather. The Electro-Oceanic underwater connectors on the load cells allowed each replacement of the wires by divers. However, because of the small changes in voltage associated with these transducer signals, those connectors were probably responsible for an excessive amount of electrical noise and drift in many of the records. Four of the load cells were recovered at the end of the test program; and although they were somewhat scarred by 2 years of service underwater, posttest calibrations indicated they were still operating normally.

4.05 Embedded Strain Gages. Except for minor connection problems, the 16 embedded strain gages operated normally throughout the test program. Strains in the concrete proved to be much lower than originally anticipated, and most of the data collected during the first winter were in the noise region. This problem was corrected on 26 May 1983 when the gains of all the gages were doubled. Data collected from this time on were suitable for analysis.

4.06 Strain Gaged Connector Bolts. As described previously, the first flexible connectors were destroyed before any measurements could be made by four 1-in.-diam strain gaged bolts located at the top and bottom of each connector. In the rigid connection configuration, each of the four corner, 1-1/4-in.-diam by 11-ft-long, bolts had a strain gage bridge inserted in a 0.15-in.-diam hole that was drilled 17 in. into the bolt. While the rigid connection was being made, the bolts were submerged in water, and all the gages were damaged. Readings were obtained for a short period of time from only one of the bolts. The second pair of flexible connectors was instrumented also with two 2-in.-diam load sensing bolts each. All four bolts were operational initially, and data were collected for a number of storms; but one by one, they all failed over the 2 months that the second flexible connector was being tested. Failure of the gages was due to the leads being twisted as the bolts rotated in their holes. Two of the leads were completely twisted off, and the other two were wrapped into balls around the heads of the bolts. Some data were obtained from these bolts during a number of storms that occurred in the last 2 months of testing.

4.07 Pressure Transducers. All of the pressure transducers that were

mounted on the south side of the breakwater were lost in the first 3 months of testing. An electrical conduit attached to the side of the floats was the main support for the transducers. The conduit, installed as part of the breakwater construction contract, was not able to resist wave forces and debris impacts. As each section of conduit was torn off, the attached transducers went with it. Transducers mounted on the bottom of the float fared somewhat better. All survived physically, but electrical leads to four of them were damaged during the test period. Three of the gages operated continuously. Parts of the side-mounted transducers were recovered by divers, new housings were made, and they were reattached in August 1983. The new attachment method, designed by the University, worked very well; and all of the transducers provided data throughout the rest of the test.

4.08 Anemometer. A Weather Measure anemometer was mounted on top of the fixed piling at the test site. This type of instrument was selected because it combined a relatively low cost and adequate reliability for the short duration of the test program. In January 1983 a backup anemometer was mounted on top of the newly added deckhouse at an elevation of approximately 10 ft. Both of the anemometers were replaced once during the test program.

4.09 Accelerometers. The water-tight compartments in which the accelerometers were to be mounted were usually completely filled with salt water. The University's original housing for the accelerometers was not designed to be hermetically sealed, and saltwater corrosion of the accelerometers was a problem initially. After modifications were made to the housings, a considerable amount of acceleration data were obtained during the later portions of the test program.

4.10 Current Meter. The Marsh-McBirney electromagnetic current meter was mounted on the 4-in.-diam conduit attached to the bottom of the concrete breakwater. Because collecting current data was assigned a low priority, the meter was not installed until well into the test program. After it was installed, erratic data were collected for a short time before it failed entirely. When the meter was recovered at the end of the test, the sensor appeared to have been damaged either at the time of its installation or by debris that was carried under the breakwater by tidal currents.

4.11 Relative Motion Sensor. The relative motion sensor was the most elaborate transducer designed and fabricated by the University. It was fastened between the two concrete units only during the test of the second flexible connector design in January and February 1984. The sensor was removed and replaced twice for repairs because water leaked past the rubber boots which surrounded the sliding and rotating parts. The quantity of data obtained from this transducer is yet to be determined.

5.0 Data Analysis. Original planning for the monitoring program did not address details of the methods and equipment required for processing the data to provide basic statistical data and auto and cross-spectral analyses. The University of Washington planned to use in-house data processing equipment and graduate student assistants for writing data analysis programs.

Because of the effort that was expended in attending to the problems that arose during the initial installation of the monitoring equipment, the development of data analysis procedures did not receive full attention until November 1983. Although results from the first of the data tapes to be analyzed indicated that several key transducers might not be operating properly, data analysis techniques had not been refined enough to pinpoint the problems. Efficient maintenance of the data acquisition system was found to require rapid analysis of the data tapes as they were retrieved from the breakwater, but the capacity of the University's microcomputer was taxed, and data analysis was tedious and time consuming. Work on software was at a fairly advanced point when the computer failed. Repeated repair attempts were futile. Finally the University was authorized to purchase a new and more powerful machine. By the beginning of the second year of monitoring, computer programs for spectral analysis, filtering, and removing signal drift had been developed. The capability to analyze data tapes quickly during the last 4 months of the project helped dramatically in the early detection and repair of problems in the data acquisition system and the monitoring transducers.

6.0 Monitoring Cost. The initial cost reimbursable contract with the University of Washington was for 2 years at an estimated $280,000. Unanticipated costs for repair and replacement of equipment added $79,000, and

extension of the monitoring program by 1 year increased the total program cost from $230,000 to $589,000. This $589,000 was distributed as follows: $140,000 for initial purchase and fabrication of hardware, $20,000 for support equipment, $202,000 for salaries of University personnel, $92,000 for University overhead, $105,000 for repair parts and materials, and $30,000 for data analysis equipment. An estimated $90,000 in equipment was returned to the Corps at the end of the monitoring program.

APPENDIX F

REFERENCES

F-1. Christensen, D. R., "Installation, Operation, and Maintenance Manual for Breakwater Data Acquisition System," Water Resources Series Technical Report No. 91, University of Washington, Department of Civil Engineering, Seattle, Washington, 1984.

F-2. Miller, R. W., Christensen, D. R., Nece, R. E., and Hartz, B. J., "Rigid Body Motion of a Floating Breakwater: Safekeeping Predictions and Field Measurements," Water Resources Series Technical Report No. 84, University of Washington, Department of Civil Engineering, Seattle, Washington, 1984.

F-3. Ratnayake, S. C. B., Christensen, D. R., Nece, R. E., and Hartz, B. J., "Linear and Nonlinear Dynamic Response of Floating Breakwaters in Directional Seas," Water Resources Series Technical Report No. 90, University of Washington, Department of Civil Engineering, Seattle, Washington, 1984.

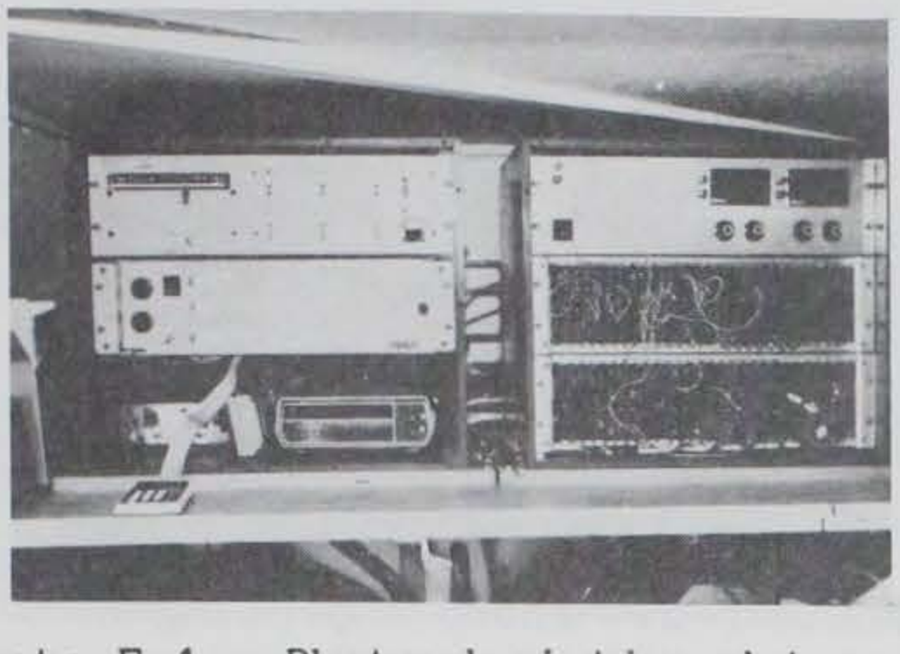

Photo F-1. Photo depicting data acquisition system (data logger on left, signal conditioning cards on right).

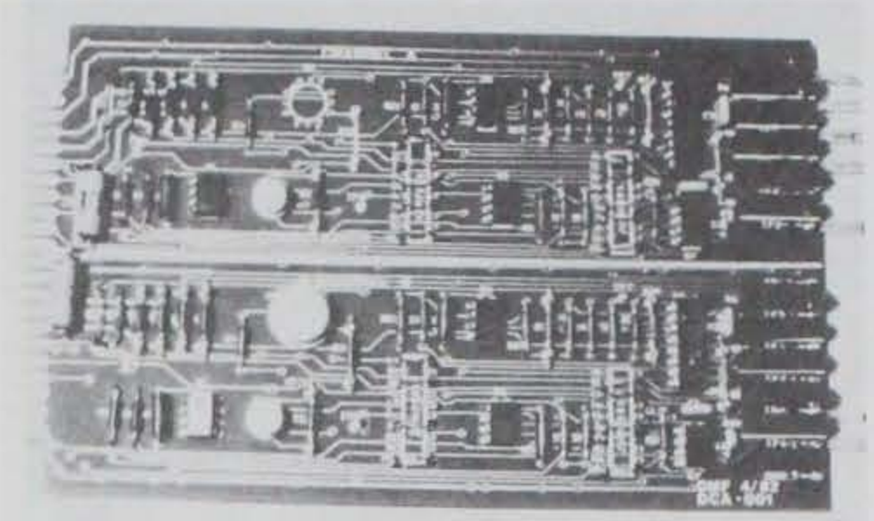

Photo F-2. Photo depicting signal conditioning cards.

Photo F-3. Attaching anchor force load cell to anchor line.

Photo F-4. Strain gages being attached to the load cell.

Photo F-5. Photo depicting 25-ft-high spar buoys.

Photo F-6. Photo depicting pressure sensor on bottom of float.

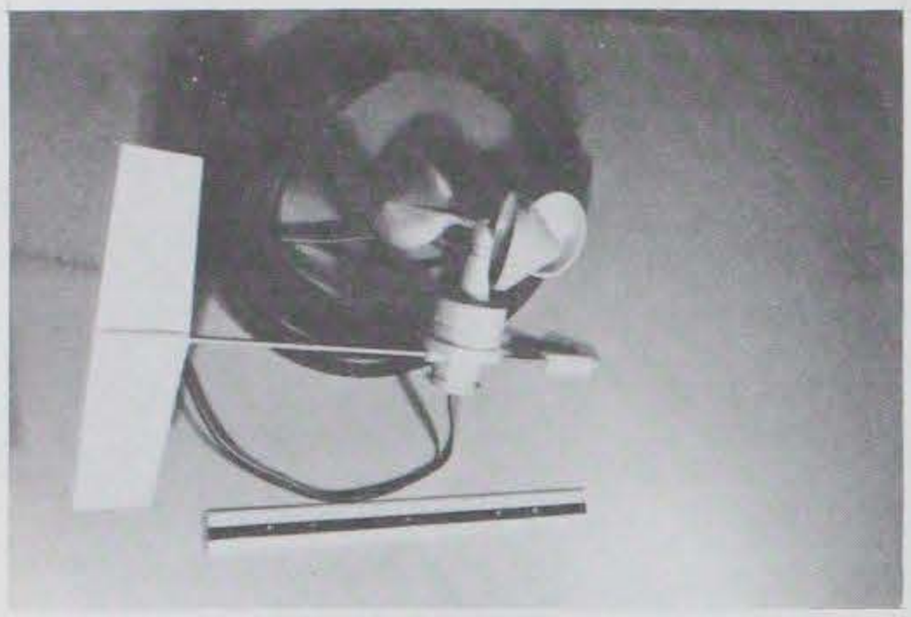

Photo F-7. Photo depicting Weather Measure anemometer.

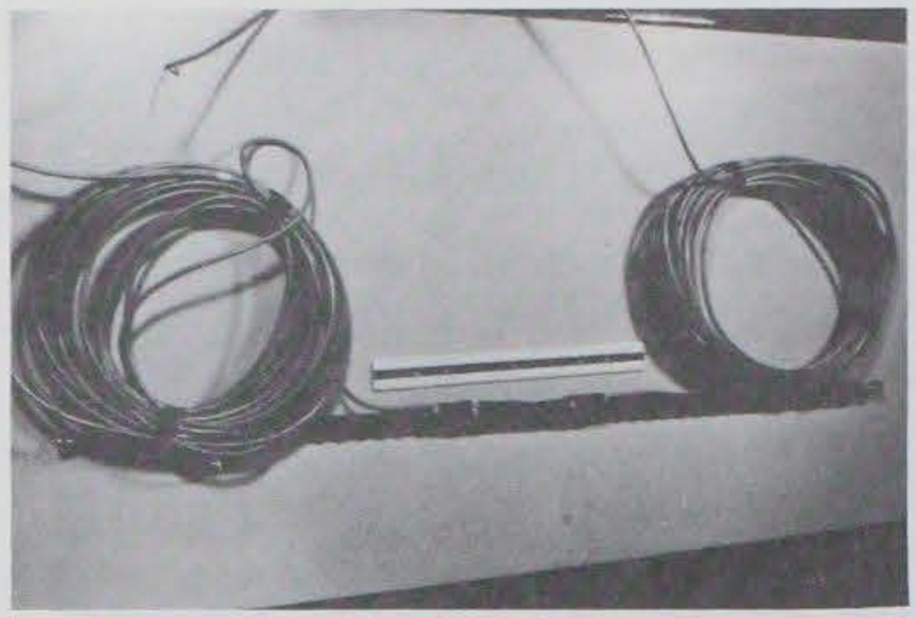

Photo F-8. Photo depicting a rebar embedment strain gage.

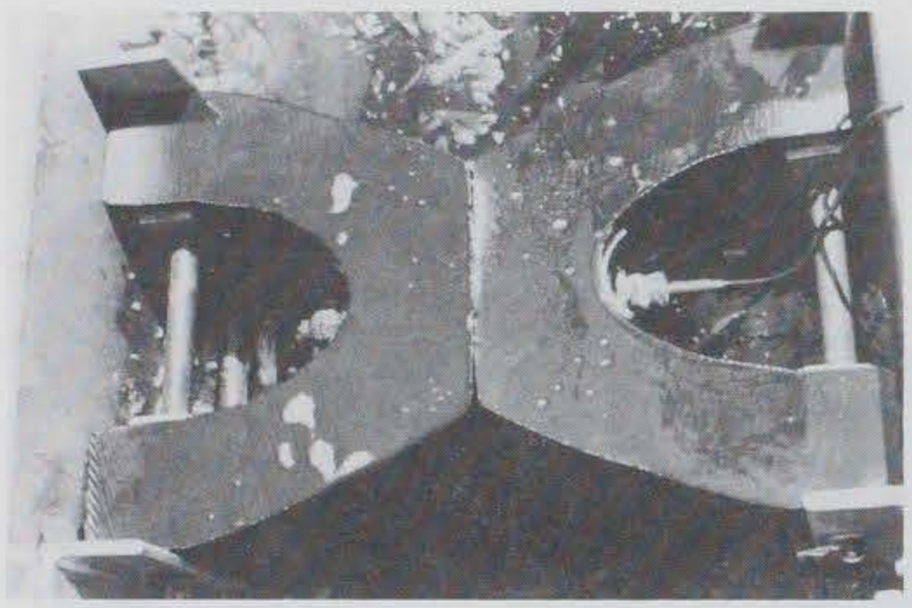

Photo F-9. Photo depicting load sensing bolt in vertical fender connection.

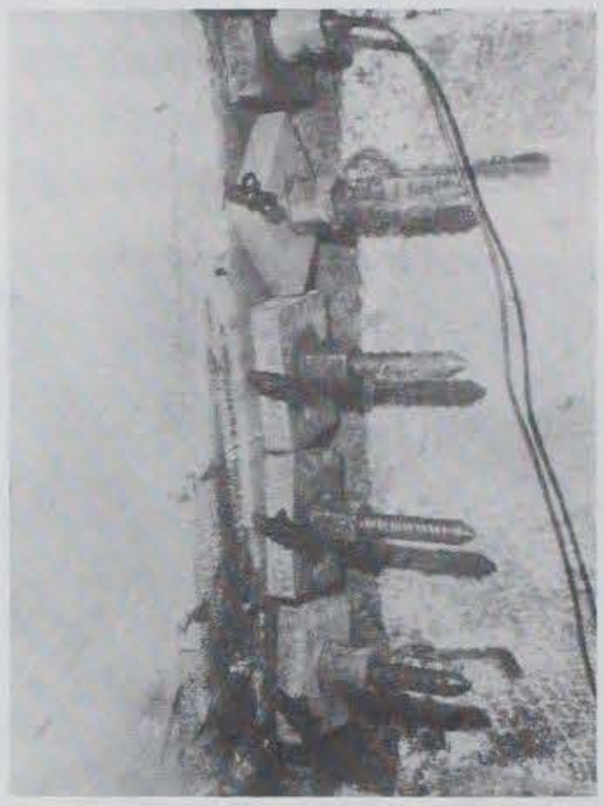

Photo F-10. Strain gages measuring loads in the corner bolts of the rigid connection.

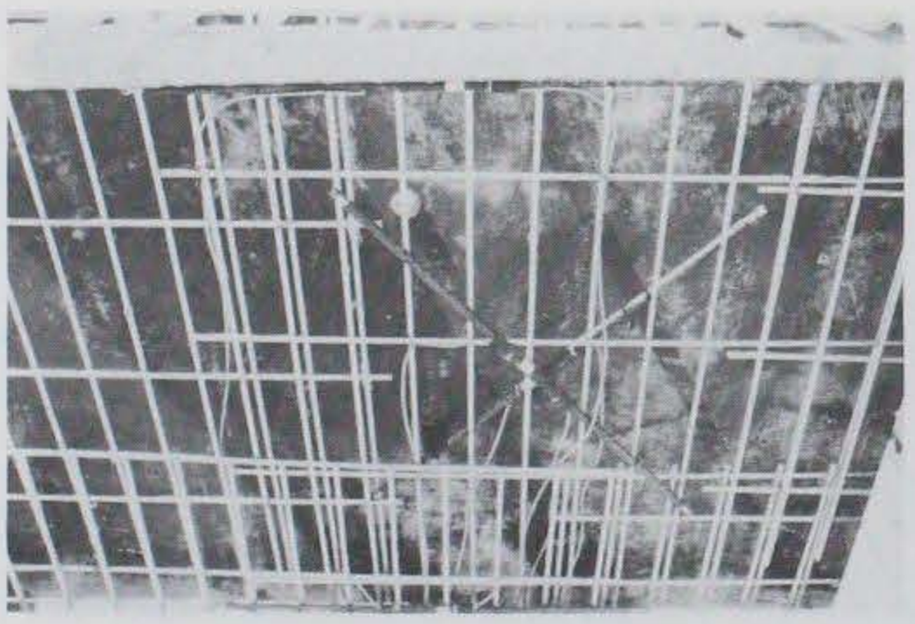

Photo F-11. Photo depicting embedded strain gages in sidewall and upper and lower edges.

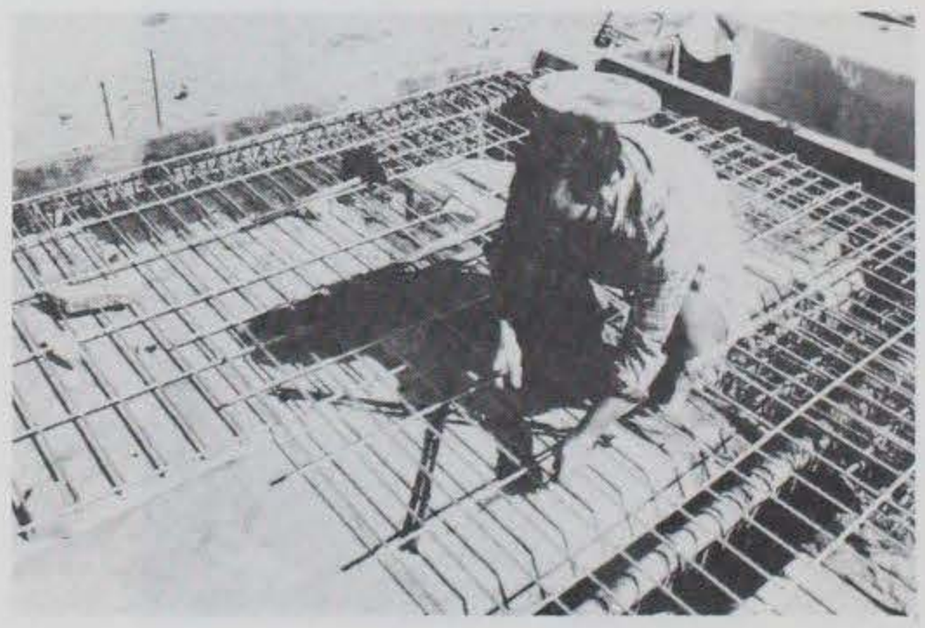

Photo F-12. Strain gages being placed in deck during construction of concrete float.

Photo F-13. Photo depicting typical working conditions during first summer.

Photo F-14. Photo showing secondary hatch to keep waves from washing into the equipment compartment.

Photo F-15. Photo depicting piling that supported the tide gage and anemometer.

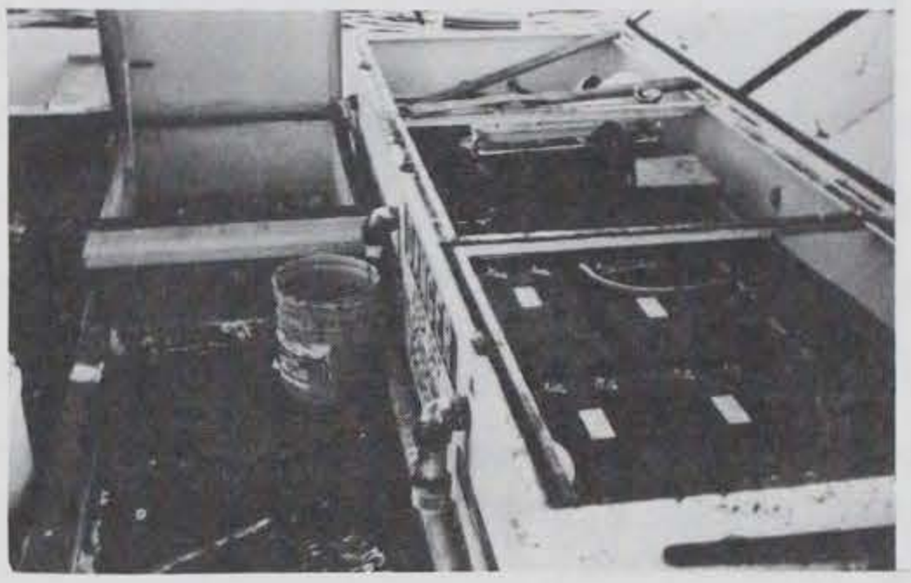

Photo F-16. Photo showing original storage box for the generator and batteries.

Photo F-17. Working under adverse conditions inside the float.

Photo F-18. A large log destroying several wave buoys and pressure transducers.

Photo F-19. Photo showing drifting kelp typical of debris which caused damage continuously.

Photo F-20. A diver installing a new electrical lead to an anchor force load cell.

Photo F-21. Photo depicting deck-house which greatly improved working conditions.

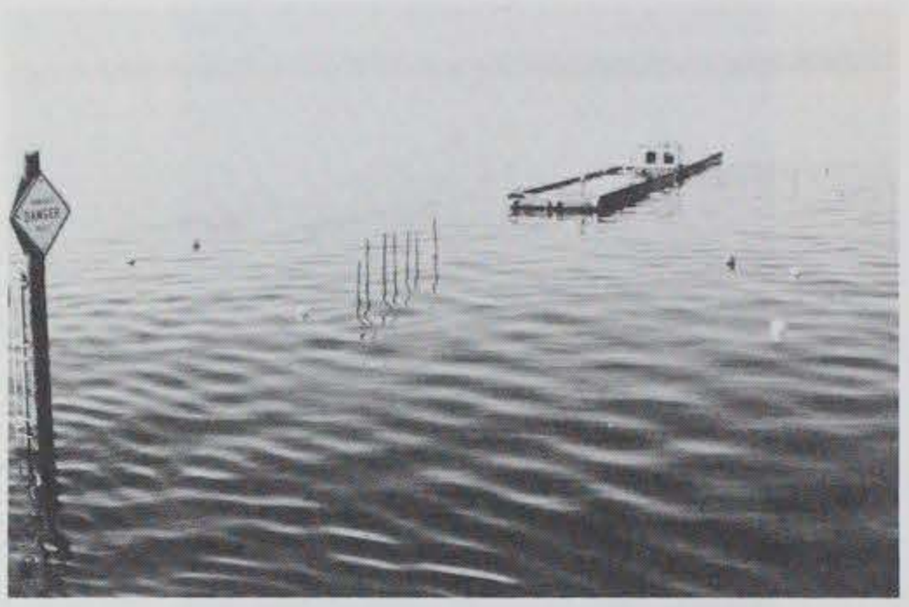

Photo F-22. Photo showing the wave array anchored in the vacant pipe-tire breakwater location.

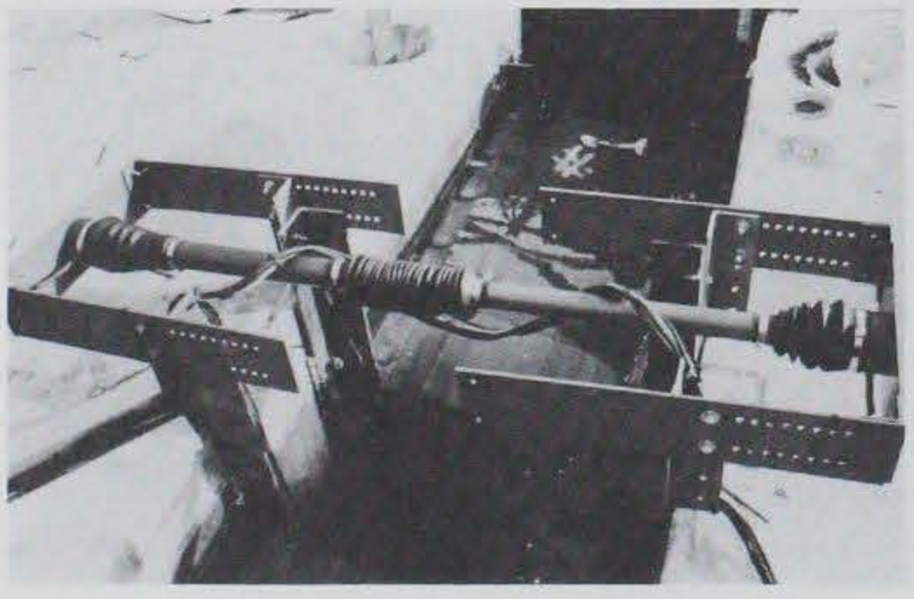

Photo F-23. Photo showing relative motion sensor which was used when the horizontal fender connector was tested.

Photo F-24. A Waverider buoy collecting additional wave data.

APPENDIX G

TEST RESULTS

1.0 Introduction. During the course of the Prototype Floating Breakwater Project, 121 data tapes containing approximately 20 megabytes of data per tape were collected. The parameters that were measured included incident and transmitted waves, wind speed and direction, anchor line forces, stresses in the concrete units, relative float motion, rotational and linear accelerations, pressure distribution on the concrete breakwater, water and air temperatures, and tidal current data. The data analysis methods for wave attenuation and anchor force measurement results are presented in this appendix. Analysis of the Prototype Test data will continue, and results will be presented in future reports.

2.0 Method of Data Analysis. The data analysis process was carried out in two steps: (a) retrieving measurements from the data tapes and (b) analyzing statistical data. In the field, the Data Acquisition System (DAS) collected a 1-min-long record of data every 2 hr. Summary statistics of these data were computed automatically and recorded on the tape. (Summary statistics included the mean, minimum, maximum, and standard deviation.) After the statistics were recorded, the DAS would check to see if any of the preset thresholds on selected parameters were exceeded. If triggered, the DAS would initiate a time series collection during which 512 sec of data were collected from each of 80 channels. The sampling rate was 4 Hz for all data collection (240 samples per channel for a 1-min record and 2,048 samples per channel for a time series).

After each data tape was retrieved from the breakwater, a summary or map was made showing how many 1-min records and time series were recorded on the tape. Included in the mapping of the tape was a listing of the 1-min summary statistics. Figure G-1 is an example of a tape summary for tape number 54, and figure G-2 presents the statistics for 1-min record number 12. The tape summary shows also how many glitches exist and where they are on the tape. A glitch is any spot on the tape where the tape drive cannot retrieve the data. (Normally only a few samples of data per channel are lost when a glitch occurs,

STATISTICAL RECORD AND GLITCH MAP

TAPE IN : 7/12/83 5:00 AM
TAPE OUT : 7/14/83 11:00 AM
TAPE # 54

TRACK 1

SR1 TS1 *
SR2 TS2
SR3 TS3
SR4 TS4 *
SR5 TS5
SR6 TS6 *
SR7 TS7

TRACK 2

SR8 TS8 *
SR9 TS9
SR10 TS10
SR11 TS11
SR12 TS12
SR13 TS13
SR14 TS14

TRACK 3

SR15 TS15
SR16 TS16
SR17 TS17
SR18 TS18
SR19 TS19 *
SR20 TS20

TRACK 4

SR21 TS21

LEGEND

SR = ONE MINUTE RECORD STATISTICS
TS = TIME SERIES
* = GLITCH

FIGURE G-1. Data Tape Summary Sheet

1 MIN. STATISTICAL DATA SUMMARY

TAPE # 54
TAPE IN : 7/12/83 5:00 AM
TAPE OUT : 7/14/83 11:00 AM
OF SAMPLES = 120
TAPE TRACK = 2
1 MIN REC. No. = 12 7/13/83 4:59 AM

QUANTITY/CH.#	MEAN	STD.DEV	MAX	MIN
ANCH.FORCE(7)	2662.54	33.23	2722	2526
ANCH.FORCE(8)	614.25	1468.34	4095	0
TIDE HT(16)	914.84	39.93	984	788
VERT.ACC(61)	115.43	8.51	127	55
WIND SP.(73)	95.93	6.78	109	82
WIND DIR.(75)	236.60	13.50	254	168

SINGLE SAMPLE VALUES

CURR.VEL.X(77)	255
CURR.VEL.Y(78)	255
WIND SP. (74)	77
WIND DIR.(75)	234
-10V (83)	138
+10V (84)	114
-24V (85)	156
+24V (86)	91
-5V (87)	127
+5V (88)	125
WATER TEMP (89)	0

FIGURE G-2. One-Minute Record Statistics Sheet

and the time series is still of value. There is no apparent cause for a glitch, but it is probably a function of temperature and/or a malfunction of the DAS.)

Once the mapping was completed, the 2,048 measurements that were made for each

of the 80 channels during a time series were reformatted, and summary statistics were computed. An example of the time series summary statistics is shown in figures G-3 and G-4. In figure G-3 the tape number, 1-min record number, and scale factors are shown. The scale factor converts the data recorded on the tapes to physical units. For example, when the data recorded

Summary of Statistical Data for West Point Floating Breakwater Project 7/12/83 to 7/14/83
Number of samples per event = 2048 Sampling Rate = 4.00 hertz
1 Days 0 Hrs. 3 Min. from beginning of tape (All Min, Max values Measured from Zero Mean)
Tape Number 54
1 Minute Record Number 12
Time Series Number 12

SUMMARY OF SCALE FACTORS

CH.NO.	1	2	3	4	5	6	7	8	9	10
L CODE	LNWC	LNEC	UNWC	USWC	UNEC	USEC	LSWC	LSEC	LNT	UNT
SFACT.	.027	.027	.027	.027	.027	.027	.027	.027	.019	.019

CH.NO.	11	12	13	14	15	16	17	18	19	20
L CODE	UST	LST	FRS	FRC	FRN	TIDE	INC BUOY	WV-NW	WV-NE	WV-SW
SFACT.	.019	.019	1.000	1.000	1.000	.012	1.000	.031	.031	.031

CH.NO.	21	22	23	24	25	26	27	28	29	30
L CODE	WV-SE	P1-NU	P2-NL	P3-BNC	P4-BEO	P5-BEI	P6-BCC	P7-BWI	P8-BWO	P9-BSC
SFACT.	.031	.004	1.000	.004	.004	.004	.004	1.000	.004	.004

CH.NO.	31	32	33	34	35	36	37	38	39	40
L CODE	P10-SCU	P11-SW1	P12-SW2	P13-SW3	P14-SCL	P15-SE3	P16-SE2	P17-SE1	P18-EP1	P19-EP2
SFACT.	1.000	1.000	1.000	1.000	1.000	1.000	1.000	1.000	1.000	1.000

CH.NO.	41	42	43	44	45	46	47	48	49	50
L CODE	P20-EP3	P21-EP4	P22-EP5	P23-EP6	NULE	NBLE	SBLE	SULE	NT1	NT2
SFACT.	1.000	1.000	1.000	1.000	1.470	1.470	1.470	1.470	1.470	1.470

CH.NO.	51	52	53	54	55	56	57	58	59	60
L CODE	BT1	BT2	UT1	UT2	ST2	ST1	NULC	NBLC	SULC	SBLC
SFACT.	1.470	1.470	1.470	1.470	1.470	1.470	1.470	1.470	1.470	1.470

CH.NO.	61	62	63	64	65	66	67	68	69	70
L CODE	W VERT	W HORZ	W ROT	E VERT	E HORZ	E ROT	WVR	WHR	EVR	EHR
SFACT.	1.000	1.000	1.000	1.000	1.000	1.000	1.000	1.000	1.000	1.000

CH.NO.	71	72	73	74	75	76	77	78	79	80
L CODE	CLM	CRM	WIND SP	WIND SP	WIND DIR	WIND DIR	N-S	E-W	CON1	CON2
SFACT.	1.000	1.000	.400	.400	1.412	1.412	1.000	1.000	1.000	1.000

FIGURE G-3. Time Series Summary Statistics, Tape Number, 1-Min Record Number, and Scale Factors

PROBLEM (MIN = MEAN) → 3

PROBLEM (NO DATA) → 6

PROBLEM (BAD CHANNEL) → 20

CH.NO.	1	2	3	4	5	6	7	8	9	10
MAX.	4.905	.000	24.141	.617	5.193	.000	4.293	46.588	1.478	6.722
MIN.	-5.949	.000	-9.825	-87.970	-3.177	.000	-5.211	-63.977	-.764	-6.046
MEAN	40.023	.000	9.825	109.948	3.177	.000	78.651	63.977	15.166	13.114
STDEV.	2.025	.000	7.806	7.077	1.735	.000	2.533	54.578	.451	2.184

CH.NO.	11	12	13	14	15	16	17	18	19	20
MAX.	.507	4.062	.000	.000	28.027	1.263	25.505	.000	.523	.000
MIN.	-.956	-.080	.000	.000	-19.973	-3.393	-18.495	.000	-.469	.000
MEAN	12.945	.080	.000	.000	1719.973	10.593	178.495	.000	3.290	7.905
STDEV.	.133	.356	.000	.000	7.596	.612	11.287	.000	.203	.000

CH.NO.	21	22	23	24	25	26	27	28	29	30
MAX.	.000	.049	13.466	.000	.027	.000	.000	.000	.000	.000
MIN.	.000	-.043	-10.534	.000	-.029	.000	.000	.000	.000	.000
MEAN	7.905	.607	151.534	.000	.065	.000	1.020	255.000	1.020	1.020
STDEV.	.000	.019	4.378	.000	.011	.000	.000	.000	.000	.000

CH.NO.	31	32	33	34	35	36	37	38	39	40
MAX.	8.742	122.883	5.776	7.662	6.746	7.532	7.018	76.342	155.875	9.214
MIN.	-8.258	-132.117	-.224	-9.338	-8.254	-10.468	-8.982	-102.658	-99.125	-90.786
MEAN	12.258	132.117	.224	128.338	153.254	127.468	123.982	178.658	99.125	245.786
STDEV.	2.810	86.428	.659	3.210	2.896	3.267	3.267	38.563	46.894	20.313

CH.NO.	41	42	43	44	45	46	47	48	49	50
MAX.	78.061	.000	13.039	81.570	22.626	20.435	32.575	12.726	5.761	5.960
MIN.	-111.939	.000	-6.961	-98.430	-25.884	-22.195	-36.515	-13.734	-4.529	-4.330
MEAN	176.939	255.000	135.961	155.430	240.504	258.865	255.545	232.764	188.279	157.210
STDEV.	41.846	.000	3.345	24.777	8.007	5.478	10.587	5.238	1.657	1.481

CH.NO.	51	52	53	54	55	56	57	58	59	60
MAX.	6.160	9.358	5.461	13.405	6.932	11.853	18.674	11.044	8.873	20.052
MIN.	-5.600	-11.222	-4.829	-10.115	-9.238	-8.727	-16.606	-6.596	-5.827	-22.578
MEAN	167.300	177.332	200.339	211.505	170.938	141.027	122.446	172.706	121.957	165.168
STDEV.	1.412	3.064	1.508	2.895	2.176	2.638	5.481	2.008	1.460	6.088

CH.NO.	61	62	63	64	65	66	67	68	69	70
MAX.	21.912	28.423	22.507	1.273	13.200	.000	166.392	166.935	166.977	168.185
MIN.	-23.088	-24.577	-23.493	-1.727	-2.800	.000	-52.608	-55.065	-54.023	-53.815
MEAN	116.088	120.577	124.493	101.727	2.800	255.000	88.608	88.065	88.023	86.815
STDEV.	7.212	9.387	7.034	.495	3.180	.000	80.383	80.634	80.645	81.231

CH.NO.	71	72	73	74	75	76	77	78	79	80
MAX.	205.157	7.122	49.637	50.639	.589	.049	.000	.000	29.921	28.569
MIN.	-49.843	-21.878	-16.763	-16.561	-23.415	-8.423	.000	.000	-24.079	-24.431
MEAN	49.843	247.878	52.363	51.361	359.470	360.011	255.000	255.000	70.079	69.431
STDEV.	98.930	8.692	11.954	11.520	2.349	.468	.000	.000	8.987	8.990

FIGURE G-4. Time Series Summary Statistics, Channel Statistics for BW54R12, Tape Number 54, and 1-Min Record Number 12

for channel 16 (the tide gage) is multiplied by 0.012, the values are converted to units of feet. An explanation of the acronyms used in figure G-3 and the physical units of each channel is found in Table G-1. Figure G-4 provides a listing of the channel statistics for BW54R12, tape number 54, and 1-min record number 12. Sensor and DAS malfunctions can be evaluated to a limited extent by examining the channel statistics. In figure G-4 some of the problems that occur on the summary statistics are shown. Additional information on system performance was obtained from point by point (row) plots of the data. These row plots were particularly useful for evaluating electrical noise and null point drift.

The final step in the statistical analysis was the production of spectral plots of the data from selected channels using fast Fourier transforms (FFT's). Because these plots show the variation of energy with frequency, the data were filtered a final time to remove energy contributions which were caused by effects with frequencies outside the range of interest. A 0.08 Hz "low pass" filter was used to remove the long period effects, such as tidal variations, and a 1.0 Hz "high pass" filter was used to remove the contribution of very short period phenomena such as ripples. Results of the spectral analysis were used to calculate, statistically, the significant wave heights and peak (highest 1 percent) anchor loads; and breakwater wave transmission coefficients, C_t, were determined by comparing the incident and transmitted wave spectra.

3.0 Data Results. The data presented are based on the summary statistics and the results of the FFT's. Assuming the data follow a Rayleigh distribution, the following relationships exist:

$$x_s \tilde{=} x_{mo} = 4\sigma$$

$$\bar{x} = 0.6265x_s = 2.51\sigma$$

$$x_{10} = 1.27x_s = 5.08\sigma \quad \text{and}$$

$$x_1 = 1.67x_s = 6.68\sigma$$

where

x_s = significant value or average of highest one third

x_{mo} = significant value based on energy

σ = standard deviation

$\bar{x}$ = mean

x_{10} = average of highest 10 percent

x_1 = average of highest 1 percent (reference A-1)

The Rayleigh distribution assumption was checked by looking at several time series for wave heights, anchor forces, strains, pressures, and accelerations. When the data are examined, the significant or 1 percent value is only one factor involved. Since the response of floating structures to waves is very dependent on wave period, the period of peak energy density, T_p, of the incident wave field was calculated from the FFT, as shown in figure G-5. The peak energy period of the incident wave field appears to be an important parameter to consider because the peak energy period of other data such as the anchor forces and concrete strains often corresponded to the measured T_p. When the periods did not correspond they were normally shifted by one spectral bandwidth which could be a function of the averaging done when calculating the

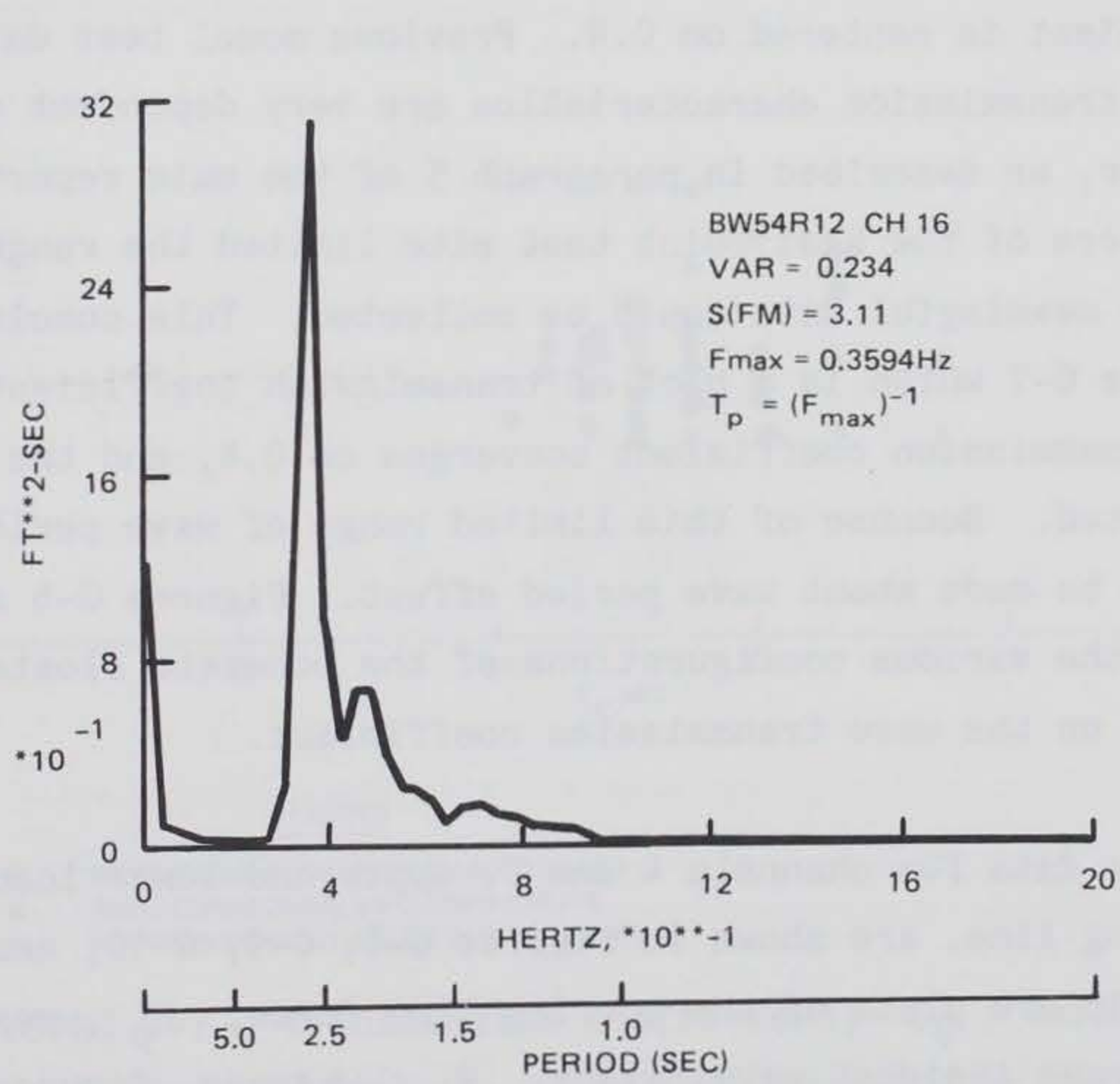

FIGURE G-5. Results of Fast Fourier Transform

FFT. Peak values of the anchor force data were of the most interest, but because the data were filtered to remove high frequency noise the peaks were not valid, and a statistical value of the average of the highest 1 percent was used to represent the peak force.

3.01 Concrete Breakwater. Several configurations of the concrete breakwater existed during the test program; however, because of structural damage to the breakwater or to the DAS malfunction, data, as listed in Table G-2, exist for only three of the five configurations tested. The three configurations are

a. The two concrete floats rigidly connected with clump weights.

b. The two concrete floats rigidly connected without clump weights.

c. The two concrete floats flexibly connected without clump weights.

Figures G-6 and G-7 show wave transmission characteristics of the three floating breakwater configurations. In figure G-6 the wave transmission coefficient, C_t , is plotted versus the incident wave height, H_i . The transmission coefficient is centered on 0.4. Previous model test data show that, normally, wave transmission characteristics are very dependent on the wave period. However, as described in paragraph 5 of the main report, the geographical features of the West Point test site limited the range of wave periods for which meaningful data could be collected. This conclusion is confirmed by figure G-7 which is a plot of transmission coefficient versus wave period. The transmission coefficient converges on 0.4, and the range of wave periods is limited. Because of this limited range of wave period, no definite conclusions can be made about wave period effect. Figures G-6 and G-7 indicate also that the various configurations of the concrete floats had no significant effect on the wave transmission coefficient.

The anchor force data for channels 4 and 7, upper and lower load cells on the southwest mooring line, are shown in figures G-8, G-9, G-10, and G-11. Figures G-8 and G-10 are plots of the mooring line force, F_p , measured in one mooring line versus incident wave height, H_i ; whereas, figures G-9 and G-11 present the mooring line force versus the wave period of peak energy density,

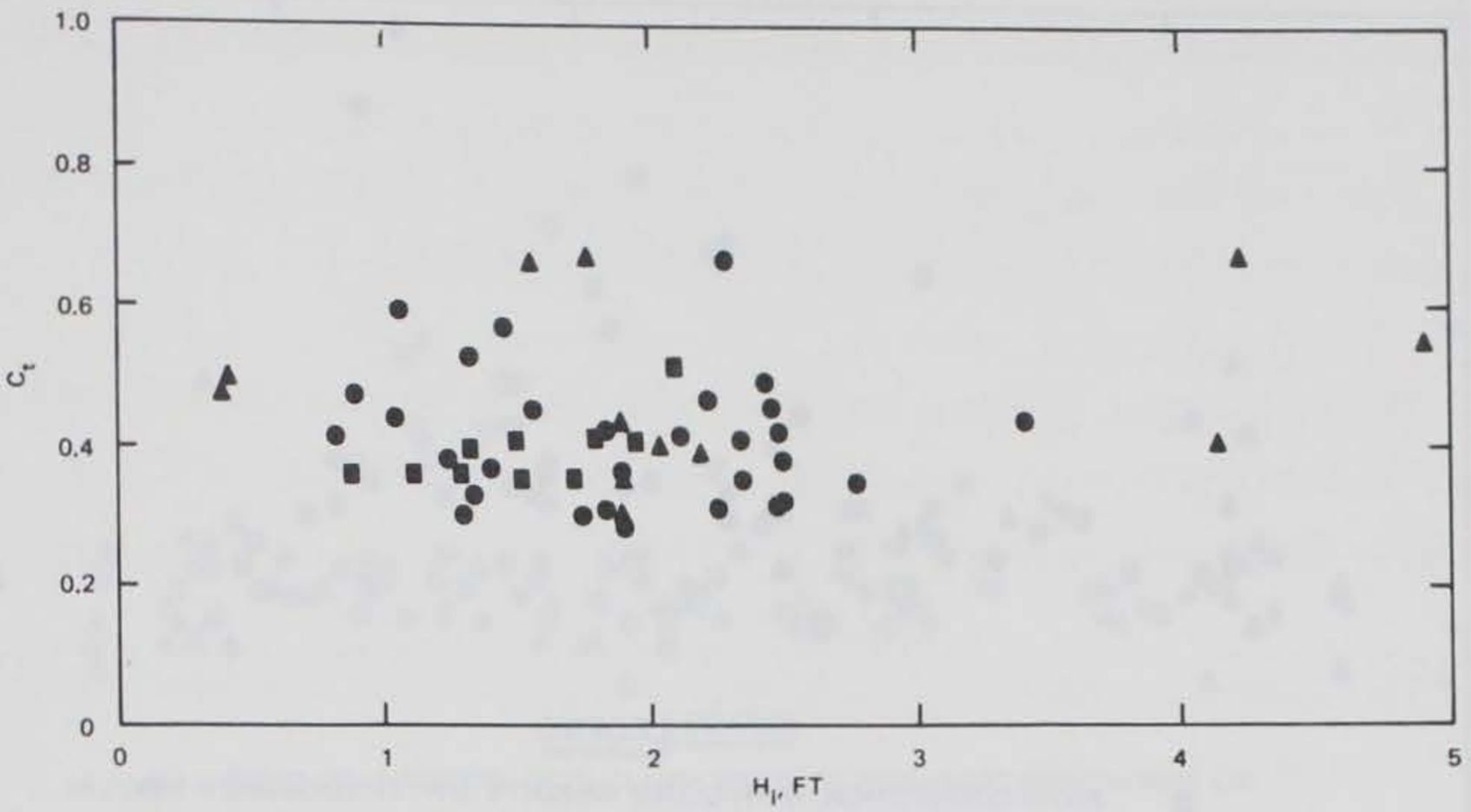

FIGURE G-6. Transmission Coefficient, C_t , versus Incident Wave Height, H_i , Concrete Breakwater

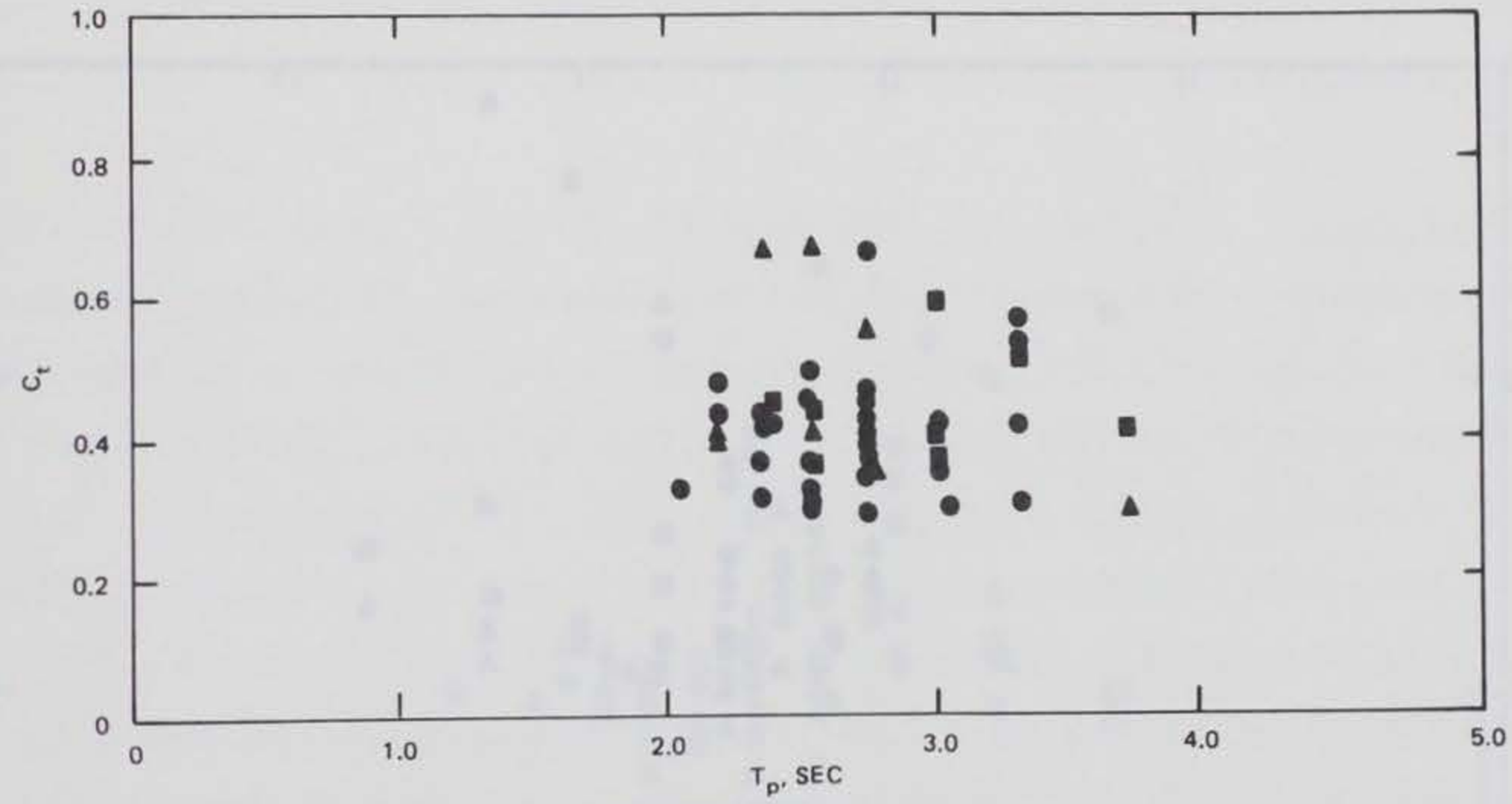

FIGURE G-7. Transmission Coefficient, C_t , versus Wave Period, T_p , Concrete Breakwater

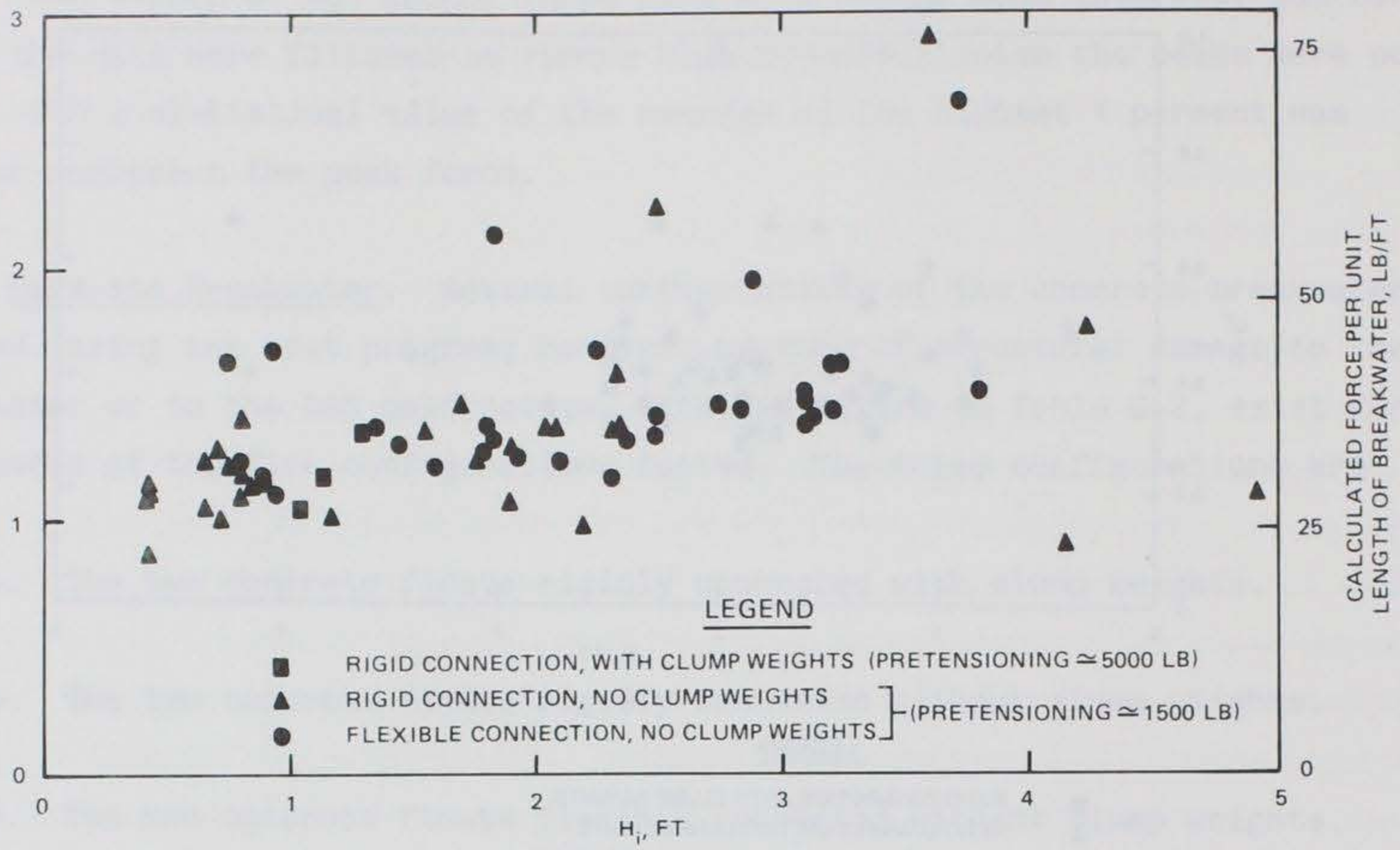

FIGURE G-8. Peak Anchor Line Force, F_p, versus Incident Wave Height, H_i, Concrete Breakwater (Channel 4)

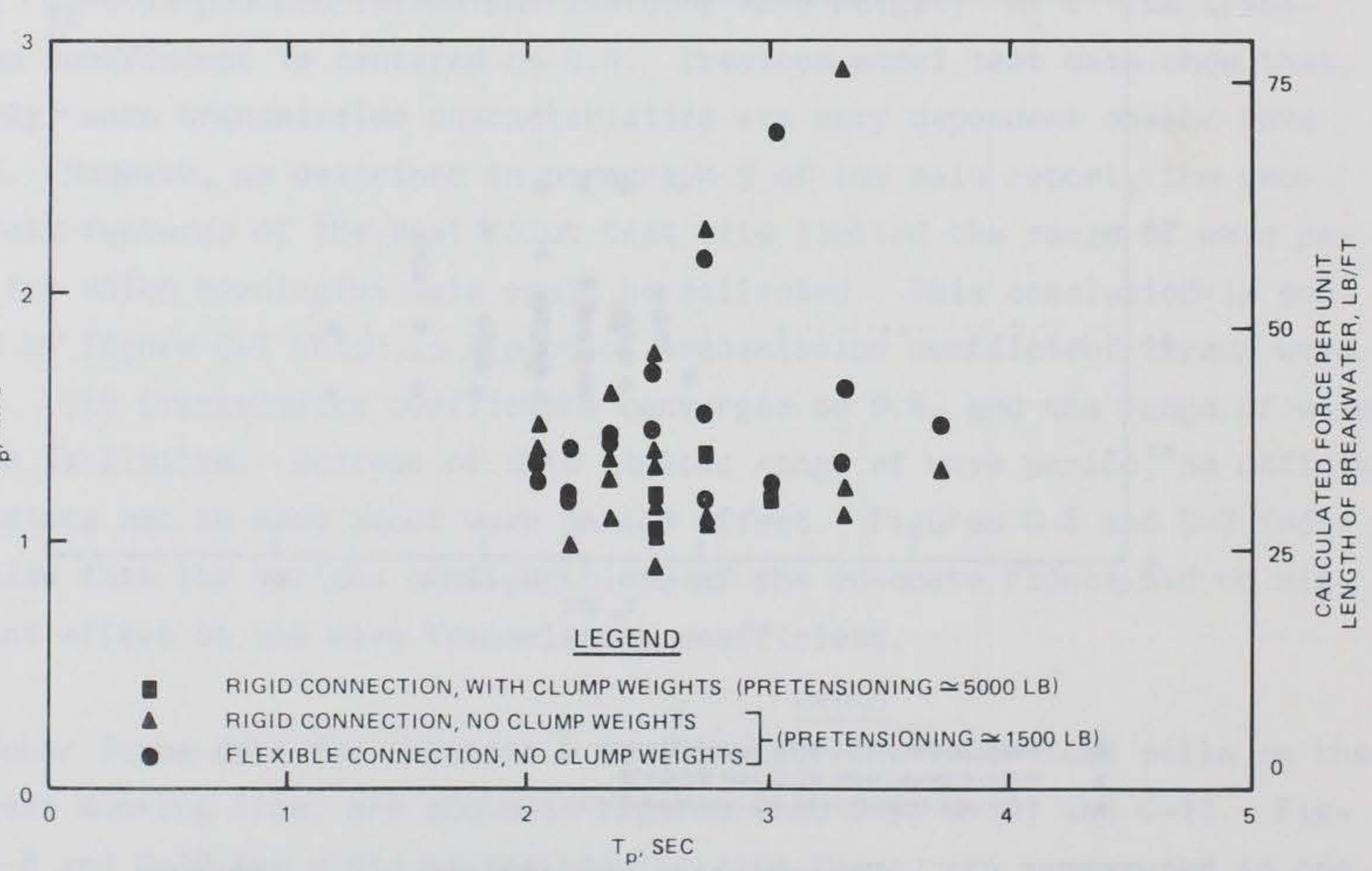

FIGURE G-9. Peak Anchor Line Force, F_p, versus Wave Period, T_p, Concrete Breakwater (Channel 4)

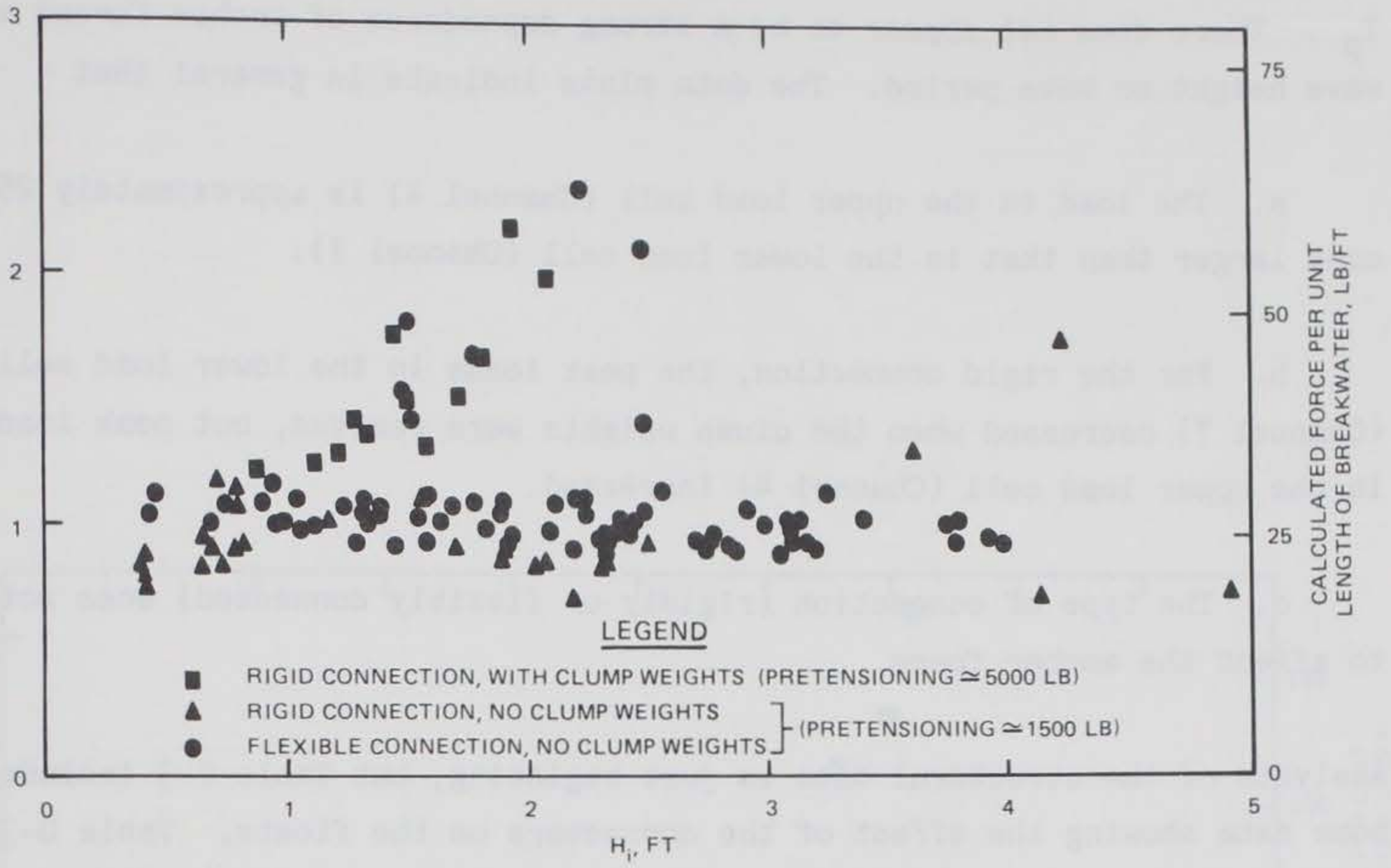

FIGURE G-10. Peak Anchor Line Force, F_p, versus Incident Wave Height, H_i, Concrete Breakwater (Channel 7)

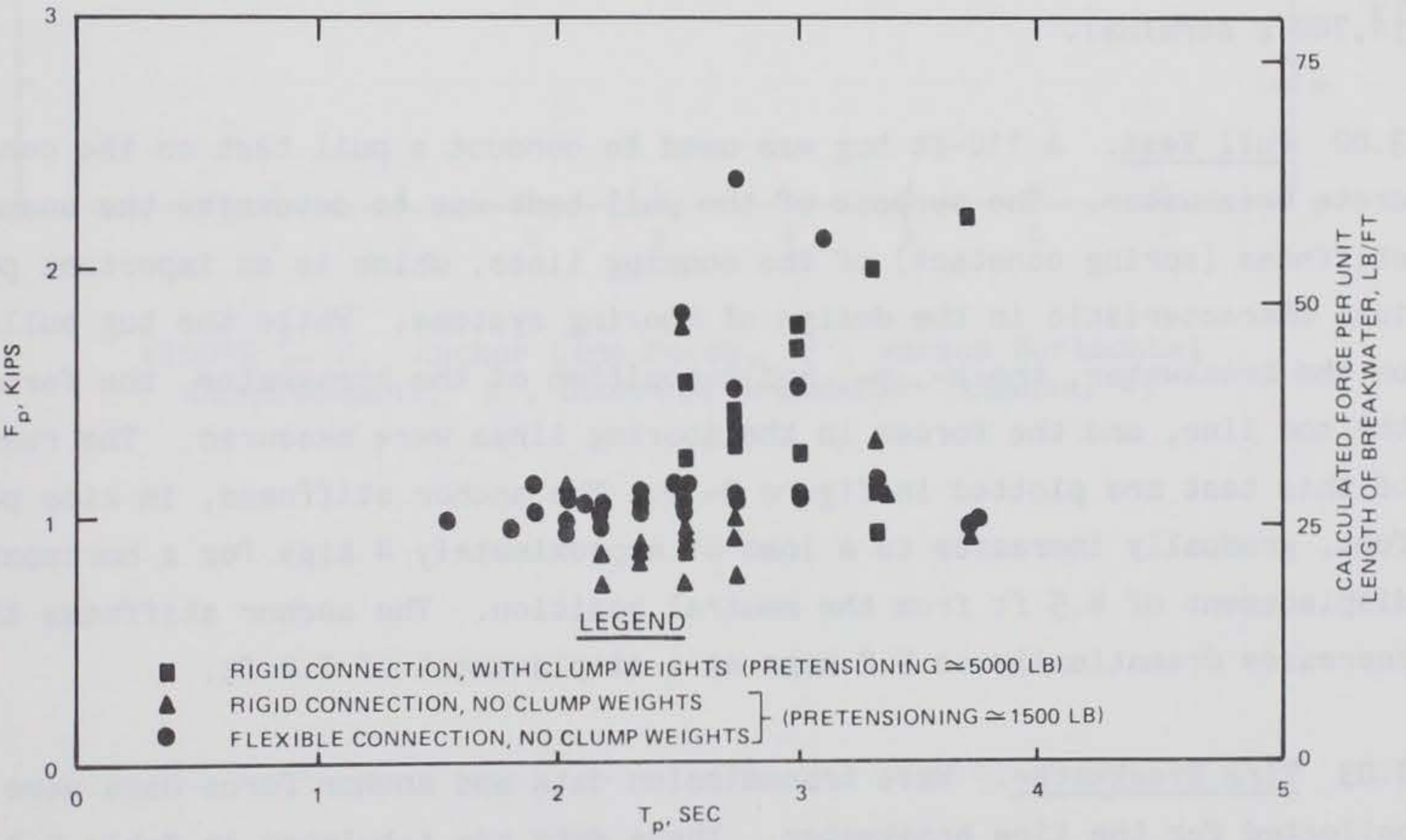

FIGURE G-11. Peak Anchor Line Force, F_p, versus Wave Period, T_p, Concrete Breakwater (Channel 7)

T_p . There does not appear to be a strong dependence of anchor forces versus wave height or wave period. The data plots indicate in general that

a. The load in the upper load cell (Channel 4) is approximately 25 percent larger than that in the lower load cell (Channel 7).

b. For the rigid connection, the peak loads in the lower load cell (Channel 7) decreased when the clump weights were removed, but peak loads in the upper load cell (Channel 4) increased.

c. The type of connection (rigidly or flexibly connected) does not seem to affect the anchor force.

Analysis of the structural data is just beginning, but Table G-3 includes some data showing the effect of the connectors on the floats. Table G-3 is a listing of strain magnitudes as measured by the longitudinal strain gages in the east end and center of the west float, Channels 45-48. The strains are very low, especially when compared to the strain values recorded when the float was lifted from the construction platform and placed in the water (1,700 μ strains).

3.02 Pull Test. A 110-ft tug was used to conduct a pull test on the concrete breakwater. The purpose of the pull test was to determine the anchor stiffness (spring constant) of the mooring lines, which is an important physical characteristic in the design of mooring systems. While the tug pulled on the breakwater, the x-, y-, and z-position of the breakwater, the force on the tow line, and the forces in the mooring lines were measured. The results of this test are plotted in figure G-12. The anchor stiffness, in kips per foot, gradually increases to a load of approximately 4 kips for a horizontal displacement of 4.5 ft from the neutral position. The anchor stiffness then increases dramatically to 5.2 kips at a displacement of 5.2 ft.

3.03 Tire Breakwater. Wave transmission data and anchor force data were collected for the tire breakwater. These data are tabulated in Table G-4 and graphically presented in figures G-13 through G-16. Figures G-13 and G-14 are plots of the wave transmission coefficient versus incident wave height and

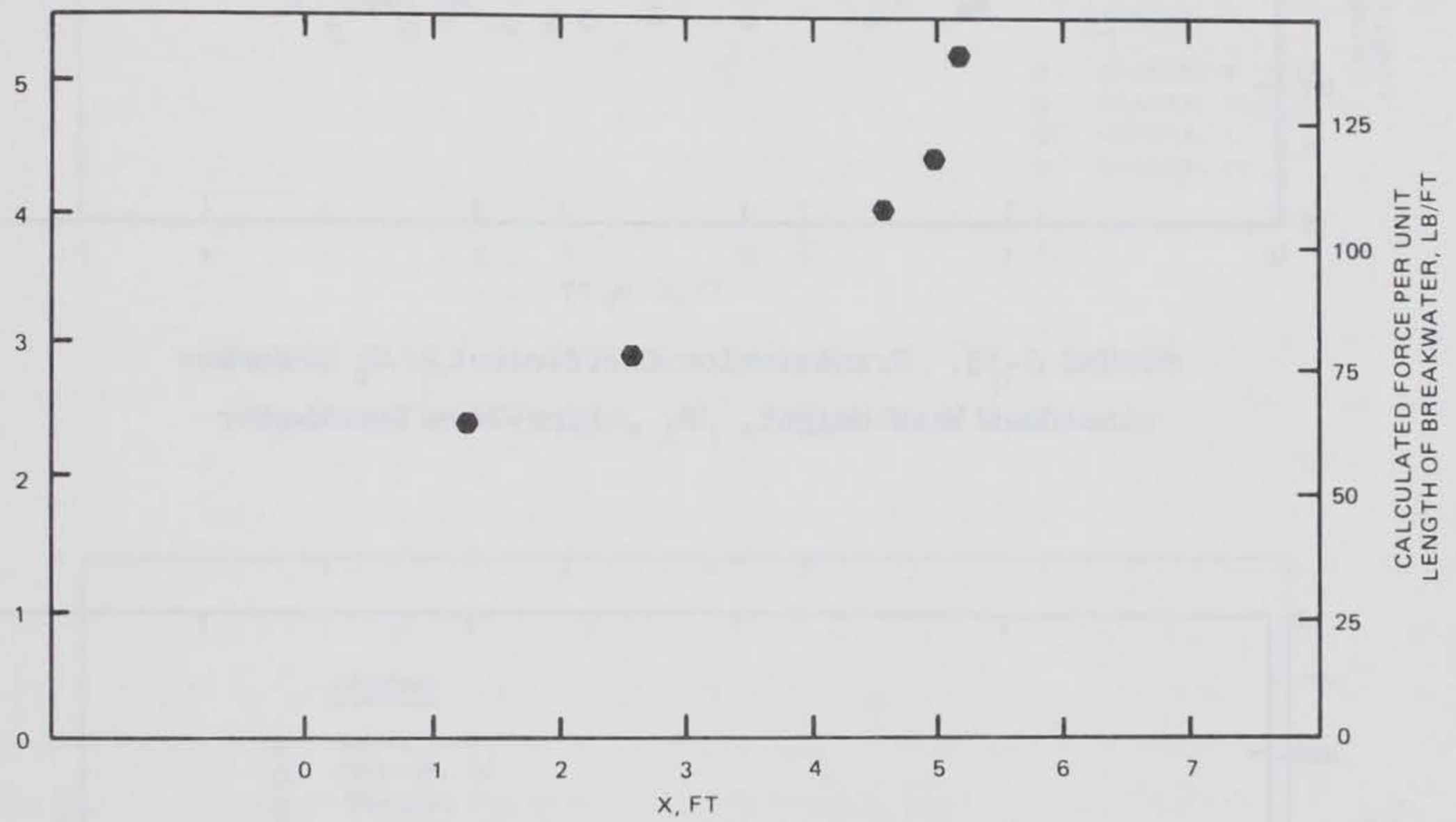

FIGURE G-12. Anchor Line Force, F , versus Horizontal Displacement, X , Concrete Breakwater (Channel 4)

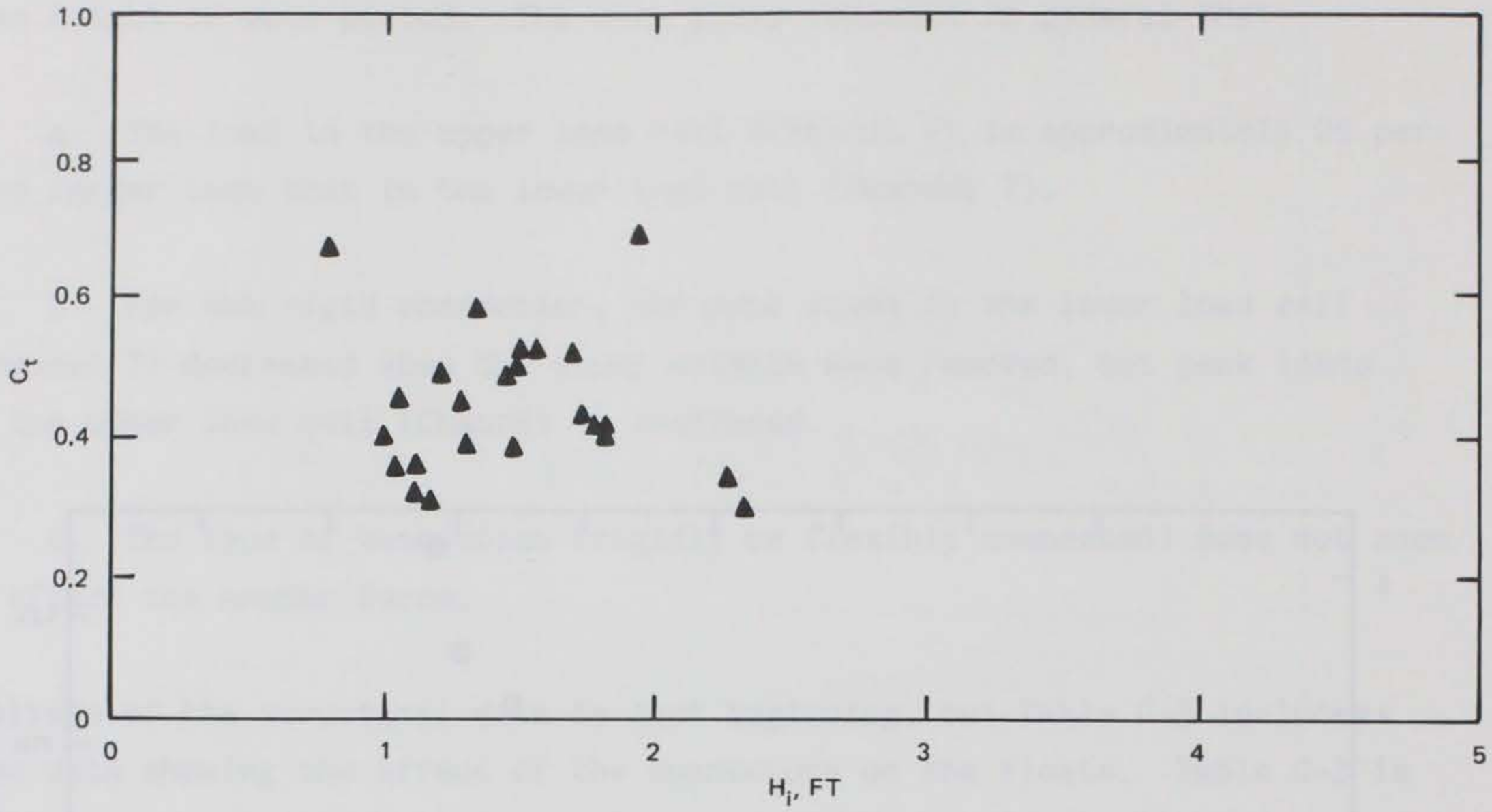

FIGURE G-13. Transmission Coefficient, C_t , versus Incident Wave Height, H_i , Pipe-Tire Breakwater

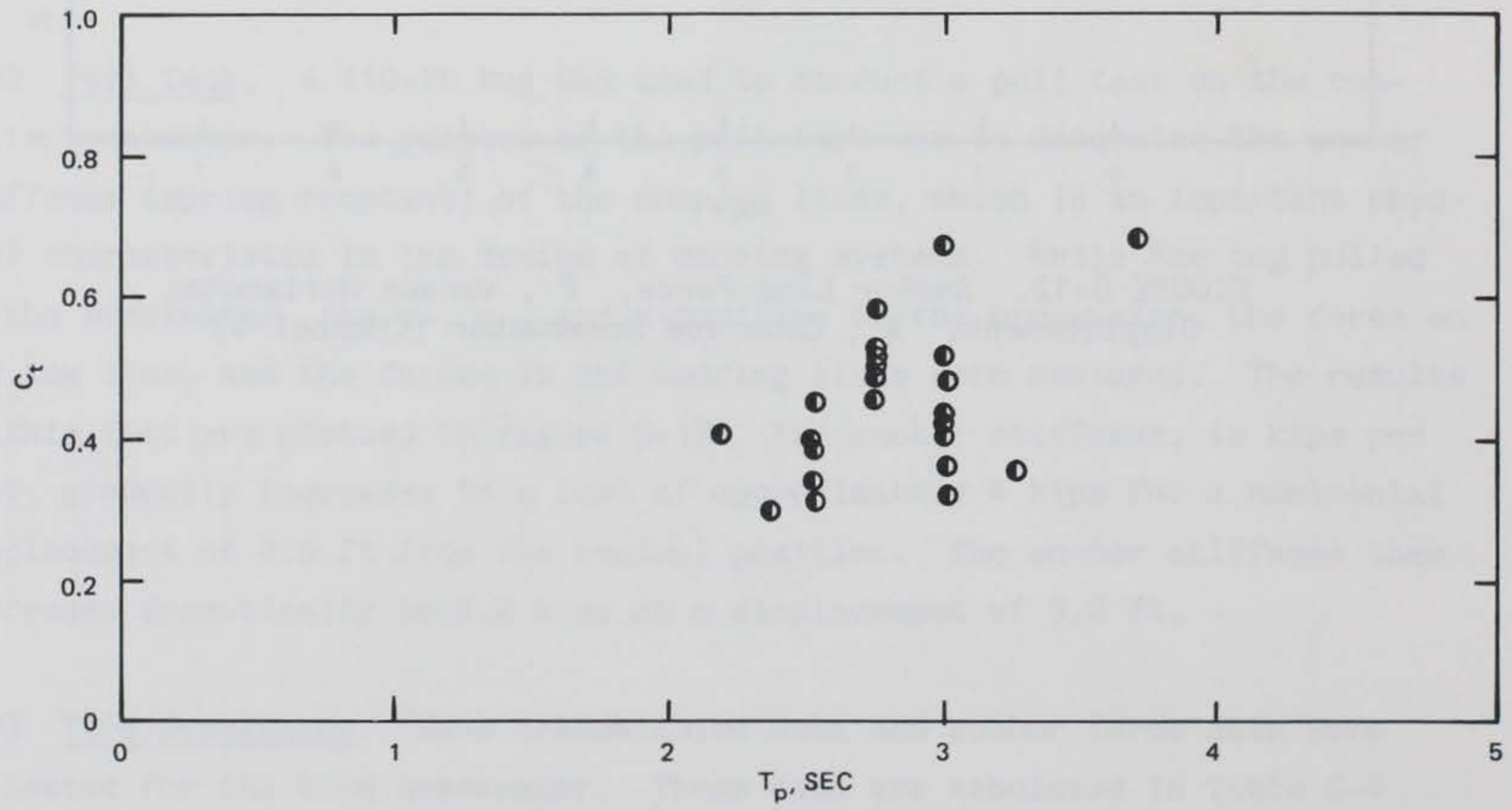

FIGURE G-14. Transmission Coefficient, C_t , versus Wave Period, T_p , Pipe-Tire Breakwater

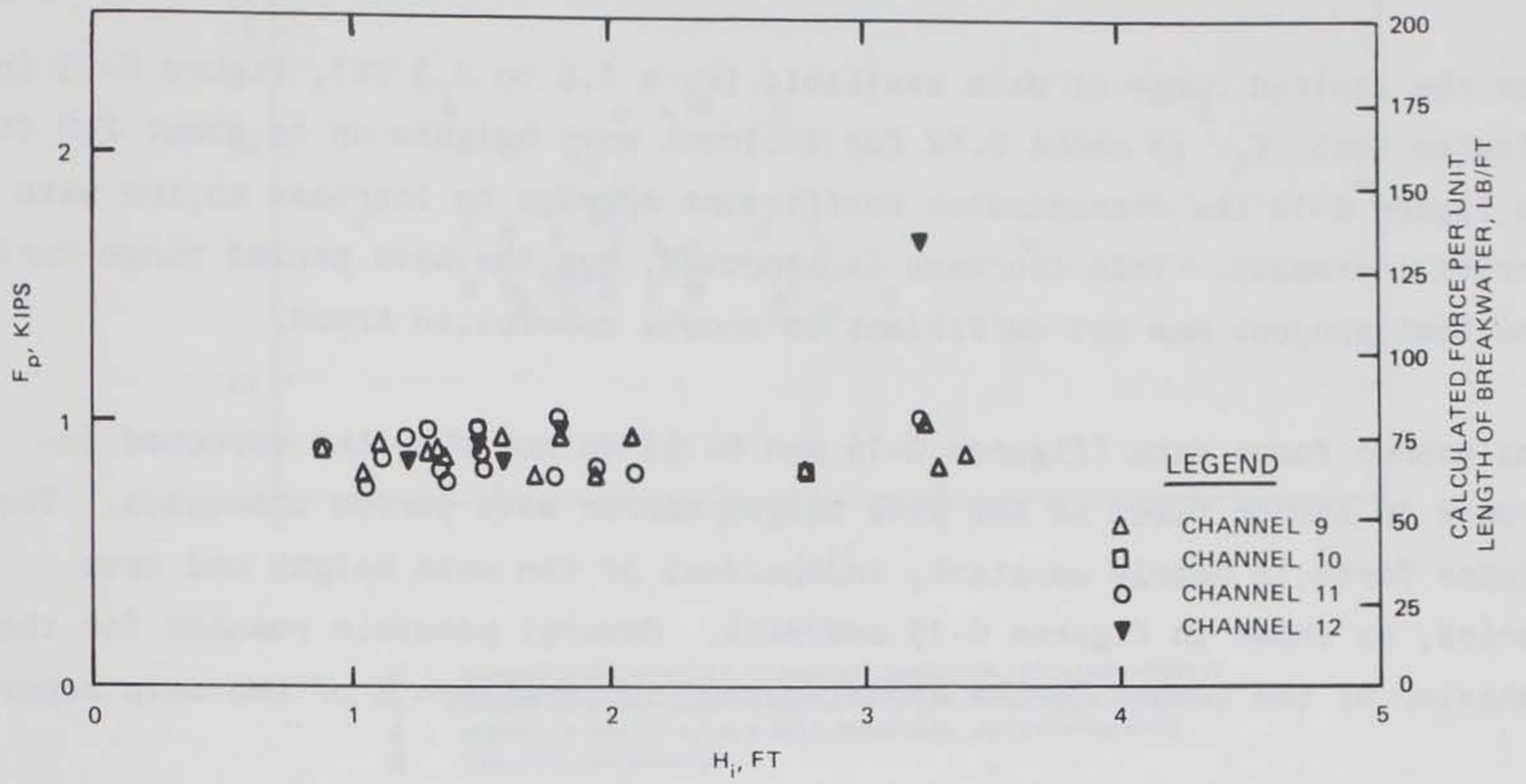

FIGURE G-15. Peak Anchor Line Force, F_p, versus Incident Wave Height, H_i, Pipe-Tire Breakwater

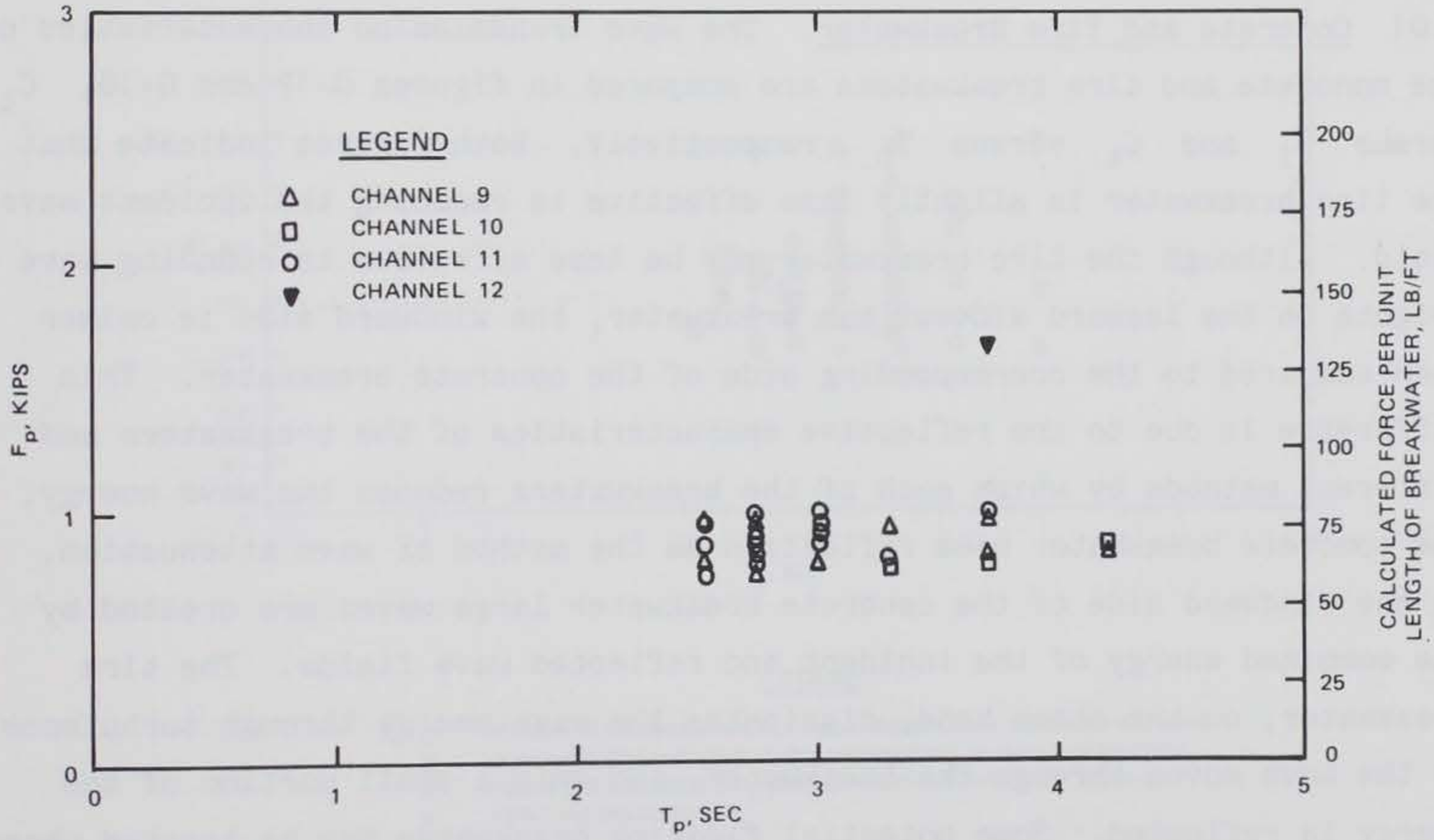

FIGURE G-16. Peak Anchor Line Force, F_p, versus Wave Period, T_p, Pipe-Tire Breakwater

wave period, respectively. Figures G-15 and G-16 present the peak anchor forces versus incident wave height and wave period, respectively.

For the limited range of data available (H_i = 1.0 to 2.3 ft), figure G-13 indicates that C_t is about 0.42 for incident wave heights up to about 2.0 ft. In figure G-14 the transmission coefficient appears to increase as the wave period increases. This increase is expected, but the wave period range during the test project was not sufficient to show a conclusive trend.

The anchor force data (figures G-15 and G-16) do not show the expected increase in anchor force as the wave height and/or wave period increases. The anchor force is nearly constant, independent of the wave height and wave period, as shown in figures G-15 and G-16. Several possible reasons for the behavior of the anchor forces are discussed in paragraph 5 of the main report.

4.0 Comparisons. Two comparisons will be made--one comparing the results of the two breakwaters and another comparing these data to previous data obtained from model studies.

4.01 Concrete and Tire Breakwater. The wave transmission characteristics of the concrete and tire breakwaters are compared in figures G-17 and G-18, C_t versus H_i and C_t versus T_p, respectively. Both figures indicate that the tire breakwater is slightly less effective in reducing the incident wave field. Although the tire breakwater may be less effective in reducing wave heights on the leeward side of the breakwater, the windward side is calmer when compared to the corresponding side of the concrete breakwater. This difference is due to the reflective characteristics of the breakwaters and different methods by which each of the breakwaters reduces the wave energy. The concrete breakwater uses reflection as the method of wave attenuation. On the windward side of the concrete breakwater large waves are created by the combined energy of the incident and reflected wave fields. The tire breakwater, on the other hand, dissipates the wave energy through turbulence as the wave moves through the breakwater, and only a small portion of the energy is reflected. Some potential floating breakwater may be located where the reflected waves in front of the concrete breakwater would be unacceptable. A tire breakwater would be a potential alternative in this situation.

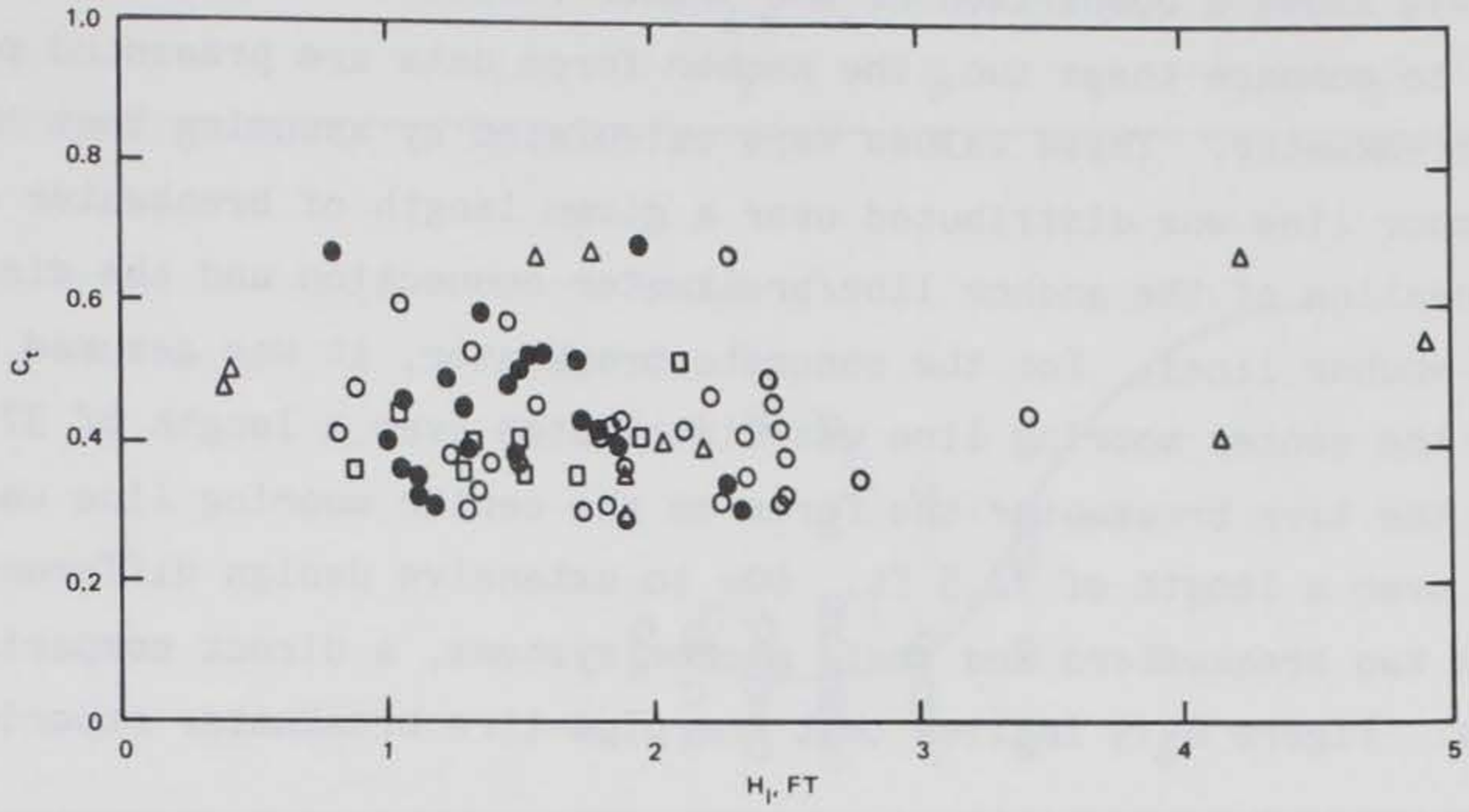

LEGEND

- ○ CONCRETE BREAKWATER, FLEXIBLE CONNECTION, NO CLUMP WEIGHTS
- □ CONCRETE BREAKWATER, RIGID CONNECTION, WITH CLUMP WEIGHTS
- △ CONCRETE BREAKWATER, RIGID CONNECTION, NO CLUMP WEIGHTS
- ● PIPE-TIRE BREAKWATER

FIGURE G-17. Transmission Coefficient, C_t, versus Incident Wave Height, H_i

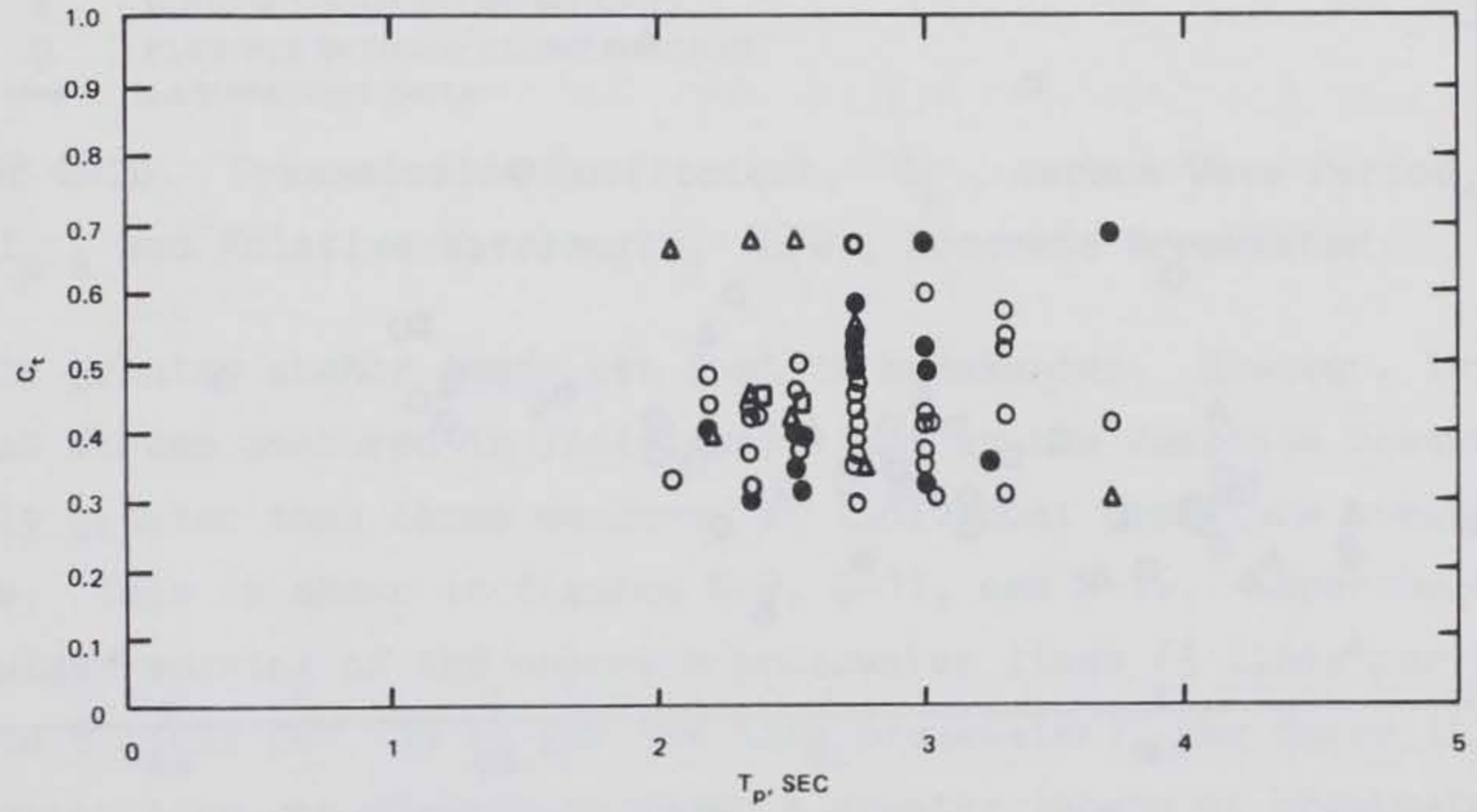

LEGEND

- ○ CONCRETE BREAKWATER, FLEXIBLE CONNECTION, NO CLUMP WEIGHTS
- □ CONCRETE BREAKWATER, RIGID CONNECTION, WITH CLUMP WEIGHTS
- △ CONCRETE BREAKWATER, RIGID CONNECTION, NO CLUMP WEIGHTS
- ● PIPE-TIRE BREAKWATER

FIGURE G-18. Transmission Coefficient, C_t, versus Wave Period, T_p

Figure G-19 shows a comparison of the anchor forces for the two breakwaters. In order to compare these two, the anchor force data are presented per linear foot of breakwater. These values were calculated by assuming that the force in an anchor line was distributed over a given length of breakwater depending on the location of the anchor line/breakwater connection and the distance to adjacent anchor lines. For the concrete breakwater, it was assumed that the force on the center mooring line was distributed over a length of 37.5 ft and that for the tire breakwater the force on the center mooring line was distributed over a length of 12.5 ft. Due to extensive design differences between the two breakwaters and their anchor systems, a direct comparison is difficult. Figure G-19 implies that the pipe-tire breakwater experienced

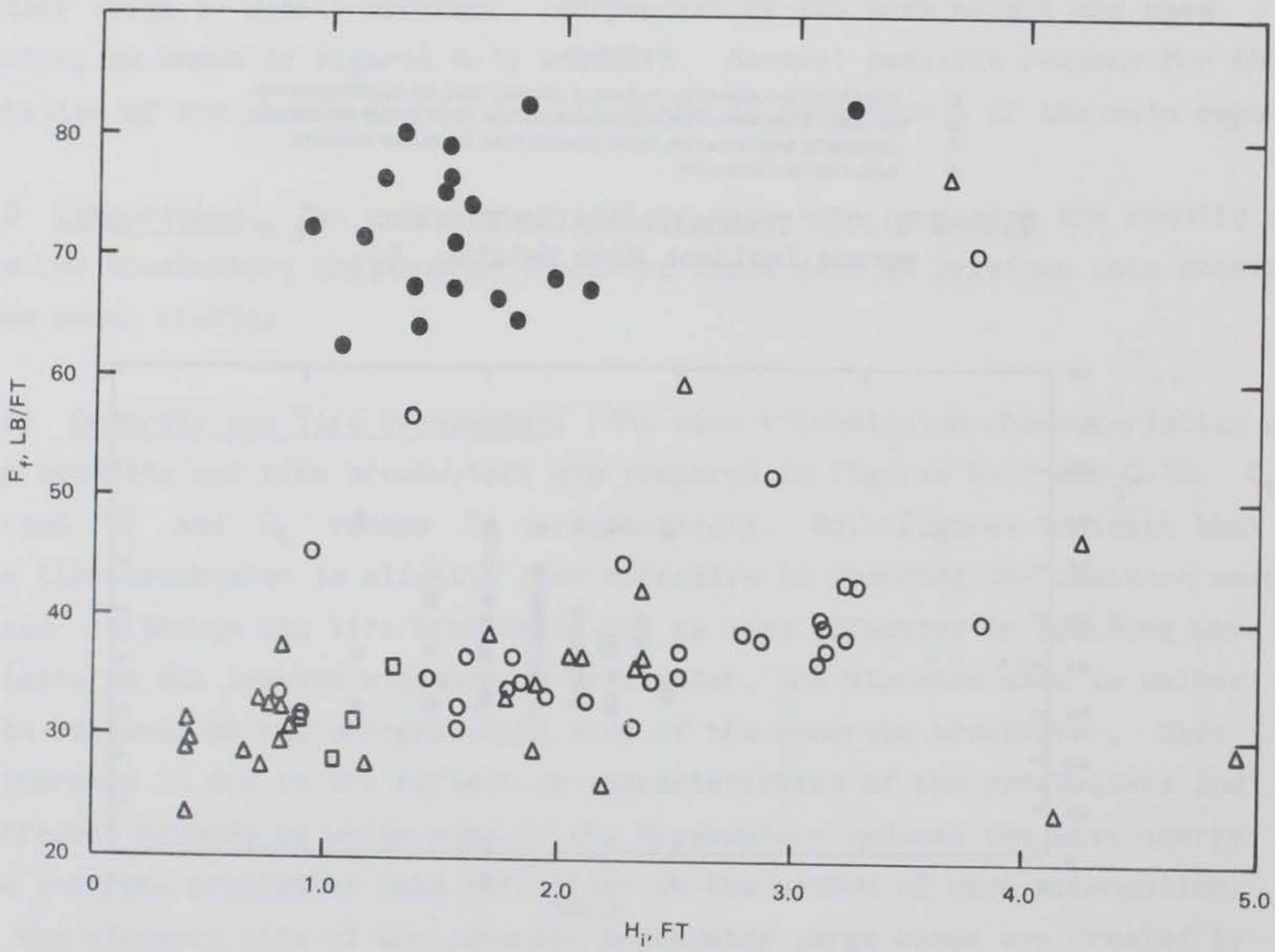

LEGEND

- △ CONCRETE, RIGID CONNECTION, WITH CLUMP WEIGHTS
- □ CONCRETE, RIGID CONNECTION, NO CLUMP WEIGHTS
- ○ CONCRETE, FLEXIBLE CONNECTION, NO CLUMP WEIGHTS
- ● TIRE BREAKWATER

FIGURE G-19. Anchor Line Force per Foot of Breakwater, F_t , versus Incident Wave Height, H_i

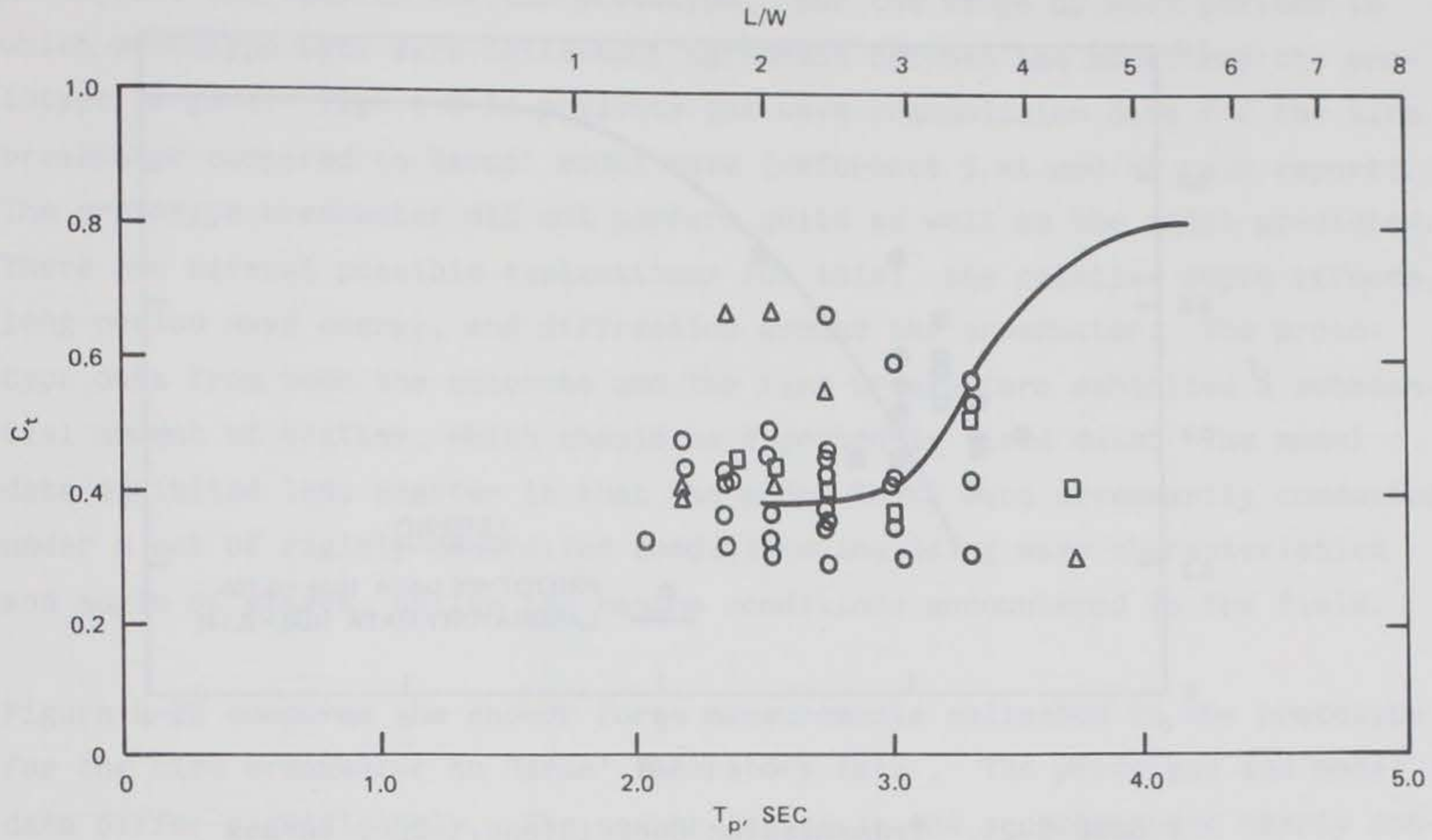

LEGEND

- □ RIGID WITH CLUMP WEIGHTS
- △ RIGID WITHOUT CLUMP WEIGHTS
- ○ FLEXIBLE WITHOUT CLUMP WEIGHTS
- — LABORATORY DATA

FIGURE G-20. Transmission Coefficient, C_t, versus Wave Period, T_p, and Relative Wavelength, L/W, Concrete Breakwater

significantly greater anchor loads per foot of breakwater. However, it should be noted that forces measured in individual lines on the concrete breakwater were actually greater than those measured in individual pipe-tire breakwater anchor lines. This is shown in figures G-9, G-11, and G-16. Nevertheless, because of wider spacing of the concrete breakwater lines (3 lines per 75 ft as opposed to 9 lines per 100 ft for the tire breakwater), the force in a concrete breakwater line was distributed over a greater length of breakwater.

4.02 Model Data. Figures G-20 through G-22 compare the prototype data to earlier model data. In figure G-20, the relationship between the wave transmission coefficient and wave period for the concrete breakwater is compared to model data collected for East Bay Marina (reference 2 at end of main report). The data for East Bay Marina were chosen because the width and draft of the

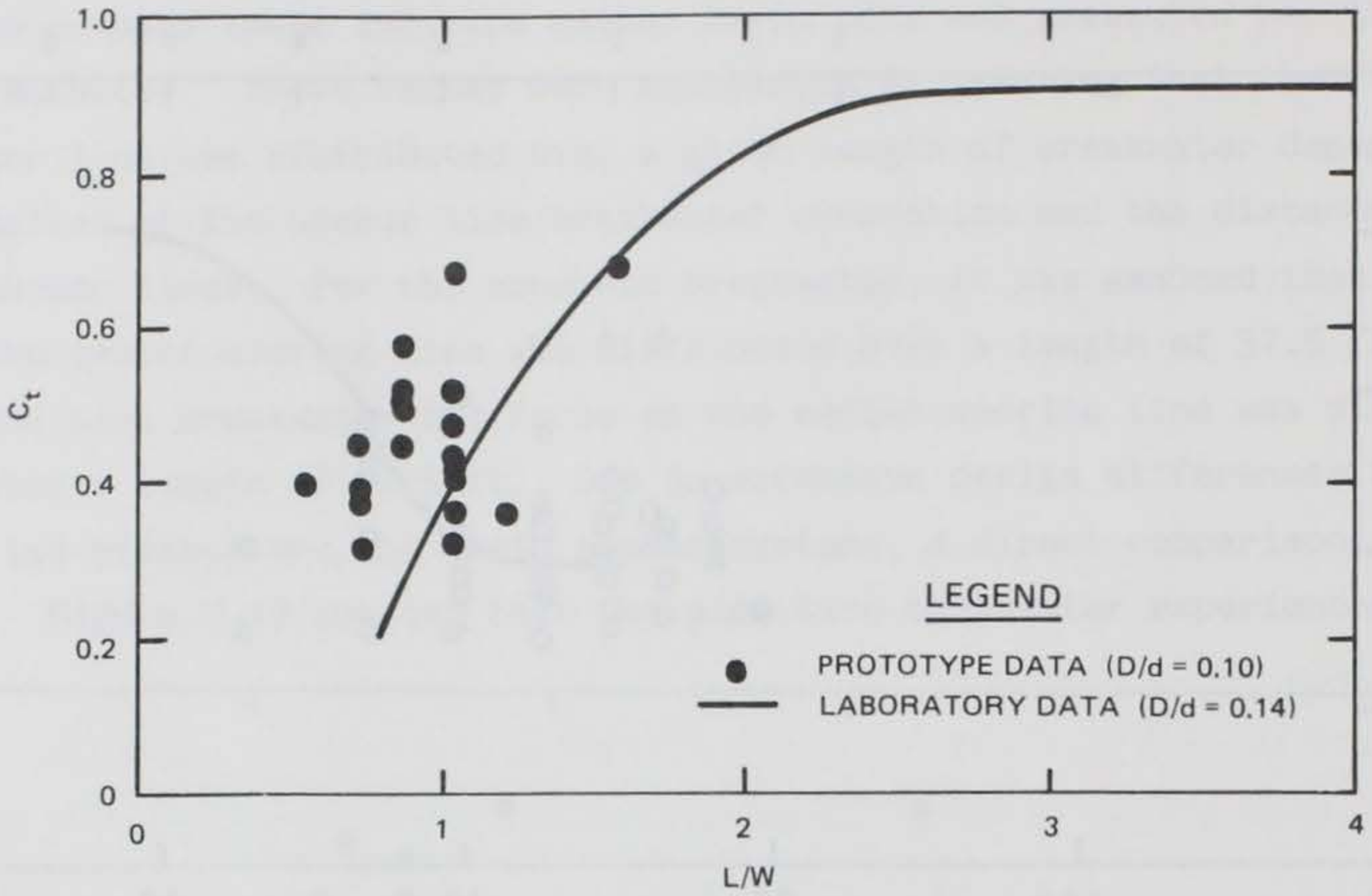

FIGURE G-21. Transmission Coefficient, C_t , versus Relative Wavelength, L/W , Pipe-Tire Breakwater

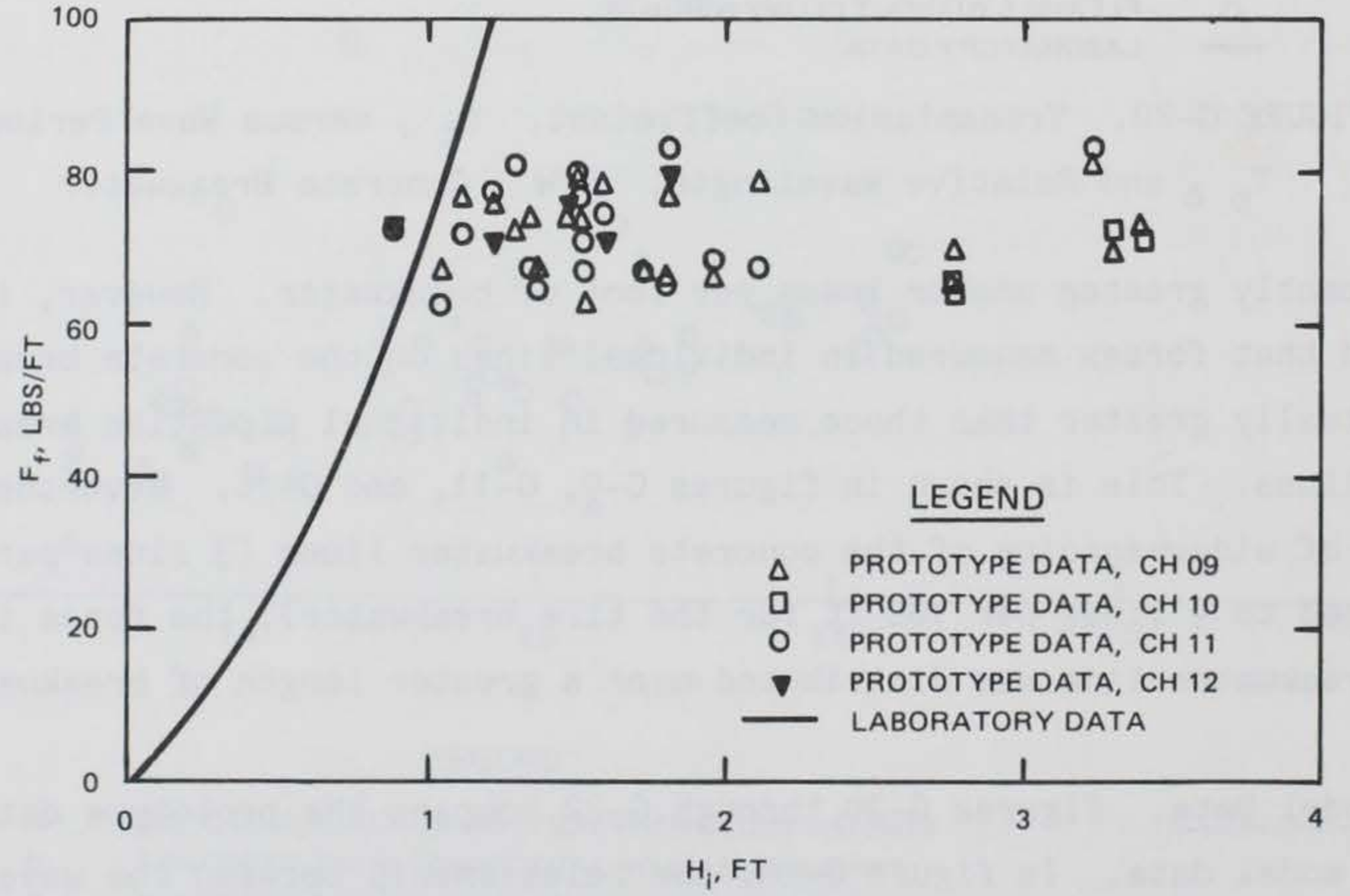

FIGURE G-22. Anchor Line Force per Foot of Breakwater, F_t , versus Incident Wave Height, H_i , Pipe-Tire Breakwater

model were the same as for the prototype. For the range of wave periods in which prototype data were collected, agreement between the model and the prototype is good. Figure G-21 presents the wave transmission data for the tire breakwater compared to Harms' model data (reference 5 at end of main report). The prototype breakwater did not perform quite as well as the model predicted. There are several possible explanations for this: the relative depth effects, long period wave energy, and diffraction around the breakwater. The prototype data from both the concrete and the tire breakwaters exhibited a substantial amount of scatter, which should be expected in field data. The model data exhibited less scatter in that the model tests were necessarily conducted under a set of rigidly controlled conditions including wave characteristics and angle of attack, unlike the random conditions encountered in the field.

Figure G-22 compares the anchor force measurements collected in the prototype for the tire breakwater to Harms' laboratory data . The prototype and model data differ significantly. The anchor forces in the prototype are nearly constant with an increasing wave height, while the model anchor forces increase with an increasing wave height. The difference between the prototype and model results probably is related to dissimilarities in the anchor system and test conditions. The actual tire mat geometry was the same; however, there were significant differences in the depth of water, anchoring system design, mooring line elasticities, and ratio of breakwater draft to water depth.

5.0 Conclusions. A large amount of data were collected during this project, and a number of valuable conclusions have been reached at this stage of the analysis. The results indicate the following:

a. Current methods of predicting wave transmission are adequate, although in critical areas a model study may be required. A model study is recommended when wave periods larger than 4 sec are expected at a proposed site.

b. Actual anchor loads can be significantly lower than what models or theory predict, but the loads may be drastically influenced by factors such as mooring line elasticity and depth of water. Further studies related to this area are being addressed in the general research and development studies.

c. The concrete and tire breakwaters performed very well and are feasible options to reduce wave energy. When choosing either structure, one should consider the method of energy dissipation. The concrete breakwater reflects the waves causing a rougher environment windward of the breakwater; whereas the tire breakwater uses energy dissipation which reduces the amount of reflection.

TABLE G-1

TRANSDUCER INPUT SUMMARY SHEET

Channel No.	Location Code	Location	Physical Units
Anchor Line Forces			
1	LNWC	Lower northwest on concrete breakwater	kips
2	LNEC	Lower northeast on concrete breakwater	
3	UNWC	Upper northwest on concrete breakwater	
4	USWC	Upper southwest on concrete breakwater	
5	UNEC	Upper northeast on concrete breakwater	
6	USEC	Upper southeast on concrete breakwater	
7	LSWC	Lower southwest on concrete breakwater	
8	LSEC	Lower southeast on concrete breakwater	
9	LNT	Lower north tire breakwater	
10	UNT	Upper north tire breakwater	
11	UST	Upper south tire breakwater	
12	LST	Lower south tire breakwater	
Fixed References			
13	South		
14	Center	(never installed)	
15	North		
Wave Heights			
16	TIDE	Tide gage	ft
17	INC	Incident wave buoy	
18	NW	Northwest wave buoy	
19	NE	Northeast wave buoy	
20	SW	Southwest wave buoy	
21	SE	Southeast wave buoy	
Dynamic Pressures			
22	NU	North upper	psi
23	NL	North lower	
24	BNC	Bottom north center	
25	BEC	Bottom east center	
26	BEI	Bottom east inner	
27	BCC	Bottom center	
28	BWI	Bottom west inner	
29	BWO	Bottom west outer	
30	BSC	Bottom south center	
31	SCU	South center upper	

(Continued)

TABLE G-1 (Continued)

Channel No.	Location Code	Location	Physical Units
Anchor Line Forces			
Dynamic Pressures (Continued)			
32	SW1	Southwest number 1	psi
33	SW2	Southwest number 2	
34	SW3	Southwest number 3	
35	SCL	South center lower	
36	SE3	Southeast number 3	
37	SE2	Southeast number 2	
38	SE1	Southeast number 1	
39	EP1	East pontoon number 1	
40	EP2	East pontoon number 2	
41	EP3	East pontoon number 3	
42	EP4	East pontoon number 4	
43	EP5	East pontoon number 5	
44	EP6	East pontoon number 6	
Concrete Strains			
45	NULE	North upper longitudinal on east end of pontoon	με
46	NBLE	North bottom longitudinal on east end of pontoon	
47	SBLE	South bottom longitudinal on east end of pontoon	
48	SULE	South upper longitudinal on east end of pontoon	
49	NT1	North transverse number 1	
50	NT2	North transverse number 2	
51	BT1	Bottom transverse number 1	
52	BT2	Bottom transverse number 2	
53	UT1	Upper transverse number 1	
54	UT2	Upper transverse number 2	
55	ST2	South transverse number 2	
56	ST1	South transverse number 1	
57	NULC	North upper longitudinal at center of pontoon	
58	NBLC	North bottom longitudinal at center of pontoon	
59	SULC	South upper longitudinal at center of pontoon	
60	SBLC	South bottom longitudinal at center of pontoon	

(Continued)

(Sheet 2 of 3)

TABLE G-1 (Concluded)

Channel No.	Location Code	Location	Physical Units
Anchor Line Forces			
Accelerometer Data			
61	WVA	West vertical	ft/sec^2
62	WHA	West horizontal	
63	WRA	West rotational	
64	EVA	East vertical	
65	EHA	East horizontal	
66	ERA	East rotational	
Relative Motions			
67	WVR	West vertical rotational displacement	deg
68	WHR	West horizontal rotational displacement	
69	EVR	East vertical rotational displacement	
70	EHR	East horizontal rotational displacement	
71	CLM	Center longitudinal motion	
72	CRM	Center rotational motion	
Wind Speed and Direction			
73	WS1	Wind speed at tide gage	mph
74	WS2	Wind speed at instrument house	
75	WD1	Wind direction at tide gage	deg
76	WD2	Wind direction at instrument house	
Current Velocity			
77	N-S	North-South	ft/sec
78	E-W	East-West	

TABLE G-2

WAVE ATTENUATION AND ANCHOR LINE FORCE DATA, CONCRETE BREAKWATER

Incident Wave Height (ft)	Transmitted Wave Height (ft)	Transmission Coefficient	Wave Period (sec)	Anchor Line Force (lb) Channel 4	Anchor Line Force (lb) Channel 7
Rigid Connection with Clump Weights					
1.58			2.75		1,315
1.21			2.75		1,276
1.82			3.01		1,670
1.46			3.01		1,755
1.50	0.62	0.41	2.75		1,495
1.49			2.54		1,536
1.12	0.40	0.36	3.01	1,167	1,244
1.04	0.46	0.44	2.54	1,042	1,120
1.95	0.80	0.41	3.71		2,178
2.10	1.09	0.52	3.32		1,982
1.79	0.74	0.41	3.01		1,673
1.32	0.52	0.39	2.75		1,351
1.52	0.54	0.36	2.75		1,403
1.72	0.61	0.36	3.01		1,501
1.29	0.47	0.36	2.75	1,346	1,424
0.88	0.32	0.36	2.54	1,174	1,214
0.98	0.44	0.45	2.40		
Rigid Connection Without Clump Weights					
3.61			3.32	2,879	1,296
1.56	1.03	0.66	2.05	1,369	1,109
0.80				1,410	1,149
0.80			3.32	1,209	1,076
0.75				1,216	848
0.70				1,229	915
0.40	0.19	0.48		1,082	835
0.42	0.21	0.50		1,102	762
0.41				1,162	882
0.41				868	815
2.32			2.53	1,349	842
2.35			2.35	1,376	855
2.34			2.35	1,583	875
2.08			2.53	1,369	855
4.22	2.82	0.67	2.53	1,744	1,744
4.90	2.69	0.55	2.75	1,089	755
4.14	1.70	0.41	2.53	888	721

(Continued)

TABLE G-2 (Continued)

Incident Wave Height (ft)	Transmitted Wave Height (ft)	Transmission Coefficient	Wave Period (sec)	Anchor Line Force (lb) Channel 4	Anchor Line Force (lb) Channel 7
Rigid Connection Without Clump Weights (Continued)					
2.19	0.86	0.39	2.19	975	721
1.89	0.84	0.44	2.35	1,082	868
1.77	1.18	0.67	2.35	1,242	822
2.04	0.82	0.40	2.19	1,369	842
1.90	0.57	0.30	3.71	1,283	888
1.70			2.05	1,456	908
2.50			2.75	2,244	928
1.17			2.53	1,022	1,015
0.71			2.53	1,022	1,189
0.80			3.32	1,096	908
0.65			2.75	1,055	962
0.83			2.53	1,142	928
1.90	0.67	0.35	2.78		1,062
Flexible Connection Without Clump Weights					
1.83	0.57	0.31	3.32	1,303	
1.80				1,376	
3.73			3.03	2,632	
1.31	0.70	0.53	3.32		
1.06	0.63	0.59	3.01		
0.88	0.42	0.48	2.19	1,182	
1.72	0.52	0.30	2.75		
1.46	0.83	0.57	3.32		
1.84	0.78	0.42	2.75	2,131	
2.35	0.83	0.35	3.01		
2.47	0.78	0.32	2.35		
1.29	0.39	0.30	2.53		935
2.50	0.96	0.38			
2.22			2.53		1,102
2.44	1.21	0.50	2.53		
2.77	0.96	0.35	2.75		
1.24	0.47	0.38	2.75		1,069
0.68			1.92		1,015
1.00					1,015
2.49			2.75		1,403
1.07	0.57	0.53	3.75		989
0.43			2.35		1,049
0.82	0.34	0.42	2.38		

(Continued)

TABLE G-2 (Continued)

Incident Wave Height (ft)	Transmitted Wave Height (ft)	Transmission Coefficient	Wave Period (sec)	Anchor Line Force (lb) Channel 4	Anchor Line Force (lb) Channel 7
Flexible Connection Without Clump Weights (Continued)					
2.13	0.89	0.42	3.32		1,089
3.75					1,002
1.39					1,082
2.49	1.05	0.42	3.01		2,111
2.23	1.04	0.47	2.75		2,345
1.50	0.56	0.37	2.53		1,810
2.57			2.50		1,129
0.90			2.35		1,089
0.46			1.92		1,129
1.05			2.53		1,109
1.32			2.13		1,049
0.73			3.01		1,076
2.75					908
1.55			2.53		1,022
2.34	0.97	0.41	2.35		
1.90	0.69	0.36	2.35		1,096
1.88	0.82	0.44	2.19		1,049
2.92			2.35		1,055
1.38	0.51	0.37	2.53		1,042
2.33					949
3.41	1.49	0.44	2.35		1,022
1.70			2.75		1,076
1.90	0.56	0.30	2.75		1,069
1.78				1,262	1,089
1.57				1,202	1,109
0.93				1,690	1,162
0.80				1,249	1,102
1.64					1,002
3.26			3.32	1,603	1,136
2.22			3.01	1,236	1,082
1.94			2.05	1,249	969
2.26	0.71	0.31	2.53	1,663	1,109
2.50	0.81	0.32	2.35	1,403	1,049
1.34	0.44	0.33	2.19	1,369	1,002
1.32	0.60	0.45	2.75	1,156	1,089
3.10				1,496	987
3.22				1,610	949
2.38			2.75		1,015
2.77			3.71	1,450	942

(Continued)

TABLE G-2 (Concluded)

Incident Wave Height (ft)	Transmitted Wave Height (ft)	Transmission Coefficient	Wave Period (sec)	Anchor Line Force (lb) Channel 4	Anchor Line Force (lb) Channel 7
Flexible Connection Without Clump Weights (Continued)					
2.46	1.13	0.46	2.53		1,029
2.85				1,430	922
2.38				1,309	969
2.88				1,944	902
2.97	1.74	0.59			
3.11				1,476	949
3.10				1,356	1,022
3.14			2.35	1,396	1,029
3.80			2.75	1,490	1,022
2.29	1.52	0.66	2.75		
3.00					1,015
1.83					982
1.57					949
2.78					962
1.11					995
0.96					1,002
2.71					942
3.78					949
2.10					975
2.18					915
3.98					949
3.06					895
3.93			1.82		955
2.44	0.79	0.32	1.55		975
1.92			2.05		935
2.31			2.05		942
2.32			2.19	1,162	955
3.22			2.53	1,430	915
2.50	1.00	0.40	2.05	1,316	1,062
1.44	0.59	0.41	3.32	1,309	915

(Sheet 4 of 4)

TABLE G-3

CONCRETE BREAKWATER STRAIN MEASUREMENTS

Incident Wave Height (ft)	Wave Period (sec)	Channels Strain (μs) 45	46	47	48	57	58	59	60
Rigid Connection with Clump Weights									
2.10	3.32	28	18	18	4	10	--	4	12
1.52	2.75	15	8	10	4	6	--	4	7
Rigid Connection Without Clump Weights									
1.90	3.71	19	21	3	1	16	7	7	17
2.50	2.75	27	28	3	1	23	10	8	25
Flexible Connection Without Clump Weights									
1.46	3.01	10	14	10	4	8	17	14	8
1.92	2.75	10	14	11	4	12	7	6	13

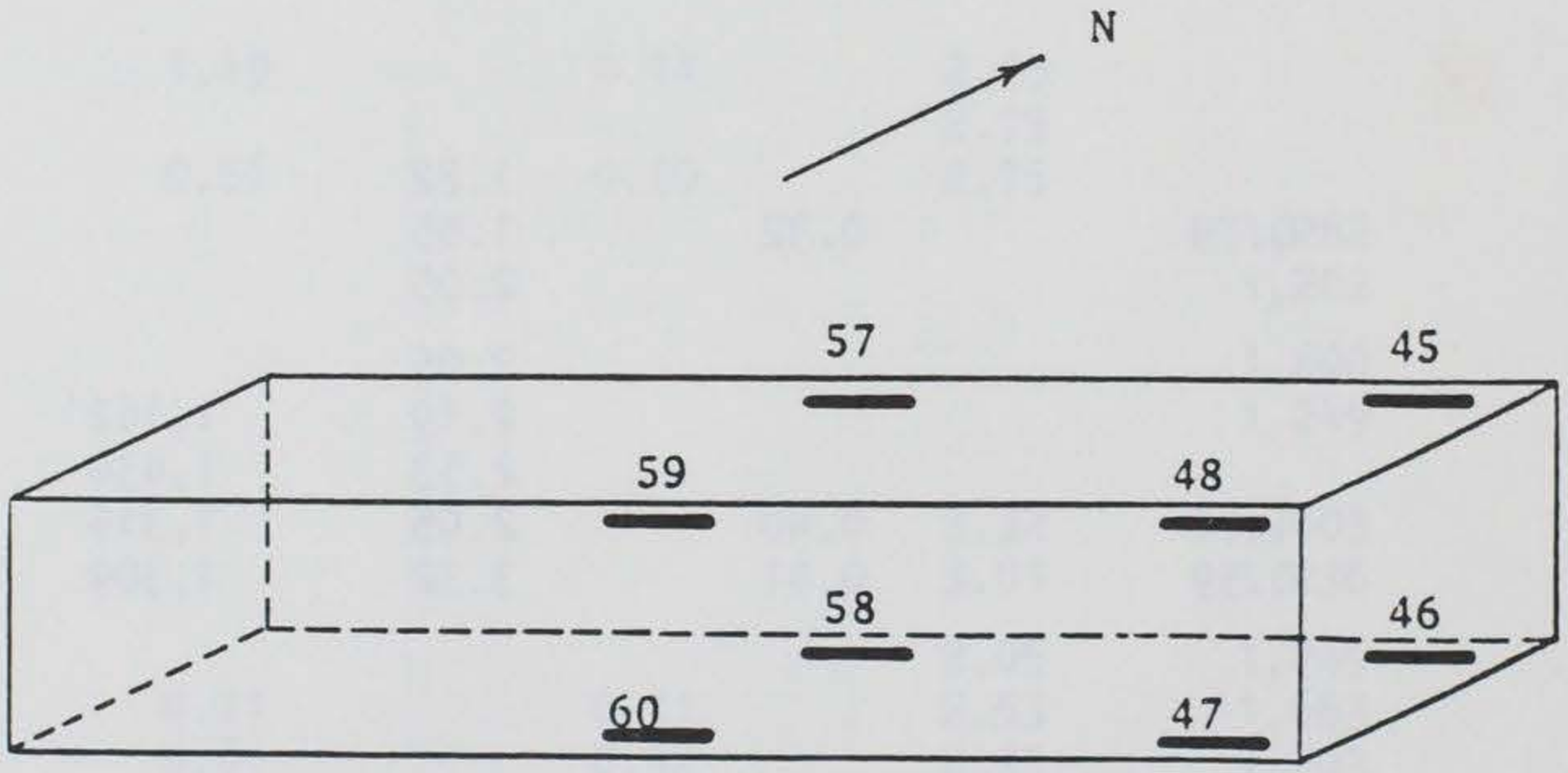

Strain Gage Location Sketch

TABLE G-4

WAVE ATTENUATION AND ANCHOR LINE FORCE DATA, PIPE-TIRE BREAKWATER

Incident Wave Height (ft)	Transmitted Wave Height (ft)	Transmission Coefficient	Wave Period (sec)	Anchor Line Force (lb) Channel 9	Channel 10	Channel 11	Channel 12
2.75			3.32	791	783		
2.76			3.71	838	783		
3.29			4.20	838	865		
3.38			4.20	873	857		
1.51			2.75	887		855	
1.34				888		813	
3.22			3.71	974		989	1,678
1.58	0.83	0.52	2.75	940		895	855
1.21	0.59	0.49	2.75	910		922	847
1.82	0.75	0.41	3.01	927		995	952
1.46	0.70	0.48	3.01	912		905	918
1.50	0.75	0.50	2.75	960		920	
1.49	0.57	0.38	2.54	952		955	
1.12	0.36	0.32	3.01	920		862	
1.04	0.84	0.81	2.54	802		748	
1.95	1.33	0.68	3.71	792		818	
2.10			3.32	942		808	
1.79	0.75	0.42	3.01	792		780	
1.36	0.79	0.58	2.75	815		770	
1.52	0.79	0.52	2.75	755		807	
1.72	0.89	0.52	3.01	798		797	
1.31	0.51	0.39	2.53				
1.29	0.58	0.45	2.75	867		965	
1.17	0.37	0.31	2.53				
1.05	0.38	0.36	3.01				
1.06	0.48	0.45	2.53				
1.00	0.40	0.40	3.00				
0.88	0.20	0.23	2.54	875		868	
0.80	0.54	0.67	3.00				
1.83	0.72	0.40	2.19				
2.38	0.72	0.30	2.35				
2.32	0.78	0.34	2.53				
1.74	0.74	0.43	3.00				
1.12	0.40	0.36	3.26				

APPENDIX H

CHRONOLOGY OF MAJOR EVENTS

5 Feb 81	The prototype test is authorized and the Floating Breakwater Prototype Test Program Working Group is established by M. G. Heiberg.
26-27 Feb 81	Meeting to set groundwork for prototype test and to delineate program responsibilities is held in Seattle.
8 May 81	Prototype design document is completed.
12 Jun 81	Meeting of working group is held in Seattle (working group approves design document and authorizes proceeding with plans and specifications).
27 Jul 81	Meeting of working group is held to review draft plans and specifications.
5 Aug 81	Plans and specifications are completed.
14 Aug 81	Plans and specifications are approved.
11 Sep 81	Monitoring contract is awarded to University of Washington for $280,000.
28 Sep 81	Construction contract is awarded to American Construction for $576,000.
24 Mar 82	Construction of pipe-tire breakwater is begun.
29 Apr 82	Pipe-tire breakwater is completed.
27 Apr-4 May 82	Anchor piles are driven at West Point test site.

28 May 82	First module of concrete breakwater is placed.
10 Jun 82	Second module is placed.
17 Jun 82	Pipe-tire breakwater is anchored at West Point.
28 Jun 82	Concrete modules are launched and connected.
1 Jul 82	Upon arrival of concrete breakwater at West Point anchoring is begun.
16 Jul 82	Concrete breakwater anchor lines are tensioned to 5,000 lb and ± 1,000 lb.
19 Jul 82	District Engineer inspection of breakwater is conducted.
22 Jul 82	First concrete breakwater flexible connector repair is completed.
3 Aug 82	Instrumentation conduit is installed by electrical contractor.
6 Aug 82	Secondary hatch is installed (to allow access to instrumentation compartment).
9 Aug 82	Final inspection of breakwater construction (connector failure noted) is conducted.
26 Aug 82	Second flexible connector repair is completed.
13 Sep 82	Test site is inspected by working group.
3 Oct 82	Failure of U-shaped connector is detected.
5 Oct 82	Emergency fendering is installed between concrete floats.

6 Oct 82	First storm of winter, with 30-knot winds from the south, is experienced.
15 Oct 82	Concrete floats are disconnected and fendered.
22 Oct 82	Second major storm, with southerly winds of 25 knots and gusts to 38 knots, is experienced.
26 Oct 82	Third storm, with southerly winds of 31 knots and gusts to 41 knots (horizontal timbers torn from wood fender), is experienced.
28 Oct 82	Data Acquisition System is installed and turned on.
8 Nov 82	West end of east float is flooded, requiring emergency pumping.
13 Dec 82	Test site is inspected by working group.
21 Dec 82	65-knot southerly winds (highest during test) are experienced.
29 Dec 82	Emergency repairs are made to concrete breakwater fendering system.
9-10 Jan 83	24 hr of southerly winds continously exceeding 30 knots is experienced.
11 Jan 83	Emergency pumping is again required (east end of east float).
31 Jan 83	Boat wake test No. 1 is conducted.
8 Feb 83	Concrete breakwater is unanchored and towed to U. S. Army Corps of Engineers work area at Lake Washington Ship Canal.

9-24 Feb 83	Rigid connection is made between floats.
25 Feb 83	Rigidly connected concrete breakwater is reanchored.
13-14 Mar 83	Strong southerly winds to 35 knots are experienced.
15 Mar 83	Onboard data acquisition system is reactivated.
30 Mar 83	Test site is inspected by working group.
9-10 Apr 83	Strong southerly winds to 25 knots are experienced.
22 Apr 83	Boat wake test No. 2 is conducted.
9-10 Jun 83	Strong southerly winds to 26 knots are experienced.
13 Jun 83	First serious structural damage to pipe-tire breakwater (broken pipe No. 2 from west end) is noted.
23 Jun 83	Test site is inspected by working group.
5 Jul 83	Pipe-tire breakwater is removed from test site.
12 Jul 83	Second pipe (No. 1 from west end) is found broken.
18 Aug 83	Pull test/boat wake test No. 3 is conducted.
10 Sep 83	Strong southerly winds, to 26 knots, are experienced.
19 Sep 83	Clump weights are removed from concrete breakwater anchor lines.
20 Sep 83	Strong northerly winds, of 20 knots, are experienced.
9 Oct 83	Strong northerly winds are experienced.

22 Oct 83	Strong southerly winds, of 20-25 knots, are experienced.
29 Oct 83	Boat wake test No. 4 is conducted.
1 Nov 83	Concrete breakwater is removed and towed to Lake Washington Ship Canal.
2-30 Nov 83	New horizontal fender flexible connector is installed.
1 Dec 83	Concrete breakwater is reinstalled at West Point.
8 Dec 83	Strong southerly winds, of 25 knots, are experienced.
12 Dec 83	Test site is inspected by working group.
20 Dec 83	Strong northerly winds are experienced.
2-4 Jan 84	Strong southeasterly winds, of 27 knots, are experienced.
23-26 Jan 84	Strong southerly winds, of 30 knots, are experienced.
31 Jan 84	Concrete breakwater is unanchored and towed to Lake Washington Ship Canal.
5 Mar 84	Concrete breakwater is anchored at Corps' marina project at Friday Harbor, Washington.